



**Electropermeabilization of inner and outer cell
membranes with microsecond pulsed electric fields :
effective new tool to control mesenchymal stem cells
spontaneous Ca²⁺ oscillations**

Hanna Hanna

► **To cite this version:**

Hanna Hanna. Electropermeabilization of inner and outer cell membranes with microsecond pulsed electric fields: effective new tool to control mesenchymal stem cells spontaneous Ca²⁺ oscillations. Cellular Biology. Université Paris Saclay (COMUE), 2016. English. NNT: 2016SACLS493. tel-01687535

HAL Id: tel-01687535

<https://theses.hal.science/tel-01687535>

Submitted on 18 Jan 2018

HAL is a multi-disciplinary open access archive for the deposit and dissemination of scientific research documents, whether they are published or not. The documents may come from teaching and research institutions in France or abroad, or from public or private research centers.

L'archive ouverte pluridisciplinaire **HAL**, est destinée au dépôt et à la diffusion de documents scientifiques de niveau recherche, publiés ou non, émanant des établissements d'enseignement et de recherche français ou étrangers, des laboratoires publics ou privés.

THÈSE DE DOCTORAT
DE
L'UNIVERSITÉ PARIS-SACLAY
PRÉPARÉE À
L'UNIVERSITÉ PARIS-SUD 11

ÉCOLE DOCTORALE N° 569

Innovation Thérapeutique : du Fondamental à l'Appliqué

Spécialité : Pharmacotechnie et Biopharmacie

Par

Mr. Hanna Hanna

Electropermeabilization of inner and outer cell membranes with microsecond pulsed electric fields: effective new tool to control mesenchymal stem cells spontaneous calcium oscillations

Thèse présentée et soutenue à Villejuif, le 13 Décembre 2016

Composition du Jury :

M. Combettes Laurent	Directeur de recherche, INSERM	Président du jury
M. O'Connor Rodney	Professeur, Ecole des Mines de Saint Etienne	Rapporteur
M. Satkauskas Saulius	Professeur, Vytautas Magnus University	Rapporteur
Mme Fromigué Olivia	Chargé de recherche, INSERM	Examinatrice
M. Percherancier Yann	Chargé de recherche, CNRS	Examineur
M. Mir Lluís M.	Directeur de recherche, CNRS	Directeur de thèse
M. André Franck M.	Chargé de recherche, CNRS	Co-encadrant de thèse

Table of contents

Abbreviations	5
Preface	9
I. State of the art	13
1 The Biomembranes	15
1.1 The plasma membrane	15
1.1.1 Historical view	15
1.1.1.1 The Fluid-Mosaic Model	16
1.1.2 Plasma membrane composition	17
1.1.2.1 Lipids	17
1.1.2.1.1 Phospholipids	17
1.1.2.1.2 Glycolipids	19
1.1.2.1.3 Sterols	20
1.1.2.1.4 Lipid phases in plasma membrane	20
1.1.2.2 Proteins	22
1.1.2.3 Carbohydrates	23
1.1.2.4 Lipid rafts	24
1.1.2.5 The asymmetry of the plasma membrane	25
1.1.3 The dynamic nature of the plasma membrane	26
1.1.4 The plasma membrane functions	28
1.1.4.1 Lipids functions	28
1.1.4.1.1 Compartmentalization	28
1.1.4.1.2 A selectively permeable barrier	28
1.1.4.1.3 Signal Transduction in response to external stimuli	29
1.1.4.2 Proteins functions	29
1.1.4.2.1 Selective permeability: transport proteins	29
1.1.4.2.2 Signal transduction: receptor proteins	31
1.1.4.2.3 Other functions	33
1.1.5 Resting membrane potential	33
1.2 The organelles membranes	35
1.2.1 Eukaryotic cell compartmentalization	35
1.2.2 Organelles membranes composition	36
1.2.3 The endoplasmic reticulum	38
1.2.3.1 The largest membranes network of the cell	38
1.2.3.2 A highly permeable membrane?	39
1.2.3.3 The largest calcium store of the cell	40
1.2.3.4 The KDEL sequence	41
1.3 The continuity of the cellular membranes	42
1.3.1 Vesicular transport	42
2 Calcium regulation in the cell	45
2.1 The importance of the calcium in the organisms and the cell physiology	45
2.2 Calcium-signaling system	45
2.2.1 Principal components of the calcium increase step	46
2.2.1.1 Voltage-operated calcium channels	47

2.2.1.2	Receptor-operated calcium channels	48
2.2.1.3	Inositol-1,4,5-triphosphate receptor	49
2.2.1.4	Ryanodine receptor	50
2.2.1.5	Two-pore calcium channels	50
2.2.1.6	Store-operated calcium channels	51
2.2.1.7	Calcium-induced calcium release (CICR)	52
2.2.2	Principle components of the calcium decrease step	52
2.2.2.1	Plasma membrane Ca^{2+} -ATPase	53
2.2.2.2	Sarco/endoplasmic reticulum Ca^{2+} -ATPase	53
2.2.2.3	Plasma membrane $\text{Na}^+/\text{Ca}^{2+}$ exchanger	54
2.2.2.4	Mitochondrial voltage-dependent anion channel	54
2.2.2.5	Mitochondrial calcium uniporter	55
2.2.3	Calcium buffers and effectors	55
2.2.4	How the calcium spatial and temporal signaling is decoded by the cell?	56
2.2.4.1	Calcium sparks, oscillations and waves	56
2.2.4.2	Calcium-sensitive enzymes and transcription-factors	58
2.3	Different calcium-related mechanisms in the cell	59
2.3.1	Mitochondria-associated membranes and apoptosis	59
2.3.2	Other mechanisms and functions	60
2.4	Studying calcium signaling: the calcium markers	61
2.4.1	Fluorescent Ca^{2+} -sensitive dyes	61
2.4.2	Genetically encoded Ca^{2+} indicators	63
3	<i>Mesenchymal stem cells and differentiation</i>	65
3.1	Mesenchymal stem cells	65
3.1.1	Human adipose Mesenchymal stem cells	66
3.1.2	Calcium oscillations in MSCs	68
3.1.3	Calcium oscillations between MSCs and differentiated cells	69
3.2	Mesenchymal stem cells differentiation	70
3.2.1	Differentiation into osteoblasts	71
3.2.1.1	Osteogenic-induction factors	72
3.2.1.2	The importance of the extracellular matrix in osteogenic differentiation	73
3.2.1.3	Osteodifferentiation markers	73
3.2.2	Differentiation into adipocytes	74
3.2.2.1	Adipogenic-induction factors	74
3.2.2.2	Adipogenic markers	75
3.2.3	Differentiation into neuronal cells	75
3.2.3.1	Neurogenic-induction factors	76
3.2.3.2	Neurogenic markers	76
3.3	Effects of physical stimuli on the MSCs differentiation	77
3.3.1	Effect of mechanical stimulation	77
3.3.2	Effect of the electric, electromagnetic fields and the membrane potential	78
4	<i>Membranes electroporation</i>	81
4.1	A brief historical view	81
4.2	The electroporation principle	82
4.2.1	The induced transmembrane potential	83
4.2.2	The permeabilization threshold	85

4.3	Some factors that influence the permeabilization threshold and impact the electropermeabilization outcomes	86
4.3.1	The impact of the electric field amplitude	86
4.3.2	The impact of the pulse duration	88
4.3.3	The impact of the number of the pulses	88
4.3.4	The impact of the pulses frequency	88
4.3.5	The impact of the cell shape and diameter	89
4.3.6	The impact of the plasma membrane properties and lipid composition	90
4.3.7	The impact of the medium composition [conductivity]	91
4.3.8	The impact of the cell confluence or density	92
4.3.9	The impact of the temperature	92
4.4	Electroporation vs electropermeabilization	93
4.4.1	Electroporation: the direct effect of the pulse	93
4.4.2	Electropermeabilization: the long-lasting effect of the pulse	93
4.5	Indices of membrane permeabilization	94
4.5.1	The permeabilization markers	94
4.5.2	The membrane conductivity	95
4.6	The different kinds of pulses used in electroporation	95
4.6.1	The millisecond pulsed electric fields	95
4.6.2	The microsecond pulsed electric fields	96
4.6.3	The nanosecond pulsed electric fields	97
4.7	Some applications of the membrane electropermeabilization	98
4.7.1	Electrochemotherapy	98
4.7.2	Electrogenettransfer	99
4.7.3	Electrofusion	99
II.	Research hypotheses and objectives	101
III.	Results	105
1	Electropermeabilization of Inner and Outer Cell Membranes with Microsecond Pulsed Electric Fields: Quantitative Study with Calcium Ions (article n°1)	107
2	Electrical Control of Calcium Oscillations in Mesenchymal Stem Cells Using Microsecond Pulsed Electric Fields (article n°2)	135
3	In vitro Osteoblastic differentiation of mesenchymal stem cells generates cell layers with distinct properties (article n°3)	153
4	Supplementary data	175
4.1	Effect of a one 100 μ s pulse applied once a day on the osteodifferentiation of human-adipose mesenchymal stem cells	176
4.2	Examples of electro-induced calcium spikes and spontaneous calcium oscillations	187
IV.	Discussion and Perspectives	193
V.	Discussion en langue française	199
VI.	References	207

ABBREVIATIONS

AM: acetoxymethyl
AGPR: asialoglycoprotein receptor
2-APB: 2-Aminoethoxydiphenyl borate
Asc: ascorbic acid
ATP: adenosine triphosphate
BAPTA: 1,2-bis(o-aminophenoxy)ethane-N,N',N'-tetraacetic acid
BHA: butylated hydroxyanisole
βME: β-mercaptoethanol
BSP: bone sialoprotein
CaM: calmodulin
CAM : cell adherence molecule
CaMKII: calmodulin-dependent protein kinase II
cAMP: cyclic adenosine monophosphate
CCV: clathrin-coated vesicle
CD: cluster of differentiation
C/EBP: CCAAT/enhancer binding proteins
cGMP: cyclic guanosine monophosphate
CHO: Chinese Hamster Ovary (cells)
CICR: calcium-induced calcium release
CL: cardiolipin
CNGC: cyclic-nucleotide-gated channel
Col1: collagen type 1
CREB: cAMP response element-binding protein
CSFD: Ca²⁺-sensitive fluorescent dye
DAG: diacylglycerol
Dex: dexamethasone
DMSO: dimethyl sulfoxide
ECM: extracellular matrix
ECT: electrochemotherapy
EGT: electrogenetransfer
EGTA: ethylene glycol tetraacetic acid
EP: equilibrium potential
ER: endoplasmic reticulum
ERK: extracellular signal-regulated kinases
ESC: embryonic stem cell
FAK: focal adhesion kinase
FABP4: fatty-acid binding protein 4
FRAP: fluorescence recovery after photobleaching
FRET: Förster resonance energy transfer
GalCer: galactosylceramide
GDP: guanosine di-phosphate

GFP: green fluorescent protein
 GlcCer: glucosylceramide
 G2P: glycerol 2-phosphate
 GPCR: G protein-coupled receptor
 GPI: glycosylphosphatidylinositol
 GPL: glycerophospholipid
 GqPCRs: Gq protein-coupled receptors
 GRP: glucose-regulated protein
 GSL: glycosphingolipid
 GTP: guanosine tri-phosphate
 GUV: giant unilamellar vesicle
 haMSC: human adipose mesenchymal stem cell
 hbMSC: human bone marrow mesenchymal stem cell
 ICR: Ion channel receptor
 ICRAC: Ca^{2+} release-activated Ca^{2+} current
 Ig : immunoglobulin
 IL : interleukin
 IMM: inner mitochondrial membrane
 IP_3 : inositol triphosphate
 IP_3R : inositol triphosphate receptor
 iPS: induced pluripotent stem cell
 LDL: low density lipoprotein
 LGC: ligand-gated channels
 LOX: lipoxygenase
 MAM: mitochondria-associated membrane
 MAPK: mitogen-activated protein kinase
 MCU: mitochondrial calcium uniporter
 MD: molecular dynamic
 MIX: 1-methyl-3-isobutylxanthine
 MP: membrane potential
 MSC: mesenchymal stem cell
 NAADP: nicotinic acid adenine dinucleotide phosphate
 NCX: $\text{Na}^+/\text{Ca}^{2+}$ exchanger
 NFAT: nuclear factor of activated T cells
 NF- κB : nuclear factor-kappa B
 NGF: nerve growth factor
 NMDAr: N-methyl-D-aspartate receptor
 NP: Nernst potential
 NT: neurotransmitter
 OMM: outer mitochondrial membrane
 PAF: platelet activating factor
 PDGF: platelet-derived growth factor
 PEF: pulsed electric field
 PhA: phosphatidic acid
 PhC: phosphatidylcholine

PhE: phosphatidylethanolamine
 PhG: phosphatidylglycerol
 PhI: phosphatidylinositol
 PhS: phosphatidylserine
 PI: propidium iodide
 PIP2: phosphatidylinositol 4,5-bisphosphate
 PKA: protein kinase A
 PKC: protein kinase C
 PLB: phospholamban
 PLC: phospholipase C
 PM: plasma membrane
 PMCA: plasma membrane calcium ATPase
 PPAR γ : peroxisome proliferator-activated receptor γ
 PR : purinergic receptor
 PrSN: presynaptic neuron
 PSN: postsynaptic neuron
 RER: rough endoplasmic reticulum
 RhoA: Ras homolog gene family, member A
 RME: receptor-mediated endocytosis
 RNA: ribonucleic acid
 ROCC: receptor-operated calcium channel
 RTKs: receptor tyrosine kinases
 Runx2: Runt-related transcription factor 2
 RyR: ryanodine receptor
 SACC: Stretch-activated calcium channel
 SAM : substrate adhesion molecule
 SDS: Sodium dodecyl sulfate
 SDS-PAGE: SDS polyacrylamide-gel electrophoresis
 SER: smooth endoplasmic reticulum
 SERCA: sarcoplasmic/endoplasmic reticulum calcium ATPase
 SH2: Src Homology 2 domain
 SM: sphingomyelin
 SMOC: second messenger-operated channel
 STIM: Stromal interaction molecule
 SOCC: store-operated calcium channel
 SOCE: store-operated calcium entry
 SR: sarcoplasmic reticulum
 TGF- β : transforming growth factor beta
 TRPC: transient receptor potential cation channel
 TPC: two-pore channel
 VA: valproic acid
 VDAC: voltage-dependent anion channel
 VGC: voltage-gated channels
 VOCC: voltage-operated calcium channel

PREFACE

The calcium is a universal second messenger that controls, either directly or indirectly, many basic cellular functions, such as proliferation, differentiation, apoptosis and vesicular trafficking. Hence, the control of cytosolic calcium concentrations may be a useful tool to study and control such processes in physiological and pathological conditions. The electroporation is a widely used technique in research, medicine, food industry and many biotechnological processes, in order to permeabilize the plasma or/and the organelles membranes to normally non-permeant molecules such as genetic materials, drugs or ions such as calcium. Therefore, this research work deals with 1) the generation of electro-induced calcium spikes in the cells using 100 μ s electric pulses (by the electroporabilization of the plasma membrane alone or together with the endoplasmic reticulum membranes), 2) the use of these pulses to control the spontaneous calcium oscillations in mesenchymal stem cells.

The first chapter of this manuscript is dedicated to the description of the state of the art, giving the reader the key elements necessary for a deep understanding of this research work, whose objectives are then addressed in the second chapter. The concepts specifically presented are: cell and organelles membranes, calcium regulation in the cell, the mesenchymal stem cells calcium oscillations and the cell electroporation. The guiding principle was the understanding of the mechanisms underlying the electroporabilization of internal membranes by microsecond pulsed electric fields, and also studying the control of spontaneous calcium oscillations by these pulses.

In the third chapter the results are described. First, the electroporabilization of inner and outer cell membranes with a single 100 μ s pulse is demonstrated by using the calcium as a permeabilization marker. Then, the fine control of calcium oscillations in mesenchymal stem cells using microsecond pulsed electric fields is evaluated. In addition, a further investigation of the mesenchymal stem cells differentiation into osteogenic, adipogenic and neurogenic lineages was also assessed. These results are presented as three research articles. Finally, a global synthesis of the results is presented in the discussion sections (in English as well as in French) where perspectives and future works are also addressed.

I. STATE OF THE ART

1 THE BIOMEMBRANES

1.1 THE PLASMA MEMBRANE

The plasma membrane (PM) is a common structure to all living organisms, whether animal, plants, unicellular or multicellular. However, its composition is not the same for all the organisms. The plasma membrane is the boundary between the cell and its environment, and it makes only 5 to 10 nm wide (Karp 2010). It regulates what enters and exits the cell. Cells must maintain an appropriate amount of molecules to function inside them (Uzman 2003), thus, each cell has to exchange molecules with its environment (selective nutrient absorption, secretion of molecules in the cellular environment). The plasma membrane defines the rules of these exchanges between the cell and its environment.

1.1.1 Historical view

The lipid nature of the cell membrane was first correctly intuited by Quincke in 1888, who noted that a cell generally forms a spherical shape in water and, when broken in half, forms two smaller spheres. The only other known material to exhibit this behavior was oil. He also noted that a thin film of oil behaves as a semi-permeable membrane, precisely as predicted (Loeb 1904). Based on these observations, Quincke asserted that the cell membrane comprised a fluid layer of fat less than 100 nm thick (Hertwig et al. 1895). Later on, Ernest Overton made the hypothesis that to pass the cell membrane a molecule must be at least sparingly soluble in oil, hence lipophilic and/or amphiphilic (Overton 1895).

In 1935, Hugh Davson and James Danielli proposed a model of the cell membrane in which a phospholipid bilayer lay between two layers of globular proteins (Danielli & Davson 1935). The phospholipid bilayer had already been proposed for the first time by Gorter and Grendel in 1925 (Gorter & Grendel 1925), but the flanking proteinaceous layers of the Davson-Danielli's model were novel and intended to explain Danielli's observations on the surface tension of lipid bilayers. In 1957, David Robertson, based on electron microscopy studies, establishes the "Unit Membrane Hypothesis". This, states that all membranes in the cell, *i.e.* plasma and organelle membranes, have the same structure: a bilayer of phospholipids with monolayers of proteins at both sides of it (Robertson 1959, 1960).

The Davson-Danielli model predominated until Singer and Nicolson proposed the fluid mosaic model in 1972 (Singer & Nicolson 1972). This model included the transmembrane proteins, and eliminated the flanking protein layers that were not well-supported by experimental evidence. It is now known that the phospholipid head groups are sufficient to explain the measured surface tension observed by Danielli.

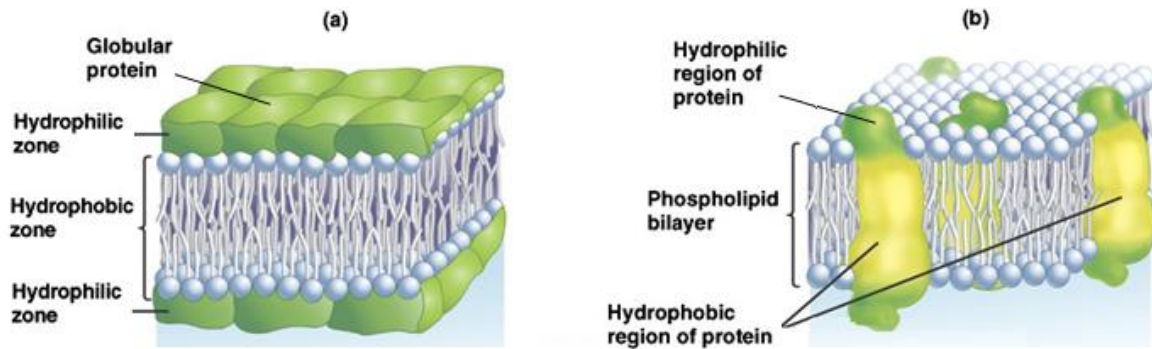


Figure 1: two generations of membrane models, (a) original Davson-Danielli trilayer model, (b) current fluid-mosaic model (adapted from <http://www.uic.edu/classes/bios/bios100/lectures/membranes.htm>).

1.1.1.1 The Fluid-Mosaic Model

In 1972 the Fluid-Mosaic Membrane Model was proposed (Singer & Nicolson 1972). According to this model, the two leaflets of biological membranes are asymmetric and divided into subdomains composed of specific proteins or lipids, allowing spatial segregation of biological processes associated with membranes. The previous models, presenting proteins as sheets neighboring a lipid layer, rather than incorporated into the phospholipid bilayer, were not well supported by microscopy, and did not permit to explain the dynamic membrane properties as well as the changes in structure and behavior of cell membranes under different temperatures (Nicolson 2014).

The nature of the membrane proteins was studied by Unwin and Henderson (1984). They found that the portion of the protein that spans the lipid bilayer is hydrophobic in nature (similar to the lipids forming the bilayer) and arranged in a three-dimensional shape, often in the form of an alpha helix (Unwin & Henderson 1984).

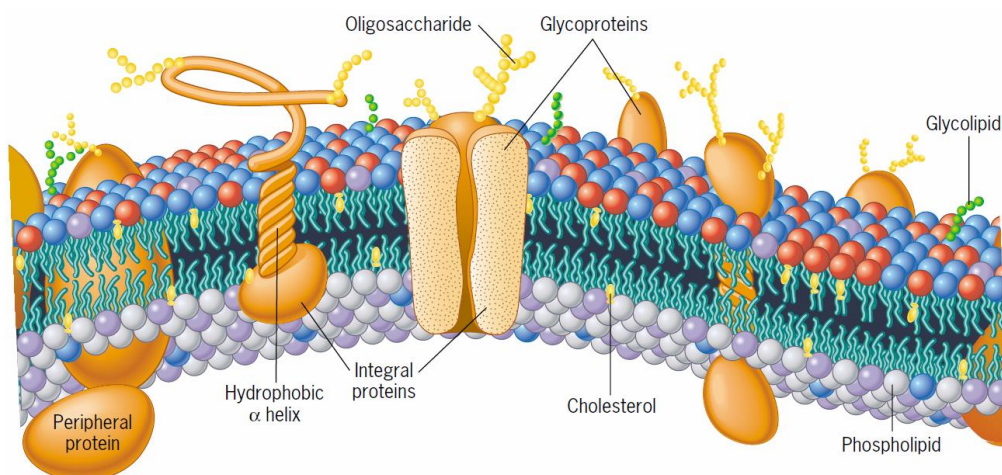


Figure 2: a current representation of the plasma membrane showing the same basic fluid- mosaic model organization as that proposed by Singer and Nicolson (Karp 2010).

1.1.2 Plasma membrane composition

The PM is composed of lipids and proteins and contains carbohydrates which are attached to them (*Figure 2*). The phospholipid bilayer forms a stable barrier between two aqueous compartments: the inside and the outside of the cell. The proteins embedded within the PM carry out specific functions such as selective transport of molecules and cell-cell recognition. The ratio of lipid to protein in a membrane depends on the type of cellular membrane (plasma vs. endoplasmic reticulum vs. Golgi), the type of organism (bacterium vs. plant vs. animal), and the type of cell (liver vs. muscle vs. bone) (Karp 2010).

1.1.2.1 Lipids

Lipids are water-insoluble biomolecules that are highly soluble in organic solvents such as chloroform. Membranes contain a wide diversity of lipids, all of which are amphipathic; that is, they contain both hydrophilic and hydrophobic regions. Lipids constitute approximately 50% of the PM mass (Cooper 2000a).

1.1.2.1.1 Phospholipids

Most membrane lipids contain a phosphate group, which makes them phospholipids. Because most membrane phospholipids are built on a glycerol backbone (*Figure 3*), they are called phosphoglycerides or glycerophospholipids and they represent the major structural lipids in eukaryotic membranes. Their hydrophobic portion is a diacylglycerol (DAG), which contains two saturated or cis-unsaturated fatty acyl chains of various lengths. The fatty acyl chains are unbranched hydrocarbons approximately 14 to 24 carbons in length. A membrane fatty acid may be fully saturated, monounsaturated, or polyunsaturated. Phosphoglycerides often contain one unsaturated and one saturated fatty acyl chain (Alberts et al. 2002a). The insaturations create an angle in the aliphatic chain and play an important role in the membrane fluidity.

Two of the hydroxyl groups of the glycerol are esterified to fatty acids; the third is esterified to a hydrophilic phosphate group. Membrane phosphoglycerides have an additional group linked to the phosphate, most commonly either choline (forming phosphatidylcholine, PhC), ethanolamine (forming phosphatidylethanolamine, PhE), serine (forming phosphatidylserine, PhS), or inositol (forming phosphatidylinositol, PhI) (*Figure 4*). These groups, together with phosphate, form at one end of the phospholipid the highly hydrophilic head group (*Figure 3*).

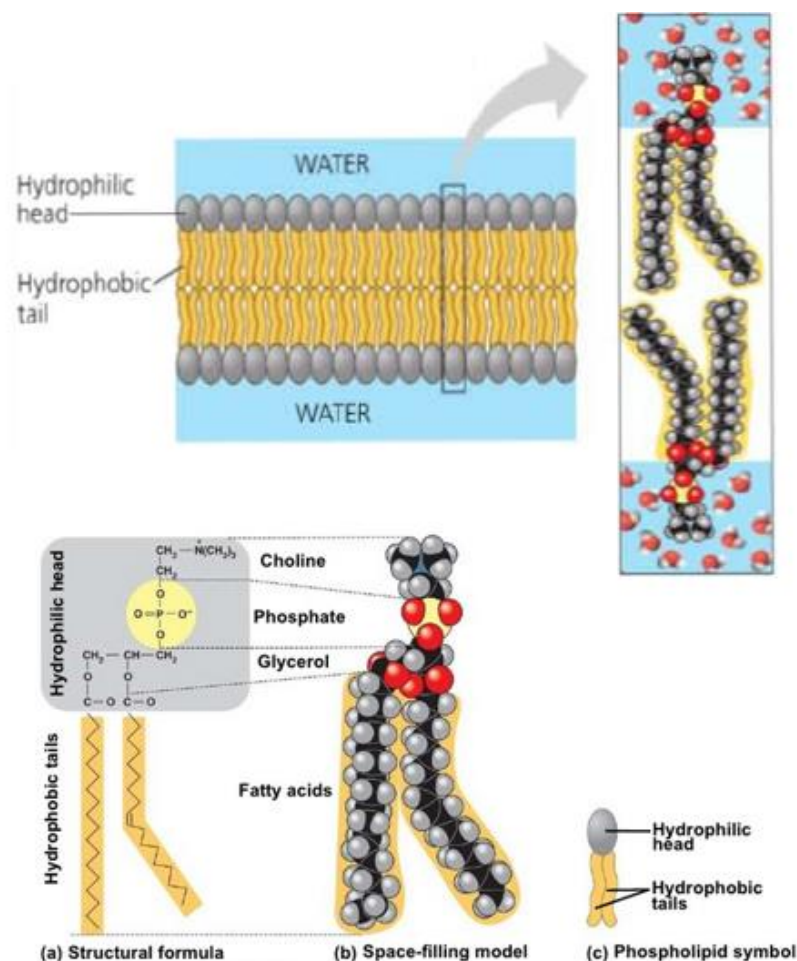


Figure 3: phospholipid bilayer (cross section) and the structure of a phospholipid (Campbell and Reece, 2007).

PhC accounts for >50% of the phospholipids in most eukaryotic membranes and has a cylindrical molecular geometry. Most PhC molecules have one cis-unsaturated fatty acyl chain, which renders them fluid at room temperature. PhE assumes a conical molecular geometry because of the relatively small size of its polar headgroup (van Meer et al. 2008). The inclusion of PhE in PhC bilayers imposes a curvature stress onto the membrane, which is used for budding, fission and fusion (Marsh 2007). At physiologic pH, the head groups of PhS and PhI have an overall negative charge (anionic head group), whereas those of PhC and PhE are neutral (zwitterionic head group).

Lipids with a small area ratio of polar head to acyl chain (creating a cone shape) induce negative curvature, lipids with an equal head to chain area ratio (creating a cylinder shape) are neutral, and those with a much larger head compared with the acyl chain area (creating an inverted cone shape) induce a positive curvature (Holthuis and Menon, 2014). Non-bilayer lipids are those who induce a curvature in the PM, like PhE and cardiolipin (CL). They may be used to accommodate membrane proteins and modulate their activities (Vance & Vance 2008). An additional factor that contributes to curvature stress in biomembranes is the asymmetric distribution of various lipids between the two bilayer leaflets (van den Brink-van der Laan et al. 2004) (*cf.* 1.1.2.5).

Another class of membrane phospholipids, called sphingolipids, are derivatives of sphingosine, an amino alcohol that contains a long hydrocarbon chain (Figure 4). Sphingolipids consist of sphingosine linked to a fatty acid (R of Figure 4) by its amino group to form a ceramide. The various

sphingosine-based lipids have additional groups esterified to the terminal alcohol of the sphingosine moiety (Karp 2010). If the substitution is PhC, the molecule is sphingomyelin (SM), which is the only phospholipid of the membrane that is not built with a glycerol backbone and is one of the major sphingolipids in mammalian cells.

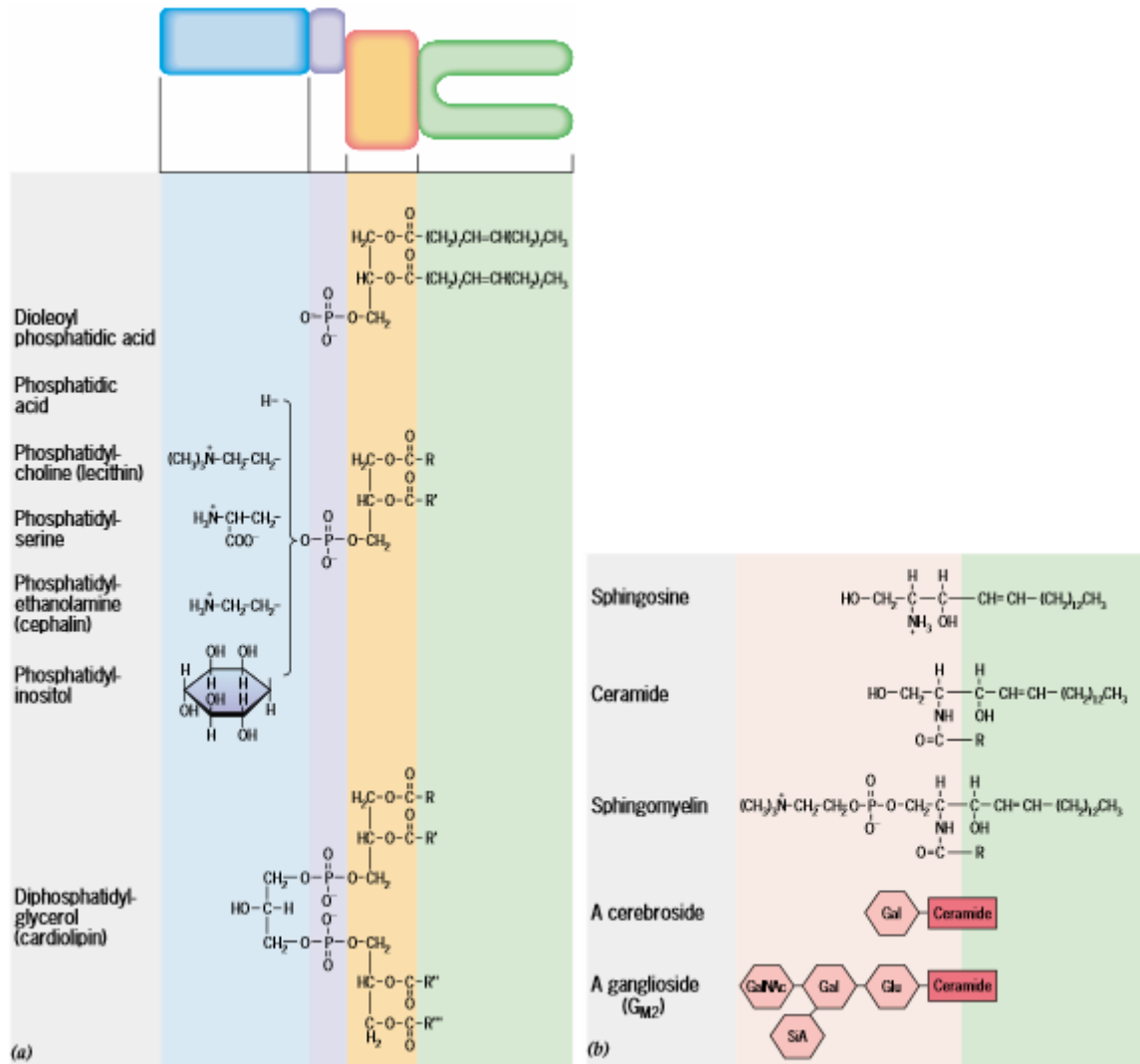


Figure 4: (a) The structures of phosphoglycerides, (b) The structures of sphingolipids. Sphingomyelin is a phospholipid; cerebroside and gangliosides are glycolipids (Karp, 2010).

1.1.2.1.2 Glycolipids

Another class of sphingolipids are the glycolipids or glycosphingolipids (GSLs), that contain mono-, di- or oligosaccharides based on glucosylceramide (GlcCer) and sometimes galactosylceramide (GalCer) (Meer & Lisman 2002). Such glycolipid with a simple carbohydrate are called cerebroside (Figure 4.b). Gangliosides are GSLs with an oligosaccharide and a terminal sialic acids. Glycolipids play crucial role in cell function. They are particularly enriched in the nervous system. The GalCer comprise nearly 30% of lipids in myelin sheaths of oligodendrocytes and Schwann cells, in which they are thought to participate in axon insulation and saltatory conduction of the action potential (Norton & Cammer

1984). The fungal toxins, called fumonisins, which inhibits the synthesis of glycolipids, disturb cell growth, cell death, cell-cell interactions and communication from the outside of the cell to the interior (Riley et al. 2001). Sphingolipids have saturated (or trans-unsaturated) tails so they are able to form taller, narrower cylinders than PC lipids of the same chain length and they pack more tightly, adopting the solid 'gel' or s_o phase (cf. 1.1.2.1.4); they are fluidized by sterols (van Meer et al. 2008).

1.1.2.1.3 Sterols

Sterols are the major non-polar lipids of cell membrane: cholesterol predominates in animal cells whereas ergosterol predominates in yeast cells (van Meer et al. 2008). Cholesterol may constitute up to 50 percent of the lipid molecules in the animal cells PM and it is absent from the PM of most plant and all bacterial cells. Cholesterol is smaller than the other lipids of the membrane and less amphipathic (Karp 2010).

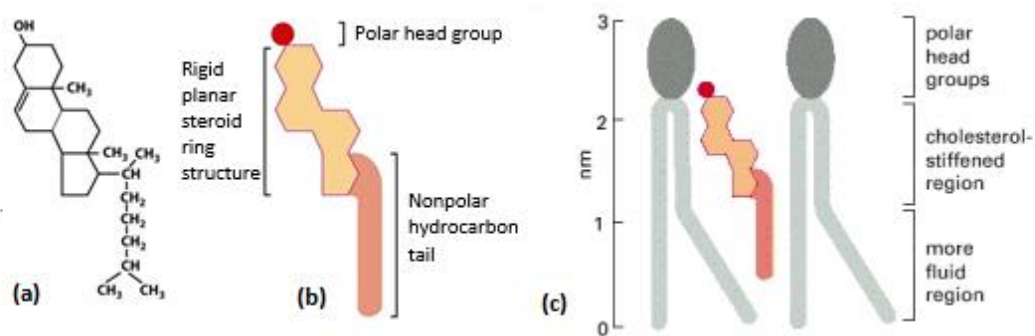


Figure 5 : (a) structural formula of the cholesterol, (b) Schematic drawing, (c) a cholesterol molecule interacting with two phospholipid molecules in one monolayer of a lipid bilayer (Alberts et al., 2002).

The backbone of cholesterol consists of a rigid, fused four-ring system (Figure 5). A single hydroxyl group forms the polar headgroup that faces the aqueous milieu while the hydrocarbon tail is positioned towards the bilayer interior. The small headgroup of cholesterol is insufficient to shield the hydrophobic ring system from water molecules, so the neighbouring lipids fulfil this role. This may favour interactions of cholesterol with other lipids that have larger headgroups. This is known as the umbrella model (Ikonen 2008).

Cholesterol determines the permeability, fluidity, and mechanical properties of the membranes (Ohvo-Rekilä et al. 2002). It increases the order of fluid-phase phospholipid acyl chains, giving rise to the formation of the liquid-ordered (lo) phase (Almeida 2009) (cf. 1.1.2.1.4). Through this process, it is also involved in the formation of highly ordered nano-scale membrane domains called lipid rafts (Niemelä et al. 2007) which play an important role in numerous cellular functions (cf. 1.1.2.4).

1.1.2.1.4 Lipid phases in plasma membrane

The PM lipids can exist in multiple possible phase states that determine the fluidity of this latter. This fluidity depends on the temperature and the PM composition.

At lower temperatures, membrane lipid bilayers undergo a reversible change of state from a fluid (disordered) L_D to a nonfluid (ordered) S_0 array of the fatty acyl chains (*Figure 6*). The temperature at the midpoint of this transition is called the transition temperature. The change of state accompanying a temperature increase is called the order-disorder transition (Mansilla et al. 2004). The transition temperature is a function of many factors such as the membrane lipid composition, the saturation degree and the length of the fatty acid chain in addition of the presence of cholesterol. Phospholipids with saturated chains pack together more tightly than those containing unsaturated chains. The greater the degree of unsaturation of the fatty acids of the bilayer, the lower the temperature before the bilayer gels. The introduction of one double bond in a molecule of stearic acid for example can lower the melting temperature from 70°C to 13°C (Karp 2010).

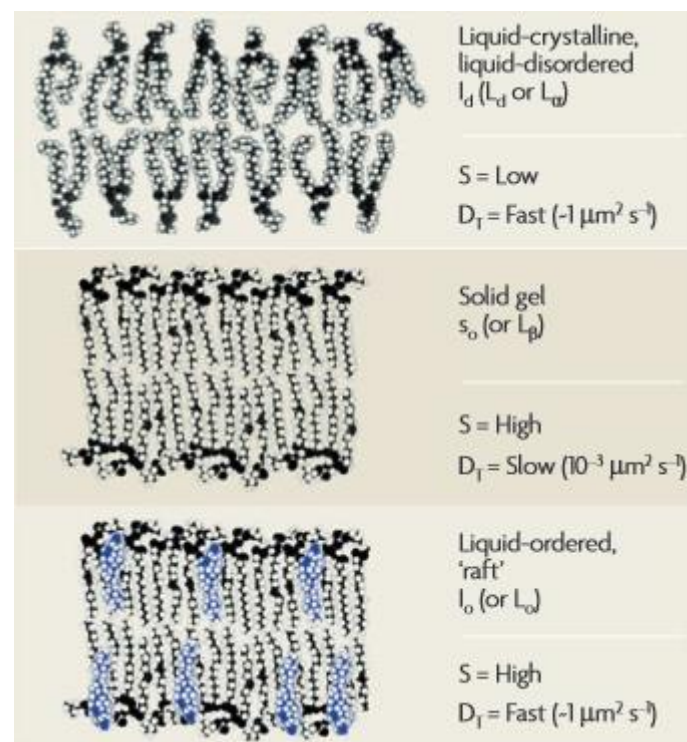


Figure 6: lipid phases in plasma membrane. S: the order parameter of a segment of acyl chain, D_T : the translational diffusion coefficient (van Meer et al. 2008).

The presence of cholesterol tends to abolish sharp transition temperatures and decreases the permeability of the PM (Cooper 1978). At relatively higher temperatures (e.g. 37°C), cholesterol makes the membrane less fluid by restraining phospholipid movement. However, because cholesterol also hinders the close packing of phospholipids, it lowers the temperature required for the membrane to solidify. Thus, cholesterol plays a role of a "temperature buffer" for the membrane, resisting changes in membrane fluidity that can be caused by changes in temperature (Campbell n.d. et al., 2008).

The membrane fluidity plays a key role in membrane assembly (from preexisting membranes and many cellular processes, including cell movement, cell growth, cell division, formation of intercellular junctions and vesicular trafficking. An example of the importance of the membrane fluidity in the life cycle is the adaptation of plants that tolerate extreme cold, such as winter wheat. In these plants, the percentage of unsaturated phospholipids increases in autumn, increasing the fluidity of PM, which keeps the membranes from solidifying during winter.

1.1.2.2 Proteins

There are much less proteins molecules than lipids molecules in the PM (about 50 lipids molecules for each protein), but given they are much larger, they constitute about 50% of PM mass. Approximately, 30% of all active genes encode membrane proteins of which approximately one-third are G-protein coupled receptors (GPCRs) (von Heijne 2007).

The primary structure of a protein is the amino-acids sequence. Alpha helices and beta-sheets are the two types of stable secondary structures, they are located at the core of the protein, whereas random coils, loops or turns are in its outer regions. Tertiary structure describes the packing of alpha-helices, beta-sheets and random coils with respect to each other on the level of one whole polypeptide chain. Then quaternary structure describes the spatial organization of many chains present in a complex protein.

The maturation of membrane proteins is directed by an initial specific glycosylation in the endoplasmic reticulum (ER). Correct glycosylation is guaranteed by the lectin chaperones calnexin and calreticulin before vesicular transport to the Golgi apparatus and later transfer to the PM (Trombetta & Parodi 2003).

The membrane proteins are associated in different ways with the lipid bilayer (*Figure 7*), and they are amphipathic like lipids; their quaternary structure displays hydrophilic parts and hydrophobic parts, in particular at the level of the transmembrane domain. Membrane proteins can span a membrane once in a single pass such as guanylate cyclase (an enzyme of the G protein signaling cascade that synthesizes cGMP from GTP) or up to 19 times such as voltage-dependent Ca^{2+} channels (Remm & Sonnhammer 2000). The most frequent are proteins with a single transmembrane spanning segment followed by those with two to seven such segments. The great majority of the membrane-spanning segments of polypeptide chains form an alpha helix when they traverse the bilayer (Alberts et al. 2002b). The first evolution of the original fluid-mosaic model presented by Singer and Nicolson was the integration of proteins in the lipid bilayer which the hydrophobic part was an alpha helix as suggested first by Unwin and Henderson (*cf.* 1.1.1.1, *Figure 1. b* and *Figure 2*).

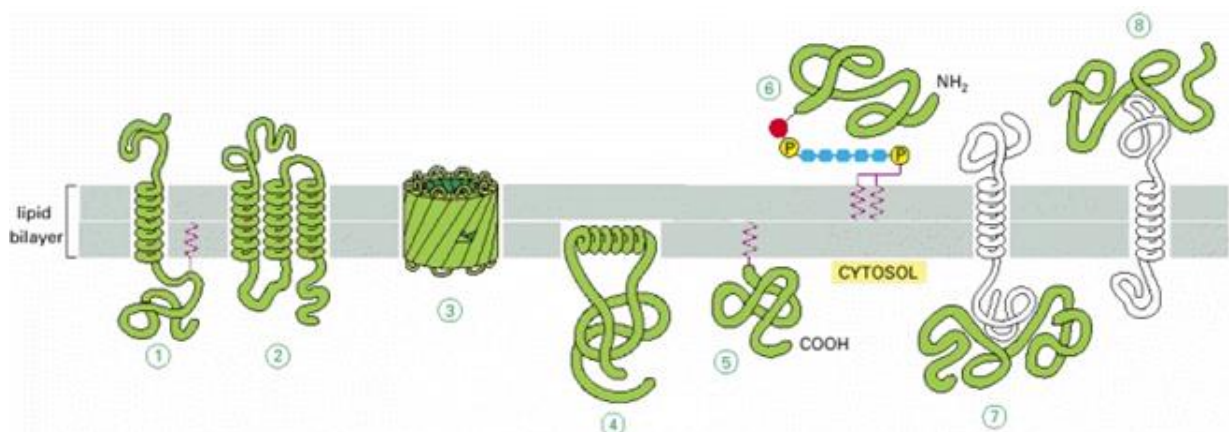


Figure 7 : Various ways of membrane proteins association with the lipid bilayer (Alberts et al. 2002b).

Membrane proteins can be grouped into three distinct classes:

a. *Integral proteins* : penetrate the lipid bilayer

Called also transmembrane proteins, integral proteins have some parts in the outside of the lipid bilayer and some others integrated in the lipid bilayer by multiple ways : a single α helix, multiple α helices, or a rolled-up β sheet (a β barrel) (*Figure 7: 1, 2 and 3 respectively*). Some of these “single-pass” and “multipass” proteins have a covalently attached fatty acid chain inserted in the cytosolic lipid monolayer.

b. *Lipid-anchored proteins*: exposed at only one side of the membrane.

Some of these proteins are anchored to the cytosolic surface by an amphipathic α helix that partitions into the cytosolic monolayer of the lipid bilayer through the hydrophobic face of the helix (*Figure 7: 4*). Others are attached to the bilayer solely by a covalently attached lipid chain—either a fatty acid chain or a prenyl group—in the cytosolic monolayer (*Figure 7: 5*), or via an oligosaccharide linked to a molecule of phosphatidylinositol in the noncytosolic monolayer (*Figure 7: 6*).

c. *Peripheral proteins* : located entirely outside of the lipid bilayer

Many proteins are attached to the membrane only by noncovalent interactions with other membrane proteins (*Figure 7: 7 and 8*).

1.1.2.3 Carbohydrates

A carbohydrate is a biological molecule consisting of carbon, hydrogen and oxygen atoms, usually with a hydrogen:oxygen atom ratio of 2:1, and with an empirical formula $C_m(H_2O)_n$. The PM of eukaryotic cells contain carbohydrates that are covalently linked to both lipids and proteins. More than 90 percent of the membrane’s carbohydrates are covalently bonded to proteins to form glycoproteins; the remaining proportion is covalently linked to lipids to form glycolipids. Membrane carbohydrates are short, branched chains of fewer than 15 sugar units (Campbell & Reece 2007). Depending on the species and cell type, the carbohydrate content of the PM ranges between 2 and 10 percent by weight (Karp 2010).

The carbohydrate projections play a role in mediating the interactions of a cell with another cell and with its environment. Infection by pathogenic microorganisms is often initiated by their adhesion to appropriate target cell via a carbohydrate. Enteric bacteria *Escherichia coli* binds to D-mannose of the urinary and gastrointestinal tracts epithelial cells via their lectins (Sharon 1987).

Oligosaccharides may be attached to several different amino acids by two major types of linkages seen on *Figure 8*: the N-glycosidic linkage and the O-glycosidic linkage. The carbohydrates of the glycolipids of the red blood cell PM determine whether a person’s blood type is A, B, AB, or O.

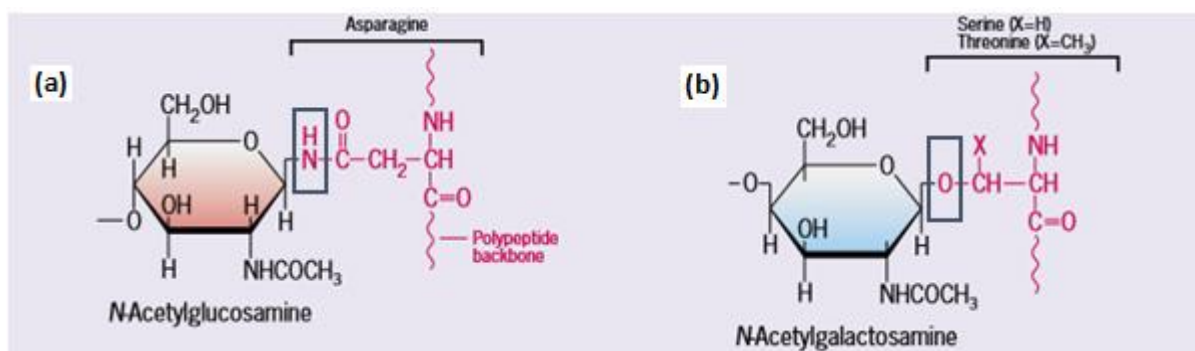


Figure 8 : Two types of linkages that join sugars to a polypeptide chain. (a) The N-glycosidic and (b) the O-glycosidic linkage (Karp 2010).

1.1.2.4 Lipid rafts

Lipid rafts are specialized membrane domains that contain high concentrations of cholesterol, glycosphingolipids, sphingomyelin, gangliosides and saturated phospholipids. Bulk PM containing these components in a smaller concentration together with unsaturated glycerophospholipids (GPL), is more fluid than lipid rafts. The rafts are liquid-ordered regions that are resistant to extraction with cold nonionic detergents such as Triton X-100. They are small in size, but may constitute a relatively large fraction of the PM.

Lipid rafts are involved in the regulation of signal transduction; a variety of proteins involved in cell signaling have been shown to partition into lipid rafts (Pike 2003). Lipid rafts contain many fatty acylated proteins that play key roles in regulating cellular structure and function. The two most common forms of protein fatty acylation are modification with myristate, a 14-carbon saturated fatty acid, and palmitate, a 16-carbon saturated fatty acid (Resh 1999).

Lipid rafts play important role in membrane trafficking (Simons & Ikonen 1997). Sphingolipid-cholesterol rafts are involved in transporting protein in the endocytic pathways (Danielsen 1995). Caveolae, small PM invaginations are a subset of lipid rafts. Glycosylphosphatidylinositol (GPI)-linked proteins are members of lipid rafts and are often used as markers for these domains (Schnitzer et al. 1995). Analysis of the rate of lateral diffusion of GPI-linked proteins as well as gangliosides, suggested that the domains are 200 nm to 300 nm in diameter (Jacobson et al. 1995).

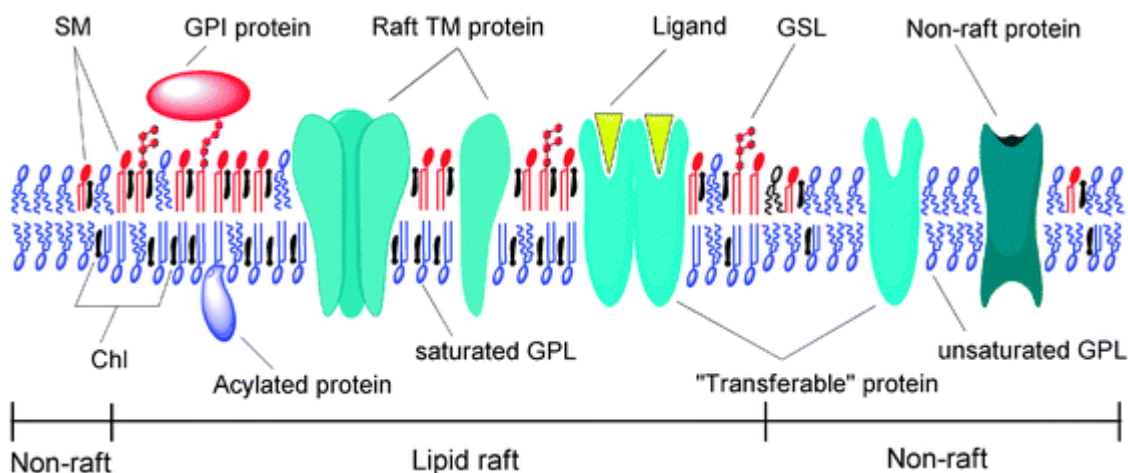


Figure 9 : the lipid raft composition. GPI: glycosylphosphatidylinositol, GPL: glycerophospholipid, GSL : glycosphingolipid, TM protein: transmembrane protein, SM : sphingomyelin. (Zhong 2011).

1.1.2.5 The asymmetry of the plasma membrane

Membranes are structurally and functionally asymmetric. The outer and inner surfaces of all known biological membranes have different components and different enzymatic activities. This asymmetry is referred to as membrane “sidedness.”

Membrane proteins have a unique orientation because they are synthesized and inserted into the membrane in an asymmetric manner. This asymmetry is preserved because membrane proteins do not rotate from one side of the membrane to the other (Berg et al. 2002a). Lipids, too, are asymmetrically distributed as a consequence of their mode of biosynthesis. The asymmetric distribution of glycolipids in the bilayer results from the addition of sugar groups to the lipid molecules in the lumen of the Golgi apparatus, which is topologically equivalent to the exterior of the cell (Alberts et al. 2014). The phospholipid asymmetry is generated in the endoplasmic reticulum (ER), where most of the membranes in a eucaryotic cell, including the plasma membrane, are synthesized. The asymmetric distribution of cholesterol and the various glycerophospholipids contribute to the lipid curvature needed to maintain cell structure and to sustain the noncrystalline state by limiting the ability to phase shift to a more rigid structure (Maxfield & Tabas 2005).

The lipid asymmetry is functionally important. The enzyme protein kinase C, for example, requires the negatively charged PS to act; when it is activated by an extracellular signal, it binds to the cytoplasmic face of the PM, where the PS is concentrated (Alberts et al. 2002a). On the other hand, the appearance of PS on the outer surface of aging lymphocytes marks the cells for destruction by macrophages, whereas its appearance on the outer surface of platelets leads to blood coagulation (Karp 2010). Another example is that of PI; these minor phospholipids concentrated in the inner leaflet are cleaved into two fragments by specific enzymes that are activated by extracellular signals. Both fragments act as diffusible mediators to relay the signal into the cell interior.

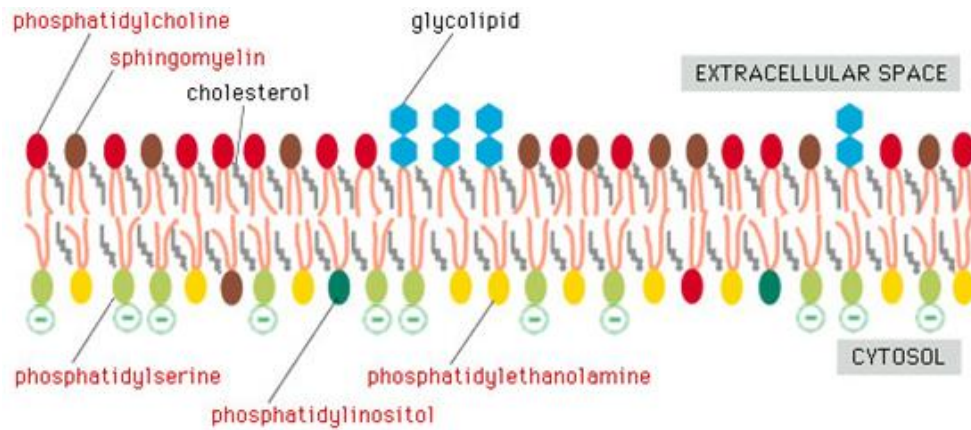


Figure 10: the asymmetric distribution of phospho and glycolipids in the plasma membrane (Alberts et al. 2002a).

1.1.3 The dynamic nature of the plasma membrane

The lipids and proteins represented in the fluid mosaic model of Singer and Nicolson are not fixed in their position. They move within the PM. Phospholipids and glycolipids can rotate freely around their axes and diffuse laterally within the membrane leaflet (Figure 11). Because such movements are lateral or rotational, the fatty acyl chains remain in the hydrophobic interior of the membrane. A typical lipid molecule exchanges places with its neighbors in a leaflet about 10^6 times per second and diffuses several micrometers per second at 37 °C. The third movement of phospholipids is the migration, or flip-flop, from one leaflet to another, and this movement is catalyzed by specific membrane proteins called *flippases*, which help maintain asymmetric gradient in the PM (Daleke 2007). However, this movement is restricted, because the transport of the polar head of a phospholipid through the hydrophobic interior of the membrane consumes a lot of energy.

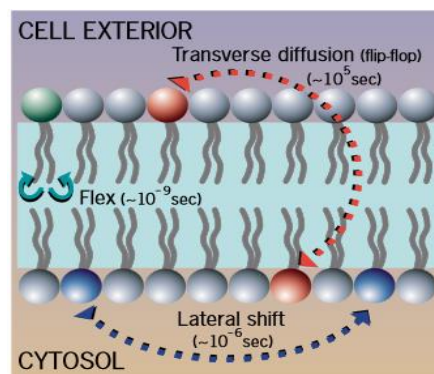


Figure 11 : The possible movements of phospholipids in a membrane and the approximate time scales over which they occur (Karp 2010).

Like lipids, membrane proteins are able to move laterally within the PM (*lateral diffusion*) and they can rotate about an axis perpendicular to the plane of the bilayer (*rotational diffusion*) but they do not tumble (*flip-flop*) across the lipid bilayer (Alberts et al. 2002b).

One of the first experiments to demonstrate that membrane proteins could move within the membrane was that of Larry Frye and Michael Edidin in 1970 (Frye & Edidin 1970). Cells from established tissue culture lines of mouse and human origin were marked by different fluorescent antibodies against membrane proteins and then fused together with Sendai virus (*Figure 12*). The heterokaryons bearing both mouse and human surface antigens were then followed by the indirect fluorescent antibody method. At the beginning the rhodamine labeled antibodies (against human membrane) were localized at one part of the heterokaryons and the fluorescein labeled antibodies (against mouse membrane) at the other part. Within 40 min following fusion, total mixing of both parental antigens occurred in over 90% of the heterokaryons (Frye & Edidin 1970).

Because they are bigger, the proteins move more slowly than the phospholipids. Protein-rich regions of the PM, about 1 μm in diameter, separate lipid-rich regions. Phospholipids are free to diffuse within such a region but not from one lipid-rich region to an adjacent one. The lateral diffusion rate of a mobile protein in an intact membrane is 10 -30 times lower than that of the same protein embedded in synthetic liposomes. This suggests that the mobility of integral proteins in intact membranes is restricted by interactions with the rigid submembrane cytoskeleton. (Lodish et al. 2000a).

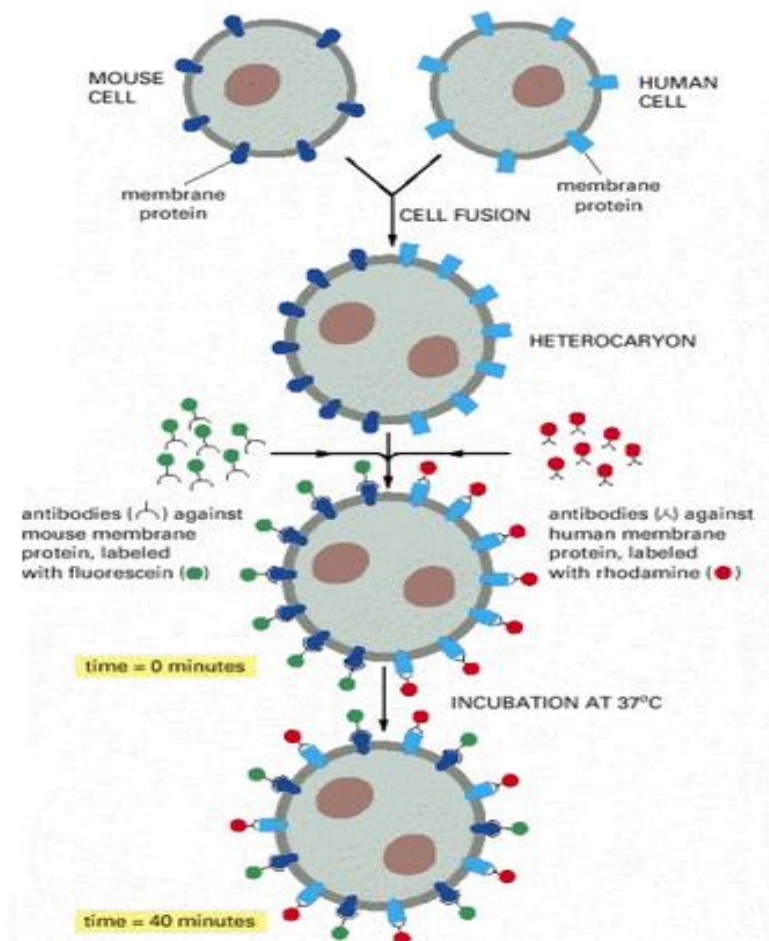


Figure 12 : An experiment demonstrating the mixing of PM proteins on mouse-human hybrid cells (Alberts et al. 2002b).

1.1.4 The plasma membrane functions

1.1.4.1 Lipids functions

1.1.4.1.1 *Compartmentalization*

The PM constitutes a scaffold that encloses the contents of the cell and allows specialized activities to proceed without external interference. At the same time, membranes provide the means of communication between the extracellular and intracellular compartments. This compartmentalization is the basic role of the PM that enables segregation of specific chemical reactions.

Due to its fluid structure, the PM is able to conserve its architecture even when the external conditions, such as temperature and pH, change. In addition to the barrier function, lipids provide membranes with the potential for budding, tubulation, fission and fusion, characteristics that are essential for cell division, biological reproduction and intracellular membrane trafficking via endocytosis and exocytosis (*cf.* 1.3.1). Lipids also allow particular proteins in membranes to aggregate, and others to disperse (van Meer et al. 2008). To do their job, the cells need to be able to change shape and this ability impose changes and plasticity in the PM. For example, some immune cells, such as neutrophils, engulf bacteria and viruses, so they need to change their shape to 'swallow' them by phagocytosis (Nordenfelt & Tapper 2011).

1.1.4.1.2 *A selectively permeable barrier*

The lipids are amphipatic: they have hydrophobic moieties that tend to self-associate, and hydrophilic moieties that tend to interact with aqueous environments and with each other. This property enables the cells to segregate their internal constituents from the external environment. The PM controls what enters and what exits the cell, and allows some substances to cross it more easily than others, phenomenon called the selective permeability.

The selective permeability of biological membranes to small molecules allows the cell to control and maintain its internal composition. Only small uncharged molecules can diffuse freely through phospholipid bilayers (*Figure 13*). Small nonpolar molecules, such as O₂ and CO₂, are soluble in the lipid bilayer and therefore can readily cross the PM. Small uncharged polar molecules, such as H₂O, also can diffuse through membranes, but larger uncharged polar molecules, such as glucose, cannot (Cooper 2000a). Non polar hydrophobic molecules such as steroid hormones can diffuse through the PM. However, charged molecules, such as ions, are unable to diffuse through a phospholipid bilayer regardless of size; even H⁺ ions cannot cross a lipid bilayer by free diffusion. The ions pass across the membrane via specific transmembrane proteins which act as transporters (discussed in *section 1.1.4.2.1*) that determine, with the lipid bilayer, the selective permeability of the PM.

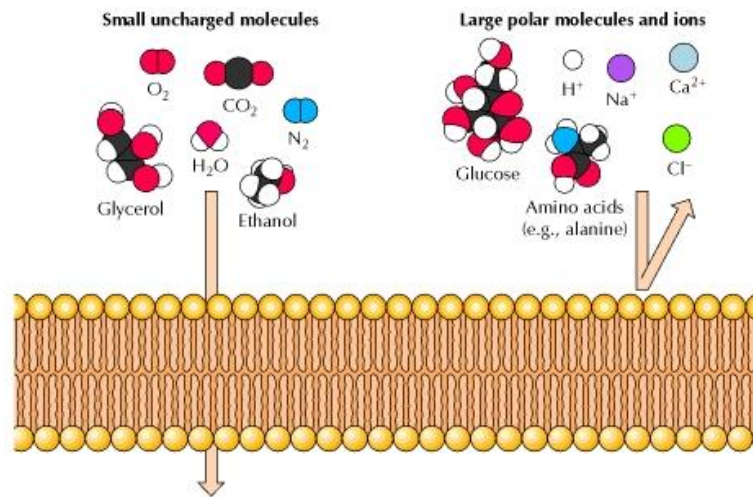


Figure 13 : permeability of phospholipids bilayer (Cooper 2000a).

1.1.4.1.3 Signal Transduction in response to external stimuli

The PM plays a critical role in the response of a cell to external stimuli, and in the propagation of stimuli by signal transduction. Lipids can act as first and second messengers in this signal transduction. For example, the phospholipase C (PLC) is a cytosolic enzyme translocated to the PM when activated by the Gq protein-coupled receptors (GqPCRs). This enzyme catalysis the reaction of PIP₂ (phosphatidylinositol 4,5-biphosphate) hydrolysis into inositol triphosphate (IP₃) and Diacylglycerol (DAG), two important second messengers in the cell leading to calcium (Ca²⁺) release and protein kinase C (PKC) activation (Falkenburger et al. 2013). Additional examples of biologically active lipids are arachidonic and docosahexaenoic acids ω -6, present mostly in PhE, PhC, and PhI, which can be liberated by activated phospholipases A₂ (Serhan et al. 1996). When oxidized, these fatty acids produce the prostaglandins and leukotrienes families of compounds, most of which activate members of the G protein-coupled receptor (GPCR) family, and key effectors in the process of inflammation and many other cellular processes.

1.1.4.2 Proteins functions

1.1.4.2.1 Selective permeability: transport proteins

PM proteins can serve as transporters whose functions include creating and/or maintaining concentration gradients of electrolytes, water, nutrients, metabolic cofactors, and other essential molecules; extruding toxic substances; and recapturing neurotransmitters and many other substances (MÜLLER et al. 2008). The two main types of transport are the passive and the active transport.

a- Passive transport : channel and carrier proteins

The diffusion of a substance across the PM is called passive transport because it does not need an energy depense from the cell. The concentration gradient itself represents potential energy and drives diffusion. Many polar molecules and ions impeded by the lipid bilayer of the membrane diffuse

passively with the help of transport proteins. This phenomenon is called facilitated diffusion. The tendency of an electrolyte to diffuse between two compartments depends on two gradients: a chemical gradient, determined by the concentration difference of the substance between the two compartments, and the electric potential gradient, determined by the difference in charge. Together these differences are combined to form an electrochemical gradient (Karp 2010). At the electrochemical equilibrium the chemical and electrical gradients are equal in magnitude.

An exemple of a nonelectrolyte is the water molecules that are small enough to cross through the phospholipid bilayer, however the rate of water movement by this route is relatively slow because of its polarity. The passage of water occurs via channel proteins known as aquaporins. Each aquaporin allows entry of up to 3 billion water molecules per second (Campbell & Reece 2007). The aquaporins are considered channel proteins that function by having a hydrophilic channel that certain molecules or atomic ions use as a tunnel through the PM (*Figure 14*). The channel proteins are one of two general classes of membrane transport proteins and they group aquaporins and ions channels. Many ions channels function as gated channels, which open or close in response to a chemical or electrical stimulus and allow the passage of inorganic ions such as sodium (Na^+), potassium (K^+), calcium (Ca^{2+}), and chlore (Cl^-) across the PM (Cooper 2000b). For example, stimulation of a nerve cell by certain neurotransmitter molecules open gated channels that allow sodium ions to enter the cell (chemical stimulation). Later on, an electrical stimulus activates the ion channel protein that rush out potassium ions from the cell (Friedman 2008).

The other classe of transport proteins are the carrier proteins. These proteins do not form open channels but act like enzymes to facilitate the passage of specific molecules across the PM. These proteins are specific for the substance they translocate and their shape changes are triggered by the binding and release of the transported molecule. For example, the glucose enters the red blood cells rapidly via specific carrier protein: the glucose transporter, so selective that it even rejects fructose, a structural isomer of glucose.

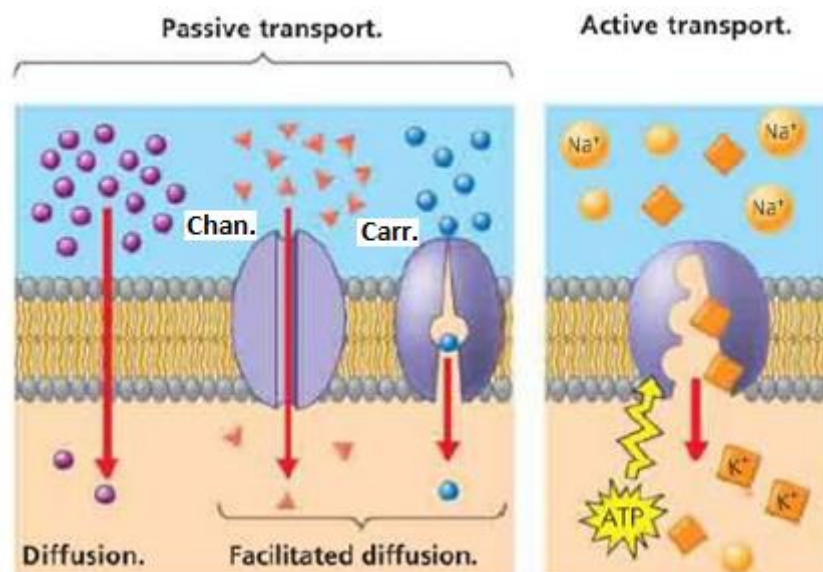


Figure 14 : passive and active transport. Chan : channel protein, Carr : carrier protein. (Campbell n.d. et al., 2008).

b- Active transport: carrier proteins

Some transport proteins can move solutes against their concentration gradients. This process is called active transport and it is coupled to ATP (adenosine triphosphate) hydrolysis as a source of energy. All the proteins implicated in this transport are carrier proteins rather than channel proteins. Active transport enables a cell to maintain internal concentrations of small solutes that differ from concentrations in its environment. For example, compared with its surroundings, an animal cell has a much higher concentration of K^+ ions and a much lower concentration of Na^+ ions (Campbell & Reece 2007). The PM helps maintaining these steep gradients by pumping sodium out of the cell and potassium into the cell. One way ATP can power active transport is by transferring its terminal phosphate group directly to the pump protein. This can induce the protein to change its shape in a manner that translocates a solute bound to the protein across the membrane. One of the very important transport system that works this way is the sodium-potassium pump, which exchange 3 Na^+ for 2 K^+ across the PM (Morth et al. 2011). This pump plays an important role in the establishment of a membrane potential (discussed in 1.1.5).

1.1.4.2.2 Signal transduction: receptor proteins

Membrane proteins can function as receptors for extracellular ligands (signaling molecules) A membrane receptor may have a binding site with a specific shape that fits the shape of a chemical messenger, such as a hormone. The external messenger causes a shape change in the protein that relays the message to the inside of the cell. The three largest protein families in this category are: G protein-coupled receptors (GPCR), receptor tyrosine kinases (RTK) and ion channel receptors.

a- G protein-coupled receptors

A GPCR is a PM receptor that has seven α helix spanning the membrane, containing a signaling molecule binding site and a segment that interacts with G-proteins. Many ligands (sensory stimuli, neurotransmitters, chemokines and hormones) use GPCRs. The binding of the ligand to the GPCR activates a specific G protein located on the cytoplasm side. A G protein is made up of three subunit: α , β and γ (Dupré et al. 2012) (*Figure 15*). There are four main families of G proteins: G_s , G_q , $G_{i/o}$ and $G_{12/13}$ (Ellis 2004) that are expressed by different genes and differ in the α subunit composition, the effector, the cellular effects, and the receptor that are coupled with.

In its inactive form, the G protein is bound to a guanosine di-phosphate (GDP) by its α subunit. When a signaling molecule binds to the extracellular side of the GPCR, this latter is activated; its structure changes and its cytoplasmic side binds to an inactive G protein, causing a guanosine triphosphate (GTP) to displace the GDP. This activates the G protein and leads to the dissociation of GTP-bound α subunit from $\beta\gamma$ subunit and their dissociation from the receptor. The GTP-bound α subunit diffuses along the membrane and binds to a membrane bound enzyme called the effector, and activates it. Among effectors, there is the adenylyl cyclase (it generates the cyclic adenosine monophosphate (cAMP) that activate the protein kinase A (PKA)), PLC (generates IP_3 and DAG), many ions channels and voltage operated calcium channels (VOCC) (*Figure 15*). The free $G_{\beta\gamma}$ complex act also as a signaling molecule, and activates other second messengers like phosphatidyl inositol 3 kinase, and ion channels like L-type calcium channels (cf. 2.2.1.1), and G protein-regulated inwardly rectifying

potassium channels (GIRK) (Mark & Herlitze 2000). G protein functions as a GTPase enzyme, then hydrolyses GTP to GDP, leaves the effector and returns to its original state.

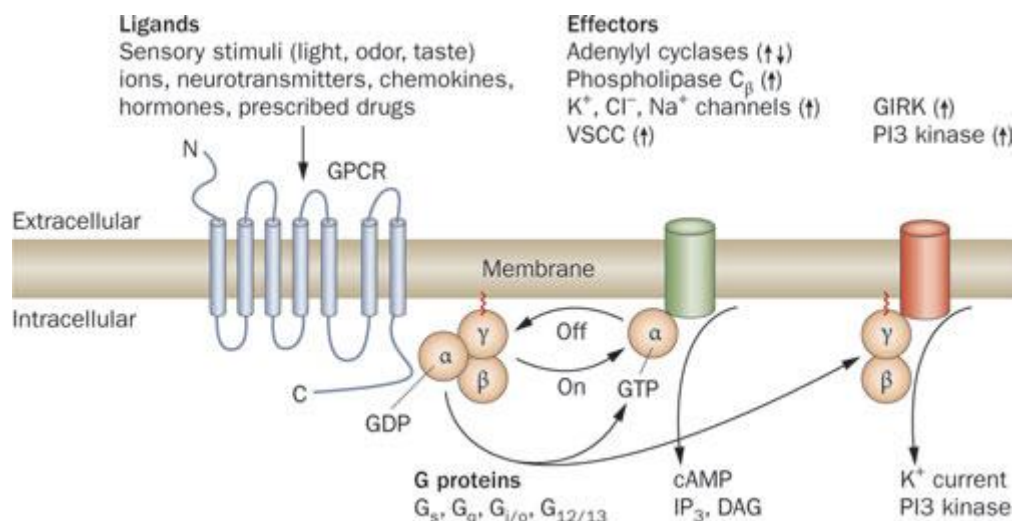


Figure 15 : binding of ligand to GPCR causes conformational change in the G coupled protein and leads to activate (or inhibit) many effectors. For example α_s and α_i will stimulate and inhibit adenylyl cyclase, respectively; α_q will activate PLC (all the terms of the figure are explained in the text) (Vassart & Costagliola 2011).

b- Receptor tyrosine kinases

The RTKs are metabotropic receptors (like GPCRs) but they differ from the GPCRs by their enzymatic (kinase) activity and the ability of a single ligand-binding event to trigger many pathways. Different RTKs recruit different collections of intracellular signaling proteins, producing different effects; however, certain components seem to be used by most RTKs. These include, for example, the PLC_γ (that functions in the same way as the PLC_β activated by GPCRs) and Ras (a small GTP-binding protein, bound by a lipid tail to the cytoplasmic face of the PM). All RTKs activate Ras; some examples are the platelet-derived growth factor (PDGF) receptors which mediate cell proliferation in wound healing (Andrae et al. 2008), and nerve growth factor (NGF) receptors which prevent certain neurons from dying in the developing nervous system (Marshall 1995).

c- Ion channel receptors

Ion channel receptors (ICR) or ionotropic receptors are transmembrane molecules that can open or close a hydrophilic channel that would allow smaller particles to get in and out of the cell. They act as a gate when the receptor shape changes. When a signaling molecule binds to an extracellular specific site of the receptor, the gate opens or closes, allowing or blocking the flow of specific ions, such as Na⁺, Ca²⁺, K⁺ or Cl⁻. When the ligand dissociates from the receptor, the gate closes and ions no longer move. The two major categories of gated channels are:

- ✓ **Voltage-gated channels (VGC):** whose conformational state depends on the difference in ionic charge on the two sides of the PM. They open transiently in response to a change in the membrane potential (*cf.* 1.1.5). The Ca²⁺ VGC in the axon terminal of a presynaptic neuron

(PrSN) allow Ca^{2+} entry and fusion of neurotransmitters (NT) vesicles with PrSN membrane and release of NT in the synaptic space.

- ✓ **Ligand-gated channels (LGC):** whose conformational state depends on the binding of a ligand which is usually not the solute that passes through the channel (Karp 2010). Like the VGC, they are very important in the nervous system. Many NT receptors are LGC.

Ionotropic receptors (ICR) act quickly. As soon as a ligand binds to them, they change shape and allow ions to flow in. They remain open for few milliseconds (Marieb & Hoehn 2006). On the other hand, metabotropic receptors (GPCR and RTK), take a longer time, depending on the number of steps (secondary messengers) required, to produce a response. They remain open from seconds to minutes (Kandel et al. 2000).

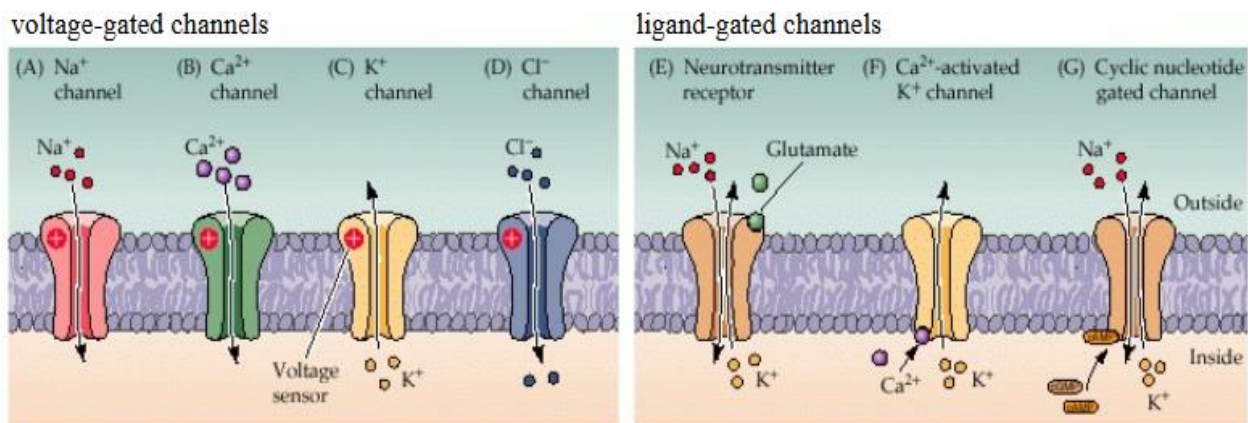


Figure 16 : examples of voltage and ligand-gated channels (Purves et al. 2001).

1.1.4.2.3 Other functions

In addition to transport and signal transduction, PM proteins exhibit a lot of other functions. They serve as structural molecules that maintain the size and the polarity of the cells. (MÜLLER et al. 2008). They bind, noncovalently, to the microfilaments or other elements of the cytoskeleton which help maintaining cell shape (Campbell n.d. et al., 2008). Membrane proteins act as adhesion molecules that allow attachment of adjacent cells to each other. In addition, they play a role in cell-cell recognition as they serve as identification tags recognized specifically by the PM proteins of other cells. They allow cells to communicate and to detect changes in their environment. And finally, the PM proteins could exhibit enzymatic activity, and carry out sequential steps of metabolic pathways.

1.1.5 Resting membrane potential

The free-energy change when an uncharged solute (a nonelectrolyte) diffuses across a membrane depends on the magnitude of the concentration gradient and it is given by

$$\Delta G = RT \ln \frac{[Ci]}{[Co]}$$

Where ΔG is the free-energy change, R is the gas constant, T is the absolute temperature, and $[Ci]/[Co]$ is the ratio of the concentration of the solute on the inside (i) and outside (o) surfaces of the membrane.

The free-energy change for the diffusion of an electrolyte into the cell is

$$\Delta G = RT \ln \frac{[Ci]}{[Co]} + zF\Delta Em$$

where $RT \ln \frac{[Ci]}{[Co]}$ is the chemical gradient ($\Delta G_{\text{Chemical}}$) and $zF\Delta Em$ is the electrical gradient ($\Delta G_{\text{Electrical}}$). z is the charge of the solute, F is the Faraday constant, and ΔEm is the potential difference (in volts) between the two compartments.

At equilibrium $\Delta G_{\text{Electrical}}$ and $\Delta G_{\text{Chemical}}$ are equal, hence:

$$RT \ln \frac{[Ci]}{[Co]} = zF\Delta Em_{\text{eq.}}$$

$$\text{Solving the } \Delta Em_{\text{eq.}}, \text{ we get: } \Delta Em_{\text{eq.}} = \frac{RT}{zF} \ln \frac{[Ci]}{[Co]}$$

The last equation is known as the Nernst equation. The Nernst equation allows us to calculate the potential that will be established across the membrane based on the valence and concentration gradient of an ion (provided that only this ion channels are present). This potential is also referred to as the Nernst potential (NP). The NP for any given ionic species is the membrane potential at which the ionic species is in equilibrium (Vidal-Iglesias et al. 2012). Therefore, the NP for an ion is referred to as the equilibrium potential for that ion.

The practical case of plasma membrane include several ions on either side, not only one. The Goldman-Hodgkin-Katz equation is used to calculate the equilibrium potential (EP) in the case of many ions surrounding the membrane (Engelking 2002). The EP of a membrane surrounded by a solution containing sodium (Na^+), potassium (K^+), and chlore (Cl^-) is:

$$\Delta Em_{\text{eq.}} = \frac{RT}{F} \ln (C_{\text{Na}^+} [\text{Na}^+]_o + C_{\text{K}^+} [\text{K}^+]_o + C_{\text{Cl}^-} [\text{Cl}^-]_i / C_{\text{Na}^+} [\text{Na}^+]_i + C_{\text{K}^+} [\text{K}^+]_i + C_{\text{Cl}^-} [\text{Cl}^-]_o)$$

Where C is the ion conductance (or permeability coefficient). Note that the terms i (for inside) and o (for outside) are reversed for Cl^- compared with K^+ and Na^+ because it has a valence of -1. The equilibrium potential for K^+ ions is -90 mV, -70 mV for Cl^- and +60 mV for Na^+ .

All cells have electrical potential energy across their plasma membranes. The cytoplasm is negative in charge relative to the extracellular medium because of an unequal distribution of anions and cations on opposite sides of the PM. The voltage across a membrane, called a membrane potential (MP), ranges from about -4.5 (Veech et al. 1995) to -200 millivolts (mV) (Campbell n.d. et al., 2008) indicating that the inside of the cell is negative relative to the outside. This is why the MP favors the passive transport of cations into the cell and anions out of the cell. For neurons, typical values of the

resting potential range from -70 to -80 millivolts. Some membrane proteins that actively transport ions against their electrochemical gradient contribute to the membrane potential. An example is the Na^+/K^+ pump seen in section 1.1.4.2.1 b, which pumps three sodium ions out of the cell for every two potassium ions it pumps into the cell. This process makes a net transfer of one positive charge from the cytoplasm to the extracellular medium and stores energy as voltage. Such transport protein that generates voltage across a membrane is called an electrogenic pump. The sodium-potassium pump is the major electrogenic pump of animal cells. The main electrogenic pump of plants, fungi, and bacteria is a proton pump, which actively transports hydrogen ions (protons) out of the cell (Sperelakis 2012).

1.2 THE ORGANELLES MEMBRANES

1.2.1 Eukaryotic cell compartmentalization

The eukaryotic cell organelles are specialized structures that have characteristic shapes, and provide different local environments that facilitate perform specific metabolic functions needed for growth, maintenance, and reproduction of the cell. The [Figure 17](#) summarizes the different organelles of a eukaryotic cell, their relative structures and functions. Not mentioned in this figure are the endosomes, specialized vesicles in sorting of endocytosed material.

On the average, the membrane-enclosed organelles together occupy nearly half the volume of a eucaryotic cell. In terms of its area and mass, the plasma membrane is only a minor fraction of the membranes in most eucaryotic cells. It is possible to separate one type of organelle from another by differential centrifugation. The cytoskeleton plays an important role in the characteristic distributions of the organelles. The localization of the Golgi apparatus close to the nucleus and of the ER throughout the entire cytosol is due to interactions with intact microtubules. If the microtubules are experimentally depolymerized with a drug, the Golgi apparatus fragments and disperse throughout the cell, and the ER network collapses toward the cell centre (Alberts et al. 2002a).

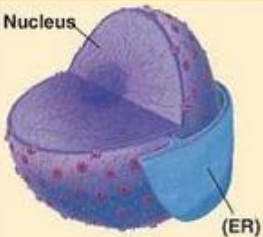

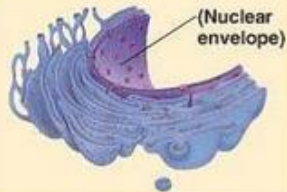






	Cell Component	Structure	Function
The eukaryotic cell's genetic instructions are housed in the nucleus and carried out by the ribosomes	Nucleus 	Surrounded by nuclear envelope (double membrane) perforated by nuclear pores. The nuclear envelope is continuous with the endoplasmic reticulum (ER).	Houses chromosomes, made of chromatin (DNA, the genetic material, and proteins); contains nucleoli, where ribosomal subunits are made. Pores regulate entry and exit of materials.
	Ribosome 	Two subunits made of ribosomal RNA and proteins; can be free in cytosol or bound to ER	Protein synthesis
The endomembrane system regulates protein traffic and performs metabolic functions in the cell	Endoplasmic reticulum 	Extensive network of membrane-bound tubules and sacs; membrane separates lumen from cytosol; continuous with the nuclear envelope.	Smooth ER: synthesis of lipids, metabolism of carbohydrates, Ca^{2+} storage, detoxification of drugs and poisons Rough ER: Aids in synthesis of secretory and other proteins from bound ribosomes; adds carbohydrates to glycoproteins; produces new membrane
	Golgi apparatus 	Stacks of flattened membranous sacs; has polarity (<i>cis</i> and <i>trans</i> faces)	Modification of proteins, carbohydrates on proteins, and phospholipids; synthesis of many polysaccharides; sorting of Golgi products, which are then released in vesicles.
	Lysosome 	Membranous sac of hydrolytic enzymes (in animal cells)	Breakdown of ingested substances, cell macromolecules, and damaged organelles for recycling
	Vacuole 	Large membrane-bounded vesicle in plants	Digestion, storage, waste disposal, water balance, cell growth, and protection
Mitochondria and chloroplasts change energy from one form to another	Mitochondrion 	Bounded by double membrane; inner membrane has infoldings (cristae)	Cellular respiration
	Chloroplast 	Typically two membranes around fluid stroma, which contains membranous thylakoids stacked into grana (in plants)	Photosynthesis
	Peroxisome 	Specialized metabolic compartment bounded by a single membrane	Contains enzymes that transfer hydrogen to water, producing hydrogen peroxide (H_2O_2) as a by-product, which is converted to water by other enzymes in the peroxisome

Figure 17 : the different eukaryotic cell organelles – their structure and function (Campbell n.d. et al., 2008).

1.2.2 Organelles membranes composition

The basic structure and composition of PM and organelles membranes are similar. Each membrane is held together via noncovalent interaction of hydrophobic fatty acid tails. However, each

organelle has a unique composition of membrane lipids and proteins suited to that membrane's specific functions. For example, enzymes embedded in the membranes of mitochondria function in cell respiration. In the endoplasmic reticulum (ER), there is a relative abundance of certain glycerophospholipids on the cytoplasmic face of the membrane with sphingolipids being predominantly located on the luminal surface (MÜLLER et al. 2008). All the other lipids are symmetrically distributed between the two leaflets of the ER membrane (Devaux & Morris 2004).

Most of the enzymes involved in phospholipids synthesis are membrane associated. In mammalian cells, the smooth ER synthesises nearly all the major classes of lipids including cholesterol and ceramid. This is why the phospholipid asymmetry of the PM is generated in the ER (Csala et al. 2006b). The asymmetric distribution of glycolipids in the bilayer results from the addition of sugar groups to the lipid molecules in the lumen of the Golgi apparatus, which is topologically equivalent to the exterior of the cell (Alberts et al. 2014).

Like the outer leaflet of the PM, the luminal surface of internal organelles is enriched in choline-based lipids such as phosphatidylcholine (PC) and sphingomyelin. However, there is less cholesterol in the organelles membranes and the amount differs between organelles. It is higher in the endosomes and golgi apparatus than in the ER and mitochondria (van Meer et al. 2008). The *table 2* shows the approximate lipid composition by weight of different membranes.

The difference in membrane composition is correlated to lipid synthesis and function of each organelle. For example, the ER is the major site of PC synthesis and its membrane can contain until 60% of PC. Another example is that of mitochondria; phospholipids specifically required for mitochondrial function such as cardiolipin and PE are synthesized in mitochondrial membrane (Zinser et al., 1991). Therefore mitochondrial membrane presents a large amount of cardiolipin, specially the inner mitochondrial membrane (IMM). It is important to mention that 75% of IMM as well as chloroplasts membranes are proteins involved in ATP production (Alberts et al. 2002b).

LIPID	PERCENTAGE OF TOTAL LIPID BY WEIGHT					
	LIVER CELL PLASMA MEMBRANE	RED BLOOD CELL PLASMA MEMBRANE	MYELIN	MITOCHONDRION (INNER AND OUTER MEMBRANES)	ENDOPLASMIC RETICULUM	<i>E. COLI</i> BACTERIUM
Cholesterol	17	23	22	3	6	0
Phosphatidylethanolamine	7	18	15	25	17	70
Phosphatidylserine	4	7	9	2	5	trace
Phosphatidylcholine	24	17	10	39	40	0
Sphingomyelin	19	18	8	0	5	0
Glycolipids	7	3	28	trace	trace	0
Others	22	13	8	21	27	30

Table 1 : Approximate Lipid Compositions of Different Cell Membranes (Alberts et al. 2002a).

The Golgi and endosomal membranes display an asymmetric lipid distribution, with SM and GSL on the luminal side, and with PS and PE enriched on the cytosolic side (Devaux & Morris 2004).

There is an exchange of phospholipids between the different organelles. Newly synthesized phospholipids can move between membranes by routes that are independent of the vesicular traffic that carries membrane proteins. This routes include zones of apposition and contact between donor

membranes, source of specific phospholipids, and acceptor membranes unable to synthesize the necessary lipids (Voelker 2005). For example, the PS synthesized in the ER is exchanged with mitochondria via mitochondria-associated ER membrane (Gaigg et al. 1995). In mitochondria, the PS is transformed to PE via PS decarboxylase. The Golgi uses also this enzyme to synthesize the PE (Voelker 2005), and it is also specialized in sphingolipids and GSL synthesis (Futerman & Riezman 2005).

1.2.3 The endoplasmic reticulum

1.2.3.1 The largest membranes network of the cell

The ER is the most extensive membrane system in a eucaryotic cell (*Figure 18*) and accounts more than half the total membrane in many eukaryotic cells (Campbell n.d. et al., 2008). In a typical mammalian cell, the area of the ER membrane is 20–30 times greater than that of the PM (Alberts et al. 2009).

The ER is a network of flattened sacs and branching tubules that extend throughout the cytoplasm. There are two distinct, though connected, regions of the ER that differ in structure and function: the smooth ER (SER) and the rough ER (RER) also called *ergastoplasm*. Rough ER has ribosomes on the outer surface of the membrane and thus appears rough through the electron microscope. Smooth ER lacks ribosomes on its outer surface. The RER lies immediately adjacent to the nucleus, and its membrane is continuous with the outer membrane of the nuclear envelope. The SER consists of tubules network extended throughout the entire cytosol and found, in some regions of the cell, in near proximity of the PM (Hay 2012). An interesting aspect of tubule formation is that the high membrane curvature of a tubule occurs along only two dimensions (Shibata et al. 2006).

The sacs and tubules are all interconnected by a single continuous membrane so that the organelle has only one large, highly convoluted and complexly arranged lumen (internal space). Many FRAP and FLIP (fluorescence loss in photobleaching) experiments have provided evidence that the membranes and luminal spaces of the ER are continuous throughout the cell, and that RER and SER form an interconnected membrane system (Subramanian & Meyer 1997, Dayel et al. 1999, Nehls et al. 2000). The lumen of the ER (cisternal space) often takes up more than 10 percent of the total volume of a cell (Csala et al. 2006a). In plant cells, the ER forms one continuum throughout the plant, via plasmodesma (Denecke 2001).

Cells specialising in the production of proteins will tend to have a larger amount of RER whilst cells producing lipids and steroid hormones will have a greater amount of SER. Larger and more homogeneous forms of the smooth ER are found in the adrenal and testes cells that secrete large amounts of steroids, in muscle cells where the sarcoplasmic reticulum that modulates Ca^{2+} levels control muscle contraction, and in liver cells that make large amounts of enzymes for detoxification (Shibata et al. 2006). It was shown that expression of a single ER protein at high levels can induce the formation of an ordered ER domain in which this protein becomes highly enriched. For example, the expression of IP_3 receptor (IP_3R) at very high levels causes the formation of ER cisternal stacks in COS cells (Takei et al. 1994), and overexpression of ryanodine receptor (RyR) results in the formation of closely apposed flat ER cisterna in CHO cells (Takekura et al. 1995).

The ER lumen is a highly viscous environment compared to the cytoplasm; the diffusion of green fluorescent protein (GFP) in the continuous ER lumen was found to be 9 to 18 fold slower than its diffusion in water and 3 to 6 fold slower than GFP diffusion in the cytoplasm (Dayel et al. 1999). The gel-like consistency of the ER lumen is due to the very high concentrations of resident proteins of the ER (chaperones including disulfide isomerase, binding immunoglobulin protein (BiP), calreticulin, calnexin) (Koch 1987). The ER is the starting point of the secretory pathway. It serves as an entry point for proteins destined for other organelles, as well as for the ER itself.

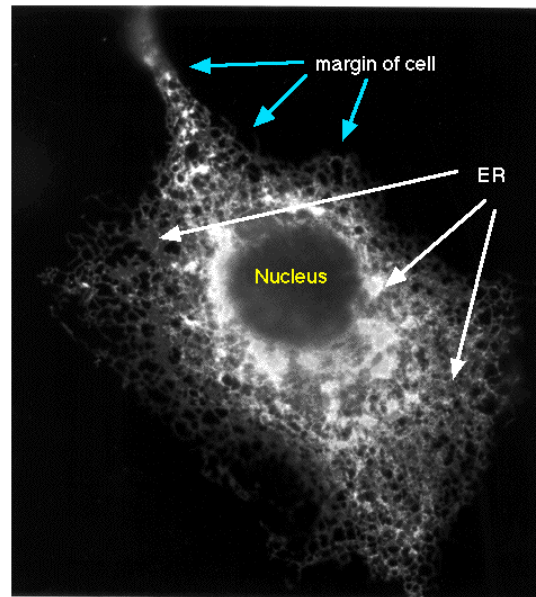


Figure 18 : immunofluorescence micrograph of ER being labeled with a monoclonal antibody against chicken fibroblast ER calcium ATPase (<http://www.bio.davidson.edu/courses/genomics/method/IMF.html>).

1.2.3.2 A highly permeable membrane?

Although the plasma and lysosomal membranes are considered to be highly impermeable, the situation with the ER membrane is not the same. The lipid composition of the ER membranes is different to that of other cell compartments. It has a large abundance of phosphatidylcholine and a very low concentration of cholesterol. It is also very fluid and disordered due to its large proportion of unsaturated fatty acids (Csala et al. 2006b). The lipid composition of the RER and SER membranes is the same, but the RER has also abundant translocon pores (Denecke 2001). The translocon is a complex of several proteins that transports newly formed polypeptides into the lumen of the ER. It forms a translocation channel in the hydrophobic lipid bilayer of the ER. The transiently open translocon may allow non-selective fluxes (Roy & Wonderlin 2003). In addition, there is no difference in pH between the ER lumen and the cytosol, in contrast to the other compartments in the secretory pathway, which are more acidic (Wu et al. 2000).

Despite an extensive exchange of material by membrane trafficking, the ER membrane and PM are remarkably different (*Figure 19*). The ER membrane is thinner than the PM due to the nearly absence of cholesterol and the shorter length of acyl chain, and presents major packing defects due to the high amount of unsaturated acyl chains and small head groups comparing to the PM. The surface

charge is determined by the presence of anionic lipids such as PS and PI; the PM and ER membrane have respectively a negative and a neutral cytoplasmic surface charge adapted for the barrier function of the first and the biogenic function of the second. The length and geometry of transmembrane domains (TMD) of the ER and PM proteins are also different. The transition from a thin and loosely packed membrane (ER) into a thick and rigid one (PM) occurs in the *trans*-Golgi where sterol supply and sphingolipid production are held (Holthuis et al. 2001).

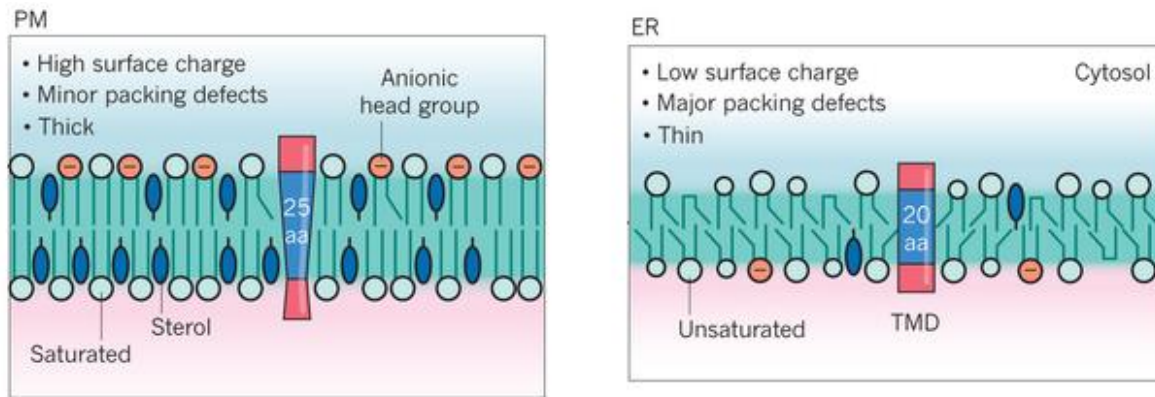


Figure 19: differences between plasma membrane (PM) and endoplasmic reticulum (ER) membrane. TMD: transmembrane domain (Holthuis & Menon 2014).

Low cholesterol and high protein content (enzymes, translocons, receptors) of ER membrane might increase leakiness by making the membrane structure less ordered (Papahadjopoulos et al. 1972). Due to this and to its high fluidity, the ER membrane is permeable to small molecules less than 5 kDa (Le Gall et al. 2004). However, it remains poorly permeable to Ca^{2+} ions which stops them from leaking back into the cytosol, due to powerful sarcoplasmic/endoplasmic reticulum Ca^{2+} ATPase pump (SERCA), and to the Ca^{2+} -binding proteins within the ER lumen (Meldolesi & Pozzan 1998). This shows that high-capacity active processes surpass the velocity of passive transmembrane fluxes of Ca^{2+} .

1.2.3.3 The largest calcium store of the cell

The ER is the largest store of releasable Ca^{2+} in the cell (Ashby & Tepikin 2001). The SER sequesters almost all of the Ca^{2+} from the cytosol (Karp 2010). This is achieved via the SERCA, and the Ca^{2+} -binding proteins within the ER lumen. The concentration of free ER Ca^{2+} ions is much lower than the total (Le Gall et al. 2004). Ca^{2+} ion release and reuptake occurs in response to extracellular signals (Csala et al. 2006b). Some cells have SER further specialized; this is the example of the sarcoplasmic reticulum (SR), found in muscle cells. When a muscle cell is stimulated by a nerve impulse, Ca^{2+} ions are released into the cytosol and trigger contraction of the cell. The terminal cisternae of the SR are juxtaposed to the cell surface T tubules to form the triad in skeletal muscle (Franzini-Armstrong & Jorgensen 1994).

A study of Subramanian and Meyer (Subramanian & Meyer 1997) using GFP-tagged luminal markers, shows that the structural continuity of the ER was preserved during short Ca^{2+} transients or Ca^{2+} store depletion. In contrast, the structural continuity of ER Ca^{2+} stores was disrupted by persistent Ca^{2+} increases (using 1 μM of ionomycin, a Ca^{2+} ionophore) that lasted longer than 10 minutes. A similar disruption in ER structure has been shown to occur transiently during fertilization of mouse

(Mehlmann et al. 1995), starfish oocytes (Jaffe & Terasaki 1994) and sea urchin eggs (Terasaki et al. 1996).

The mean concentration of the Ca^{2+} in the cytosol varies between 100 and 400 nM (Schantz 1985, Ratto et al. 1988), whereas it varies almost between 50 μM and 1 mM in the RE (Hofer & Machen 1993, Chatton et al. 1995). In plants, the vacuoles represent the major Ca^{2+} store within the cell (Canut et al. 1993).

1.2.3.4 The KDEL sequence

The synthesis of the proteins in the cell begins on the ribosomes in the cytosol. The exceptions are the few mitochondrial and chloroplast proteins that are synthesized on ribosomes inside these organelles (Harris et al. 1994, O'Brien 2003). The fate of any protein molecule synthesized in the cytosol depends on its amino acid sequence, which can contain a sorting signal that directs the protein to the organelle in which it is required. Proteins that lack such signals remain as permanent residents in the cytosol. This has been shown by experiments in which the sequence is either deleted or transferred from one protein to another by genetic engineering techniques. Deleting a signal sequence from an ER protein, for example, converts it into a cytosolic protein, while placing an ER signal sequence at the beginning of a cytosolic protein redirects the protein to the ER (Alberts et al. 2009).

Some proteins made in the ER are destined to function there. They are retained in the ER (and are returned to the ER when they escape to the Golgi apparatus) by a C-terminal sequence of four amino acids called an ER retention signal or KDEL sequence in mammals and HDEL sequence in yeasts (Munro & Pelham 1987); K for lysine, D for aspartic acid, E for glutamic acid, L for Leucine and H for histidine. This retention signal is recognized by a membrane-bound receptor protein in the ER and Golgi apparatus.

ER luminal proteins, especially those present at high levels can be passively incorporated into COPII vesicles and transported to the Golgi ([Figure 20](#)). Many such proteins bear a C-terminal KDEL (Lys-Asp-Glu-Leu) sequence that allows them to be retrieved. The KDEL receptor, located mainly in the *cis*-Golgi network and in both COPII and COPI vesicles, binds proteins bearing the KDEL sorting signal and returns them to the ER. This retrieval system prevents depletion of ER luminal proteins such as those needed for proper folding of newly made secretory proteins. The binding affinity of the KDEL receptor is very sensitive to pH (Lodish et al. 2007). The small difference in the pH of the ER and Golgi favors binding of KDEL-bearing proteins to the receptor in Golgi-derived vesicles and their release in the ER.

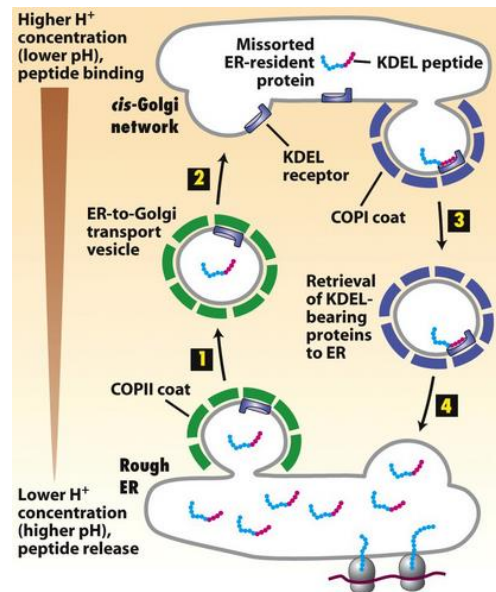


Figure 20 : Role of the KDEL receptor in retrieval of ER-resident luminal proteins from the Golgi. KDEL sequence is colored in red (Lodish et al. 2007).

1.3 THE CONTINUITY OF THE CELLULAR MEMBRANES

Many of the different membranes of the eukaryotic cell are part of the endomembrane system. The membranes of this system are related either through direct physical continuity or by the transfer of membrane segments as small vesicles. The luminal continuity between PM and ER for example are essential features of membrane flow and normal cell function (Hay 2012). There is also a continuity between RER and SER membranes and nuclear envelop. The Golgi apparatus is closely associated with the ER and recent observations suggest that parts of the two organelles are so close, that some chemical products probably pass directly between them without vesicles.

The smooth ER is where vesicle budding and fusion take place, as well as zones of contact with other organelles membranes, possibly for the purpose of delivering lipids to them (Shibata et al. 2006). For example, couplings between ER and the PM can be observed as seen before in skeletal muscle but also in nonmuscle cells with a highly differentiated ER network such as squid giant axon (Metuzals et al. 1997) or cerebellar Purkinje cells (Takei et al. 1994). Moreover, ER membranes may form contacts with the OMM, for the transport of certain lipids into the mitochondrion (Perkins et al. 1997).

1.3.1 Vesicular transport

The interior of the ER, Golgi apparatus, endosomes and lysosomes, communicate extensively with one another and with the outside of the cell by means of small vesicles. This phenomenon permits the membrane transport between cellular organelles in the secretory and endocytic pathway. Secretory and endocytic organelles are connected by bidirectional vesicular transport as shown in [Figure 21](#). Vesicles bud from one membrane and fuse with another, carrying membrane components and soluble proteins between cell compartments.

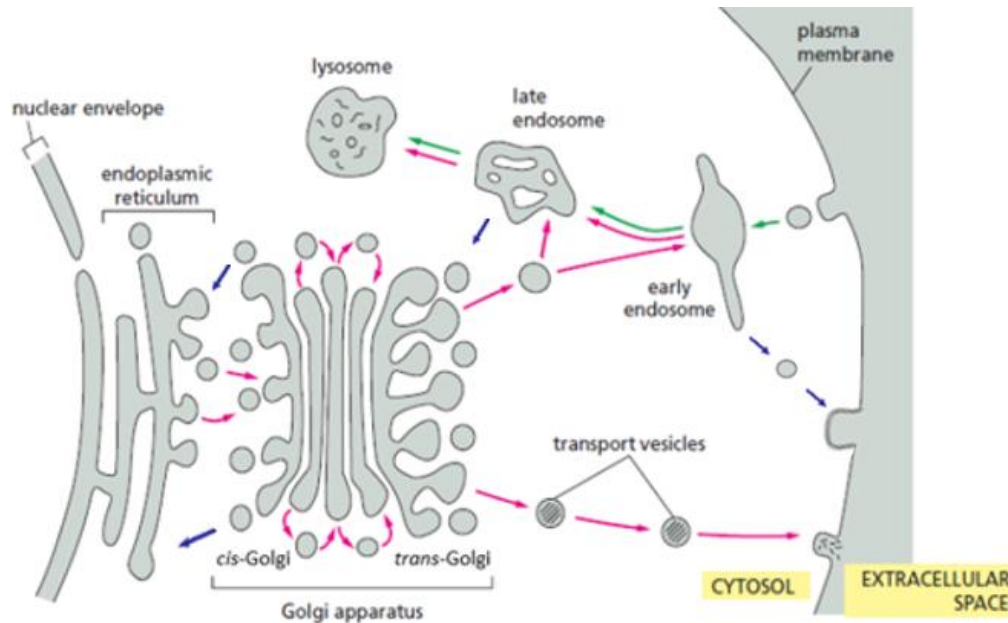


Figure 21 : vesicular trafficking between the endomembrane system and the plasma membrane. In Pink: secretory pathways, in green: endocytic pathways and in blue: retrieval pathways (Alberts et al. 2009).

Each transport vesicle have a distinctive protein coat and are therefore called coated vesicles. Some examples of coated vesicles are:

- **Clathrin-coated vesicles (CCV)** are involved in material transport from the *trans*-Golgi or the PM to the endosomes.
- **COPI vesicles** are involved in transporting molecules from the *cis*-Golgi to the ER (Figure 20).
- **COPII vesicles** are involved in transporting molecules from ER to the *cis*-Golgi (Figure 20) and from one part of the Golgi apparatus to another.

After budding from a cellular compartment, the vesicle sheds its coat to be able to interact with the target membrane. The vesicle is transported by motor proteins that move along cytoskeletal fibers such as kinesin and dynein. The kinesin move toward the exterior whereas dynein move toward the interior of the cell by using ATP (Garrett & Grisham 2000 p. 537).

2 CALCIUM REGULATION IN THE CELL

2.1 THE IMPORTANCE OF THE CALCIUM IN THE ORGANISMS AND THE CELL PHYSIOLOGY

Calcium (Ca^{2+}) is essential for all living organisms. It forms part of cell walls and is an essential constituent of leaves, and a major material used in mineralization of bones, teeth, and exoskeleton. In many animals, it is the most abundant ion by mass. Hence, it is an important component of healthy diet.

Ca^{2+} is a primordial element and a key regulator of many physiological processes occurring in many organisms. It is important for blood clotting, muscle contraction, egg fertilization, cell proliferation, learning, memory and neuronal transmission. On the cellular scale, it constitutes one of the most important second messengers in the cell. It regulates many important cellular processes such as metabolism, ATP synthesis, apoptosis, vesicle trafficking, exo and endocytosis, cellular motility, membrane excitability, cellular growth, proliferation and differentiation, control of gene expression and many other functions.

2.2 CALCIUM-SIGNALING SYSTEM

Because of its extremely importance, the cells have developed a sophisticated machinery responsible for Ca^{2+} regulation and to maintain the intracellular cytoplasmic calcium concentration stable, taking into account that any uncontrolled excess of this concentration could be highly toxic for the cell, resulting in cell death. Each cell has its unique set of Ca^{2+} signaling system components, in a way to create calcium transients with specific spatial and temporal properties. *Figure 22* shows the principles channels and receptors implicated in the generation of Ca^{2+} pulses in the cell, and the different physiological effects of calcium transients.

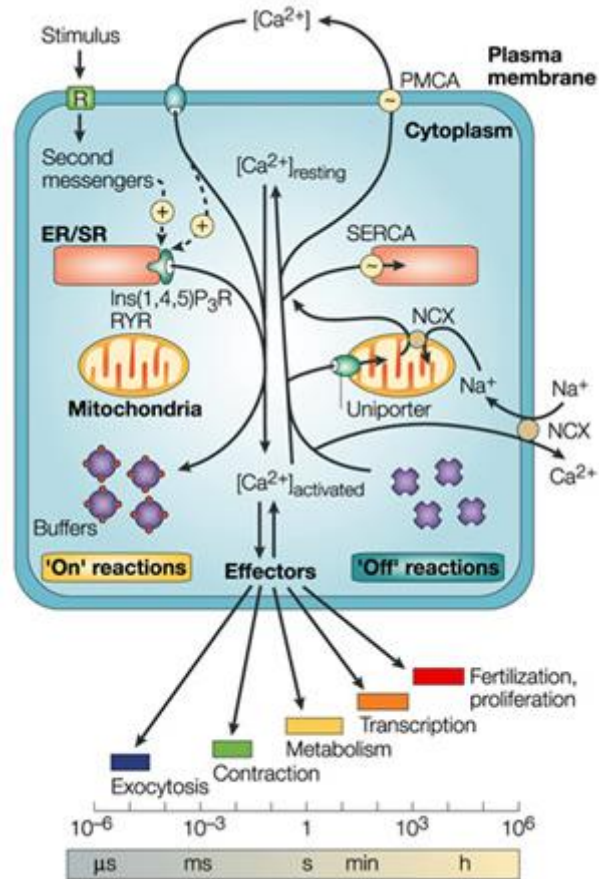


Figure 22 : Examples of some components of the “on” and “off” reactions governing the calcium signaling systems. Red circles = Ca²⁺, IP3R: inositol-1,4,5-triphosphate receptor, NCX: Na⁺/Ca²⁺ exchanger, PMCA: plasma membrane Ca²⁺-ATPase, RyR: ryanodine receptor, SERCA: Sarco/endoplasmic reticulum Ca²⁺-ATPase, Red circles: calcium. The buffers are the proteins that attach to cytosolic Ca²⁺, leaving a very small percentage of free Ca²⁺ (Berridge et al. 2003).

2.2.1 Principal components of the calcium increase step

The first step of a Ca²⁺ transient is an increase of cytosolic the Ca²⁺ concentration. The Ca²⁺ may enter from the extracellular medium in response to a variety of stimuli or may be released from the internal stores, mostly the endoplasmic (ER) or sarcoplasmic (SR) reticulum. The entry of Ca²⁺ from the external medium could be enhanced by extracellular agonists, membrane depolarization, mechanical stretch or depletion in the internal Ca²⁺ stores. Many channels types are implicated in the external Ca²⁺ entry like the voltage-operated Ca²⁺ channels (VOCC), the receptor-operated Ca²⁺ channels (ROCC), the store-operated Ca²⁺ channels (SOCC) and the second-messenger-operated Ca²⁺ channels (SMOCC). The calcium release from the ER/SR is mainly due to the inositol-1,4,5-triphosphate receptor (IP₃R) and the ryanodine receptor (RyR). Stimuli that induce the entry of extracellular Ca²⁺ lead to the formation of second messengers that release internal Ca²⁺ from the ER/SR. One of the most important second messengers is the IP₃. Finally, Ca²⁺ can also be released by two-pore [calcium] channels (TPC) located on lysosomes and endosomes.

2.2.1.1 Voltage-operated calcium channels

VOCC are activated by membrane depolarization and lead to calcium entry from the outside due to the change in membrane potential. These channels are mainly present in the excitable cells, but can also be present, at low levels, in other cells not considered excitable such as the immune system cells (Cahalan et al. 2001). The rapid Ca^{2+} fluxes across the VOCCs initiate diverse physiological fast cellular processes; in endocrine cells for example, it mediates hormones secretion (Yang & Berggren 2006). In cardiac, skeletal and smooth muscle cells, it mediates contraction, either directly through the cytosolic increase of Ca^{2+} concentration or indirectly by calcium-induced calcium release (see *section 2.2.1.7*) (Bers 2002). In neurons, it mediates synaptic transmission (Catterall & Few 2008). The Ca^{2+} entering the cytosol via the VOCC regulates also slow cellular processes such as many biochemical processes, enzymatic functions, and gene expression (Flavell & Greenberg 2008).

The VOCC are heteromultimers composed of 4 subunits: α_1 , α_2 - δ , β , and γ (Hille 2001). The main subunit is the α_1 . According to their pharmacological and biophysical properties, the VOCC can be divided into five types: L type (long-lasting), P/Q (Purkinje), N (Neural/Non-L), R (residual), T (transient). All of them are medium to high-voltage-activated except the T type which is low-voltage activated (Snutch et al. 2013). Table 3 gives the α_1 subunits that can form each channel type, their principles physiological functions and blockers, and inherited diseases caused by their abnormal functions.

The L-type channels are the most understood pharmacologically. They can be inhibited by the dihydropyridines (nifedipin, nicardipin, nisoldipin), the phenylalkylamines (verapamil) or benzothiazepines (diltiazem). They require strong depolarization to be activated, have large conductance and are slowly inactivated. The N, P, Q and R-type can be selectively blocked by snail or spider toxins. They have medium conductance, and intermediate inactivation kinetics (Hille 2001). The T-type have low-conductance and they are called transient because they are rapidly inactivated (Perez-Reyes & Lory 2006). They can be blocked by mibefradil, which is also a blocker of other VOCC (Viana et al. 1997). The VOCC blockers are used to cure many diseases such as hypertension (Felizola et al. 2014) and traumatic brain injury (Kriegelstein et al. 1996).

Ca ²⁺ current type	α 1 Subunits	Specific blocker	Principal physiological functions	Inherited diseases
L	Ca _v 1.1	DHPs	Excitation-contraction coupling in skeletal muscle, regulation of transcription	Hypokalemic periodic paralysis
	Ca _v 1.2	DHPs	Excitation-contraction coupling in cardiac and smooth muscle, endocrine secretion, neuronal Ca ²⁺ transients in cell bodies and dendrites, regulation of enzyme activity, regulation of transcription	Timothy syndrome: cardiac arrhythmia with developmental abnormalities and autism spectrum disorders
	Ca _v 1.3	DHPs	Endocrine secretion, cardiac pacemaking, neuronal Ca ²⁺ transients in cell bodies and dendrites, auditory transduction	
	Ca _v 1.4	DHPs	Visual transduction	Stationary night blindness
N	Ca _v 2.1	ω -CTx-GVIA	Neurotransmitter release, Dendritic Ca ²⁺ transients	
P/Q	Ca _v 2.2	ω -Agatoxin	Neurotransmitter release, Dendritic Ca ²⁺ transients	Familial hemiplegic migraine, cerebellar ataxia
R	Ca _v 2.3	SNX-482	Neurotransmitter release, Dendritic Ca ²⁺ transients	
T	Ca _v 3.1	None	Pacemaking and repetitive firing	
	Ca _v 3.2		Pacemaking and repetitive firing	Absence seizures
	Ca _v 3.3			

Table 2 : different types of VOCC. DHP, dihydropyridine; ω -CTx-GVIA, ω -conotoxin GVIA from the cone snail *Conus geographus*; SNX-482, a synthetic version of a peptide toxin from the tarantula *Hysterocrates gigas* (Catterall 2011).

2.2.1.2 Receptor-operated calcium channels

The transport of Ca²⁺ through ROCC depends on the binding of a ligand which is usually not the solute that passes through the channel, but causes conformational changes in the channel in a way that allows the passage of the Ca²⁺ (alone or with other cations) to the cell. In the nervous system for example, the N-methyl-D-aspartate receptor (NMDAr) is a non-selective ionotropic channel that allows positively charged ions to cross the PM. When activated by glutamate, aspartate or glycine, it allows the passage of Ca²⁺ and Na⁺ into the cell and the flow of K⁺ outside the cell. The NMDAr is 10 times more permeable to the Ca²⁺ than Na⁺ (Dityatev & El-Husseini 2006). The Ca²⁺ flux through this receptor is crucial for many nervous functions such as learning, memory and synaptic plasticity (Tsien et al. 1996).

The P₂X purinergic receptors are another type of ionotropic ROCC. They open in response to external ATP binding and allow the entry of Ca²⁺ and Na⁺ into the cell and the activation of various Ca²⁺-sensitive intracellular processes. The cations entry cause membrane depolarization and facilitate voltage-sensitive Ca²⁺ entry in excitable cells through the activation of VOCCs (Koshimizu et al. 2000). The P₂X can be found in many tissues and they have a lot of physiological roles. They modulate synaptic transmission and neural-glia interactions in the nervous system. They participate in the contraction initiation of the heart, skeletal and smooth muscle including that of the urinary bladder and the vas deferens (Burnstock 2006).

2.2.1.3 Inositol-1,4,5-triphosphate receptor

The IP3R is a ER glycoprotein complex activated by the second messenger IP3 and acting as a Ca^{2+} channel that releases the Ca^{2+} from the ER, the Golgi and the endolysosomal vesicles (Kew & Davies 2010), and from the mitochondria (Decuyper et al. 2011). In Golgi, the IP3Rs are 2-3 fold less than in the ER (Pinton et al. 1998), which explains the reduced amount of Ca^{2+} release from it.

A very wide range of external stimuli, such as hormones and neurotransmitters, activating GPCRs (G-protein coupled receptors) or RTKs (receptors tyrosine kinase), lead to the activation of phospholipase C (PLC β and γ respectively) and the formation of IP3. Other forms of PLC are activated by an increase in cytosolic Ca^{2+} concentration (PLC δ) or through Ras signaling (PLC ϵ) (Berridge et al. 2003). The IP3R plays a very important role in the transduction of the external stimuli to specific intracellular Ca^{2+} signals. These signals are characterized by complex patterns of spatial and temporal properties that are expressed by Ca^{2+} waves and oscillations specific for each cell type. The dynamics of IP3 production depends on the receptor type being activated, the G protein it is coupled to and the type of PLC activated further (Wal et al. 2001). For example, histamine, thrombin and lysophosphatidic acid receptors give small, slow and long Ca^{2+} transients, whereas Neurokinin A and bradykinin receptors give large and rapid Ca^{2+} transients.

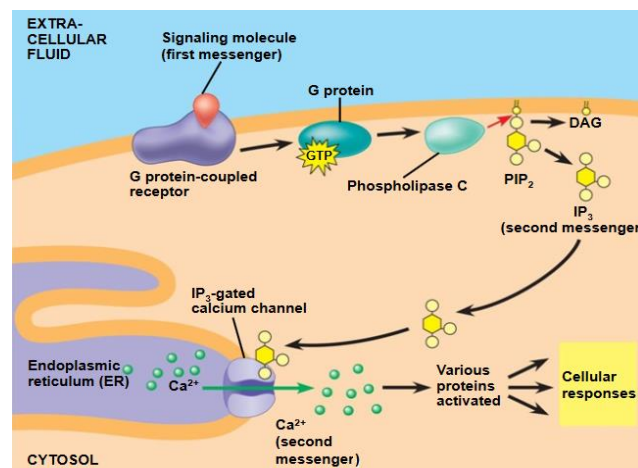


Figure 23 : an example of steps leading to Ca^{2+} release from IP3R (the first step is the attachment of a ligand to a GPCR) (Campbell & Reece 2007).

In nonexcitable cells, Ca^{2+} signaling is typically initiated by receptor-triggered production of IP3 and the subsequent Ca^{2+} release from the ER (Liou et al. 2005). During mammalian egg fertilization for example, the IP3 is responsible for triggering the Ca^{2+} oscillations necessary to activate the egg after activation of PLC ζ (zeta) (Saunders et al. 2002). The IP3R is blocked by the Aminoethoxydiphenyl borate (2-APB) (Xiao et al. 2010).

2.2.1.4 Ryanodine receptor

The RyRs are Ca^{2+} release channels found on the ER/SR. They are named after the plant alkaloid ryanodine, to which they show a high affinity. They are found in different tissues but their highest density is in striatic (cardiac and skeletal) muscles (Fill & Copello 2002). In mammals, there are 3 RyR isoforms (RyR 1, 2 and 3). The RyRs are activated by calcium (Ca^{2+} -induced Ca^{2+} release) and by the second messenger Cyclic ADP-ribose (cADPR) which also contributes to Ca^{2+} -induced Ca^{2+} release (CICR). The cADPR functions either directly by binding to the RYR or indirectly through accessory proteins such as the FK506-binding protein 12.6 (FKBP12.6) (Figure 24), a subunit associated to the RyR (Noguchi et al. 1997). The calmodulin (CaM) is another accessory protein needed in cADPR-induced Ca^{2+} release, either directly (Lee et al. 1994) via a calmodulin binding domain (Rodney et al. 2005), or indirectly through phosphorylation of RyR via the CaM kinase II (Takasawa et al. 1995). cADPR constitutes a physiological agonist of RyR. Other agonists such as caffeine and pentifylline activate the RyR by potentiating sensitivity to Ca^{2+} . cADPR sensitizes the receptor to Ca^{2+} in a manner similar to caffeine but with much higher potency (Lee 1993). The RyR can be blocked by dantrolene (Zhao et al. 2001) or ryanodine (Ostrovskaya et al. 2007).

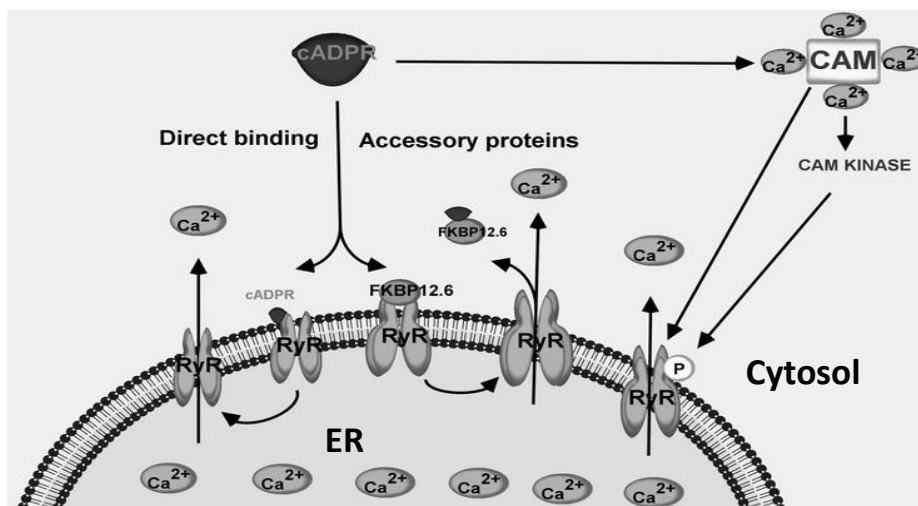


Figure 24 : RyR activation via cADPR (Deshpande et al. 2005).

2.2.1.5 Two-pore calcium channels

They are called TPCs because of their unusual structure combining 2 pores in tandem. These channels are mainly present in the endolysosomal system which constitutes an acidic Ca^{2+} store playing an important role in Ca^{2+} regulation in parallel to the ER stores. Three subtypes of TPCs have been characterized in the endolysosomal system : TPC1 and TPC3 present on endosomes, and TPC2 present on lysosomes (Zhu et al. 2010). All the TPCs are nicotinic acid adenine dinucleotide phosphate (NAADP)-gated, because they are activated by the NAADP. The release of Ca^{2+} from TPCs cause a further release of Ca^{2+} from the IP3R and the RyR by CICR (*cf.* 2.2.1.7).

2.2.1.6 Store-operated calcium channels

The major Ca^{2+} entry pathway from the outside, in electrically nonexcitable cells, is the store-operated calcium entry (SOCE), in which the emptying of the intracellular Ca^{2+} stores leads to Ca^{2+} influx across the SOCC (Parekh & Putney 2005).

Many PM receptors are coupled to a G protein (GPCR) including some ROCC. The receptor can be coupled to a Gq protein (that activates PLC) or a Gs protein (that activates adenylyl cyclase) as shown in [Figure 25](#). Also the receptors tyrosine kinase activates PLC. The PLC generates the IP_3 that cause the release of Ca^{2+} from the ER via the IP_3R . When the ER stores are filled of calcium, this latter inhibits the action of a calcium sensor called Stromal interaction molecule 1 (STIM1), a single transmembrane ER protein (Liou et al. 2005) that can be found also with a lesser percentage (10%) on the PM (Saitoh et al. 2011). The release of Ca^{2+} from the ER results in its dissociation from STIM1, which in turn activates the SOCCs of the PM. STIM1 can also activate the adenylyl cyclase (Lefkimmatis et al. 2009). Another form of STIM protein is the STIM2, that is a weaker activator of Orai channels (see below) than STIM1 (Bird et al. 2009) but a more sensitive sensor of ER luminal Ca^{2+} (Brandman et al. 2007).

The Orai proteins (3 members: Orai 1, 2 and 3) form the pore of the SOCC, and contain the site of interaction with STIM1. Ca^{2+} signaling through the SOCC plays an important role in the activation and proliferation of the T lymphocytes after an antigen recognition. If a mutation occurred in STIM1 or Orai1 protein, it leads to the absence of Ca^{2+} influx and subsequent severe combined immunodeficiency (SCID) (Qu et al. 2011).

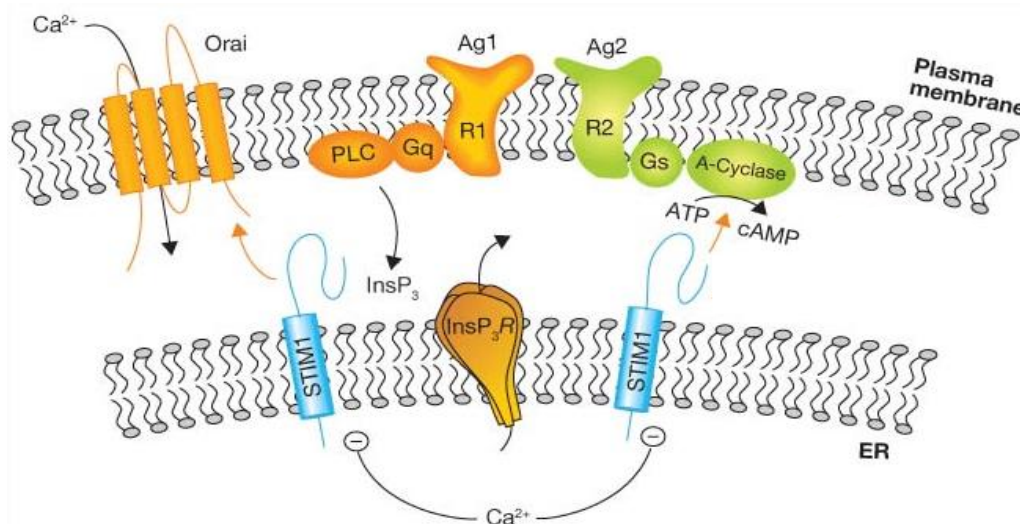


Figure 25 : steps leading to SOCC activation. Ag : agonist, R : receptor, (Putney 2009).

SOCCs play an important role in maintaining Ca^{2+} oscillations (see also 2.2.4 and 3.1.2) (a series of repetitive spikes of Ca^{2+} that occur in many types of cells and constitute a physiological response for many stimuli (Berridge 1990)) by refilling the ER Ca^{2+} following store depletion (Parekh & Putney 2005). The inflowing calcium current that results from the Ca^{2+} flow through the SOCCs is called Ca^{2+} release-activated Ca^{2+} current (ICRAC). The activity of SOCC could be modulated by 2-APB; at low concentrations, the 2-APB activates the SOCC whereas at high concentrations it causes transient increase activity followed by a total inhibition (Prakriya & Lewis 2001). The 2-APB prevents also the

STIM from moving toward PM by clustering it in the cell (Zeng et al. 2012). Other inhibitors can also be used to block the SOCCs such as lanthanum (La^{3+}), gadolinium (Gd^{3+}), cadmium (Cd^{2+}), zinc (Zn^{2+}) (Gore et al. 2004) and diethylstilbesterol (Zakharov et al. 2004).

2.2.1.7 Calcium-induced calcium release (CICR)

One of the key controllers of Ca^{2+} signaling in the cell is the Ca^{2+} itself; a cytosolic increase in Ca^{2+} concentration leads to further Ca^{2+} release from the ER/SR via the IP₃R and RyR, thus establishing a positive feedback. This phenomenon is called Ca^{2+} -induced Ca^{2+} release. The IP₃R and RyR have a Ca^{2+} “sensor” which is a site for cytosolic Ca^{2+} binding: a small amount of Ca^{2+} near the receptor will cause it to release more Ca^{2+} . Two examples of CICR are mentioned in [Figure 26](#). The first one is the CICR from IP₃R and RYR after the activation of TPC of the acidic Ca^{2+} stores (the endolysosomal system) by the NAADP (*see also* 2.2.1.5). The second one is the activation of RyR after a Ca^{2+} entry through VOCCs. This latter is crucial for excitation-contraction coupling in cardiac and skeletal muscle (Capes et al. 2011). Note that the larger spacing between Ca^{2+} release sites, the lower efficacy of CICR (FOSKETT et al. 2007).

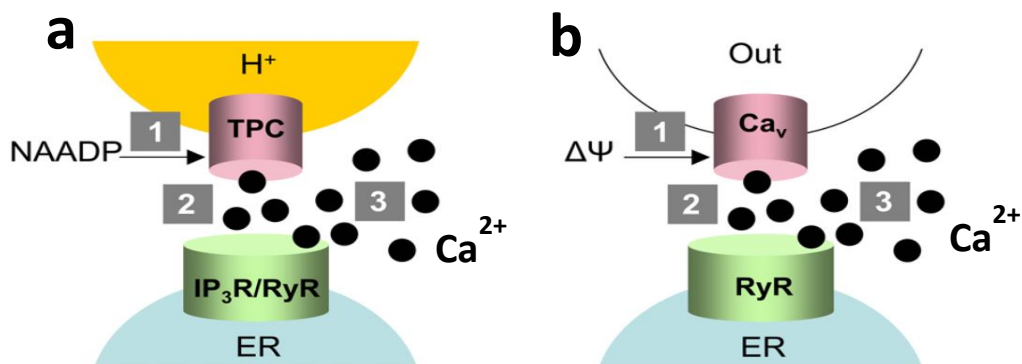


Figure 26 : two examples of CICR. a : after TPC activation by NAADP, b : after Ca^{2+} entry from VOCC (Patel & Docampo 2010).

2.2.2 Principle components of the calcium decrease step

Any uncontrolled excess of the cytosolic calcium concentration could be toxic for the cell. However, there is a very large transmembrane electrochemical gradient of Ca^{2+} between cytosol and the external medium or between cytosol and the ER/SR, that favors the entry of the Ca^{2+} from the exterior, or the release of Ca^{2+} from the inner Ca^{2+} stores, to the cytosol. Therefore, the cell, to keep low concentrations of Ca^{2+} for proper cell signalling, has developed a specific machinery to pump the excess of Ca^{2+} to the external medium or to the ER/SR and mitochondria via specific pumps and exchangers. There is also the Ca^{2+} buffers, proteins that remove the excess Ca^{2+} by binding it to specific sites on them.

2.2.2.1 Plasma membrane Ca^{2+} -ATPase

The PMCA serves to pump the Ca^{2+} from the cytosol to the external medium. As it is an ATPase, it drives the Ca^{2+} against its electrochemical gradient. Its function is vital for keeping a suitable Ca^{2+} concentration in the cell necessary for homeostasis. And because it pumps the Ca^{2+} to the extracellular medium, it participates to the regulation of Ca^{2+} concentration outside the cell. The PMCA is a PM transport protein that belongs to the family of P-type primary ion transport ATPases. These proteins are ions pumps responsible for active transport of cations and capable to auto-phosphorylate a highly conserved aspartate (Asp) residue of their pumps by using the ATP as a source of energy. They have at least 2 different conformations called E1 (in presence of saturating concentrations of Ca^{2+}) and E2 (Ca^{2+} free).

The PMCA is present in all the human tissues in 4 different isoforms (PMCA 1, 2, 3 and 4). It plays important role in regulating synaptic transmission (Jensen et al. 2007). However, the PMCA activity is not always advantageous; in breast cancer, the PMCA2 lowers the cytosolic Ca^{2+} concentration and hence decreases the calcium-induced apoptosis (*c.f* 2.3.1) in malignant cells (VanHouten et al. 2010). As all P-type pumps, PMCA is inhibited by lanthanum La^{3+} and vanadate. Other more specific inhibitors are usually used such as thapsigargin, carboxyeosin and caloxin peptides (Szewczyk et al. 2008).

2.2.2.2 Sarco/endoplasmic reticulum Ca^{2+} -ATPase

Like the PMCA, the SERCA belongs also to the family of P-type primary ion transport ATPases. It has the same structure as the PMCA but it is situated in the ER/SR membrane. It oscillates also between 2 conformational structures E1 and E2. As PMCA, it uses ATP as a source of energy to pump Ca^{2+} from cytosol to the ER lumen (against its concentration gradient) : the mean concentration of Ca^{2+} in the cytosol being between 100 and 400 nM (Schantz 1985, Ratto et al. 1988), whereas it varies between 50 μM and 1 mM in the RE (Hofer & Machen 1993, Chatton et al. 1995).

There are 3 paralogs of SERCA (SERCA 1, 2 and 3) encoded respectively by the genes ATP2A1, 2 and 3 and expressed at various levels in different cell types. SERCA1 is the most studied one with an available detailed 3D structure (Toyoshima et al. 2000). SERCA1 is a fast switch pump expressed essentially in skeletal muscle (Odermatt et al. 1996). The slow-switch SERCA2a is mainly expressed in heart and smooth muscle (SERCA2b is found in muscle and non-muscle cells) (Foundation 2003). SERCA3 is expressed in non-muscle tissues such as blood platelets, lymphocytes, mastocytes, epithelial and endothelial cells (Wuytack et al. 1995). SERCA genes are absent from yeast and some other fungi genomes (Wuytack et al. 2002).

Together with PMCA, SERCA plays a crucial role to restore the relaxation state of muscle cells after contraction, by eliminating the Ca^{2+} excess from the cytosol (MacLennan et al. 1997). Mutations in SERCA1 lead to delayed muscle relaxation and brody disease characterized by stiffness, cramps and impairment of skeletal muscle relaxation (Odermatt et al. 2000). Mutations in SERCA3 results in the impairment of endothelial cells Ca^{2+} signaling and defective endothelium-dependent relaxation of vascular smooth muscle (Liu et al. 1997). SERCA is inhibited by thapsigargin, cyclopiazonic acid (CPA),

tetrabromobisphenol A (TBBPA) or vandamate (Michelangeli & East 2011) and it is activated by istaroxime (Khan et al. 2009), CDN1134 and CDN1163 (Gruber et al. 2014).

2.2.2.3 Plasma membrane $\text{Na}^+/\text{Ca}^{2+}$ exchanger

$\text{Na}^+/\text{Ca}^{2+}$ exchanger (NCX) has a very important role in removing Ca^{2+} from the cytoplasm. It does not have the high affinity of Ca^{2+} ATPases such as PMCA but on the other hand, it does have a high capacity and rapidity to remove Ca^{2+} (until five thousand Ca^{2+} ions per second), while the PMCA has a low transport capacity for Ca^{2+} (Carafoli et al. 2001). Hence, the essential role of PMCA is to maintain the cytosolic Ca^{2+} (by binding even low augmentation of Ca^{2+}) and of NCX is to counteract large cytosolic Ca^{2+} variations especially in excitable cells (by pumping rapidly a large increase of Ca^{2+}) (Brini & Carafoli 2011). Note that the PMCA and the PM NCX are the main regulators of the long-term resting intracellular Ca^{2+} concentrations (Strehler & Zacharias 2001).

NCX is an antiporter that uses the electrochemical gradient of Na^+ to transport 3 Na^+ ions into the cell in exchange to one Ca^{2+} ion. The NCX is found on PM, ER and mitochondria (Sisalli et al. 2014). There are three subtypes of NCX (NCX1, 2 and 3) particularly abundant in excitable tissues and all of them exist in the brain (Shenoda 2015). The NCX1 was the first to be purified in canine cardiac cells (Philipson et al. 1988), and the 2 other subtypes were later found in rat hippocampus cultures (Thurneysen et al. 2002).

PM NCX plays important roles in neuronal signalling, cardiac excitation-contraction coupling, and Ca^{2+} reabsorption in the kidney (Lytton 2007). In heart, NCX plays an important role in cardiac cell relaxation, and its expression is remarkably higher in the first postnatal developmental stages of neonatal animals (Artman et al. 1995, Huang et al. 2005) before the SR (sarcoplasmic reticulum) reaches its functional maturity. Its dysfunction leads to many heart problems such as diastolic dysfunctions, cardiac arrhythmias, ischemia, and hypertrophy (Menick et al. 2007). Hence, NCX inhibitors such as dronedarone, amiodarone, bepridil may have cardioprotective effects (Iwamoto et al. 2007). NCX is a promising target for drugs to treat ischemia in neural, cardiac and renal tissues (Yamashita et al. 2003).

2.2.2.4 Mitochondrial voltage-dependent anion channel

The Mitochondrial voltage-dependent anion channel (VDAC) known also as mitochondrial porin is a β barrel protein with 19 transmembrane beta-strands found in the outer mitochondrial membrane (OMM). It represents the most abundant protein of the OMM. As its name refers, it is voltage-dependent: it has a partially closed state when the membrane potential (MP) is between -30 and +30 mV, and has a conductance of 2 nS. When it is opened it has a conductance of 4 nS (Hiller et al. 2010).

Ca^{2+} flux across the OMM occurs mainly via VDAC. It was shown that there is a physical link between VDAC and IP3R on the ER via the chaperone glucose-regulated protein 75 (GRP75) (Szabadkai et al. 2006). This neighboring enhances mitochondrial Ca^{2+} uptake from ER (*Figure 28*). The VDAC is not only an important regulator of Ca^{2+} transport across the OMM but is also involved in the transport of

ATP, ADP, many ions such as K^+ and Na^+ and many metabolites such malate and pyruvate of the Krebs cycle (that generates ATP). Ca^{2+} is a cofactor for many Krebs cycle enzymes such as isocitrate dehydrogenase and pyruvate dehydrogenase. VDAC, by regulating Ca^{2+} permeability, controls ATP production and regulates Ca^{2+} homeostasis and apoptosis (Shoshan-Barmatz & Gincel 2003).

2.2.2.5 Mitochondrial calcium uniporter

The mitochondrial calcium uniporter (MCU) is a Ca^{2+} channel located in the inner mitochondrial membrane IMM (*Figure 28*). The Ca^{2+} itself is a regulator of the MCU; it activates the channel indirectly via the Calmodulin-dependent Protein Kinase II (CaMK II) and this activation occurs with a time constant of 6 seconds. Then, on the other hand, the increase in Ca^{2+} concentration inhibits Ca^{2+} transport with a time constant of 17 seconds (Rizzuto et al. 2009). The MCU has low-affinity at micromolar Ca^{2+} cytosolic concentrations but high affinity mitochondrial Ca^{2+} uptake can occur at nanomolar concentrations (Santo-Domingo & Demaurex 2010). This biphasic dependence on cytosolic Ca^{2+} concentration allows mitochondrial Ca^{2+} oscillations, and prevents further Ca^{2+} uptake and accumulation in mitochondria when cytosolic Ca^{2+} elevation is prolonged (Moreau et al. 2006). The mitochondrial Ca^{2+} oscillations are important to control many mitochondrial metabolic processes such as ATP production, NADPH elevation and stimulation of mitochondrial enzymes such as deshydrogenases (Robb-Gaspers et al. 1998)

MCU is activated by spermine (Litsky & Pfeiffer 1997) and plant flavonoids especially the kaempferol (Montero et al. 2004). Its activity can be modulated, in a concentration-dependent manner, by adenine nucleotides, in the order of effectiveness $ATP > ADP > AMP$ (Litsky & Pfeiffer 1997) and it is inhibited by Rhutenium red (Bae et al. 2003).

2.2.3 Calcium buffers and effectors

The Ca^{2+} constitutes a highly versatile signal for the cell and the information carried within its variable spatial and temporal signaling needs to be suitably decoded. The cells have specific classes of proteins that act as Ca^{2+} sensors that decode the information embedded in Ca^{2+} signal before passing it on to targets. This decoding process is based on specific conformational changes in the sensor proteins (Carafoli et al. 2001). After an increase of cytosolic Ca^{2+} concentration, most of the Ca^{2+} binds to Ca^{2+} -binding proteins that function as Ca^{2+} buffers or Ca^{2+} effectors, and a very few amount of Ca^{2+} remains free in the cytosol. These proteins can control both the amplitude and the recovery time of Ca^{2+} transients (Berridge et al. 2003).

Examples of cytosolic buffers are calretinin, calbindin D-28 and parvalbumin. There is also the ER/SR buffers and chaperones such as calreticulin (the predominant one), calnexin, calsequestrin, glucose-regulated protein 78 and 94 (GRP 78 and GRP 94). The ER Ca^{2+} buffers reduce ER free Ca^{2+} concentration and helps SERCA in its pumping function by reducing the concentration gradient between the ER and the cytoplasm. The Ca^{2+} binding of these proteins is characterized by its affinity and capacity (kinetic). For example, calretinin, calbindin D-28 and calreticulin are low-affinity but high-capacity binding protein whereas parvalbumin has higher affinity but slower binding-kinetics for Ca^{2+} .

Golgi Ca^{2+} buffers are Cab45, P54/NEFA, and CALNUP (nucleobindin). In mitochondria, Ca^{2+} is not bound to buffering proteins but precipitated as insoluble salt CaPO_4 (Prins & Michalak 2011).

The buffering capacity of a cell is measured by Ca^{2+} -binding ratio K_s . Cells with low buffering capacity such as adrenal chromaffin cells and motoneurons ($K_s=40$) generate rapid Ca^{2+} dynamics comparing with high buffering capacity cells such as hippocampal or cerebellar Purkinje neurones ($K_s=2000$). Low endogenous Ca^{2+} buffering may cause pathophysiological conditions such as excitotoxic stress and motoneuron disease (Palecek et al. 1999).

Ca^{2+} effectors are Ca^{2+} -binding protein that control many cellular functions depending on the binding or not of Ca^{2+} . Hence, the calcium, through the interaction with these proteins, regulates a wide variety of cellular processes such contractile processes, intracellular transport and trafficking, secretory functions, intracellular communication, glycolysis and mitosis (Petersen et al. 2005). Some examples of Ca^{2+} effectors are calmodulin (CaM), troponin C, synaptotagmin, annexin, neuronal Ca^{2+} sensor family (NCS-1), visinin-like proteins (VILIP), hippocalcin, recoverin and guanylate-cyclase-activating proteins (Berridge et al. 2003).

2.2.4 How the calcium spatial and temporal signaling is decoded by the cell?

Every cell sets the suitable combination of Ca^{2+} channels and pumps subtypes in order to respond to its own requirements in Ca^{2+} signaling and to control effectively its physiological specific functions. For example, cells such cardiomyocytes, myocytes and stereocilia, which recover very rapidly after a Ca^{2+} spark have the fastest isoforms of PMCA (PMCA 3f and 2a), whereas Jurkat cells that takes more time to recover (up to one minute) have the slow PMCA 4b (Caride et al. 2001). Even the distribution of Ca^{2+} channels and pumps different isoforms is specific, especially in polarized cells. For example, in pancreatic acini, SERCA2a is expressed in the luminal pole, whereas SERCA2b is expressed in the basal pole. Whereas in salivary gland acinar and duct cells, SERCA3 is found in the basal pole and SERCA2b in the luminal one (Lee et al. 1997).

2.2.4.1 Calcium sparks, oscillations and waves

The regulation of intracellular Ca^{2+} concentrations is a complex phenomenon using several mechanisms and a wide number of Ca^{2+} channels and pumps essentially in the PM, the ER/SR and a possible contribution of mitochondria, Golgi and the endolysosomal system. This complexity is manifested in spatial and temporal domains by Ca^{2+} sparks, oscillations (repetitive spikes) or waves.

An example of Ca^{2+} spark and wave is shown on [Figure 27](#). Ca^{2+} sparks are generated by low and intermediate IP_3 concentrations, whereas Ca^{2+} wave is generated by a high concentration of IP_3 resulting from a high concentration of extracellular agonists. In detail, at low IP_3 concentration, individual IP_3R of the ER are opened and localized spatiotemporally elevations in cytosolic Ca^{2+} concentration called Ca^{2+} “sparks” or “blips” occur at discrete release sites (Parker et al. 1996) ([Figure 27](#)). These sites are spaced at intervals of several microns and represent clusterings of IP_3R (FOSKETT et al. 2007). At intermediate concentrations of IP_3 , many IP_3R within a cluster are activated generating

Ca²⁺ “puffs”. The released Ca²⁺ stimulates other IP₃R within the cluster by CICR. And at higher levels of IP₃ concentration, Ca²⁺ released at one cluster site can trigger Ca²⁺ release at other adjacent sites by CICR, and the localised Ca²⁺ signal propagates from an IP₃R cluster to another as a Ca²⁺ wave (Bootman & Berridge 1996, Callamaras et al. 1998). Generated Ca²⁺ waves are the spatial and temporal summation of individual Ca²⁺ sparks (Cheng et al. 1996), that can propagate in a continuous (without deformation) or a saltatory (burst-like) manner (Dawson et al. 1999). The Ca²⁺ wave propagates at a velocity of a few tens of microns per second by successive cycles of Ca²⁺ release, diffusion, and CICR (Berridge 1997a). The Ca²⁺ signal can either propagate to the entire cell (Rooney & Thomas 1993), or remain localised in specific subcellular regions (Allbritton & Meyer 1993).

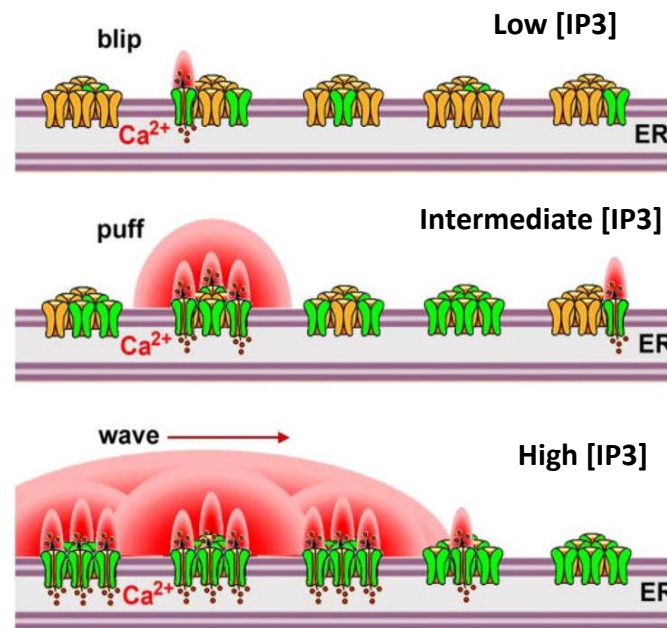


Figure 27 : generation of Ca²⁺ wave by increased IP₃ concentration and CICR. In green : open receptor (FOSKETT et al. 2007).

Spontaneous Ca²⁺ waves have been observed in both excitable and nonexcitable cells (Lipp & Niggli 1996). In cardiac tissue, Ca²⁺ waves propagated in and between cardiac myocytes but their functions remains unclear. These waves result from spontaneous localized Ca²⁺ sparks and are not dependent from membrane depolarization. However, they can cause membrane depolarization and under some circumstances induce an action potential (Stuyvers et al. 2000). In all cases, spontaneous Ca²⁺ releases in a cardiomyocyte are regarded as potential arrhythmogenic process in the heart (Fedida et al. 1987). In cardiac trabeculae, Ca²⁺ waves propagate at low velocity ($\approx 30 \mu\text{m/s}$) and over a limited distance throughout the muscle (Wier et al. 1997). Kaneko *et al.* demonstrated three distinct types of Ca²⁺ waves in Langendorff-perfused rat heart, depending on localized Ca²⁺ concentration. Under quiescence, the waves occurred sporadically (3.8 waves/min/cell), with a velocity of $84 \mu\text{m/s}$. In regions with higher basal levels of Ca²⁺, Ca²⁺ waves occurred more frequently (28 waves/min/cell) and propagated at a higher velocity ($116 \mu\text{m/s}$) with occasional intercellular propagation. In regions with much higher basal Ca²⁺ concentration, waves occurred with a high incidence (133 waves/min/cell) (Kaneko et al. 2000).

Ca²⁺ waves exist also in the intestine where they control specific behavioral motor patterns governed by neural activities timing. For example, the defecation motor program in *Caenorhabditis elegans* consists of three stereotyped motor steps with precise timing, which start by a periodic

calcium spike in a pacemaker cell. The IP3R is necessary for this periodic behavior and its inhibition blocks the second and third motor steps (Teramoto & Iwasaki 2006). Gap junctions are also crucial for the intercellular Ca^{2+} wave propagation. The absence of pannexin gap junctions in mutant animals affects the reliability of the pacemaker cell and the wave propagation (Peters et al. 2007)

2.2.4.2 Calcium-sensitive enzymes and transcription-factors

The necessity of a decoding system for the different Ca^{2+} behaviors (Ca^{2+} sparks, oscillations or waves) is of a primordial importance for the cell to ensure an adequate control of the physiological Ca^{2+} dependant processes. For example, mesenchymal stem cells (MSC) present spontaneous Ca^{2+} oscillations (discussed in details in *section 3.1*) at different frequencies depending on whether they are pluripotent or on the route of differentiation (Pullar 2011). In these cells for example, the Ca^{2+} code is embedded within the spontaneous Ca^{2+} oscillations frequency and the cell should have the suitable translating system for decoding the Ca^{2+} message in order to control oscillations frequency-dependent cell responses such as gene expression, proliferation and differentiation.

Many Ca^{2+} -sensitive enzymes are responsible of the decoding of Ca^{2+} signals, such as calmodulin-dependent protein kinases (CaMK), PKC, adenylyl cyclase, calcineurin, Ca^{2+} -activated proteases (calpain I and II), myosin light chain kinase (MLCK), phosphorylase kinase, IP3-kinase, cyclic AMP phosphodiesterase, endothelial and neuronal nitric oxide synthase (NOS) (Berridge et al. 2003).

The CaM Kinase II (CaMKII) for example can decode the frequency of Ca^{2+} oscillations into distinct amounts of kinase activity. The frequency response of CaMKII is also modulated by the individual Ca^{2+} spikes duration and amplitude (De Koninck & Schulman 1998). These CaMKII features may present an important role in the control of MSC pluripotency and differentiation, due to the Ca^{2+} oscillations frequency differences between the pluripotent MSC and MSC on the routes of differentiation to many cellular lineages (cf. *section 3* for details). As seen in *section 2.2.2.5*, the CaMKII responds to cytosolic Ca^{2+} concentration changes by activating the MCU. The mutation in CaMKII was correlated with the lack of Ca^{2+} wave propagation and coordination of the muscle contraction in *Caenorhabditis elegans* intestine (Teramoto & Iwasaki 2006).

In addition to Ca^{2+} -sensitive enzymes, there is the Ca^{2+} -sensitive transcription factors that participate also in the decoding of Ca^{2+} signals, such as nuclear factor of activated T cells (NF-AT), nuclear factor-kappa B (NF- κ B), Oct/OAP, cyclic AMP response element-binding protein (CREB) and CREB-binding protein (CBP).

For example, NF-AT is expressed in many cells such as MSC (*Figure 34*) and T lymphocytes, both of them presenting Ca^{2+} oscillations. These oscillations depend on, between others, IP3R Ca^{2+} release and Ca^{2+} entry from SOCC (MSC Ca^{2+} oscillations are discussed in details in *section 3.1.2*). In MSC, Ca^{2+} oscillations are important in controlling the proliferation and differentiation of the cells (Pullar 2011), and in T lymphocytes, they play crucial role in activating these latter after antigen binding to T-cell receptor (TCR) (Lewis 2003). It was shown that the Ca^{2+} oscillations act as a frequency encoding system rather than amplitude encoding because it is the frequency that varies most often with stimulus strength. For example, the interleukin-2 (IL-2) and IL-8 gene expression is sensitive to oscillations frequency that activate either NF-AT or NF- κ B. Rapid Ca^{2+} oscillations stimulate the expression of the

three transcription factors NFAT, NF- κ B and Oct/OAP, whereas less frequent oscillations activate only the NF- κ B (Dolmetsch et al. 1998).

2.3 DIFFERENT CALCIUM-RELATED MECHANISMS IN THE CELL

2.3.1 Mitochondria-associated membranes and apoptosis

The regions of tightly apposition of ER/SR and mitochondria are called mitochondria-associated membranes (MAM) (Patergnani et al. 2011). *Figure 28* shows an example of Ca^{2+} trafficking between ER and mitochondria. Upon to an agonist (the IP_3) stimulation, the ER IP_3R are activated and release Ca^{2+} . And as several mitochondria are within 20-100 nm of the ER, the released Ca^{2+} is transmitted to these adjacent mitochondria via MCU and VDAC (in connection with IP_3R via Grp75). Hence, mitochondrion acts as a Ca^{2+} buffer that shapes cellular Ca^{2+} signals. In pancreatic acinar cells for example, Ca^{2+} waves are always generated in the apical pole. These waves must be very robust in order to reach the basolateral pole due to mitochondria clustering between apical and basal poles of the cell, and because this mitochondrial clustering can retain any Ca^{2+} excess (see also section 2.2.4).

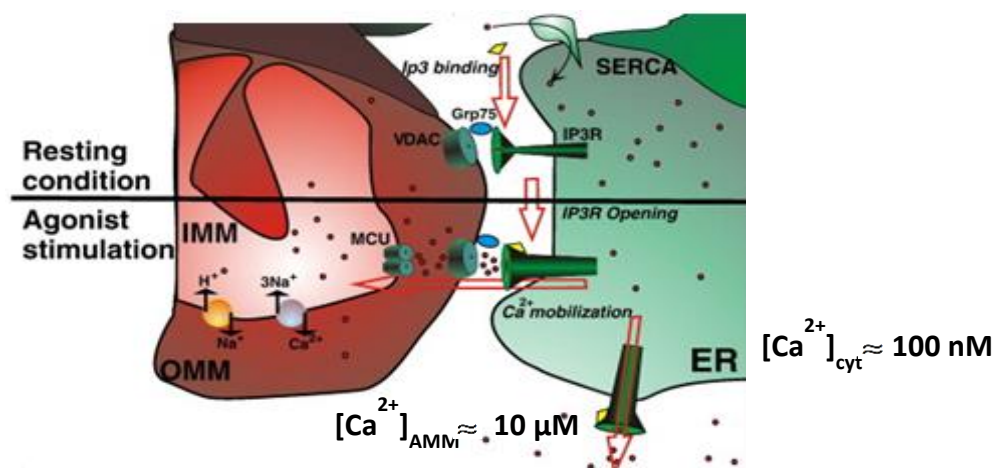


Figure 28: mitochondria–ER contact sites and Ca^{2+} handling showing the connection between IP_3R and VDAC , and further implication of MCU and NCLX (Rizzuto et al. 2009). Ca^{2+} concentrations in AMM and cytosol are taken from Santo-Domingo and Demareux, 2010.

Among many regulatory functions such as autophagy regulation, Ca^{2+} control the ATP production rate in mitochondria by activating Ca^{2+} -sensitive mitochondrial dehydrogenases (pyruvate-, α -ketoglutarate- and isocitrate-dehydrogenases) of the Krebs cycle (McCormack et al. 1990). On the other side, mitochondrial Ca^{2+} overload caused by agonist hyperstimulation results in bioenergetic catastrophe and cell death (Celsi et al. 2009). Therefore, mitochondria responds to Ca^{2+} elevations either by increasing the cell energy supply or by triggering the cell death program of apoptosis. Nevertheless, even slow and steady cytosolic Ca^{2+} concentrations can be sensed by the mitochondria that tune high affinity mode of Ca^{2+} uptake on (cf. section 2.2.2.5). This latter transforms small cytosolic Ca^{2+} concentrations increase into sustained increases in mitochondrial Ca^{2+} concentrations which initiate the signalling cascade of apoptosis (Santo-Domingo & Demareux 2010).

The RyR generates Ca^{2+} sparks and participate also with the IP3R to Ca^{2+} release from ER, that controls ATP synthesis in many cell types such as cardiomyocytes (Broun et al. 2013) and pancreatic β cells (Tsuboi et al. 2003). In these latter, ATP production potentiates glucose-stimulated insulin release.

2.3.2 Other mechanisms and functions

In addition to enzymatic function regulation, mitochondrial respiration and metabolics, cell bioenergetics (ATP production), survival, apoptosis and autophagy control, Ca^{2+} regulates a very wide band of cellular proteins and mechanisms. Ca^{2+} regulates gap junctions opening: an increase in cytosolic Ca^{2+} concentrations in apoptotic cells close the gap channels, which is an effective way to isolate these cells and to avoid transferring the apoptotic signal to adjacent cells. This mechanism is not effective in cancerous cells, and the failure to disrupt cell coupling is a way to propagate cell death via Ca^{2+} signals (Krutovskikh et al. 2002).

Ca^{2+} is important for cell interactions with its environment. Many cell-adhesion molecules (CAM) (for cell-cell interaction) and substrate-adhesion molecules (SAM) (for cell-ECM interaction) are Ca^{2+} dependent, such as immunoglobulins (Ig), cadherins (responsible of the contact inhibition process) (Hirano et al. 1987), selectins (implicated in Leukocyte extravasation), integrins (links between cytoskeleton and the proteins of the basal lamina such as fibronectin, laminin and collagen). The CAM and SAM are present in tight junctions, gap junctions, cell-cell, and cell-matrix junctions. In all cell-adhesion junctions, the transmembrane CAMs are linked to the cytoskeleton via various adapter proteins in cytoplasmic plaques (Lodish et al. 2000b). The cadherins and other CAMs play also important role in survival and differentiation of pluripotent stem cells and of human trophoblast (Coutifaris et al. 1991, Li et al. 2012).

Ca^{2+} exerts an effect on cytoskeleton ; it has cytoskeletal receptor on actin filament and controls actin polymerisation (Europe-Finner & Newell 1986). A raise in cytosolic calcium causes increased polymerization of the actin microfilaments (Dushek et al. 2008). It exerts an effect on the structure and activity of myosin and tubulin (microtubules) cytoskeletons (Hepler 2016). A concentration of $10 \mu\text{M}$ of Ca^{2+} , in presence of CaM, inhibits microtubule assembly in vitro (Marcum et al. 1978). In muscle, calcium binds to troponin C which cause tropomyosin to be displaced along the actin filament, exposing myosin-binding sites and permitting contraction to occur. Ca^{2+} , by controlling cytoskeleton remodeling, controls cell shape changes, cell division, and cell movements and motility including phagocytosis, secretion and locomotion (Bennett & Weeds 1986).

Ca^{2+} is a crucial factor for membrane repair and resealing by lysosome exocytosis. Reddy *et al.* showed that an elevation in intracellular Ca^{2+} concentrations triggers fusion of lysosomes with the PM, and that this process is regulated by the lysosomal synaptotagmin isoform Syt VII. The inhibition of Syt VII by specific antibodies or the use of recombinant Syt VII prohibited lysosomal exocytosis and membrane resealing (Reddy et al. 2001).

Ca^{2+} modulates the activity of many PM channels such as Ca^{2+} -activated K^+ channels (BK channels) and Ca^{2+} -activated Cl^- channels (CaCC). In arterial smooth muscle cells for example, intracellular Ca^{2+} controls both contraction and relaxation. While the contraction phenomenon has been already discussed, the relaxation is mediated by local Ca^{2+} sparks from the SR that activate BK channels (Brenner et al. 2000). CaCCs play important roles in epithelial secretion of electrolytes and

water, regulation of neuronal and cardiac excitability, regulation of vascular tone and sensory transduction (Hartzell et al. 2005).

All the examples cited above are ones from countless events and processes controlled by Ca^{2+} . Ca^{2+} is a universal and the most versatile intracellular messenger implicated in cell growth, development and death, and it is not false to think that in every cellular process there is a certain implication of Ca^{2+} whether directly or indirectly.

2.4 STUDYING CALCIUM SIGNALING: THE CALCIUM MARKERS

Whole-cell configuration of the patch clamp technique (Neher & Sakmann 1976) can measure ionic currents flowing through single protein channels of the PM. It is an indirect technique to monitor membrane Ca^{2+} currents by using ion-sensitive microelectrodes. However, this technique only measures Ca^{2+} concentration underneath the PM and not the bulk Ca^{2+} concentration (Lipp & Niggli 1996). The recent development of fluorescent Ca^{2+} -indicators is a more sensitive and reliable technique to measure Ca^{2+} concentration variations in living cells, and subsequent cellular and subcellular aspects of Ca^{2+} regulation.

The first experiments that visualized intracellular Ca^{2+} changes (Ridgway & Ashley 1967) used a Ca^{2+} -sensitive bioluminescent protein called aequorin, extracted from the luminescent hydromedusan, *Aequorea victoria* (Shimomura et al. 1962). Actually, a very large palette of fluorescent Ca^{2+} indicators is available, and allow the measure of a broad spectrum of Ca^{2+} concentrations ranging from $< 50 \text{ nM}$ to $> 50 \text{ }\mu\text{M}$ (Paredes et al. 2008). Ca^{2+} indicators are either intensimetric (single wavelength) or ratiometric (2 excitation or 2 emission wavelengths) dyes. The ratiometric indicators are less sensitive to images artifacts, photobleaching, leakage or uneven dye loading, and their use is advantageous over the intensimetric markers because they give quantitative informations on the Ca^{2+} concentrations. These indicators excite and emit at different wavelengths depending on whether they are Ca^{2+} -free or Ca^{2+} -bound states.

The choice of a Ca^{2+} indicator depends on the Ca^{2+} signal to be measured and the type of the experiment. Intensimetric markers are more sensitive to even a modest Ca^{2+} changes (their intensity change is easily detectable) but give only qualitative data. The difference in intensities between Ca^{2+} -free and Ca^{2+} -bound indicator is smaller with ratiometric markers but these latter are more useful for quantitative analysis (and can be used for qualitative analysis).

2.4.1 Fluorescent Ca^{2+} -sensitive dyes

The Ca^{2+} -sensitive fluorescent dyes (CSFDs) are chemical indicators based on BAPTA, a non-fluorescent Ca^{2+} chelator derived from EGTA (ethylene glycol tetraacetic acid) with high selectivity for Ca^{2+} over Mg^{2+} ions (Tsien 1980), associated with a fluorescent chromophore. Actually, a wide variety of Ca^{2+} indicators is available, with differences in Ca^{2+} affinity, and cell permeability in addition to a large excitation and emission spectra ranging from ultraviolet to the infrared. The fluorescence intensity of a CSFD depends on the Ca^{2+} concentration. Ca^{2+} signalling can be studied by loading the

cell with a CSFD such as fura-2, fluo-3, fluo-4, indo-1, quin-2 or calcium Green-1. Each of them has its strong and weak points. For example, among the cited indicators, fura-2 and indo-1 give quantitative Ca^{2+} measurements because they are ratiometric markers (*Figure 29*), the others being intensimetric. Fluo-3 has a higher affinity to Ca^{2+} than Calcium green-1, but this latter is about 5-fold brighter than fluo-3 at saturating Ca^{2+} levels (Eberhard & Erne 1991). The *Table 3* shows the properties of some CSFDs.

Indicator	Kd for Ca^{2+} (nM)	Excitation (nm), emission (nm)	Notes
Calcium Green-1	190	490ex 531 em	single wavelength
Fluo-3	325	506 ex 526 em	single wavelength
Fluo-4	345	494 ex 516 em	single wavelength
Fura-2	145	363/335 ex 512 em	dual excitation/ single emission
Indo-1	230	488 ex 405/485 em	single excitation/dual emission

Table 3 : some examples of Ca^{2+} indicators and their properties. Kd :dissociation constant - the concentration of Ca^{2+} at which half the indicator molecules are bound with Ca^{2+} at equilibrium (Paredes et al. 2008).

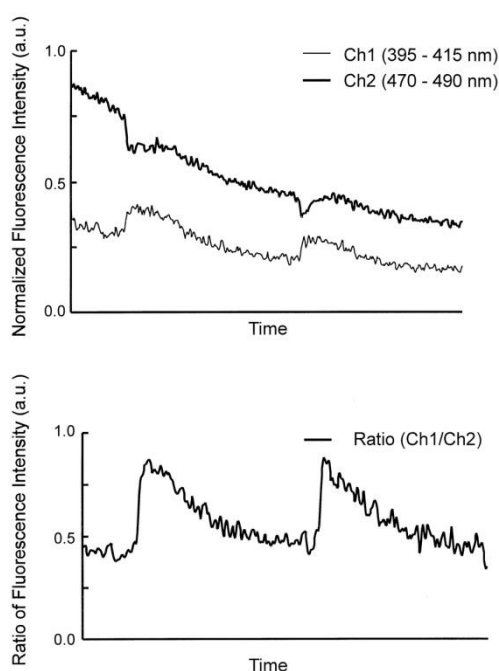


Figure 29 : Ratiometric measurement of cytosolic Ca^{2+} concentration using indo-1 (Takahashi et al. 1999).

All the Ca^{2+} indicator dyes cited above are hydrophilic by their nature, and do not cross the PM. So, they are oftenly coupled to a lipophilic ester group, called acetoxymethyl (AM) group, to facilitate their diffusion across the PM. The AM ester masks the chelator carboxyl group of the dye. Once inside the cells, the AM esters are cleaved from the dye by specific esterases called acetyl esterases. The cleavage of the AM group liberates the chelator part of the dye, allowing it to bind free Ca^{2+} , and traps the dye in the cytosol; the dye, without its lipophilic ester group, comes back to its hydrophilic nature

and can not therefore leak from the cell. Markers with AM groups are dissolved in dimethylsulfoxide (DMSO) before being used, after the corresponding dilution, in the extracellular medium of the cells. Pluronic-F127 can also be used to facilitate the dispersion of the dye in the medium (Kao et al. 2010).

2.4.2 Genetically encoded Ca^{2+} indicators

Protein-based genetically encoded Ca^{2+} indicators (GECIs) are engineered fluorescent protein chimeras that change in function of Ca^{2+} concentrations fluctuations. These powerful tools were developed first in the laboratory of Roger Tsien, the same person who contributed to the development of the green fluorescent protein (GFP) (Tsien 1998), already reported by Shimomura *et al.* in the jellyfish *Aequorea victoria* (Shimomura et al. 1962). The GECIs are not loaded to the cell like CSFDs, but transfected as encoding plasmids. Roger Tsien Lab deposited such plasmids at Addgene for distribution to the research community (https://www.addgene.org/Roger_Tsien/). Some examples of such plasmids are the pcDNA-D1ER and the pcDNA-4mtD3cpv (the D1ER and 4mtD3cpv are second generation cameleon Ca^{2+} sensors targeted to ER and mitochondria respectively) (Palmer et al. 2004, 2006). The pcDNA-D1ER for example, codes for a Ca^{2+} marker protein containing a KDEL sequence in its C-terminal side and this sequence targets the marker to the ER (*cf.* 1.2.3.4).

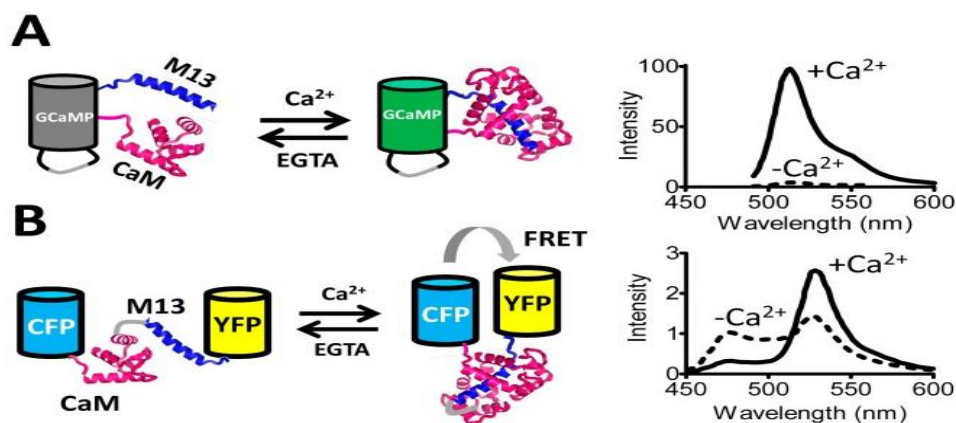


Figure 30 : example of A. a single fluorescent protein Ca^{2+} indicator (GCaMP), and B. two fluorescent protein Ca^{2+} indicator (cameleon, FRET: fluorescence resonance energy transfer (Lindenburt & Merckx 2014)).

The fluorescent GECIs are based essentially on GFP or one of its color variants, yellow (YFP), red (RFP) or cyan fluorescent protein (CFP), which are suitable for Förster resonance energy transfer (FRET), and a Ca^{2+} buffer (the CaM) (Miyawaki et al. 1997), with its binding peptide M13 derived from myosin light chain kinase (Porumb et al. 1994). Two important classes of GECIs are the single fluorescent protein type, such as GCaMP (Nakai et al. 2001), pericams (Nagai et al. 2001), GECOs (Zhao et al. 2011) and Camgaros (Baird et al. 1999), that are dim in the absence of Ca^{2+} and bright when bound to Ca^{2+} , and the two fluorescent protein (FRET) type such as cameleons (Miyawaki et al. 1997) and TN-XL (Mank et al. 2006), that have FRET signal increased upon Ca^{2+} binding.

Another category of GECIs are the bioluminescent ones ; they use a donor chemiluminescent protein, such as aequorin or a luciferase that does not require an external light excitation and instead of FRET, used the BRET (bioluminescent resonance energy transfer) to excite a GFP (or one of its derivatives) upon the binding of Ca^{2+} . The GFP can be linked directly to aequorin such as in GFP-aequorin and upon the binding of Ca^{2+} to aequorin, the BRET occurs, just like it exists naturally in the jellyfish *Aequorea victoria*. In the BRAC indicator and Nano-lantern (Ca^{2+}), there is a CaM and its binding peptide M13 between the aequorin and the yellow fluorescent protein (Venus) or the monomeric red fluorescent protein (mRFP1) (Curie et al., 2007).

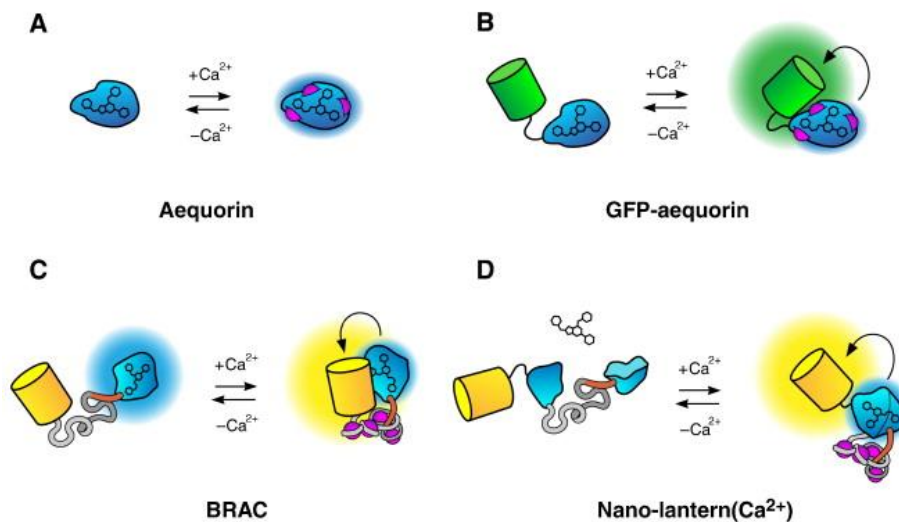


Figure 31 : bioluminescent Ca^{2+} indicators (Pérez Koldenkova & Nagai 2013).

The GFP-aequorin and Nano-lantern directly depend on Ca^{2+} binding in an intensimetric way : the signal intensity of aequorin and therefore the BRET depends on the Ca^{2+} concentration (Saito et al. 2012), whereas BRAC can be used as a ratiometric probe because the binding of Ca^{2+} modulates the BRET ratio by changing the distance between the donor and acceptor proteins (Saito et al. 2010).

3 MESENCHYMAL STEM CELLS AND DIFFERENTIATION

3.1 MESENCHYMAL STEM CELLS

Mesenchymal stem cells (MSCs) are multipotent stromal cells (Dominici et al. 2006) originated from the embryonic mesoderm (mesenchyme) and present in many adult tissue such as bone marrow (bMSC), adipose tissue (aMSC), muscle, dermis, umbilical cord and around blood vessels (as pericytes) (Caplan & Bruder 2001, Lee et al. 2004, Malgieri et al. 2010). These cells have the ability to self-renew and to differentiate into a wide variety of cells including mesodermal (osteoblasts, fibroblasts, chondrocytes, adipocytes, muscle, tendocytes, ligaments), ectodermal (neurons, epithelial cells) and endodermal (endothelial, pancreatic and liver cells) lineages (Friedenstein et al., 1974; Kopen et al., 1999; Krause et al., 2001; Marappagounder et al., 2013; Pittenger et al., 1999; Woodbury et al., 2002). The MSCs have the capacity to form cell types from alternative layers of their embryogenesis origin (both endodermal and ectodermal tissue), a process termed 'transdifferentiation'.

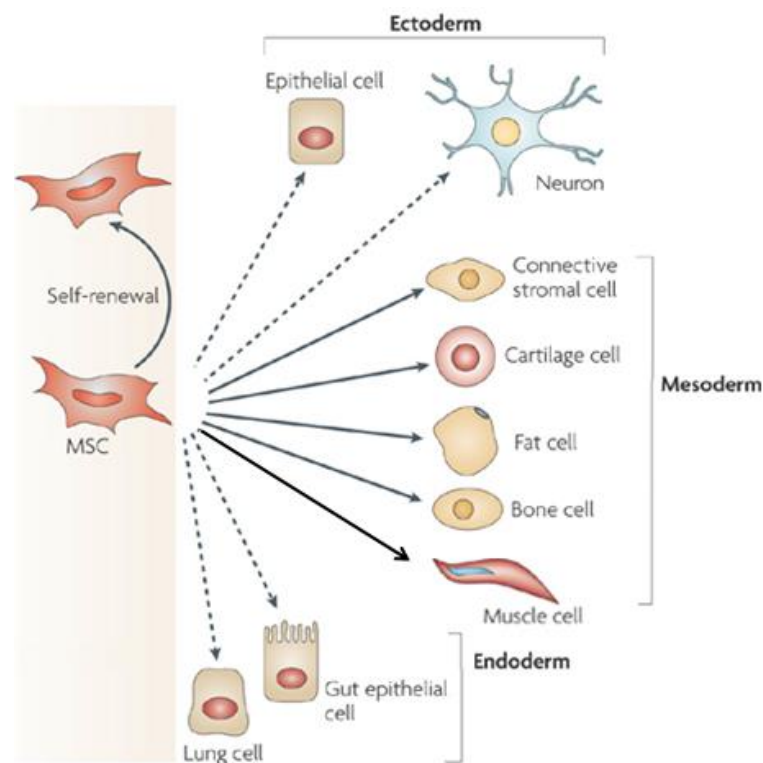


Figure 32 : The multipotency of MSCs. Solid arrows: differentiation into mesenchymal lineages, dashed arrows : differentiation into cells from unrelated germ lineages (transdifferentiation) (Uccelli et al. 2008).

The non-hematopoietic MSCs of bone marrow were discovered by Friedenstein, who called them stromal cells (Friedenstein et al. 1968, 1970, 1974). He described clonal, plastic adherent cells capable of differentiating into osteoblasts, chondrocytes and adipocytes. The first experiments using MSCs, called them fibroblast (because they are fibroblast-like cells) or marrow (because extracted from

the bone marrow) stromal cells (Piersma et al. 1985). The term « mesenchymal stem cell » was popularized by Caplan in the early 1990s (Caplan 1991), and later on, the Mesenchymal and Tissue Stem Cell Committee of the International Society for Cellular Therapy (ISCT), state that, to define MSCs, they should have minimal criteria: be plastic adherent when maintained in standard culture conditions, express certain specific cellular markers and lack others (see below) and must differentiate to osteoblasts, chondroblasts and adipocytes in vitro (Dominici et al. 2006).

As they are adult stem cells, MSCs have lower differentiation potency than embryonic stem cells (ESC) (Thomson et al. 1998) and induced pluripotent stem cells (iPS) (Cyranoski 2008), but they are advantageous over the two because of the ethical issues correlated with the use of ESC and the production cost issues of the iPS. The use of MSCs seeded in biomaterial scaffolds have been used in order to heal organs and tissues defects. They have been used also for cell delivery (without a scaffold) (Marion & Mao 2006). MSCs have Immunosuppression effects, they can inhibit T lymphocytes proliferation or induce their tolerance in vivo, and regulate many immune cells functions such as neutrophils activation and dendritic cells antigen presentation. They can also release anti-apoptotic and anti-inflammatory molecules (Uccelli et al. 2008), hence being tissue protective. All these properties make the MSCs excellent candidates for regenerative medicine.

Depending on the species and the tissue source, MSCs express different levels of clusters of differentiation (CD) markers such as CD13, CD29 (Integrin beta-1), CD44, CD90, CD71 (transferrin receptor), CD73 (ecto-5'-nucleotidase) CD105 (endoglin), and CD271 (low-affinity nerve growth factor receptor). They lack the immune cells co-stimulatory molecules CD40, CD80 and CD86, and the haematopoietic markers CD14, CD34 and CD45 and HLA (human leucocyte antigen)-DR (Lindroos et al. 2011, Ullah et al. 2015)

3.1.1 Human adipose Mesenchymal stem cells

Human aMSC (haMSC) are derived from the adipose tissue. They are more available than other MSC like the human bMSC (HbMC) because they are easily accessible in higher number and without painful procedures of extraction. In addition, they have phenotypes, surface markers (Gronthos et al. 2001) and gene expression profile similar to those of the HbMSC. They are also easier to maintain and proliferate than HbMSC (Lee et al. 2004), and capable to differentiate into, at least, osteogenic, chondrogenic, adipogenic, myogenic and neurogenic lineages in vitro (Gimble et al. 2007). Other studies showed also the haMSC capacity of differentiation into cardiomyocytes (van Dijk et al. 2008) hepatocytes (Seo et al. 2005), endothelial (Miranville et al. 2004, De Francesco et al. 2009) and pancreatic (Timper et al. 2006) cells. All these characteristics make the haMSC one of the ideal MSC to use (Lindroos et al. 2011) for experimental testings, cell therapy and regenerative medicine. In vitro, haMSC display a cell doubling time of 2 to 4 days (shorter doubling time than HbMSCs), depending on the culture medium and the passage number, and they express ESC markers, Sox-2, Oct-4, and Rex-1 for at least 10 passages (Izadpanah et al. 2006).

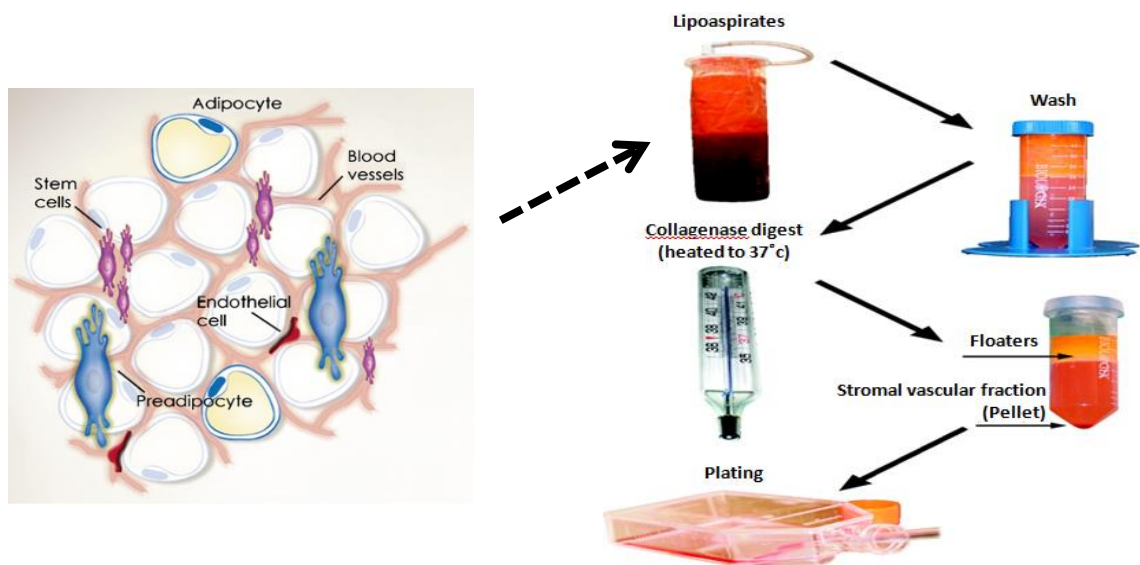


Figure 33 : schematic view of components of adipose tissue (Lindroos et al. 2011) and isolation steps of haMSC (Gimble et al. 2007).

After isolation, haMSCs are characterized by their immunophenotype (Table 4) and their differentiation potential towards adipogenic, chondrogenic and osteogenic lineages in presence of lineage-specific induction factors (Lindroos et al. 2011).

Antigen Category	Surface-Positive Antigens	Surface-Negative Antigens
Adhesion molecules	CD9 (tetraspan), CD29 (β_1 integrin), CD49 days (α_4 integrin), CD54 (ICAM-1), CD105 (endoglin), CD166 (ALCAM)	CD11b (α_b integrin), CD18 (β_2 integrin), CD50 (ICAM-3), CD56 (NCAM), CD62 (E-selectin), CD104 (α_4 integrin)
Receptor molecules	CD44 (hyaluronate), CD71 (transferrin)	CD16 (Fc receptor)
Enzymes	CD10 (common acute lymphocytic leukemia antigen), CD13 (aminopeptidase), CD73 (5' ecto-nucleotidase), aldehyde dehydrogenase	
Extracellular matrix molecules	CD90 (Thy1); CD146 (Muc18); collagen types I and III; osteopontin; osteonectin	
Cytoskeleton	α -smooth muscle actin, vimentin	
Hematopoietic		CD14, CD31, CD45
Complement cascade	CD55 (decay-accelerating factor), CD59 (protectin)	
Histocompatibility Antigen	HLA-ABC	HLA-DR
Stem cell	CD34, ABCG2	
Stromal	CD29, CD44, CD73, CD90, CD166	

Table 4 : immunophenotype of haMSCs (Gimble et al. 2007).

3.1.2 Calcium oscillations in MSCs

Ca^{2+} oscillations are a universal mode of Ca^{2+} signaling. They exist in excitable (Tsien 1983, Parri et al. 2001) and non-excitable cells (Fewtrell 1993). As seen in *section 2*, in electrically excitable cells, the major pathway of Ca^{2+} entry are the VOCCs, which play important role in proliferation and differentiation. In nonexcitable cells, Ca^{2+} oscillations are typically initiated by receptor-triggered production of IP3 (after an agonist attachment to the receptor) (Nash et al. 2001) and the subsequent Ca^{2+} release from the ER (Liou et al. 2005) which stimulates the store-operated calcium entry (SOCE) via the SOCC (Parekh & Putney 2005). The Ca^{2+} oscillations were thought, for a long time, to exist only in excitable cells. Woods *et al.* were the first to show that Ca^{2+} oscillations can occur in nonexcitable cells by demonstrating that hormone-stimulated hepatocytes present repetitive transient rises in cytoplasmic free calcium (Woods et al. 1986). In the same year, Yada et al. showed that cultured epithelial cells present synchronous oscillations of the cytoplasmic Ca^{2+} concentration (Yada et al. 1986). These studies changed the ideas that were prevalent on the fact that Ca^{2+} signals in nonexcitable cells are only amplitude encoded, to show that there is also a frequency encoded system.

The MSCs, which are nonexcitable cells, present spontaneous Ca^{2+} oscillations. As their name refers, these oscillations are spontaneous which means that they occur without agonists stimulation. The precise mechanism on how they are generated and sustained are not well understood. The major source of these oscillations is the largest intracellular Ca^{2+} store, the ER. However, Ca^{2+} entry from extracellular medium is necessary to refill the ER of Ca^{2+} and sustain Ca^{2+} oscillations. This explains why, in a Ca^{2+} free solution, the oscillations can not be sustained (Kawano et al. 2003a). Ca^{2+} release is mediated by the IP3R of the ER with no contribution of the RyRs, and Ca^{2+} influx across PM is mainly mediated by SOCCs (activated by Ca^{2+} release from ER) but also a little contribution of VOCCs (Kawano et al. 2002). The practically no contribution of RyRs to these oscillations is consistent with the fact that generally, RyRs are the main pathway of Ca^{2+} release from ER in excitable cells, and IP3Rs are the main one in nonexcitable cells (Berridge 1997b). The Ca^{2+} oscillations are inhibited by the application of La^{3+} suggesting a probable Ca^{2+} entry through non-selective cation channels (Kawano et al. 2003b).

After the increase of intracellular Ca^{2+} concentration (the first step of a Ca^{2+} oscillation), Ca^{2+} is extruded via the PMCA and PM NCX to the extracellular medium, and pumped via SERCA to the ER (Kawano et al. 2003a). Kawano *et al.* showed also that autocrine/paracrine ATP, via the activation of the purinergic receptor P_2Y_1 , contributes to the MSC spontaneous Ca^{2+} oscillations. ATP is secreted via an hemi-gap junction channel, and the stimulation of $\text{P}_2\text{Y}_1\text{R}$ activates PLC- β that produces IP3 (*Figure 34*). The Ca^{2+} oscillations modulate the activity of Ca^{2+} -activated K^+ channels (so-called BK channels), and a Ca^{2+} activated outward K^+ current could be recorded: hence, Ca^{2+} oscillations induce hyperpolarization of the membrane (Kawano et al. 2006).

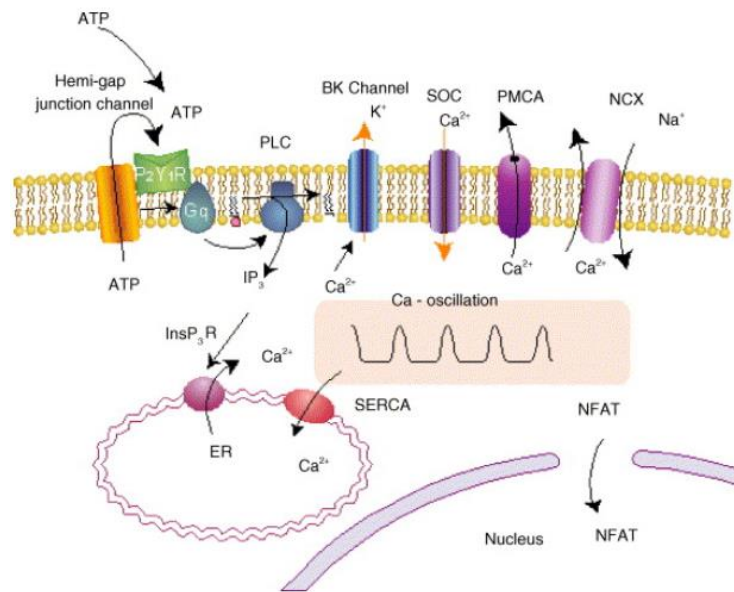


Figure 34 : mechanisms of Ca^{2+} oscillations induced by ATP autocrine/paracrine signaling (Kawano et al. 2006).

As it can be seen in Figure 34, Ca^{2+} oscillations activate the transcription factor NFAT which will be translocated to the nucleus. NFAT is dephosphorylated by Ca^{2+} /CaM-dependent phosphatase calcineurin. As seen before, the Ca^{2+} oscillations act as a frequency encoding system. The Ca^{2+} code embedded within the spontaneous Ca^{2+} oscillations frequency should be suitably translated by the cell in order to control gene expression, proliferation and differentiation (Berridge et al. 2000, 2003). NFAT is one of the Ca^{2+} -sensitive enzymes of the decoding system and its activation plays a very important role in the proliferation or the differentiation of MSC. NFAT plays a role in the process of adipocyte differentiation for example by binding to and transactivating the promoter of the adipocyte-specific gene aP2 upon fat cell differentiation (Ho et al. 1998).

The observation of the MSCs in vitro shows that not all the cells present Ca^{2+} oscillations at the same time. Some of them do not have oscillations. This difference can be related to the fact that MSCs display Ca^{2+} oscillations at the G1-S phases transition of the cellular cycle, and not all the cells in the visualisation area of an experiment are in the same phase of the cell cycle. Ca^{2+} oscillations increase levels of cell cycle regulators such as cyclins A and E and probably control cell cycle progression and proliferation, via the regulation of cyclin levels (amongst other mechanisms) (Resende et al. 2010). In addition, the MSCs presenting Ca^{2+} oscillations do not do it at the same rhythm and frequency. First the oscillations are asynchronous, and at a specific time, each cell is in a different phase of a Ca^{2+} oscillation. Secondly, the oscillations frequencies display wide variations from cell to cell. Kawano et al. observed a mean interval of 2.8 ± 1.9 minutes between an oscillation and another (Kawano et al. 2003a).

3.1.3 Calcium oscillations between MSCs and differentiated cells

The Ca^{2+} oscillations frequency is different between undifferentiated MSC and MSC on routes of differentiation and it differs between the different outcomes of differentiation (the various

differentiated cell types). While the MSCs have ordered Ca^{2+} oscillations, MSCs undergoing neuronal differentiation display disordered oscillations. The primary myoblasts present different patterns from the two, and MSC undergoing osteodifferentiation show a decrease in spontaneous Ca^{2+} oscillations frequency (Titushkin et al. 2010, Pullar 2011). This shows that each cell type (between undifferentiated MSC and differentiated cells) has its own pattern of Ca^{2+} oscillations frequency and form.

According to Titushkin *et al.*, the MSCs Ca^{2+} oscillations are suppressed after addition of neuroinductive factors, but reappear in less than 7 days after neurodifferentiation (Titushkin et al. 2010). Friel reported that sympathetic neurons displayed Ca^{2+} oscillations that do not depend on VOCCs or IP3R but on RyR (Friel 1995). Sun and colleagues observed that multipotent MSCs present 8.06 ± 2.64 Ca^{2+} spikes per 30 min of observation, and that this number decreases to 3.66 ± 2.42 after 28 days of incubation with osteoinductive factors (Sun et al. 2007). The adipocytes don't present spontaneous Ca^{2+} oscillations but different agonists such as acetylcholine can engage distinct subsystems of Ca^{2+} signaling, each of them generating oscillations with a specific temporal pattern (Turovsky et al. 2012).

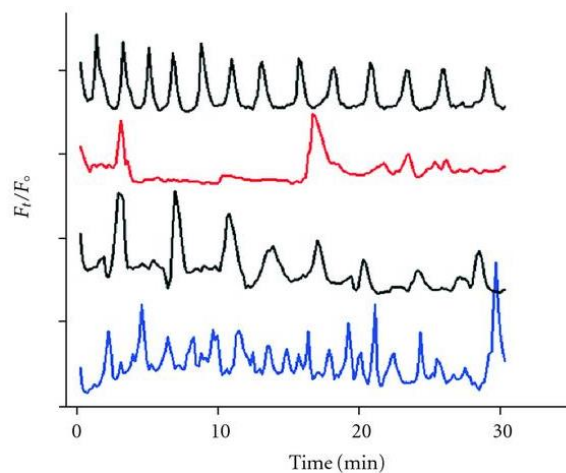


Figure 35 : different profiles of Ca^{2+} oscillations. From top to bottom: undifferentiated MSCs, MSCs undergoing osteodifferentiation (3rd week), primary myocyte, MSCs undergoing neurodifferentiation (day 5) (Titushkin et al. 2010).

As discussed before, the Ca^{2+} oscillations contain a code for the cell, and the frequency of oscillations should be suitably translated, because it controls many cell functions. The substrate rigidity for example plays crucial role in MSCs differentiation by altering the Ca^{2+} oscillations (discussed in 3.3.1) demonstrating that many stimuli (chemical and physical) on MSCs will converge to impact the Ca^{2+} signaling, and hence the control of gene expression and differentiation.

3.2 MESENCHYMAL STEM CELLS DIFFERENTIATION

As seen above, multipotent MSC can differentiate into wide variety of cellular lineages. Izadpanah *et al.* studied some properties of human and rhesus macaque (R) MSCs from bone marrow and adipose tissue. They found that the MSCs have similar multilineage differentiation capability at early passages. However, RbMSCs and haMSCs retain greater differentiation efficiency at higher passages. They found also that MSCs from all sources maintained their mean telomere length over

extended culture time (Izadpanah et al. 2006). Pittenger et al. observed a normal telomerase activity even at passage 12 (Pittenger et al. 1999).

Aksu *et al.* showed that the MSCs donor gender has an impact on osteogenic capacity of haMSCs; male haMSCs differentiate more rapidly and more effectively than female haMSCs in vitro (Aksu et al. 2008). Zhu and co-workers studied the effect of age on osteogenic and adipogenic capacity; they showed that the adipogenic potential is unchanged irrespective of the donor age but the osteogenic one decreased with increasing age (Zhu et al. 2009). These differences can be due to the difference in steroid types and functions between males and females and the variations in hormone levels with age. These differences must be taken into account when designing clinical treatments for patients (Lindroos et al. 2011).

Every MSCs differentiation has its own characteristics, markers, duration and a specific cocktail of chemicals to be added in order to obtain the specific cellular outcome. [Table 5](#) shows examples of inductive chemical factors used in some differentiation pathways.

Cell Lineage	Inductive Factors
Adipocyte	Dexamethasone, isobutyl methylxanthine, indomethacin, insulin, thiazolidinedione
Cardiomyocyte	Transferrin, IL-3, IL-6, VEGF
Chondrocyte	Ascorbic acid, bone morphogenetic protein 6, dexamethasone, insulin, transforming growth factor- β
Endothelial	Proprietary medium (EGM-2-MV; Cambrex) containing ascorbate, epidermal growth factor, basic fibroblast growth factor, hydrocortisone
Myocyte	Dexamethasone, horse serum
Neuronal-like	Butylated hydroxyanisole, valproic acid, insulin
Osteoblast	Ascorbic acid, bone morphogenetic protein 2, dexamethasone, 1,25 dihydroxy vitamin D ₃

Table 5 : examples of chemical inductive factors in order to obtain different cell lineage from MSC (Gimble et al. 2007).

MSCs produce autocrine and paracrine signals that are very important for lineage specific progression (Pittenger et al. 1999). This is why the culture medium should not be changed before 3-4 days of contact with the cells, in order to allow communication and signaling between the MSCs.

3.2.1 Differentiation into osteoblasts

MSCs osteogenic differentiation was the first differentiation to be identified by Friedenstein and co-workers in the late 1960s – early 1970s (Friedenstein et al. 1968, 1970). As the MSCs (known then as marrow stromal cells) were extracted from the bone marrow, it was not surprising that they could give rise to osteoblasts. Bruder *et al.* showed that the process of cryopreserving and thawing the cells had no effect on either their growth or osteogenic differentiation (Bruder et al. 1997), Aksu *et al.* showed that male haMSCs differentiate more rapidly and more effectively than female haMSCs in vitro

(Aksu et al. 2008), and Zhu *et al.* showed that osteogenic capacity of haMSCs appeared to decrease with increasing age of the donor (Zhu et al. 2009).

3.2.1.1 Osteogenic-induction factors

The most common factors used to mediate MSCs osteodifferentiation are dexamethasone (Dex), ascorbic acid (Asc) and β -glycerophosphate also known as glycerol 2-phosphate (G2P). The cells are first plated at a density of 10 to 15 000 cells/cm². A high cell confluence (100%) is recommended, before starting to add the osteoinductive factors, because it promotes the osteogenic differentiation. The day 1 of differentiation is the day of the first addition of the osteoinductive factors to the cells. The cells are cultured between 21 and 28 days in order to obtain osteoblasts and medium should be changed twice per week. The classical concentrations used are 10 nM for Dex, about 200 μ M of Asc and 10 to 100 mM G2P (Jaiswal et al. 1997, Pittenger et al. 1999, Lindroos et al. 2011).

Dexamethasone is a glucocorticoid steroid. Hence, it diffuses freely across the PM and has intracellular receptors. Dex contributes to osteogenic differentiation by increasing and activating (indirectly) the Runt-related transcription factor 2 (Runx2), a key transcription factor that induces osteoblast differentiation and bone formation.

Ascorbic acid enters the cells through the glucose transporters GLUT1 (Montel-Hagen et al. 2008). The Asc enhances the osteogenic differentiation by increasing the secretion of collagen type I (col1) to the extracellular matrix (ECM) and the (indirect) activation of Runx2. Asc is highly required as a cofactor for enzymes that hydroxylate proline and lysine in pro-collagen (Vater et al. 2011b) and its secretion into the ECM. Ultrastructural observations indicated that the ECM produced by Asc-treated cells is highly organized and contains well-banded collagen fibrils (Franceschi & Iyer 1992). The secretion of col1 leads to increased binding of ECM with $\alpha 2\beta 1$ integrins of the cell and the further resulting signaling of the Ras pathway, the phosphorylation of Extracellular related kinase ERK1/2, and the subsequent translocation of P-ERK1/2 to the nucleus where it activates Runx2.

Glycerol 2-phosphate: G2P enhances the mineralization of the ECM, and is critical to stimulate calcified matrix formation (already developed under the effect of Asc) (Franceschi & Iyer 1992). It is the source of phosphate needed to the formation of hydroxyapatite ($\text{Ca}_{10}(\text{PO}_4)_6(\text{OH})_2$). The alkaline phosphatase (an early osteogenic marker) plays an important role in bone ECM mineralization by removing the phosphate group from G2P. Then, the free phosphate will bind to Ca^{2+} to form the hydroxyapatite deposits. Extracellular inorganic phosphate (Pi) plays also a key role in promoting osteoblastic differentiation by regulating the expression of many osteogenic genes such as BMP2 (Tada et al. 2011) and osteopontin (Fatherazi et al. 2009).

Other osteogenic factors such as the bone morphogenetic proteins (BMPs), 1,25-Dihydroxyvitamin D3 ($1,25(\text{OH})_2\text{D}_3$) and transforming growth factor TGF- $\beta 1$ can also be used to promote osteogenic differentiation.

MSCs osteogenic differentiation was also demonstrated to occur just by cultivating MSCs with osteocytes and osteoblasts without chemical factors. Osteocytes and osteoblasts cells had synergistic

effects and produced biochemical signals to stimulate the osteogenic differentiation of MSCs (Birmingham et al. 2012).

3.2.1.2 The importance of the extracellular matrix in osteogenic differentiation

Osteogenic matrix is an essential element for the osteogenic differentiation. This matrix is secreted by the osteoblasts and, in addition to BMPs, contains growth factors, collagenous and noncollagenous proteins such as fibronectin, vitronectin, laminin, osteopontin and osteonectin (El-Amin et al. 2003). Osteoblasts must be in contact with a collagen-containing matrix before they can differentiate. This highlights the very important role of ascorbic acid in osteoblast differentiation, via the induction of collagen synthesis. The binding of osteoblasts with ECM is assured via the col1- $\alpha 2\beta 1$ integrins interaction, which leads to MAPK signaling and Runx2 phosphorylation. This step is crucial for activating osteoblast marker genes such as osteocalcin and bone sialoprotein (BSP). ECM formation is a marker of MSC differentiation to osteoblast, and it accumulates maximally after one week of culture, as collagen biosynthesis begins to diminish. After 2 weeks of culture, mineralization of ECM begins which marks the final phase of osteoblast phenotypic development (Quarles et al. 1992).

3.2.1.3 Osteodifferentiation markers

Expression of osteoblast markers follow a temporal sequence. The earliest effects of ascorbic acid for example is to stimulate type I procollagen mRNA and collagen synthesis, followed by induction of alkaline phosphatase and later on osteocalcin (Franceschi & Iyer 1992). Quarles and colleagues showed that, by the day 9 of osteodifferentiation, the cells attain confluence and stop proliferation. Downregulation of replication is associated with expression of osteoblast markers such as ALP, processing of procollagens to collagens, and progressive deposition of a collagenous ECM (Quarles et al. 1992). Later on, other bone markers can be detected (see below). The cell proliferation before mineralization is a critical process for increasing bone mass, and many physical stimuli were shown to enhance osteodifferentiation by (amongst others) increasing MSCs (on the route of osteoblasts) proliferation (Li et al. 2004, Kim et al. 2009a).

Alkaline phosphatase, found in cytoplasm and as a membrane-bound enzyme, is an early osteoblast marker (within the early stage of differentiation, from days 5 to 14 (Aubin 2001)). It is the most used marker to prove early osteogenesis in addition to col 1 (onto which the hydroxyapatite is deposited) (Rodan & Noda 1991). The Asc is essential for ALP expression and activity (Quarles et al. 1992). ALP induction is inhibited by the use of collagen formation inhibitors (Franceschi et al. 1994). The ALP can be measured quantitatively by biochemical tests relying on colorimetric enzymatic assays, or histologically by using the BCIP substrate (bromochlorylindolophosphate), a naphtol-based chemical stain (Aubin 1998, Malaval et al. 1999). Note that ALP presents a peak of expression after 2 weeks of differentiation, after which its level starts to decline (Quarles et al. 1992) while other genes are upregulated. After 3 weeks of culture, 100 nM of Dex suppresses ALP activity (Yin et al. 2006). In the study of George and colleagues (George et al. 2006), MSCs were cultured in honeycomb collagen scaffold without Dex, and the level of ALP kept increasing even after the day 14.

After 2 weeks of osteogenic differentiation (the final stage of differentiation from days 14 to 28), the late osteogenic markers (Huang et al. 2007) such as osteocalcin, osteopontin, BSPs, and osteonectin can be measured by RT-PCR (Reverse transcription polymerase chain reaction) or ELISA (enzyme-linked immunosorbent assay) (Marion & Mao 2006). Osteocalcin is an excellent marker of mature osteoblast because its expression is highly restricted in these cells (Frendo et al. 1998). Around day 16, mineralization of ECM begins. The hydroxyapatite deposits mark the final phase of osteoblast phenotypic development (Quarles et al. 1992). The mineralization in confluent monolayers can be histologically verified by Alizarin Red S or Von Kossa (silver nitrate) staining (Marion & Mao 2006).

3.2.2 Differentiation into adipocytes

The understanding and manipulation of this process may present a hope for the diminution of severity of many diseases such as obesity, diabetes and soft tissue resorption or atrophy after burns, accidents and some medications. Human immunodeficiency virus patients for example receive antiretroviral medications that may cause facial lipodystrophy, which can be socially embarrassing. Such patients would highly benefit from a tissue engineering approach that reconstruct their inadequate adipose compartment (Scott et al. 2011). Note that the adipogenic capacity of MSCs decrease with the age of the donor (Hauner et al. 1989).

3.2.2.1 Adipogenic-induction factors

Adipogenic differentiation can be induced in MSCs monolayer cultures by adding an hormonal cocktail containing dexamethasone (Dex), 1-methyl-3-isobutylxanthine (MIX), indomethacin (Ind) and insulin. There is vast inconsistency between the different recipes: between 100 and 1000 nM of Dex, 0.5 and 500 μ M of IBMX, 50 – 200 μ M of Ind, and 5 to 400 nM of insulin (Marion & Mao 2006, Styner et al. 2010, Scott et al. 2011). While a low concentration (100 nM) of Dex is used also to stimulate osteogenic differentiation, it is advised to use higher concentrations for adipogenic differentiation because higher Dex concentrations promote adipogenic differentiation and inhibit osteogenic one (Bruder et al. 1997). The treatment with the four factors mentioned above is cyclic, followed by treatment with insulin only (Maltman et al. 2011).

1-methyl-3-isobutylxanthine stimulates adipogenesis via the increase of cAMP. In details, MIX is a phosphodiesterase inhibitor that blocks the conversion of cAMP to 5'AMP, which permits the cAMP to perform its functions. cAMP decreases cell proliferation and activates the hormone sensitive lipase (HSL) which converts triacylglycerides to glycerol and free fatty acids (Gregory et al. 2005). MIX has been shown to increase the levels of the CCAAT/enhancer binding proteins (C/EBP), an essential adipogenic regulator (Cao et al. 1991).

Indomethacin is a non nonsteroidal anti-inflammatory drug (NSAID) that promotes adipogenesis by increasing both C/EBP and peroxisome proliferator-activated receptor γ (PPAR γ) (Rosen & Spiegelman 2000, Styner et al. 2010). The Ind is a ligand for PPAR γ , an early adipogenic key transcription factor that suppresses the canonical wingless (Wnt) signaling (Sekiya et al. 2004). The

inhibition of canonical Wnt signaling is primordial for the progression of adipogenesis (Gregory et al. 2005).

Insulin stimulates prenylation (addition of hydrophobic molecules) of the Ras family GTPases, which phosphorylate and activate CREB (c-AMP response element-binding protein) that, in turn, triggers the intrinsic cascade of adipogenesis (Klemm et al. 2001).

Dexamethasone exerts its effect on adipogenic differentiation by regulation of the expression of PPAR γ and CEBP α (Zilberfarb et al. 2001). While a low concentration (100 nM) of Dex is used also to stimulate osteogenic differentiation, it is advised to use higher concentrations for adipogenic differentiation because higher Dex concentrations promote adipogenic differentiation and inhibit osteogenic one (Bruder et al. 1997).

Other factors can be used to induce adipogenesis either in addition to the standard cocktail of chemicals or alone such as PARP agonists or BMP. Others can replace classical factors such as hydrocortisone (instead Dex) or thiazolidinedione (instead Ind) or forskolin (instead MIX) (Tang et al. 1999, Scott et al. 2011).

3.2.2.2 Adipogenic markers

MSCs undergoing adipogenesis undergo growth arrest at preadipocyte level before subsequent terminal differentiation into adipocytes (Gregoire et al. 1998). Early adipocytes have a spherical shape, whereas mature adipocytes are round with large perilipin-coated lipid droplets that displace nuclei to the cell periphery (Zhang et al. 2012). After one week of induction in adipogenic medium, the adipogenic markers could be detected. The key molecules and markers of early adipocytes are: accumulation of lipid vacuoles, adipogenic mRNAs and proteins production such as PPAR γ , C/EBP β , adipocyte determination and differentiation factor (ADD1), lipoprotein lipase (LPL), leptin, adiponectin and acylCoA synthetase. The markers of mature adipocytes are PPAR γ , C/EBP α , adiponectin, adipin and adipocyte fatty-acid binding protein 4 (FABP4) known also as aP2 (adipocyte protein 2) (Gregoire et al. 1998, Sekiya et al. 2004). Lipid vacuoles can be detected histologically by Oil Red O, Nile red (Aldridge et al. 2013) or boron-dipyrromethene (Bodipy) staining (Nagayama et al. 2007). Free glycerol is another indicator of triacylglycerides degradation and fatty acids synthesis by the *hormone sensitive lipase*, and it can be quantified by lysing the cells and using a glycerol kit (Pairault & Green 1979). The other adipogenesis markers can be detected either by immunocytochemistry or by RT-PCR.

3.2.3 Differentiation into neuronal cells

The MSCs differentiation to neuronal cells is a transdifferentiation because the embryogenic origin of the MSCs (the mesoderm) is different from the neuronal cells origin (the exoderm). An extensive data exists today on the MSCs neuronal differentiation ability in vitro, and many groups demonstrated that MSCs display neuronal forms and markers in a few days after culture in suitable

medium with the suitable chemical factors (Woodbury et al. 2002, Ortiz-Gonzalez et al. 2004, Jori et al. 2005).

3.2.3.1 Neurogenic-induction factors

There is a wide variety of cocktails used to induce MSCs neurogenic differentiation. These cocktails may contain one or many neuronal induction factors such as retinoic acid (RA), β -mercaptoethanol (β ME), dimethyl sulfoxid (DMSO), valproic acid, butylated hydroxyanisole (BHA), forskolin, K252a, growth factors (brain-derived neurotrophic factor, epidermal growth factor, neural growth factor), noggin factor or 5-Azacytidine (Jori et al. 2005, Mareschi et al. 2006, Liu et al. 2015). The cells are maintained in a pre-induction medium for 12-24 hours and then in an induction medium for 5-6 days. In vitro, MSCs differentiate into early neuronal cells progenitors under conditions that increase the intracellular level of cAMP (Deng et al. 2001). The co-culture of MSCs with neural cells can result also in MSCs neuronal differentiation, due to cell-cell interactions and effects of secreted soluble factors. The co-culture of MSCs with cerebellar granule neurons for example gives arise to MSC-derived neuron-like cells presenting single-action potentials and respond to several neurotransmitters such as GABA, glycine and glutamate (Wislet-Gendebien et al. 2005).

3.2.3.2 Neurogenic markers

The nestin is one of the first and very important markers for the responsive character of MSCs to extrinsic signals, and its expression in MSCs is essential for the integration of these signals (Wislet-Gendebien et al. 2005). It is essential and characteristic of neuronal precursor stem cells (after some hours of differentiation), but undetectable after 6 days of differentiation. In contrast, expression of other markers such as the Tropomyosin receptor kinase A (TrkA), also known as high affinity nerve growth factor receptor, persisted from 5 hr throughout the 6 days of differentiation (Woodbury et al. 2000). Other important neurogenic markers are the neuron-specific enolase (NSE), neuron-specific nuclear protein (NeuN), neurofilament-M (NF-M), tubule-associated unit (tau), microtubule-associated protein 2 (MAP-2) and glial fibrillary acidic protein (GFAP). With an optimal differentiation protocol, different studies showed that almost 80% of the cells express NSE and NF-M (Woodbury et al. 2000) or become immunoreactive for NeuN, nestin, and GFAP (Mareschi et al. 2006). Deng *et. al* showed that undifferentiated cultures of MSCs express some markers characteristic of neural cells such as microtubule-associated protein 1B (MAP1B), TuJ-1, NSE and vimentin. After treatment with an adequate neural induction medium, the MSCs differentiated into neuronal cells showed increased levels of both NSE and vimentin (Deng et al. 2001), and expressed tau protein in their cell body (Black & Woodbury 2001).

3.3 EFFECTS OF PHYSICAL STIMULI ON THE MSCs DIFFERENTIATION

The cell density, the optimal combination and concentration of growth factors, cytokines, basal nutrients and serum supplements have important impacts in controlling MSCs differentiation process and cell fate. Recent studies have tested also the effect of mechanical forces and electromagnetic fields on the differentiation outcomes.

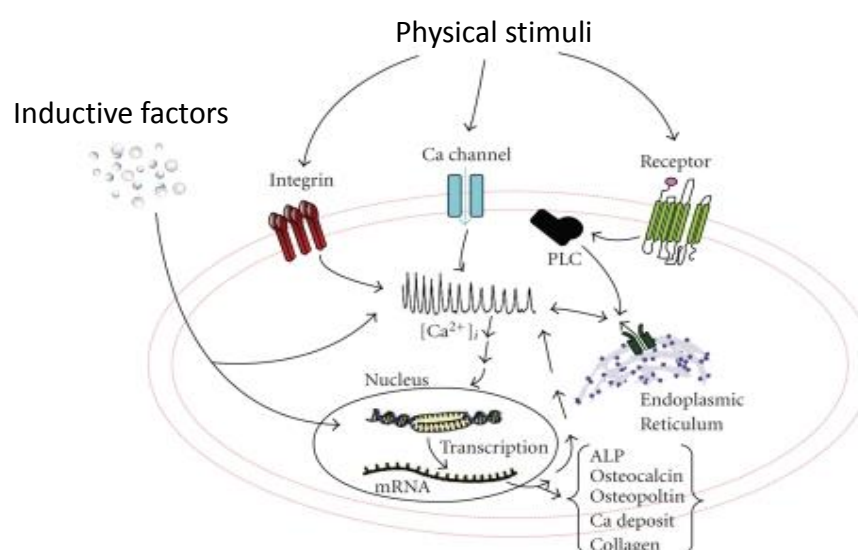
3.3.1 Effect of mechanical stimulation

The substrate rigidity plays crucial role in stem cell differentiation (Engler et al. 2006) and influences Ca^{2+} signaling. It was shown that substrate rigidity regulates Ca^{2+} oscillations via Ras homolog gene family member A (RhoA) and its downstream effector the molecule Rho-associated protein kinase (ROCK)(Kim et al. 2009b). MSCs cultured on gels with low elastic moduli displayed low RhoA activities. Lowering the substrate stiffness to 1 kPa significantly inhibited both the magnitudes and frequencies of Ca^{2+} oscillations in comparison to stiffer or more rigid substrates (Kim et al. 2009b).

Altman *et al.* showed that the application of a cyclic mechanical stimulation (translational and rotational strain) to undifferentiated MSCs embedded in a collagen gel, over a period of 21 days resulted in ligament cell lineage differentiation even without differentiation factors. The differentiated ligament cells expressed ligament markers such as oriented collagen fibers I and III and tenascin-C. They did not express bone or cartilage-specific cell markers which demonstrate the specificity of the differentiation (Altman et al. 2002). Ward and colleagues studied the effect of the application of a 3-5% tensile strain to a collagen I substrate and saw that it stimulates osteogenesis of attached human MSCs (hMSCs). This mechanical strain increased osteogenic markers expression and matrix mineralization while simultaneously reduced the expression levels of other lineage markers (chondrogenic, adipogenic, and neurogenic). They showed that mechanical strains enhanced osteogenic differentiation through the ERK MAP kinase pathway (Ward et al. 2007). Another study of Datta *et al.* underlined the synergetic effect of the combination of a mechanical stimulation and ECM and dexamethasone. They showed that rat MSCs cultured on titanium fiber mesh discs exhibit high levels of osteogenic markers when they are cultured in the presence of fluid shear stresses, ECM and dexamethasone (Datta et al. 2006). The oscillatory fluid flow was studied by another group that showed also the positive effect of such a shear stress on MSC osteodifferentiation. They showed that the mechanotransduction involved intracellular Ca^{2+} mobilization, demonstrating the role of Ca^{2+} signaling in the differentiation process (Li et al. 2004). Many other studies mentioned the effects of shear stress (Zhao et al. 2007, Kreke et al. 2008, Sharp et al. 2009) and mechanical stretch i.e. uniaxial cyclic tensile strain (Yoshikawa et al. 1997, Sumanasinghe et al. 2006), equibiaxial cyclic strain (Simmons et al. 2003), on MSCs osteodifferentiation.

Ca^{2+} oscillations play an important role in the mechanotransduction of a mechanical signal in the cells. A study of Jing *et al.* showed that tissue strain and shear stress on mouse tibia is transduced by repetitive Ca^{2+} spikes in the osteocytes. The spikes frequency and amplitude depend on the mechanical magnitude. The oscillations were inhibited by the ER depletion or the inhibition of PLC and P_2 purinergic receptors (P_2R). This study demonstrated that osteocytes respond to mechanical stimulation, in situ, by Ca^{2+} oscillations dependent on $\text{P}_2\text{R}/\text{PLC}/\text{IP}_3$ pathway (Jing et al. 2014).

Low intensity ultrasounds (LIUS) are another form of mechanical stress, and has been shown to enhance the chondrogenic differentiation. When human MSCs cultured in pellets were treated with transforming growth factor beta (TGF- β) and exposed to LIUS for 20 min every day, they displayed enhanced chondrocyte differentiation (Ebisawa et al. 2004). However when LIUS are compared to TGF- β , the LIUS were more effective in enhancing chondrogenesis, especially when the MSCs were cultivated in a fibrin-hyaluronic acid hydrogel (Choi et al. 2013).



3.3.2 Effect of the electric, electromagnetic fields and the membrane potential

application of an electrical stimulation alone failed to differentiate the MSCs, which demonstrates the synergistic effects between the soluble osteoinductive factors and the electrical stimulation. Another study showed that the exposition of hMSCs to a static biphasic electric current (BEC) promotes osteogenic differentiation. The hMSCs were exposed to a 100 Hz electrical stimulation with a magnitude of 1.5 to 15 $\mu\text{A}/\text{cm}^2$ for 250 to 25 μs respectively. The cells presented increased proliferation under the electric stimulation (ES) for 5 days (the importance of cells proliferation before bone mineralization was already discussed in 3.2.1.3), and enhanced calcium deposition after 7 days (after the electric stimulation). The osteogenic differentiation was enhanced by the mitogenic effect of BEC and the activation of VOCCs and MAPK (Erk and p38) pathway (Kim et al. 2009a). The common mechanism between the two studies cited above is the activation of the MAPK pathway by the electric stimulation, which is known to be involved in cell differentiation (Luttrell 2002, Burdon et al. 2002). However, the activation of VOCCs was not observed in the two studies: in the study of Kim *et al.*, the ES was sufficient to activate VOCCs, whereas the 0.1 V/cm used by Sun *et al.* did not alter the membrane potential because the electric field was too low.

Other studies using electrical stimulation of bone cells showed also the implication of Ca^{2+} in the effects of the ES. They suggested an increase of intracellular Ca^{2+} concentration either by the activation of VOCCs and the Ca^{2+} - CaM pathway inducing a proliferative response in the cells (Lorich et al. 1998, Brighton et al. 2001), or by the stimulation of PLC-coupled cell surface receptors, IP3-dependent intracellular processes and activation of SOCCs (Khatib et al. 2004). Electrical stimulation also induces integrin activation, redistribution, clustering and assembly of some FA proteins such as paxillin, vinculin, FAK and src (Cho 2002, Wozniak et al. 2004). Such assembly could induce the MAPK activation (Miranti & Brugge 2002) and hence cell differentiation.

Electromagnetic fields (EMF) can also promote MSCs differentiation to osteoblasts through Ca^{2+} -related mechanisms. The exposition of MSCs to pulsed EMF for 10 min every day at the same time resulted in the enhancement of the early stages of osteogenesis (first 2 weeks) through the activation of VOCCs and the increase of intracellular Ca^{2+} concentrations (Peteccchia et al. 2015). Many other studies showed also that the effects of EMF, whether beneficial or not, are mediated by VOCCs (Pall 2013).

Many reports mention the relationship between membrane depolarization and control of proliferation and differentiation. They show that proliferative and relatively immature cells exhibit depolarized membrane potentials, while terminally differentiated quiescent cells exhibit hyperpolarized membrane potentials (Cone, Jr. 1970, Cone & Tongier 1971, Binggeli & Weinstein 1986, Olivotto et al. 1996, Wonderlin & Strobl 1996, Levin 2007). A study of Sundelacruz and colleagues showed that the transmembrane potential is an essential determinant of differentiation, and that it can control the adipogenic and osteogenic differentiation of MSCs (Sundelacruz et al. 2008). They observed that the process of MSCs differentiation was accompanied by a hyperpolarization in membrane potential, and that differentiated osteoblasts and adipocytes have a hyperpolarized membrane whereas the undifferentiated MSCs have a depolarized membrane. They demonstrated that membrane depolarization, either by the addition of high concentrations of extracellular K^+ or the addition of ouabain (a Na^+/K^+ ATPase blocker), suppresses the osteogenic and adipogenic differentiation. However, hyperpolarization by ATP-sensitive K^+ channel openers pinacidil and diazoxide, during osteogenic differentiation causes upregulation of osteogenic markers (Sundelacruz et al. 2008).

4 MEMBRANES ELECTROPORATION

The plasma membrane (PM) is the physical barrier that shields the cell interior from the external medium. It preserves the integrity of the cells and controls all the exchanges between the interior and the exterior via its very wide collection of channels and receptors. Nevertheless, it would be important to cause a temporary rupture in the PM structure in order to let interesting non permeant molecules to reach the cell. Such molecules can be drugs, genetic material or chemicals compounds. The rupture of PM does not cause only the entry of certain compounds but also the leakage of internal material. The passage of ions or molecules always occurs according to the concentration gradient.

The fact of breaking the PM integrity is called membrane permeabilisation, because it will make the PM permeable to usually non permeant compounds. In its quiescent state, the cell controls what goes in and what comes out via the PM. When permeabilised, the PM loses this control but temporarily, because every uncontrolled PM permeabilization, either in space or in time may cause drastical outcomes leading to cell death. This is why, the factors that are used to cause PM permeabilization should be controlled and set carefully in order to give the desired outcomes without causing cell mortality, unless the purpose of the permeabilization is to break irreversibly the integrity of the PM.

Many chemical and physical factors can be used to permeabilize the PM. Molecules such polyethylene glycol are used for cell transfection, transformation (Bibb et al. 1978, Chang & Cohen 1979) or even to cover nanoparticles carrying drugs or DNA to the cells (Brigger et al. 2002, Cha et al. 2013). The PEG is not toxic and protects nanoparticles from the immune system (Jokerst et al. 2011). Another chemical that can permeabilize the PM is the DMSO. The DMSO is known to be a cryoprotector agent of the cells when they are frozen, but can also cause membrane permeabilization (Hempling & White 1984, Ménorval et al. 2012). The sonoporation is a physical way to permeabilise the PM by using ultrasounds. The use of microbubbles greatly enhances the outcomes of this technique. The sonoporation causes the formation of short-lived pores in the PM lasting for a few seconds, and up to 100 nm in effective diameter (Newman & Bettinger 2007). Sonoporation has been successfully used to enhance gene transfer in vitro as well as in vivo (Lan et al. 2003, Guo et al. 2004). Another physical way lays on the use of an electric field to achieve PM permeabilization and is called electroporation. It is a simple, easily applicable, very efficient and non invasive technique used in vitro and in vivo for many purposes such as cell transfection and electrochemotherapy.

4.1 A BRIEF HISTORICAL VIEW

The first works on electroporation (called also electropermeabilisation) started in the 60s with Sale and Hamilton. While studying many cell types in culture, they demonstrated that unpermeant molecules to the PM in physiological conditions can cross it after the application of an intense electric field pulse (Sale & Hamilton 1968). They observed that the degree of lysis of a cell suspension population depends on the electric field strength. In 1972, Neumann and Rosenheck showed that electric pulses of 20 kilovolts/centimeter (kV/cm) cause transient permeability changes in the membranes of vesicles storing biogenic amines. They monitored the PM permeabilisation by the

measurement of the amount of catecholamines released by these vesicles (Neumann & Rosenheck 1972). A few years later, Kinosita and Tsong published an important study showing that the exposure of an isotonic suspension of erythrocytes to an electric field (EF) of 2.2 kV/cm, makes the erythrocytes PM becomes leaky to normally impermeant ions or molecules. They demonstrated that the passage of molecules across the PM is due to the formation of pores in this latter. The size of these pores can be varied in a controlled manner and they can be resealed (Kinosita & Tsong 1977). In 1982, Neumann *et al.* drive gene transfer into mouse lyoma cells by using electric pulses and found that this technique greatly enhances the DNA transfer into the cells. After six years, Mir and colleagues achieved the electroporation of 90% of cultured NIH 3T3 cells by using 8 successive square pulses of 100 μ s and 1500 V/cm (Mir *et al.* 1988). From then on, the applications using electroporation grew considerably in biology, medicine, research and food industry.

4.2 THE ELECTROPORATION PRINCIPLE

The electroporation (or electroporation) occurs when the cells are subjected to an electric field sufficiently high. The cells are placed between two electrodes where an electric field is applied (*Figure 37*). The zones of the cells that are more subjected to the electric field, and hence more permeabilized, are the two poles facing the electrodes. According to the electric pulse parameters (electric field amplitude, pulse duration, frequency of repetition), to the cell type and to the properties of the external medium, the PM permeabilization could be reversible, as cells recover after the pulse, or irreversible, thus leading to cell death. The reversible electroporation is used to make molecules of interest enter the cell, such as therapeutic molecules, drugs or genetic material (Hofmann *et al.* 1999, Widera *et al.* 2000, Lucas & Heller 2003, Mir *et al.* 2005) and can be used to achieve cell fusion (Claude & Justin 1983). The irreversible electroporation is used to kill harmful cells such as cancerous cells in vivo (tumor ablation) (Al-Sakere *et al.* 2007), bacterial decontamination and food processings (Schoenbach *et al.* 2000, Schultheiss *et al.* 2002) or even to increase the efficiency of juice extraction from fruits (Bouzzara & Vorobiev 2000).

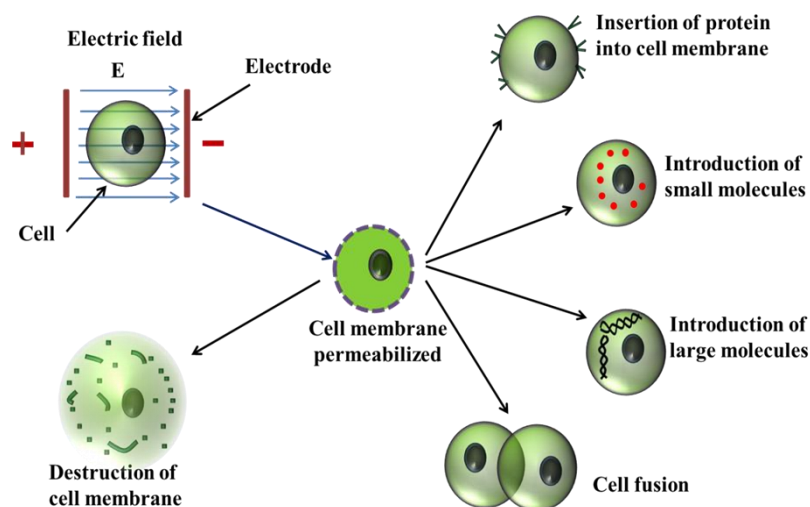


Figure 37 : the electroporation principle and applications (Subhra et al. 2013).

4.2.1 The induced transmembrane potential

In its quiescent state, the cell has a resting transmembrane potential (TMP) insured by the function of the Na^+/K^+ ATPase (*cf. section 1.1.5*). The resting TMP $\Delta\Psi_0$ ranges from about - 4.5 (Veech et al. 1995) to - 200 millivolts (mV) (Campbell n.d. et al., 2008) depending on the species and the cell type. When a cell is subjected to an electric field, an induced TMP $\Delta\Psi_i$ is added to the resting $\Delta\Psi_0$. The $\Delta\Psi_i$ is mainly due to the movements of mobile charges caused by the electrophoretic force of the electric field. This displacement of electric charges (mostly ions) causes further charging of the PM and hence the $\Delta\Psi_i$.

The charging time τ_m of a membrane is the time required to charge the surface of this membrane. The τ_m of the PM depends on the electrical parameters of the cell and the medium in which it is suspended and it is given by the equation (Cole 1937):

$$\tau_m = rC_m (\rho_c + \rho_0/2) \quad (1)$$

where C_m is the membrane capacitance (considering that the PM acts as a dielectric layer with no leakage currents), r is the cell radius, ρ_c is the resistivity of the cytoplasm, and ρ_0 is the resistivity of the extracellular medium. This equation is mainly applied to spherical cells in suspension (Deng et al. 2003).

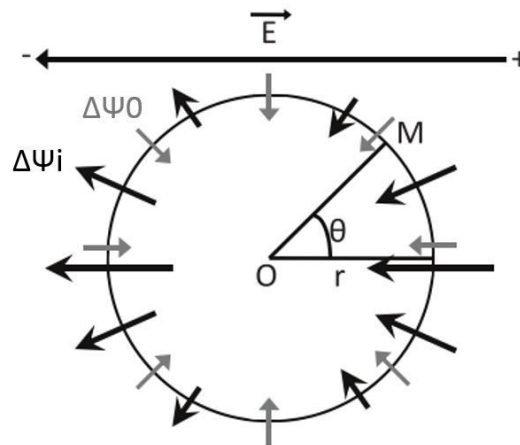


Figure 38 : representation of $\Delta\Psi_0$ and $\Delta\Psi_i$ on a cell of a radius r exposed to an electric field. The sign (+) represents the anodic side and the (-) is the cathode, (Ecoffre & Rols 2012).

The charging time of the PM is approximately 100 ns for mammalian cells (Ashton Acton 2012). By using electric pulses with longer duration than the charging time of the PM, this latter has the time to be charged, and if the electric field is high enough, to be permeabilised. Shorter pulse durations are thought to have more effects on the cell interior, and if high enough, to permeabilize the organelles membranes. However, recent studies show that, it is not obligatory that the pulse has a sufficient duration to cause membrane charging, because such observations were done with ultrashort electric pulses (Frey et al. 2006, Pakhomov et al. 2007). The $\Delta\Psi_i$ is given by Laplace equation (Pauly & Schwan 1959):

$$\Delta\Psi_i = f E r \cos \theta (1 - e^{-t/\tau_m}) \quad (2)$$

where E is the electric field amplitude, r is the cell radius, θ is the angle between the electric field direction and the normal to the surface at a specific membrane position, t is the duration of the

exposure to the electric field and τ_m is the charging time of the membrane. f is a function depending on the electrical and dimensional properties of the cell and the surrounding medium, and is given by the equation (Kotnik et al. 1997):

$$f = \frac{3\lambda_0 [3dr^2 \lambda_i + (3d^2r - d^3)(\lambda_m - \lambda_i)]}{2r^3 (\lambda_m + 2\lambda_0) \left(\lambda_m + \frac{1}{2}\lambda_i\right) - 2(r-d)^3 (\lambda_0 - \lambda_m) (\lambda_i - \lambda_m)} \quad (3)$$

where d is the PM thickness, C_m is its capacitance, λ_0 , λ_i and λ_m are the conductivities of the extracellular medium, the cytoplasm and the PM respectively.

Two simplifications can be done on equation (1): first, if the PM is considered as a perfect insulator, hence its conductivity is considered as zero, and f will be approximately $3/2$. Second, it is often assumed that τ_m is much smaller than t , and in this case e^{-t/τ_m} will be zero, and equation (2) is simplified to become the Schwan equation (Schwan 1957):

$$\Delta\Psi_i = \frac{3}{2} E r \cos \theta \quad (4)$$

As a consequence of this equation, the cells that have a large radius require a lower electric field to get their membrane permeabilized than cells having a small radius.

As it can be seen on [Figure 38](#), $\Delta\Psi_i$ is added to $\Delta\Psi_0$ at the anodic side of the cell, whereas it is against it on the cathodic side. Because the total TMP $\Delta\Psi_m$ is the addition of $\Delta\Psi_i + \Delta\Psi_0$, hence the pore formation process begins on the anodic side of the electrically stressed membrane (Hu et al. 2005, Frey et al. 2006). The charges accumulation is the highest on the 2 poles of the cell facing the 2 electrodes ([Figure 39](#)), which makes them the regions where the permeabilization occurs. On the anodic side, the PM is hyperpolarized, whereas on the cathodic one, it is depolarized. In these two regions, the total TMP $\Delta\Psi_m$ is higher than the other parts of the cell. According to Schwan equation, the 2 positions of the cell that make an angle θ of 0° or 180° with the electric field direction, are the positions where the total TMP $\Delta\Psi_m$ is the highest, and these positions are indeed in the 2 poles of the cell facing the 2 electrodes. According to the same equation, the 2 positions of the cell that are perpendicular to the electric field direction, are the positions where the total TMP $\Delta\Psi_m$ is the lowest and it is equal to zero.

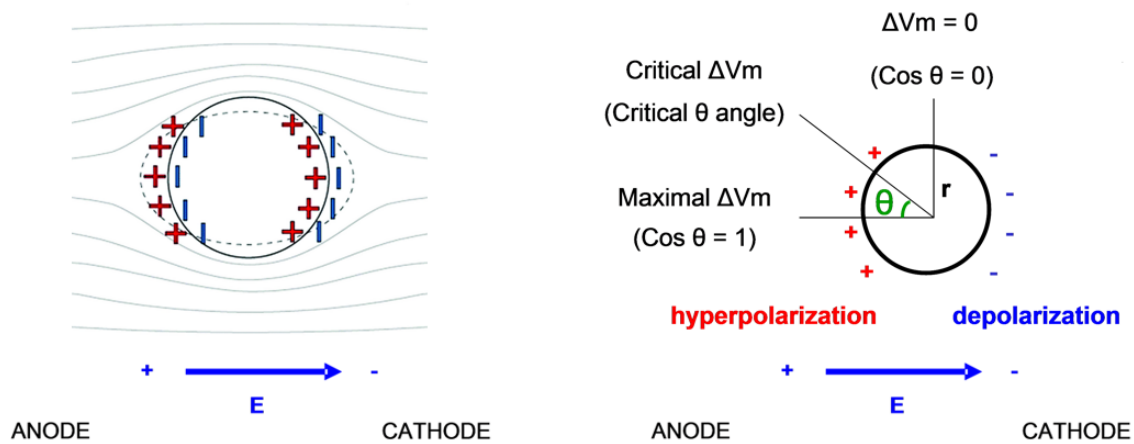


Figure 39 : left: field lines and charges distribution on the 2 poles of the cells facing the anode and the cathode, right: the total TMP (ΔV_m) at different angles relative to the electric field direction (Burgain-Chain & Scherm 2013, Vlahovska 2015).

These theoretical predictions were confirmed by many experimental studies as demonstrated by Kinoshita *et al.* (Kinoshita et al. 1988) and later on by Kotnik *et al.* (Kotnik et al. 2010). By using the voltage sensitive dye di-8-ANEPPS to determine total TMP $\Delta\Psi_m$, and the propidium iodide (PI) to monitor the transmembrane transport, Kotnik *et al.* demonstrated that the highest absolute values of $\Delta\Psi_m$ are found in the regions of the PM that face the two electrodes, and that the PI transport is mainly confined to these regions. Another important demonstration of their study was that the theoretical model is not only applicable to spherical or regular cell shapes, but also to cells with irregular shapes as can be seen in [Figure 40](#). According to this study, the cell region facing the anode is the most permeabilized.

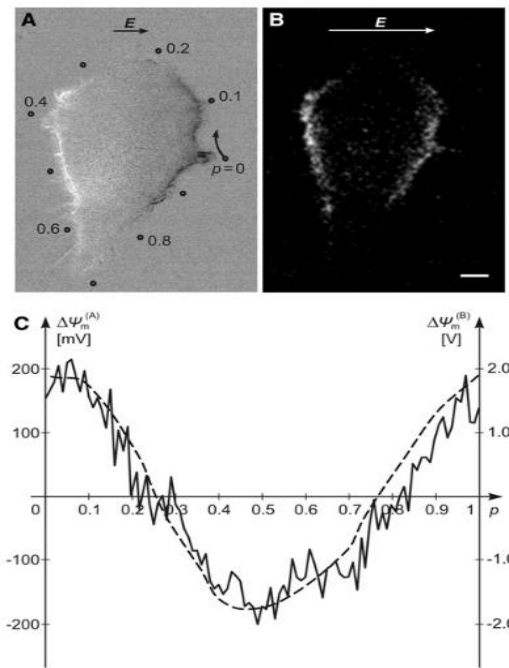


Figure 40 : local variations of the TMP of an irregular shaped Chinese Hamster Ovary (CHO) cell. A: changes in fluorescence of di-8-ANEPPS caused by a nonporating 50 ms, 100 V/cm pulse. B: PI transport caused by a porating 200 μ s, 1000 V/cm pulse, visualized in the same cell after 200 ms of exposure. The bar is 5 μ m. C: the dashed line represents the $\Delta\Psi_m$ predicted by numerical computation, and the solid line represents the $\Delta\Psi_m$ measured along the path shown in A (Kotnik et al. 2010).

4.2.2 The permeabilization threshold

The permeabilisation threshold is the level that $\Delta\Psi_i + \Delta\Psi_0$ should reach to cause changes in membrane properties and its permeabilisation. This concept was first introduced by Neumann and Rosenheck in 1972 (Neumann & Rosenheck 1972). The permeabilisation threshold is not a fixed value; it depends, between others, on the cell type, the original TMP of a cell $\Delta\Psi_0$, and the size and conformation of the permeabilization marker. Sale and Hamilton calculated the potential difference across the PM of spherical cells in suspension exposed to an electric field, and noticed that lysis occurred when the potential difference reached about 1 V in average (Sale & Hamilton 1968). The same result was obtained by 2 independent studies leaded by Coster and Simmermann in 1975 and by Kinoshita and Tsong in 1977; Coster and Simmermann worked on *Valonia utricularis* (a genus of green

algae), and demonstrated that the critical breakdown potential is 1V at 4°C. Interestingly, this potential was strongly dependent on the temperature, and decreased to 640 mV at 30°C (Coster & Simmermann 1975). Kinoshita and Tsong found that the EF necessary to permeabilize erythrocytes in suspension corresponds to a TMP of approximately 1 V (Kinoshita & Tsong 1977). Later on, Hibino et al. demonstrated that the permeabilization threshold of sea urchin eggs is 1V (Hibino et al. 1993).

However, other studies showed that the permeabilisation threshold may be under 1V. Teissié and Rols calculated a TMP, needed to permeabilise the protoplasts (cells that have their wall removed) of bacteria and plant, between 100 and 250 mV only. They demonstrated also that CHO cells are permeabilized when their TMP reaches 250 mV (Teissié & Rols 1993), a value near to the permeabilization threshold of 100 nm lipidic vesicles, that was found to be between 200 and 300 mV by Teissié and Tsong (Teissie & Tsong 1981). By using the whole cell patch-clamp technique on protoplasts derived from the tobacco culture cell line "Bright yellow-2", Wegner et al. demonstrated that an electroporation occurred when the PM was either hyperpolarized or depolarized beyond threshold values of around -250 to -300 mV and +200 to +250 mV, respectively (Wegner et al. 2011). They demonstrated also that a TMP of 800 mV is required to permeabilise a protoplast of green marine algae. As a conclusion of the studies cited above and many others in the bibliography, the permeabilisation threshold of the PM ranges from 100 to 1000 mV (1V).

4.3 SOME FACTORS THAT INFLUENCE THE PERMEABILIZATION THRESHOLD AND IMPACT THE ELECTROPORATION OUTCOMES

When the total TMP $\Delta\Psi_m$ ($\Delta\Psi_i + \Delta\Psi_o$) reaches the permeabilisation threshold, the PM loses its insulating character and becomes permeabilised. The electroporation can be quantified by the internalization of impermeant dyes or the leakage of cytoplasmic components such as ATP (Rols & Teissié 1990). In the case of a reversible electroporation, the permeabilized state of the PM lasts from some minutes (Pakhomov et al. 2007) to some tens of minutes, after which the PM returns to its original state (Wilhelm et al. 1993). The permeabilization threshold, the pore formation, extension and lifetime depend on the electric pulse parameters, the cell geometry, the PM and the medium composition.

4.3.1 The impact of the electric field amplitude

One of the most important factors of an electric pulse, which determines the permeabilisation threshold and the PM breakdown is the electric field (E) amplitude. The E amplitude determines the $\Delta\Psi_i$ that favors the development of the pores (Abidor et al. 1979). Rols and Teissié demonstrated that the fact of reaching the permeabilisation threshold is directly dependent of the electric field amplitude. When the electric field amplitude increases, the permeabilized area of the permeabilized zone increases (Rols & Teissié 1990), and larger molecules can cross the PM. If higher electric field amplitudes are applied, the percentage of permeabilized cells increases until reaching a plateau. Above

a certain value of the electric field, a mortality of the cells starts to be observed. This value is dependent on the cell type, the extracellular medium and many other factors.

Many models attempted to explain how the PM breakdown occurred after the application of an electric field. According to the bilayer lipid membrane (BLM) model (known also as bimolecular or black lipid membrane) of Crowley (Figure 41), the membrane is modeled as a homogeneous isotropic and viscoelastic layer that has insulating electrical properties. When the membrane is subjected to an electric field, a compressive electric force tends to crush it. If the compressive force exceeds a critical value, in a way that the viscoelastic force of the elastic layer could not compensate it, hence the membrane is ruptured (Crowley 1973). It should be noted that the restoring elastic force of a stretched membrane is inversely proportional to its length; the more the membrane is long, the more its restoring elastic force is small. Another model interpretation of the breakdown phenomenon is based upon the concept of structural defects in the PM, whose development is favoured by the electric field (Abidor et al. 1979). The membrane breakdown is a multistep phenomenon that can be divided into three stages: (i) growth of the membrane surface fluctuations, (ii) molecular rearrangements leading to membrane discontinuities, and (iii) expansion of the pores, resulting in the mechanical breakdown of the membrane (Dimitrov 1984). However, these models did not predict neither the effect of an electric field increase above the permeabilization threshold, nor the effect of the duration or the number of the pulses. The pore creation time has been shown to decrease as the electric field amplitude initiating it increases (Ziegler & Vernier 2008).

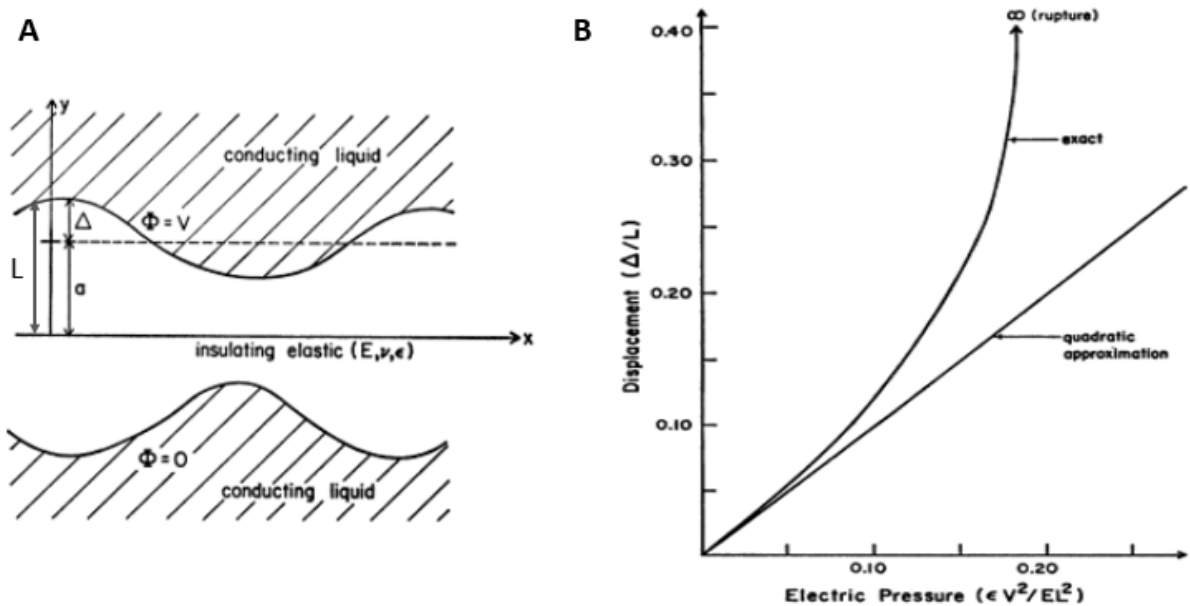


Figure 41: electrical breakdown of the membrane. A. Membrane is modeled as an electrically insulating elastic layer surrounded by a conducting liquid. B. An applied electric field squeezes the membrane, and ruptures it. a : the original semi-thickness of the membrane, L : the new semi-thickness after electric compression, $\Delta = L - a$, V : the voltage applied, ϵ : the permittivity of the membrane, E : young's modulus, a property of the membrane dependent on its capacitance and thickness (Crowley 1973).

4.3.2 The impact of the pulse duration

Another major determinant of the electroporation is the electric field duration. Frey *et al.* demonstrated that the pore size depends on the duration of the electric pulse (Frey *et al.* 2006). The microseconds to milliseconds pulses (with an EF amplitude high enough) generate relatively large pores in the PM, sufficient for the passage of large molecules such as bleomycin, siRNA and DNA plasmids. The pulses with a duration of nanoseconds are thought to create small pores in the PM that allow ions but not large molecules to pass through (Chen *et al.* 2004, Hu *et al.* 2005). Moreover, the membrane stability depends on the duration of the electric field (Tien & Diana 1967). This could be explained by the fact that the creation of an electropore is completely stochastic, hence when the pulse duration increases, the probability for a pore formation increases also. Rols and Teissié demonstrated that the permeabilisation threshold depends on the electric field amplitude, and the molecules flow across the permeabilized PM depends on the pulse duration [and the number of pulses] (Rols & Teissié 1990). The microscopic observations of individual living cells demonstrated different effects between electric pulses of different duration. A 100 μ s pulse for example induces cellular swelling and a median PM permeabilization duration of 5 minutes, whereas after a 60 ns pulse, the membrane permeability is delayed to a median of 17 minutes with no cellular swelling.

4.3.3 The impact of the number of the pulses

Mauroy *et al.* found that increased number of pulses caused lipid loss and a decrease in size of giant unilamellar vesicles (GUVs) (Mauroy *et al.* 2012). As seen above, the molecules flow intensity across the permeabilized PM depends on the pulse duration and the number of pulses (Rols & Teissié 1990). In a recent work of Silve *et al.*, it was demonstrated that a large number of pulses resulted in a large number of pores or defects in the PM. The authors showed that, with an external concentration of 3 μ M, one single 10 ns pulse of 40 kV/cm is sufficient to allow the uptake of bleomycin in 20% of cells. The same levels of cytotoxicity can be reached even with a 100 fold reduction in the external bleomycin concentration, if the number of pulses is increased 25 times (Silve *et al.* 2012). The authors found that, due to the very short half life of a nanopore (Levine & Vernier 2010), the fact of increasing the number of pulses may have the same result than the addition of the effects of each separate pulse. This means that the higher number of pulses cause additional defects (additional pores) in the PM rather than stabilizing initial ones or increasing their size. This is also demonstrated by the inverse relationship between the external concentration of bleomycin, and the number of pulses needed to cause cell death, in another words, the entry of at least 500 bleomycin molecules. A recent study of Pakhomov *et al.* showed also that increasing the pulse number resulted in increasing the pores number, not the size of pre-existing pores (Pakhomov *et al.* 2015).

4.3.4 The impact of the pulses frequency

Several studies demonstrated that electric pulses delivered at low repetition rates are more efficient in inducing electroporation. Silve *et al.* showed that, for pulses of 100 μ s, a saturation was observed below a frequency of 0.1 Hz, and that the pulses delivered at such frequencies were

more efficient than those delivered at higher ones, from 1 Hz to 7 kHz (Silve et al. 2014). This study was conducted on potato cells but other studies showed also the same tendencies on other plant tissues such as onion (Asavasanti et al. 2011) and apple (Lebovka et al. 2001), where lower frequencies (< 1 Hz) caused more damage to tissue integrity than higher ones (1 Hz to 5 kHz). Other in vivo studies are in agreement with the previous ones. Sersa *et al.* demonstrated that the electrochemotherapy (*cf.* 4.7.1) of mouse sarcoma tumors was more effective when using electric pulses trains at 1 Hz compared to 5 kHz. They explained this effect by the fact of prolonged exposition of electroporated tumors to the chemotherapeutic drugs and a greater electroporative effect (Sersa et al. 2010). The use of shorter pulses (in the nanosecond range) gave the same outcomes; a greater permeabilization is observed when pulses are delivered at very low repetition rate (Silve et al. 2014).

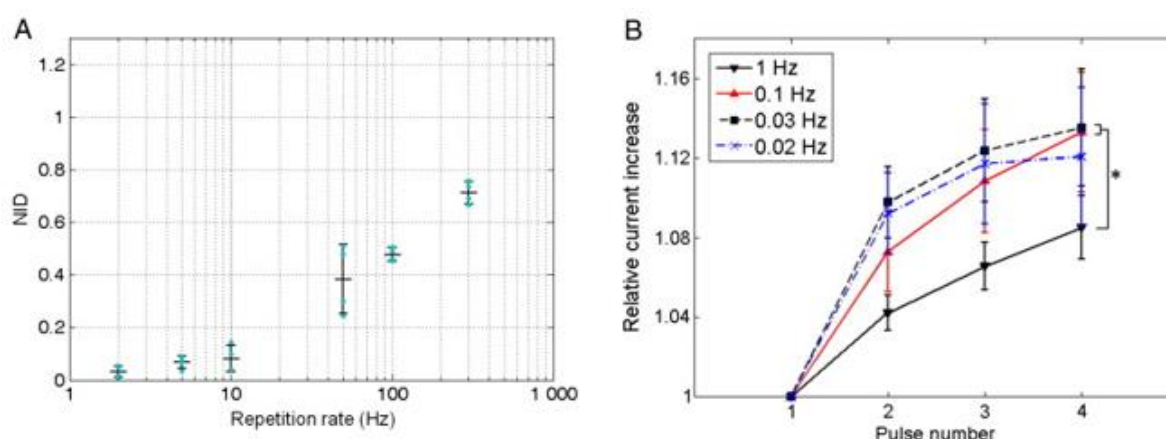


Figure 42 : Pulse repetition rate impact during the exposure to A: 300 pulses of 10 ns pulse and 40 kV/cm and B: 4 pulses of 100 μ s and 300 V/cm, NID: normalized impedance drop (Silve et al. 2014).

4.3.5 The impact of the cell shape and diameter

The Schwan equation implies that the cell size affects the electroporation outcomes. The permeabilisation threshold is inversely proportional to the diameter of the object wanted to be permeabilized. Larger GUVs for example are more affected at lower electric field strengths than the smaller ones (Mauroy et al. 2012). The restoring elastic force of a stretched membrane exposed to an electric field is inversely proportional to its length; this means that the more the size of a cell or a vesicle is large, the more the elastic force of their membranes, compensating the compressive electrical force, is small, hence they are more easily permeabilized (Crowley 1973). This is why cells in suspension need higher electric field amplitudes to be permeabilized than when they are attached and spread. This has been demonstrated in Rols and Teissié's study in 1990: the same CHO cells are not permeabilised with the same electric field amplitudes when they are in suspension or attached. A 700 V/cm pulse (of 100 μ s) was needed to observe a trypan blue entry in the cells in suspension, whereas 300 V/cm was sufficient to obtain the same effect when the cells were attached and spread (Rols & Teissié 1990).

Kotnik and colleagues performed many simulation studies that showed how the geometry and the orientation of the cells relative to the orientation of the electric field impact the induced transmembrane potential on different points of the cells (Kotnik & Miklavcic 2000, Kotnik et al. 2010).

An example in [Figure 43](#) shows a cell with 2 different radius R_1 and R_2 , and demonstrates how the cell with the highest R_2 compared to R_1 presented the highest maximum values of induced TMP, and how the shape of the curves depend on the cell geometry.

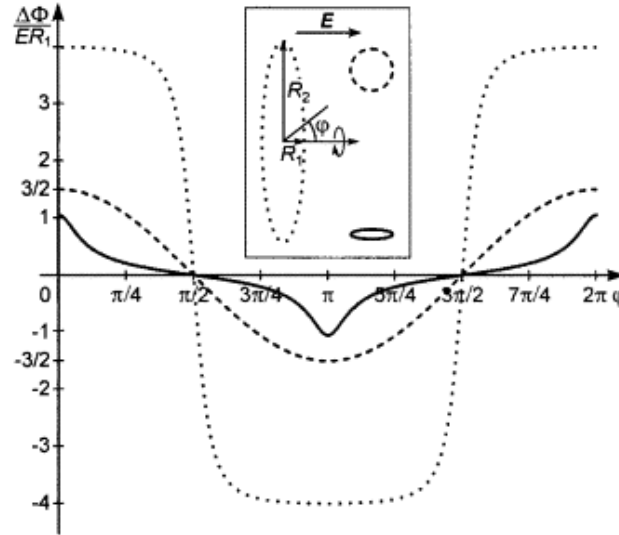


Figure 43: Left: the induced transmembrane voltage ($\Delta\Phi$) in units of ER_1 as a function of the polar angle φ for three spheroidal cells with equal R_1 and $R_2 = 1/5 R_1$ (solid line), $R_2 = R_1$ (dashed line), and $R_2 = 5 R_1$ (dotted line) (Kotnik & Miklavcic 2000).

4.3.6 The impact of the plasma membrane properties and lipid composition

The process of electroporation was demonstrated experimentally in vitro on different kinds of cells and in vivo. However, the simplest model to study the process remains the GUV which is a purely lipidic structure assembled in vitro. The GUV is being the simplest model to study membrane electroporation, because this phenomenon occurs normally in lipids-rich zones of the PM. The composition of the GUV can involve one single lipid or a combination of two or more lipids. These lipids can be either synthetic or natural. The complexity of the GUV could be monitored by adding or not the cholesterol which makes the GUV nearer in properties to the physiological PM. The rupture voltage is dependent upon the nature, the lipid composition and the physico-chemical properties of the membrane. The presence of cholesterol for example, makes higher the voltage needed to permeabilize a membrane. The measured breakdown voltage of a membrane made from cholesterol for example, is three times higher than if it was made of phosphatidylcholine (Crowley 1973). Furthermore, the electroporation threshold changes with the nature of lipids tails (whether these tails are acyl chains or methyl branched chains) and the type of linkages (whether these are ether or ester linkages). This is what showed a molecular dynamics (MD) simulation of Polak *et al.* in 2013. They used three different lipids in their study: the dipalmitoyl-phosphatidylcholine (DPPC), the diphytanoyl-phosphocholine-ester (DPhPC-ester) and the diphytanoyl-phosphocholine-ether (DPhPC-ether) ([Figure 44](#)). The electroporation of the lipid bilayers occurred at 2.3, 3 and 3.7 V for DPPC, DPhPC-ester and DPhPC-ether respectively (Polak *et al.* 2013). This shows that the addition of methyl groups in the hydrophobic tails stabilizes the lipid bilayer. Also, the ether linkage stabilizes even more the bilayer. The more the

lipid bilayer is stabilized, the more the electroporation threshold is higher. This can explain why, for example, the archaea membranes are more stable than the eukaryotes or bacteria membrane; the archaeal lipids have ether linkages that replace the ester linkages in their membranes. The archaeal lipids resist hydrolysis and oxidation and this helps these organisms to withstand the extreme conditions in which they live (Berg et al. 2002b).

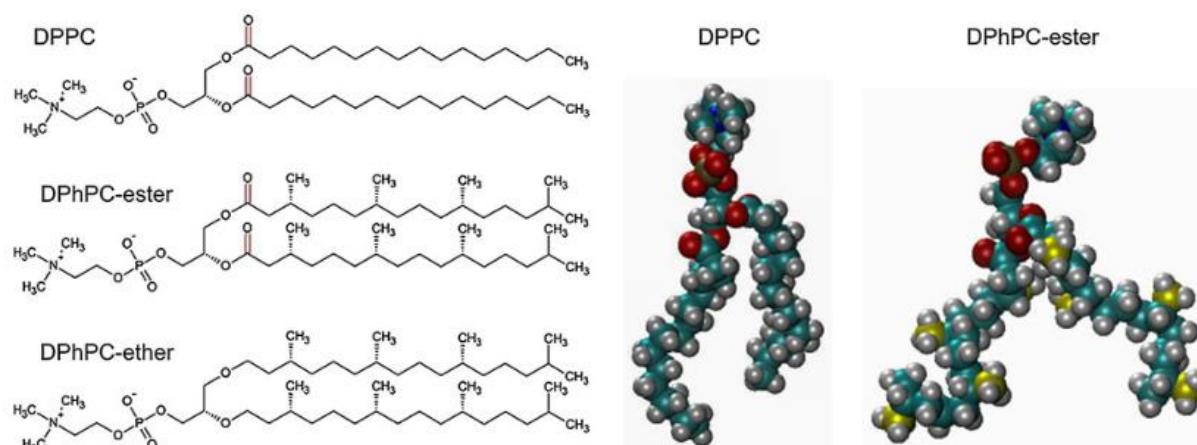


Figure 44 : Left, structures of the lipids in the study of Polak et al., Right, atoms are color-labeled in MD models (O: red, C: cyan, H: gray, P: brown), the DPhPC-ether is not shown due to similarity to the DPhPC-ester (Polak et al. 2013).

The breakdown voltage does not depend only on the composition of the PM but depends also on other properties such as, between others, the thickness of the membrane, which can be given by the equation (Michael & O'Neill 1970):

$$U > \left(\frac{\sigma h}{\epsilon_0} \right)^{1/2}$$

where h is the membrane thickness, σ is the surface tension and ϵ_0 is the dielectric constant of vacuum. The surface tension is produced by the surface charges (under the forces of the electric field) that cause the coalescence of water droplets on the water interfacial surface of the membrane (Michael & O'Neill 1970). Ziegler and Vernier also demonstrated, by molecular dynamics simulations, such a correlation between the bilayer thickness and the breakdown voltage. They showed that, the larger the phospholipid hydrocarbon tail length of a bilayer, the higher the magnitude of the field required for poration (Ziegler & Vernier 2008).

4.3.7 The impact of the medium composition [conductivity]

The medium conductivity is determined by the amount of ions present in this medium. Rosen and Sutton demonstrated, on lecithin bimolecular membranes, that the compressive electric force on the membrane bilayer is affected by the composition of the surrounding medium, especially the electrolyte concentration, and that the capacitance of the membrane depends on this concentration (Rosen & Sutton 1968). The rupture voltage of a membrane is dependent upon the composition and

the concentration of the electrolytes of the medium (Abidor et al. 1979). Silve *et al.* has demonstrated recently that the lower the conductivity of the medium, the more efficient the reversible permeabilization, whether with micro or nanosecond pulses (Silve et al. 2016). However, this effect of medium conductivity is only detected under saturation conditions, giving that the results were the same (between low and high-conductivity medium) when extreme conditions were used.

4.3.8 The impact of the cell confluence or density

Using the same electrical parameters on the same cells will give different outcomes if the cell confluence (if attached) or density (if in suspension) differs. Numerical computational studies have shown that cell density and organization impact the induced transmembrane potential (TMP) (Susil et al. 1998, Pavlin et al. 2002). High cell density resulted in an altered distribution of the TMP and a reduction of the area of the permeabilised regions. This was also shown experimentally by Pucihar *et al.* who demonstrated that, to achieve the same fraction of cells permeabilization of a suspension of 10×10^6 and 400×10^6 cells/ml, a higher electric field amplitude should be applied in the second case. Furthermore, they showed that the PI fluorescence in the cells is lower when the cell density increases, and explained this phenomenon by the fact of a reduced extracellular dye availability to the permeabilized regions of the membrane (already reduced), and the hindered diffusion into the cells (Pucihar et al. 2007).

4.3.9 The impact of the temperature

The effect of the temperature is somekind controversial: an increasing temperature will make the membrane more fluid, hence decreasing the electric field needed to permeabilize it, but in the same time the resealing of the electroporated membrane is faster. At lower temperature, the membrane is less fluid, hence its electroporation is harder but the permeabilized status remains longer due to the slower resealing of the pores. For example, while increasing the temperature from 5 to 37°C decreases the necessary voltage for electroporeabilization of Madin-Darby canine kidney epithelial cells by a factor of 2 (Díaz & Rubinsky 2004), a temperature of 4°C yielded a better protein extraction from bacterial cells (Meglič et al. 2016). For the electrotransfection, optimal conditions of pre and post-incubation temperatures should be respected: Rols *et al.* showed that a preincubation of CHO cells for 10 minutes on ice limits DNA degradation by extracellular nucleases, and a post-incubation at 37°C for 10 minutes increases the survival and transfection rate. Lowering the temperature after the pulse will stabilize the permeable pores but appeared not necessary because the DNA should be only present during the electropulsation (Rols et al. 1994).

4.4 ELECTROPORATION VS ELECTROPERMEABILIZATION

4.4.1 Electroporation: the direct effect of the pulse

The PM behaves as a leaky dielectric, and when the voltage across it reaches the permeabilisation threshold, transient aqueous pores are formed in the lipid bilayer resulting in electroporation (Weaver & Chizmadzhev 1996, Neumann et al. 1999). However, even though the electroporation is a widely used technique in biomedical sciences and food industry, the exact mechanisms underlying membrane permeabilization, and the exact nature of the permeabilised area, remain poorly understood (Escoffre et al. 2009, Miklavčič et al. 2014). Abidor et al. mentioned that the membrane defects are through-going macroscopic pores (which they named holes), that are originated from the evolution of micropores arisen in the membrane under the influence of the electric field (Abidor et al. 1979). The holes or pores theory of Abidor was echoed by many teams in the following years (Sugar & Neumann 1984, Freeman et al. 1994) and developed to assume that aqueous pores are created in the membranes (Weaver & Chizmadzhev 1996). However, no experimental study has shown what these claimed pores may look like in reality. The development of the molecular dynamics works revealed these virtual pores *in silico*. Tielman showed such pores in his computational study published in 2004. He explained that the pore formation is due to the local voltage gradient at the interface between water and lipids. The water molecules can move in this voltage gradient, which increases the probability of observing a water molecule across the plasma membrane. This passage of a water molecule causes an increase of the local field which accelerates the process and allows the enlargement of the water column formed until the formation of a completely hydrophilic pore (Tieleman 2004). These observations were later confirmed by other studies such as those of Tarek and Tokman. Tarek showed that defects in the interfacial water are formed on both sides of the membrane and eventually joining to form a hydrophilic channel (Tarek 2005). Tokman *et al.* demonstrated that pore formation is driven by the reorganization of the interfacial water molecules and that the process of poration is the same with or without lipid bilayer; it is always driven by field-induced reorganization of water dipoles at the water-lipid or water-vacuum interfaces (Tokman et al. 2013). The electro-induced pores are stabilised by the phospholipids polar heads. The lipids may also move from one leaflet to another along the hydrophilic pores. An example of this movement is the externalization of phosphatidylserine (Tekle et al. 2008).

4.4.2 Electroporimeabilization: the long-lasting effect of the pulse

The short-lasting electro-induced pores have been shown to be associated with chemical modifications of lipids which make the membrane permeable up to several hours after the application of the electric pulses (Abidor et al. 1979). The electroporimeabilization of the membrane can persist for times much longer than the pulses (Gowrishankar & Weaver 2006) and their lifetime depends on the electric field parameters (Rols & Teissié 1990). It is dependent on pulse duration and number but not on electric field amplitude which creates the electroporimeabilization. Different studies have shown that the electroporimeabilisation, that follows the creation (electroporation) and resealing of the electropores, is due to reactive oxygen species (ROS) and the oxidation reactions of the lipids. Our team has recently showed a new model reconciling the electroporation and electroporimeabilization

at the molecular level. It shows that the oxidation of the unsaturated lipids, which are the main constituent of the cell membranes, changes its physico-chemical properties and explains how the membrane stays permeable for a long time after the pulse (Breton et al. 2016). It was shown before, by MD simulations and experiments with living cells, that the oxidation of the PM lipids with oxidative agents increases the membrane susceptibility to electroporation (Vernier et al. 2009). The long permeabilisation of the membrane due to lipids oxidation can be explained by the reparation time of these oxidations. It is the exocytosis phenomenon that permits to replace the oxidized lipids with new synthesized ones.

4.5 INDICES OF MEMBRANE PERMEABILIZATION

4.5.1 The permeabilization markers

According to all the factors cited in the *section 4.3*, and depending on the combination of many of them, the electroporation could be reversible or irreversible. In general, one to eight electric pulses of a duration of 100 μ s and an electric field ranging from tens of volts to 2 kV/cm cause reversible electroporation. Higher values of these parameters may cause irreversible electroporation, depending also on the cell type and the medium properties. However, there is also an important factor, often forgotten, which is the size of the permeabilization marker. The membrane permeabilization can not be referred as a general phenomenon for all molecules but as a relative phenomenon depending on the permeabilization factors and the molecules used to measure it. For example, a set of electrical parameters may not show an internalization of yo-pro iodide to the cells, but may lead to the entry of Ca^{2+} . In this case the membrane is not permeabilized for the yo-pro but it is for the Ca^{2+} which is smaller. Hence, it is more suitable to talk about membrane permeabilization for a specific molecule but not in general. *Table 6* shows some ions, molecules and fluorescent dyes that have been used to show the degree of membrane permeabilization. It should be noted that not only the entry of permeabilization markers can demonstrate an electroporation, but also the release of some cell components such as ATP, K^+ ions or lactate dehydrogenase (Hojman et al. 2008).

Ion/molecule	Weight (Dalton)	Direction
Water	18	Entry
Potassium	39	Release
Calcium	40	Entry
Thallium	204	Entry
Yo-pro 1 iodide	375	Entry
Lucifer Yellow	443	Entry
ATP	507	Release
Propidium iodide	541	Entry
Calcein	623	Entry
Trypan blue	965	Entry

Bleomycin	1 500	Entry
siRNA	14 000	Entry
Lactate dehydrogenase	35 000	Release
DNA plasmid	3 000 000	Entry

Table 6: some frequently used permeabilization markers, respecting ascending order in weight from up to down.

4.5.2 The membrane conductivity

The PM is poorly conductive by its own. After an exposition to an electric field, the permeabilised regions of the PM are those where the TMV induced by the electric pulse exceed the permeabilisation treshold. These regions present an increased membrane conductance, related to a loss of 0.01-0.1% of the membrane area and the formation of stable conductance pores. After the pulse, the conductance decreases to lower level in less than a millisecond, leaving a moderately electroporated cell (Kinosita et al. 1988). Benz and Zimmermann showed conductance changes within few nanoseconds after the application of an electric pulse (Benz & Zimmermann 1980). The electrically conductive pores prevent permanent damage of the membrane by shunting current and limiting further TMP rise (DeBruin & Krassowska 1999). Hence, the PM conductance is an indirect method to monitor the electroporeabilisation and the passage of ions through this membrane. It has been suggested that the local defects that cause the membrane breakdown (discussed above in the model of Abidor *et al.* (Abidor et al. 1979)) are assimilated to ions channels, thus they have higher [ionic] conductivity (Parsegian 1975). Wegner *et al.* found that a transition from a low-conductance (~ 0.1 nS/pF) to a high-conductance state (~ 5 nS/pF) was observed when the PM of protoplasts derived from tobacco culture was electroporeabilized (Wegner et al. 2011). Moreover, the membrane rupture is preceeded by an increase in the level of conductivity fluctuations (Tien & Diana 1967).

4.6 THE DIFFERENT KINDS OF PULSES USED IN ELECTROPORATION

4.6.1 The millisecond pulsed electric fields

This type of pulses is used for the aims of PM permeabilization but also to enhance DNA movements *in vitro* and *in vivo*. As mentioned before, a combination of the pulse parameters impact the outcomes of the electroporation, and as the duration of this type of pulse is relatively long, the electric field should be low to permit a reversible electroporation, otherwise an irreversible electroporation occurs. For example, a set of ten electric pulses of 0.5 to 5 ms and 800 V/cm can be used to reversibly permeabilize the PM of CHO cells (Golzio et al. 2002). However, increasing the number of pulses to 15 with an electric field to 3 kV/cm causes irreversible electroporation and protein extraction from microalguea with a duration of 2 ms for each pulse (Coustets et al. 2013). A study of Mauroy *et al.* showed that the millisecond pulsed electric fields (msPEF) induce loss of lipids and membrane deformations of GUVs facing the electrodes. The permeabilization threshold depended on the vesicles size (Schwan equation). Millisecond pulses were used for carotenoid extraction from

microalgae such as *Chlorella Vulgaris*; 20 pulses of 20 ms and 5 kV/cm caused electroporation of 90% of the cells (Luengo et al. 2015).

This type of pulses revealed a specific importance in cell transfection with nucleic acids. They can generate an electrophoretic force that guides the charged molecules movement such as DNA and plasmids *in vitro* and *in vivo*. The combination of these pulses with microsecond pulses yields a higher transfection rate especially *in vivo* (discussed in the next section).

4.6.2 The microsecond pulsed electric fields

The microsecond pulsed electric fields (μ sPEF) are more used than the msPEF for the different applications of electroporation (*cf. section 4.7*). The main purpose of their use is the plasma membrane permeabilization. Due to their short duration, the heating effect resulted from such pulses is neglected (Davalos et al. 2005). They are called also high voltage (HV) pulses because the electric field used in combination with such pulses is higher than the msPEF called low voltage (LV). The μ sPEF are widely used *in vitro* and *in vivo* for the internalization of many molecules, drugs and nucleic acids. The use of one to eight 100 μ s pulse (the classical number and duration used frequently) with 0.5 to 1.5 kV/cm allowed PM permeabilization to many molecules such as bleomycin (Poddevin et al. 1991), lucifer yellow (Mir et al. 1988) or propidium iodide (Mohr et al. 2006). However, for DNA internalization, a combination of microsecond and millisecond PEF is required to obtain optimal results *in vivo*. As mentioned before, the msPEF create an electrophoretic force guiding the DNA toward or across the permeabilized cell membrane but also across the extracellular matrix [*in vivo*], and the μ sPEF cause the membrane permeabilization to the DNA molecule allowing its entry to the cell. Such combination is called HV+LV and has been widely used *in vitro* and *in vivo*. Satkauskas *et al.* showed that a combination of one HV of 100 μ s and 800 V/cm followed by one LV of 100 ms and 80 V/cm (separated by 100s) resulted in a large increase in DNA transfer. The lags between pulses can be increased to 3000 s if the HV is followed by 4 LV (Satkauskas et al. 2002). Hojman *et al.* demonstrated that the combination of one HV and one LV is less toxic and caused less disturbance of cell function comparing to 8 permeabilizing HV, which is important for efficient transgene expression (Hojman et al. 2008). André *et al.* studied in depth the combination of HV + LV in many rodent tissues such as liver, muscle, skin and tumor and confirmed the importance of this pulses combination. They found that a lag time of 1s was optimal for gene transfer and that the electrical parameters were dependent on the tissue organization and the cell size (André et al. 2008a).

The mechanisms of permeabilization induced by the microsecond and millisecond pulses is nearly the same. Due to their “relatively long duration” (larger than the plasma membrane charging time), the majority of their effects are induced on the level of the PM. The TMP induced by these pulses is mainly due to the charging of the membrane resulting from ions movements, which have the necessary time to charge the membrane.

The μ sPEFs have been widely used in research, medicine, biotechnology and food industry for the applications related to the plasma membrane permeabilization. However, recent simulation studies done by the team of James Weaver (M.I.T, Boston USA) showed that the μ sPEF could also permeabilize the organelles membranes. Due to their duration higher than the charging time of the PM, these pulses give sufficient time to small electrolytes such as ions to charge this latter. Once the

PM is permeabilized, the extracellular electric field will enter to the interior of the cell and create intracellular fields sufficient to cause an induced transmembrane voltage at the organelles membranes, to gate organelles channels and to cause organelle membranes poration (Esser et al. 2010, Weaver et al. 2012). In their simulation study, Weaver *et al.* used one pulse of 40 μ s and an electric field ranging from 1 to 7 kV. They showed that, the higher the electric field amplitude, the larger the affected regions of the PM, and the more the organelles membranes are porated.

4.6.3 The nanosecond pulsed electric fields

When the applied electric field have an ultrashort duration, less than the charging time of the PM, the field will pass through the membrane into the cytoplasm and affect the internal structures. The principle is the same as the PM permeabilization: the applied electric field should be high enough to cause the TMP across intracellular membranes to reach the permeabilisation threshold value. In this case, electroporation of these membranes occurs (Schoenbach et al. 2001a). However, the charging mechanism for intracellular membranes is not yet completely understood. Due to the very short duration of this kind of pulses, energetic effects in terms of heating (thermal effects) are negligible.

Chen *et al.* studied the effects of electrical pulses of 60 and 10 ns duration and an EF strength up to 65 kV/cm on the PM and nucleus of HL-60 cells and found that the more the pulse duration is shortened, the more its effects on PM are delayed and become smaller, and its intracellular effects increase. They found no effect of these pulses on cell viability and no thermal effect was observed even though very high pulsed electric fields were applied, because of the ultrashort pulse duration (Chen et al. 2004). By using the ANNINE-6, a fast voltage-sensitive dye, Frey *et al.* measured the voltage across the membrane of Jurkat cells exposed to 60 ns pulses of 100 kV/cm. They found that this voltage reached 1.6 V after 15 ns at the anodic pole of the cell, whereas it did not surpass 0.6 V in the same time period at the cathodic pole. This drop in voltage across the PM corresponds nearly to the entire electric field applied, which demonstrates that this electric field penetrates into the interior of the cell and organelles (Frey et al. 2006).

The nsPEFs cause, between others, the release of intracellular Ca^{2+} (Vernier et al. 2003, White et al. 2004), a transient externalization of phosphatidylserine (Vernier et al. 2004), breaching of intracellular granule membranes (Schoenbach et al. 2004), cell and nuclear shrinkage (Schoenbach et al. 2001b), enhanced expression of genes and the induction of apoptosis or necrosis at higher electric fields (Beebe et al. 2002, 2003). The Ca^{2+} release from internal stores activates the Ca^{2+} influx from PM SOCCs or capacitative Ca^{2+} entry.

In contrary to what has been thought for a long time, the nsPEF do not only affect the interior of the cells, but can also cause similar effects on the PM like longer pulses, even if their duration is under the charging time of the PM (Gowrishankar & Weaver 2006). Pakhomov *et al.* demonstrated that mammalian cells exposed to nsPEF of 60 ns and 12 kV/cm presented an increased PM conductivity which was due to the opening of stable conductance pores that were permeable to small ions such as Cl^- and alkali metal cations (Pakhomov et al. 2007). The increase in PM conductivity is one of the results and signs of electroporeabilization observed with microsecond and millisecond pulsed electric fields. Frey *et al.* showed also a change in the PM potential after using 100 ns pulses (Frey et al. 2006). The PM pores created by nsPEF may be large enough to let relatively large molecules such as yo-pro-1

iodide (Vernier et al. 2006) and bleomycin to cross the membrane. Silve *et al.* demonstrated that one single 10 ns pulse was sufficient to mediate transport of bleomycin across the membrane (Silve et al. 2012).

4.7 SOME APPLICATIONS OF THE MEMBRANE ELECTROPERMEABILIZATION

4.7.1 Electrochemotherapy

The electrochemotherapy (ECT) is a non-thermal technique used for the treatment of many types of cutaneous and subcutaneous tumor nodules. It consists on the application of an electric field combined with non- or low-permeant drugs. The ECT is now applied in over 140 clinical centers in Europe. The ESOPE study (European Standard Operating Procedures of Electrochemotherapy) performed in 2004-2005 allowed to define the standard procedures for treatment efficacy and patients safety using the standard electrical parameters consisting of 8 square-wave pulses of 100 μ s and 1-1.3 kV/cm delivered at a frequency of 1 Hz or 5 kHz (Mir et al. 2006). The most popular drugs used in ECT are bleomycin and Cisplatin. The bleomycin is a non-permeant drug that generates single and double-stranded DNA breaks. When combined with electric pulses, its cytotoxicity increases 700-fold (Orlowski et al. 1988); this can be explained by the fact that some hundreds molecules of bleomycin are enough to kill the cell (Poddevin et al. 1991). The Cisplatin is a low-permeant drug efficient by itself as an anti-cancer treatment, and its cytotoxicity is only 10-fold higher when combined with the pulses (Gehl et al. 1998). This is why the bleomycin was more often used in the *in-vivo* and clinical studies (Belehradek et al. 1991, Mir et al. 1991). As the bleomycin kills the cells by a mitotic mechanism, it will be only harmful for dividing cells and not for the quiescent ones and this is one of the most interesting features and advantages of the ECT, its ability to selectively kill the dividing cancerous cells and spare the quiescent ones. Another advantage of the ECT is the vasoconstriction and reduction in tumor blood flow in the treated zone. This ECT-associated phenomenon is called vascular lock and it permits the retaining of the drug in the treated area. This is why the ECT is a very interesting approach to treat bleeding tumors. Another vascular effect of the ECT is the destruction of the tumor endothelial cells, preventing tumor resupply in nutrients and oxygen (Cemazar et al. 2001).

The electrodes used for ECT are generally plate or needle electrode. However, in the last ten years, and due to the success of this technique, there have been many developments of new types of electrodes suitable to treat a large number of superficial and internal tumors. For example, expandable electrodes were developed to treat brain cancer, endoscopes for intraluminal tumors and finger electrodes for oral and anal cavities tumors (Breton & Mir 2012). The operation is done under local or general anesthesia.

Our team has recently shown that ECT with bleomycin induces hallmark of immunogenic cell death, promoting the possible generation of a systemic anticancer immune response (Calvet et al. 2014a). The important role of the immune system in the ECT treatments was also demonstrated by other studies: Mir *et al.* demonstrated that the rate of cured animals by ECT is increased by an injection of IL-2 (Mir et al. 1992), Roux *et al.* found that the expression of Toll-like receptor 9 (TLR9) expression is highly increased after the ECT and that combination with CpG oligonucleotides resulted in systemic

antitumor effects (Roux et al. 2008). The combination of ECT and immunotherapy was tested on several tumors and showed a higher efficiency in tumor treatment.

4.7.2 Electrotransfer

Gene electrotransfer (EGT) is a very promising and efficient technique for nonviral gene transfer *in vitro* as well as *in vivo*. The electric pulses used for EGT are the micropulses (HV), millipulses (LV) or their combination (HV+LV). *In vitro*, the HV pulses can be used alone for an efficient EGT, whereas *in vivo*, and as mentioned before, a combination of LV + HV pulses is recommended: the LV are needed to move the nucleic acids electrophoretically in the tissue to be transfected, and the HV are needed to permeabilize the tissue cells to these nucleic acids. The DNA transfer into muscle for example is dramatically enhanced and leads to highly efficient long-term gene expression (André et al. 2008a). It was tested in many animals such as rabbit, mouse, rat and monkey. Mir *et al.* showed that the plasmid DNA should be present in the tissue when the pulses are applied, and demonstrated a gene expression stability in muscle for at least 9 months (Mir et al. 1999).

The EGT is used in research and in medicine for many applications such as transfection of reporter genes, gene therapy, DNA vaccination and generation of iPS. The most common reporter genes are the ones coding for GFP (fluorescent protein), luciferase (generating bioluminescence in presence of ATP and luciferin) and β -galactosidase (generating a coloured product from the galactose glycoside X-gal). These genes are attached (or not) to another gene of interest and serve to quantify the percentage of cells and the expression level of the wanted protein. The optimal electrical parameters should be set to assure the highest transfection efficiency while preserving the cell viability or the tissue integrity. Another important application of EGT is the DNA vaccination. That consists of injecting a DNA sequence coding for a pathogenic cell epitope (such as cancerous cell), which will lead to the activation of the immune system against the cells exposing that epitope. A recent study done in our team by Calvet *et al.* used a plasmid that encodes a modified form of the human telomerase reverse transcriptase gene (*hTERT*) and its intradermal electrotransfection in mice. The transgene expression was 100-fold higher when combined to EGT than when the DNA was injected alone. After optimization of the electrical parameters including the best electrodes, the best HV pulse intensity and the best combination of HV-LV, the telomerase antigen will be used as a cancer DNA vaccine called INVAC-1 (Calvet et al. 2014b).

4.7.3 Electrofusion

If two cells are in close contact to each other, the electric field can cause their irreversible membrane fusion, a phenomenon called cell electrofusion. The electrofusion has several advantages over other fusion means such as polyethylene glycol and Sendai virus; it is more efficient, synchronous, without any added products that affect the cell viability and gives possibility to create giant polynuclear cells. This phenomenon was first observed by the team of U. Zimmermann in 1980, who realized that adhered red blood cells in an hypotonic suspension displayed membrane fusion after the application of an electric field of 830 V/cm (Scheurich et al. 1980). The next year, the same team published more papers reporting the electrofusion on many cellular models. For example, with a pulse of 50 μ s and

250 V/cm they observed the electrofusion of many plant protoplasts (Scheurich et al. 1981). In all their studies, U. Zimmermann team used the same conditions of hypotonic and low-conductive medium and applied first an external, alternating, non uniform field to cause cells to adhere. Once the cells adhered to each others, they form like a pearl chain between the electrodes and an additional external electric field of low duration and high intensity (supposed to cause membrane breakdown) was applied. Teissié and Rols showed that the electroporation is required for cell electrofusion and that the cells can be brought to contact even after their permeabilization (for cells in suspension); they applied first 5 electric pulses of 100 μ s and 0.7 to 2 kV/cm and then they centrifuged the CHO cells after about 5 minutes. They demonstrated that the 2 phenomena were not simultaneous because the electroporation occurs before the electrofusion (Teissie & Rols 1986).

The first study to demonstrate the electrofusion *in vivo* was that of Mekid and Mir on B16 murine melanoma tissue. They confirmed the observations already done *in vitro* consisting that the cells, to undergo electrofusion, they should have been electroporated; when they used 8 electric pulses of 100 μ s and 500 V/cm (electric field that electroporates a low percentage of cells), they observed four times less nuclei in giant cells than when they used 1350 V/cm. Furthermore, they confirmed another observation which is the required contact between the cells; the electrofusion was observed in melanoma tumor but not in liver or fibrosarcoma even with a higher permeabilizing field amplitude (2000 V/cm), because the cells in these latters are separated by a dense extracellular matrix (ECM). This ECM is degraded by the secreted proteases in the melanoma tissue (Mekid & Mir 2000). Most of the studies done on electrofusion used microsecond pulses in the range of 100 to several hundreds V/cm. A recent study of Rems *et al.* used the nsPEF to achieve cell electrofusion between cells of equal or different size (Rems et al. 2013). Interestingly, they showed by numerical calculations that, with nanosecond pulses, contact areas between cells are selectively electroporated. This was explained by the fact that the contact areas are surrounded by highly conductive cytoplasm (0.25 S/m) from both sides comparing to the rest of the membrane surrounded by the fusion medium of low conductance (0.01 S/m).

Cell electrofusion was used in many important biological applications such as the production of monoclonal antibodies and the antitumoral immunotherapy. The monoclonal antibodies are produced by hybridoma cells formed by the fusion of B lymphocytes (that produce antibodies) and myeloma tumour cells (immortalized cells). The fused cells have the properties of the two fused original cells: immortalization and production of antibodies. The electrofusion has been proved to be a very efficient technique (over chemicals) in inducing hybridoma formation (Lo & Tsong 1989). The generation of dendritic cell – tumor cell hybrids is another important application consisting in fusing pre-irradiated cancerous cells with dendritic cells in order to develop a vaccine (Trevor et al. 2004). The dendritic cells are antigen presenting cells that will stimulate the immune system against the cancerous cells by presenting the tumor antigen at their surfaces.

II. RESEARCH HYPOTHESES AND OBJECTIVES

Our attention was focused on the generation, control and consequences of electro-induced calcium (Ca^{2+}) spikes in the cells using one single 100 μs pulse.

Ca^{2+} is a universal intracellular messenger playing a role in plenty of cellular processes either directly or indirectly (Berridge et al. 2000). The control of the cytosolic concentration of Ca^{2+} could present a promising tool to control cell proliferation, differentiation, senescence, apoptosis and other cellular key functions. Electroporation has emerged some 50 years ago with Sale and Hamilton (Sale & Hamilton 1968). This technique showed an interesting approach to permeabilize the cells to non-permeant molecules (such as Ca^{2+} , bleomycin, genetic material). Hence, its applications concerns a lot of aspects in biotechnology, medicine, research, food and environment industry (Neumann et al. 1982, Gehl et al. 1998, Schoenbach et al. 2000, Mir et al. 2005, Potter & Heller 2011). The application of a temporary electric field results in the cellular uptake of normally non-permeant molecules to the cells. By changing the electric field intensity, the duration of the pulse, the number of pulses and their repetition frequency, the outcomes of electroporation can largely differ. The three types of pulses used frequently are the millisecond (msPEFs), microsecond (μsPEFs) and nanosecond (nsPEFs) pulsed electric fields. The μsPEFs are often used to permeabilize the plasma membrane (PM) of the cells (Mir et al. 1988, Poddevin et al. 1991). The msPEFs are used to permeabilize the PM and to assure an electrophoretic force for the uptake of large charged molecules e.g. for DNA electrotransfer (André et al. 2008b). The nsPEF have emerged recently compared to the two other types of pulses and they are applied to make a transitory permeabilization of cell organelles or to cause cell apoptosis (Beebe et al. 2002, Vernier et al. 2003). Depending on the pulse parameters, the electroporation can be reversible or irreversible.

Not all the laboratories possess the nsPEFs technology due to its high price and complexity of use. The μsPEFs technology is more available since it can be found frequently in the laboratories and is more practical to use. As said before, all the observations done with the μsPEF showed their interaction with the PM and the nsPEFs are essentially used to permeabilize the inner membranes of the cells, even though it has been also shown that these pulses can cause the formation of small pores in the PM (Gowrishankar & Weaver 2006). A couple of simulation studies done by J. Weaver and colleagues showed that it was possible, *in silico*, to permeabilize the organelles membrane with μsPEFs , that is using the so-called conventional electroporation (Esser et al. 2010, Weaver et al. 2012). In the first part of this thesis, we aimed to verify experimentally the theoretical work of J. Weaver and colleagues. We decided to use only one single 100 μs pulse. This choice was based on several reasons: first because we wanted to study the effect of a classical μsPEFs duration on the PM and on the organelles, and secondly because the application of one pulse would relieve us from the study of the effect of the frequency if several pulses were applied. We decided to use the Ca^{2+} as a permeabilization marker because it is present in the extracellular medium and in many cell organelles, mainly the endoplasmic reticulum (ER) which is the larger Ca^{2+} store in the cell. The use of two different media, with and without Ca^{2+} would allow us to know the origin of an electro-induced Ca^{2+} spike (whether it was originated from the Ca^{2+} of the extracellular medium or/and from the Ca^{2+} of the inner stores, mostly the ER).

After the assessment of the effect of one 100 μs pulse on two different kind of cells (the DC-3F cells and the human-adipose mesenchymal stem cells (haMSC)) and evaluate its effect on cell PM and ER membranes depending on electric field amplitude, this pulse was applied to control the Ca^{2+} oscillations in haMSCs. The MSCs are pluripotent cells originated from embryonic mesoderm and

present in many adult tissues (Dominici et al. 2006). These cells present a high potential to differentiate into many cell types including osteoblasts, chondrocytes and neuronal cells (Pittenger et al. 1999). Therefore, they are very interesting candidates for the regenerative medicine. These cells present spontaneous Ca^{2+} oscillations related to their differentiation state and pathway. For example, a diminution in the Ca^{2+} oscillations frequency was observed when the MSC undergo osteodifferentiation (Pullar 2011). Our second objective was to study the effect of one 100 μs pulse on the Ca^{2+} oscillations in MSC extracted from adipose tissue (haMSCs). We chose the haMSC because they are easily accessible in large number and without painful procedures of extraction (Gronthos et al. 2001). The mechanical stimulation of MSC has shown to induce their differentiation and the Ca^{2+} oscillations present an important mechanotransduction signal (Jing et al. 2014). Hence, our aim was to assess whereas one 100 μs pulse could modulate the Ca^{2+} oscillations by imposing electrically-induced Ca^{2+} spikes to the cell.

The third objective of this thesis was to apply one 100 μs pulse, already used to induce cytosolic Ca^{2+} spikes from different origins (ER, extracellular medium), on haMSC undergoing osteodifferentiation. The purpose was to assess the effect of the pulse on the duration of the period necessary to achieve mature osteoblasts. Under normal conditions (MSC incubated with osteogenic chemical factors), four weeks are needed to obtain mature osteoblasts. If the second part of the thesis would give us positive results on the control of the Ca^{2+} oscillations in MSC by one 100 μs pulse, such pulse or train of pulses could be used to control the differentiation outcomes and rapidity, since the Ca^{2+} oscillations are a major regulating factor of the differentiation. The differentiation of MSC to osteoblast is known to occur in an extensive collagen I extracellular matrix (Owen et al. 1990). Hence, we sought to develop a new protocol to dissociate the cells in this extensive matrix in order to study Ca^{2+} oscillations in the different layers separately, and analyse if there is a difference between the layers in terms of these oscillations, and in terms of pluripotent stem cells markers.

III. RESULTS

1 ELECTROPERMEABILIZATION OF INNER AND OUTER CELL MEMBRANES WITH MICROSECOND PULSED ELECTRIC FIELDS: QUANTITATIVE STUDY WITH CALCIUM IONS (ARTICLE N°1)

Many laboratories already possess the microsecond pulsed electric fields (μ sPEFs) technology that is used for many routine applications such as gene delivery, cell transfection and electropermeabilization of the plasma membrane. On the contrary, few laboratories possess the more sophisticated nanosecond pulsed electric fields (nsPEFs) generators. This latter technology is used to manipulate cell organelles permeability and it is more expensive than the μ sPEFs technology. James Weaver and his team showed, theoretically, that it is possible to permeabilize the cell inner membranes with the classical μ sPEFs, but no experimental study had shown this yet. Therefore, in the first part of this thesis, we decided to bring an experimental evidence to the theoretical work of J. Weaver and colleagues (Esser et al. 2010, Weaver et al. 2012). We used one single 100 μ s pulse to study its effect on two different cell lines and we used the Ca^{2+} as a permeabilization marker in order to create electro-induced Ca^{2+} spikes in the cells cytosol. Since Ca^{2+} is one of the most important second messengers in the cells, the use of the available μ sPEFs technique to control the Ca^{2+} in the cell and to study its consequences is of a high importance. We decided to study the effect of one single 100 μ s pulse because we had to choose electrical parameters to be used in the following parts of the thesis. One pulse is simpler than many pulses since there is no need to study the impact of the frequency if many pulses were applied. One hundred microseconds is a classical duration already used for many electroporation applications. The study of the interaction of one single 100 μ s pulse with the PM and the ER was primordial in this first part of the thesis to give us the necessary information in order to use this kind of pulse for further applications in the following parts. These results have been submitted to "Scientific Reports" in August 2016.

Electropermeabilization of Inner and Outer Cell Membranes with Microsecond Pulsed Electric Fields: Quantitative Study with Calcium Ions

Hanna Hanna ¹, Franck M. Andre ¹, Agnese Denzi ², Micaela Liberti ² and Lluís M. Mir ^{1*}

¹ Vectorology and Anticancer Therapies, UMR 8203, CNRS, Univ. Paris-Sud, Gustave Roussy, Université Paris-Saclay, 94 805 Villejuif, France.

² Department of Information Engineering, Electronics and Telecommunication (DIET), University of Rome “La Sapienza,” Rome, 00184, Italy

* To whom correspondence should be addressed.

E-mail address: luís.mir@gustaveroussy.fr

Tel. : +33 1 42 11 47 92

Laboratoire de Vectorologie et Thérapeutiques Anticancéreuses
UMR 8203 CNRS Univ Paris-Sud
Gustave Roussy
114 rue Edouard Vaillant
94805 VILLEJUIF Cédex France

Abstract

Microsecond pulsed electric fields (μ sPEF) permeabilize the plasma membrane and are widely used in research, medicine and biotechnology. For internal membranes permeabilization, nanosecond pulsed electric fields (nsPEF) are applied but this technology is not simple to use. The endoplasmic reticulum (ER) membrane electropermeabilization to Ca^{2+} ions by one 100 μ s pulse is reported here in Chinese hamster lung fibroblast (DC-3F) and human adipose mesenchymal stem cells. This electropermeabilization was achieved while cell viability was preserved. One single μ sPEF of low field amplitude is also sufficient to permeabilize the plasma membrane to Ca^{2+} ions. This study compares the electropermeabilization of the plasma membrane and the ER membrane, which are highly dependent on the cell type. The importance of the ER size, distribution and architecture in the field amplitude needed to permeabilize its membrane was revealed. This study demonstrates that μ sPEF, a simple to use technology already available in the research laboratories, can permeabilize internal membranes with the interest that μ sPEF application is easier to control than the nsPEF technology. In particular, μ sPEF, through their interaction with either the plasma or ER membranes, can be an efficient tool to modulate cytosolic calcium concentration and study Ca^{2+} roles in cell physiology.

Introduction

Cell electroporation involves the application of electric pulses in order to increase the plasma membrane (PM) permeability. This concept emerged in the mid-60s with the work of Sale and Hamilton (1968) ¹. Molecules that cannot cross the PM in normal conditions can reach the cell cytosol due to the delivery of one or several electric pulses ². Furthermore, in 1982, Neumann et al. showed that gene transfer into a cell was possible by the application of electric pulses ³.

In the quiescent state of the cell, PM behaves as an insulator. However, certain ions, such as Na⁺ and K⁺ ions are pumped by the Na⁺-K⁺ ATPase which causes ion imbalance on either side of the membrane. This imbalance creates the resting transmembrane potential difference (resting Δ TMP). When cells are subjected to an electric field, the mobile charges (mainly ions) will move under the action of the electrophoretic force generated by the electric field, which will result in a further charging of the membrane: the so-called induced Δ TMP, superposing to the resting Δ TMP. When the net Δ TMP reaches a critical value, called permeabilization threshold, the properties of the membrane change: electroporation occurs, the membrane is electropermeabilized and it loses its insulating character. Depending on the amplitude of the field and the duration of the pulses, the electropermeabilization can be reversible or irreversible. In the case of the reversible electroporation, the increased permeability of the PM persists for a few minutes and afterwards the membrane returns to its original impermeable state.

Electric pulses of a typical duration of 100 microseconds and an electric field amplitude of the order of 1000 V/cm (μ sPEF), have been widely used in many biotechnological or medical applications, notably for antitumor electrochemotherapy ^{4,5}, tumor ablation ^{6,7}, cell transfection *in vitro* ⁸ and even gene transfer *in vivo* ^{3,9}. μ sPEF have been used to permeabilize many cell types and allow internalization of non-permeant molecules such as ⁵¹Cr-EDTA ¹⁰, bleomycin ¹¹, or plasmid DNA ¹² either *in vitro* and *in vivo*. Such pulses may also be used to achieve the fusion of adjacent cells brought in contact to each other ¹³ or even to break the integrity of the cell membrane and cause cell death in the case of the achievement of irreversible electroporation ^{6,14}.

Since the early 2000s, electric pulses of a few nanoseconds to several hundreds of nanoseconds and a field strength up to 300 kV/cm are used in biology: the so-called nanosecond pulsed electric fields (nsPEF). As the pulse duration in this type of pulses is below the PM charging time, effects at the PM level decrease and effects on intracellular membranes become detectable ^{15,16}. Unlike the μ sPEF, these ultrashort pulses have already been shown to permeabilize both the PM and the organelles membranes ¹⁷.

Small ions such as calcium Ca²⁺ can be used to visualize the PM or the inner stores permeabilization through the use of fluorescent markers like Fluo-4, or Fura-2. The difference of Ca²⁺ concentration between the cytoplasm and the extracellular medium (respectively about 100 nM and 1.2-1.8 mM) and between the cytoplasm and the endoplasmic reticulum ER (respectively 100 nM and 0.05 to 1 mM) are very different: therefore, when permeabilization of the PM or ER membranes occurs, a large number of molecules will enter the cytosol with gradient-driven very fast kinetics.

In the study here reported, Ca²⁺ was used as a marker of internal or external membrane electropermeabilization in two very different types of cells exposed to one single 100 μ sPEF. Response curves of Chinese hamster lung fibroblast cells (DC-3F) and human adipose mesenchymal stem cells (haMSC) to different electric field amplitudes were achieved. Characterization of the response

included the number of cells presenting a Ca^{2+} peak in media with and without Ca^{2+} , as well as the mean amplitude of the Ca^{2+} peaks. Cell viability was also tested. The Ca^{2+} peaks detected in a medium without Ca^{2+} demonstrate that μsPEF can also permeabilize the inner membranes of the cells without causing a loss of cell viability. To our knowledge, this is the first experimental study, with cell viability investigation, that shows that “classical” μsPEF can permeabilize internal membranes of the cells. Furthermore, to explain the amplitude of the various thresholds found, a detailed analysis of the ER structure in the haMSC and DC-3F cells was also performed.

Results

HaMSC exposure to one 100 μs electric pulse

The haMSC mean radius was about 36 μm . In DMEM, cells displaying a pulse-induced Ca^{2+} peak could be detected at a field E_{PM}^0 as low as 120 V/cm (Fig. 1A). 50% of cells presented a calcium peak when pulse amplitude E_{PM}^{50} was about 210 V/cm and plateau was reached at E_{PM}^{100} of about 430 V/cm. The curve representing the percentage of cells displaying a pulse-induced Ca^{2+} peak fits with a sigmoid. An exponential increase of the calcium peaks mean amplitude (among the cells responding to the pulse) was observed between 120 and 250 V/cm, followed by no further significant increase from 450 to 1000 V/cm (Fig. 1C). Traces of the typical pulse-induced Ca^{2+} peaks are provided in supplementary Fig. S1 and S2. No permeabilization of the PM was detected after a pulse of 300 V/cm using the classical PM permeabilization marker yo-pro-1 (Supplementary Fig. S3). With yo-pro-1, permeabilization was detected at 600 V/cm.

In SMEM-EGTA, there was no free Ca^{2+} in the medium surrounding the cells. At about 500 V/cm, only few cells displayed a Ca^{2+} peak (Fig. 1B). The number of cells presenting Ca^{2+} peaks increased with the field strength, to reach 100% at 1800 V/cm. At 800 V/cm, 50% of cells responded to the pulse (E_{ER}^{50}). The curve could fit with a truncated sigmoid, between 500 and 1600 V/cm. The mean amplitude of the Ca^{2+} peaks increased rather rapidly between 500 and 650 V/cm, and very slowly for higher field amplitudes (Fig. 1D). Mean value reached a maximum of 5 a.u.. The curve fits with an exponential between 500 and 650 V/cm and with a straight line above 650 V/cm.

DC-3F cells exposure to one 100 μs electric pulse

The DC-3F cells mean radius was about 9 μm . In DMEM, 270 V/cm was the lowest field amplitude (E_{PM}^0) at which cytosolic Ca^{2+} peaks could be detected immediately after the pulse delivery (Fig. 2A). From 300 to 500 V/cm the percentage of cells presenting a Ca^{2+} peak increased from 10 to 80%. At about 600 V/cm all the cells presented a Ca^{2+} peak (E_{PM}^{100}). 50% of cells responded to the pulse when amplitude E_{PM}^{50} was about 430 V/cm. The curve fits with a sigmoid. The mean amplitude of the Ca^{2+} peaks increased monotonously between 200 and 1000 V/cm (Fig. 2C). The curve fits with an exponential. The mean amplitude of the peaks was higher than in the haMSC. Traces of the typical pulse-induced Ca^{2+} peaks are provided in supplementary Fig. S1 and S2. No PM permeabilization was detected after one pulse of 300 V/cm using yo-pro-1 (Supplementary Fig. S3). With yo-pro-1, permeabilization was detected at 600 V/cm.

In SMEM-EGTA, a high field strength (2500 V/cm) was needed to observe Ca^{2+} peaks in 20% DC-3F cells (Fig. 2B). The percentage of cells presenting a Ca^{2+} peak increased to 38% at 2750 V/cm and then decreased to 27% at 3000 V/cm. The curve between 2000 and 2750 V/cm could be fitted by an exponential. The curve presenting the mean amplitude of Ca^{2+} peaks (Fig. 2D) increased from 2 to 8 a.u. between 2500 to 2750 V/cm, and then decreased to 4 a.u. at 3000 V/cm.

Inhibition of the Voltage-Operated Calcium Channels (VOCCs)

HaMSC cells were exposed to one single 100 μs electric pulse in DMEM with or without verapamil and mibefradil, inhibitors respectively of L-type and T-type VOCCs^{18,19}. Even at the lowest electric field amplitude (150 V/cm, resulting in about 10% of cells displaying an electro-induced Ca^{2+} peak), the use of VOCCs blockers did not affect the pulse-induced Ca^{2+} peaks ($p = 0.4$, Mann Whitney test) (Fig. 3 and supplementary Fig. S4).

Inhibition of Sarco/Endoplasmic Reticulum Calcium ATPase (SERCA)

After the addition of 2 μM of thapsigargin (a SERCA inhibitor)²⁰ to haMSC in SMEM-EGTA medium, an increase of Ca^{2+} concentration was observed (Fig. 4), corresponding to the depletion of the ER Ca^{2+} store²¹. When a 2000 V/cm electric pulse (100 μs) was applied after thapsigargin application, no electro-induced Ca^{2+} peak was observed. On the contrary, the electric pulse caused a little decrease in fluo-4 fluorescence. When the same pulse (2000 V/cm) was applied without a prior addition of thapsigargin, it provoked an electro-induced Ca^{2+} peak.

Inhibition of the inositol triphosphate and ryanodine receptors

HaMSC cells were incubated with or without 2-aminoethoxydiphenyl borate (2-APB), dantrolene sodium salt, and flecainide acetate salt, inhibitors respectively of inositol trisphosphate receptor (IP3R), ryanodine receptor (RyR) 1, 2 and RyR 3²²⁻²⁴. In all the cases, Ca^{2+} peaks mean amplitude increased proportionally with the field strength (Fig. 5 and supplementary Fig. S5). No differences in the mean amplitude were observed between cells with or without inhibitors ($p = 0.1384$, 2-way ANOVA test), while there was a significant effect of the field strength applied according to the same test ($p = 0.0035$).

Comparison of the endoplasmic reticulum of the two cell types

The ER was decorated by the D1ER protein. In attached haMSC, nuclei were located at the center of the cells and completely surrounded the nuclei, occupying a large volume in the cell. The ER 3D reconstruction allowed getting precise ER dimensions. The maximal diameter of the ER was approximately 75 % of the haMSC diameter. In the attached DC-3F cells, nucleus was located in general at one side of the cell and the ER extended mainly in the other side of the cell. Maximal ER diameter did not surpass 45% of DC-3F cells diameter (Fig. 6).

Cell viability after one 100 μ s electric pulse

Up to 2000 V/cm there was no significant difference in cell mortality between haMSC unexposed (ctrl) or exposed to one pulse (Fig. 7A). haMSC viability was almost the same in the two media, with and without calcium.

In DMEM, one pulse of 1000 V/cm did not impact DC-3F cells viability (Fig. 7B). A little decrease in the apparent DC-3F cells viability, from 100 to about 87%, was observed between 1400 and 2000 V/cm. Above 2000 V/cm the number of colonies decreased with the field amplitude, with 60% of cells still making colonies at 2750 V/cm, and 40% at 3000 V/cm.

In SMEM-EGTA, a decrease of DC-3F cells viability to 60-65% was observed even at 1000 V/cm and until 1800 V/cm. At 2000 V/cm, only 50% of cells made colonies. This percentage decreased at 2200 V/cm to reach 30%, and no further decrease was found at higher field amplitudes.

Discussion

μ sPEF are an effective tool used in many domains such as research, medicine and biotechnology, for antitumor electrochemotherapy, tumor ablation, cell transfection, etc. Due to their duration, which is long enough to cause transmembrane potential changes, μ sPEF were normally supposed to solely interact with the PM and change its permeability properties if the field amplitude reached a certain value. If the investigators desire to permeabilize internal membranes, nsPEF (pulses of a few nanoseconds duration) are applied^{25,26}. Indeed, using nsPEF, internal membranes such as mitochondrial²⁷ or endosomal²⁸ membranes were shown to be permeabilized. Thus, in the case of the μ sPEF (classical duration: 100 μ s), it is widely accepted that only the external membrane is affected by the electric pulses.

Only a couple of theoretical studies simulated the effect of the μ sPEF on organelles^{29,30}, and so far, no experimental study showed such an effect. Our quantitative study demonstrates for the first time that internal membranes can be permeabilized with a single 100 μ s pulse, while preserving cell viability. The amplitude of the pulse strength is highly dependent on the cell type.

haMSC and DC-3F cells and two media, with and without calcium, were used here to study calcium peaks generation in cells exposed to one 100 μ s pulse of field amplitudes ranging from 120 to 3000 V/cm. The DC-3F cells are a hamster cell line whereas the haMSC are human primary cells. Moreover, the DC-3F cells are small cells whereas the haMSC are large ones. The origin and size difference was important for us in order to have two models of cells and to study the interaction of the electric field with their PM and ER. One single electric pulse was delivered because we recently showed that pulses repetition frequency impacts the efficacy of the PM permeabilization when several pulses are delivered³¹. Thus, the real impact of electric pulses on different cells and/or organelles is easier to evaluate if a single pulse is delivered. In ulterior studies, it will be necessary to analyze the impact of pulses repetition frequency on organelles electropermeabilization. To distinguish between PM permeabilization and internal organelles permeabilization, we used a medium with classical Ca^{2+} concentration (DMEM; 1.8 mM CaCl_2) and a medium completely deprived of Ca^{2+} (SMEM-EGTA; not only the SMEM is prepared without Ca^{2+} ions, but moreover we added EGTA to complex any remaining trace of Ca^{2+} ions). In DMEM, a Ca^{2+} peak (detected by the increase in the cytosolic Fluo-4 Ca^{2+} marker fluorescence) is mainly the result of Ca^{2+} influx from the external medium, across the PM, but a

contribution of Ca^{2+} release from inner stores cannot be excluded. On the contrary, in the SMEM-EGTA, any observed cytosolic Ca^{2+} peak must be due to Ca^{2+} released from the Ca^{2+} inner stores.

Plasma membrane permeabilization

The comparison of the two curves achieved in the presence or absence of Ca^{2+} (Fig. 1 and 2 panels A and B) demonstrates that, up to certain field amplitude, only extracellular Ca^{2+} contributes to the peak in a medium with Ca^{2+} . Indeed, in haMSC and DC-3F cells, 100% of cells in DMEM displayed a Ca^{2+} peak respectively at 450 and 700 V/cm (Fig. 1 and 2 panels A), electric field amplitudes at which no Ca^{2+} peak was detected in SMEM-EGTA (Fig. 1 and 2 panels B).

This influx of extracellular calcium induced by the electric pulse could be the result of the electropermeabilization of the cell membrane or/and the activation of VOCCs. In the literature electropermeabilization is usually reported for transmembrane potential across the plasma membrane of at least 200 mV³². But these values are based on the penetration of large fluorescent dyes such as propidium iodide which are much larger than a calcium ion. For small ions like calcium, electropermeabilization probably occurs for lower transmembrane potentials. However, activation of VOCCs occurs for even lower membrane depolarization (30-50 mV)³³. Moreover, it has been reported that nsPEF can trigger calcium influx via VOCCs³⁴. We have thus exposed MSCs to the electric pulse in presence of L-type and T-type VOCCs inhibitors. Even at the lowest electric field amplitude, the use of VOCCs blockers did not affect the pulse-induced Ca^{2+} peaks (Fig. 3 and supplementary Fig. S4). Thus, VOCCs do not participate in the calcium peaks induced by the electric pulses, which is coherent with the fact that only 10–15% of MSCs express VOCCs^{35,36}. For DC3F, since the electric field necessary to induce calcium peaks is much higher, VOCCs are probably not involved either. Therefore, in our experiments the external calcium is most likely entering the cytoplasm through the electropermeabilized membrane. Indeed, penetration of Ca^{2+} from the outside of the cell due to PM permeabilization using trains of eight 100 μs electric pulses was already known. Tumor treatment by penetration of large Ca^{2+} amounts after electroporation is even tested at the clinical level³⁷.

Endoplasmic reticulum permeabilization

The calcium peaks reported in haMSC and DC-3F cells in SMEM-EGTA (Fig. 1 and 2 panels B) demonstrate that one single 100 μs pulse can mobilize Ca^{2+} from internal vesicles. Indeed, the total absence of Ca^{2+} in the external medium implies that the electro-induced Ca^{2+} peaks can only arise from the flow of Ca^{2+} from the internal stores to the cell cytosol. Since the ER is known to be the largest store of releasable Ca^{2+} in the cell³⁸, these electro-induced Ca^{2+} peaks are probably due to the release of Ca^{2+} from the ER. To test this hypothesis, we depleted the ER calcium store by inhibiting the SERCA (that pumps the Ca^{2+} from the cytosol to the ER) by thapsigargin (Fig. 4). When the thapsigargin was added to haMSC in SMEM-EGTA, an electric pulse of 2000 V/cm did not provoke an electro-induced Ca^{2+} peak. However, when the same electric pulse was applied without a prior addition of thapsigargin, all the cells presented a Ca^{2+} peak. This demonstrate that the ER depletion by thapsigargin prohibited the appearance of the electro-induced Ca^{2+} peaks. Therefore, the major source of electro-induced Ca^{2+} spike in SMEM-EGTA is the ER. This is coherent with the mathematical cell model of Esser *et al.*²⁹ who showed that a single 40 μs electric pulse can cause transient electric perturbations of all organelle

transmembrane voltages, preferably on larger organelles such as the ER compared to smaller organelles such as the mitochondria. This is also identical to what has been reported with nsPEF where the ER was also the only appreciable source of intracellular calcium increase in response to nsPEF stimulation in a calcium free buffer ³⁹.

To assess if the Ca^{2+} peaks observed in SMEM-EGTA were the result of the ER membrane electropermeabilization or a release of Ca^{2+} through the IP3R and RyR due to cellular signaling, experiments with inhibitors of these channels were performed at three field strengths. The IP3R and RyR are the two channels from which Ca^{2+} is released from the ER: the IP3R plays an important role in the transduction of the external stimuli to specific intracellular Ca^{2+} signals ⁴⁰. Both RyR and IP3R are activated by a cytosolic increase in Ca^{2+} concentration ⁴¹. Even in the simultaneous presence of the three inhibitors, Ca^{2+} peaks always appeared in SMEM-EGTA (Fig. 5 and supplementary Fig. S5). This concentration of inhibitors was sufficient to block the natural calcium oscillation of the haMSC in presence of external calcium, and even a 4-time increase of the inhibitors concentration did not affect the pulse induced Ca^{2+} peaks observed without external calcium (data not shown). This demonstrate that these Ca^{2+} peaks are due to the release of calcium through the ER electropermeabilized membrane.

Therefore, we bring the experimental evidence to the theoretical work of J. Weaver and colleagues ^{29,30} who postulated that μsPEF can permeabilize cell organelles even though organelles radius is lower than cell radius and even if internal vesicles are shielded by the PM before the pulses delivery.

Electroporation threshold for PM and ER in haMSC and DC3F cells

Electroporation threshold for PM

The curves reporting the percentage of cells presenting a Ca^{2+} peak after one μsPEF in DMEM as a function of the field amplitude are sigmoids, with a shift to higher values of the field amplitude in the case of the DC-3F cells (approximately two times higher) (Fig. 1 and 2 panel A).

This shift could be due to the difference in cell size, the haMSC mean radius being 4 times larger than the DC-3F cells one (respectively 36 and 9 μm). Indeed, H. Schwan ⁴² and others later on ⁴³ analyzed the influence of the particle radius in the ΔTMP generated by an external field showing the reciprocal influence of the radius and the field strength. However, according to the Schwan equation $\Delta\Psi = 3/2 E \cdot R \cos \theta$ ⁴² (where E: applied field strength; R: cell radius; θ : angle between field lines and a normal to the cell surface at the point of interest; $\Delta\Psi$: value of the electrically induced ΔTMP at this point of the cell surface), the electric field amplitudes between the two cell types should have differed by a factor of four, while they only differed by a factor of two. However, the Schwan equation is strictly valid for spherical cells in suspension. For attached cells the contribution of the cell size may not be linear. Moreover, other differences between the haMSC and DC-3F cells could contribute to the variation in the permeabilization threshold such as cell shape, cell orientation and cell organization ⁴⁴ (see supplementary Fig. S6).

All our data here were achieved using Ca^{2+} which is not a classical permeabilization marker. Therefore, a classical one, like the yo-pro-1 iodide ^{17,45}, was used to compare the PM permeabilization thresholds between the two markers (Supplementary Fig. S3). The results showed no cell permeabilization to yo-pro-1 at a field lower than 600 V/cm, whereas electropermeabilization to Ca^{2+} (in Ca^{2+} -containing

medium) was partly detectable at 120 and 270 V/cm for haMSC and DC-3F cells respectively. These results confirm that the electric field threshold needed to detect cell permeabilization is lower for a small molecule (like Ca^{2+}) than for a large one.

Electroporation threshold for ER

For the two cell types, higher electric field amplitudes were needed for the ER permeabilization than for the PM permeabilization (Fig. 1 and 2 panel B versus A). For example, in haMSC, an about 4 times higher electric field amplitude was needed to observe the beginning of the permeabilization of the Ca^{2+} internal stores membranes (480 vs 120 V/cm). In the case of nsPEF, the electric field threshold reported for ER permeabilization was also greater than the threshold for PM permeabilization³⁹. This could be explained by the fact that the PM needs to be permeabilized first for the field lines to be able to penetrate inside the cell and permeabilize the cell organelles. Moreover, according to Schwan⁴² and others^{29,46}, higher field amplitudes are needed to permeabilize the organelles membranes due to the organelles smaller size.

Permeabilization of the ER is detectable as soon as 480 V/cm for MSCs (4 times higher than for their PM permeabilization) and above 2000 V/cm for DC-3F cells (7.4 times higher than for their PM permeabilization). The difference in ER size and distribution between the two cell types could contribute to this discrepancy. Indeed, while haMSC ER distributes in a large fraction of the cell and completely surrounds the nucleus (Fig. 4), DC-3F cells ER was found to be localized in a rather small part of the cell at one side of the nucleus. Moreover, the link between the organelle size and the change in their transmembrane voltage induced by the electric pulse has been reported by Esser *et al.*²⁹. Using a mathematical cell model, they showed that a single 40 μs electric pulse causes a larger change in the organelle transmembrane voltage for larger organelles.

The percentage of DC-3F cells presenting a calcium peak in a medium without Ca^{2+} reached a maximum of around 40% at 2750 V/cm then decreased at 3000 V/cm. This decrease might be attributed to the leak of fluo-4 through the plasma membrane. Indeed, the very high field strength applied (3000 V/cm) could create large pores which would lead to the fluorophore leakage and to the fluorescence decrease.

Mean amplitude of the cytosolic calcium peaks: comparison between the 2 media and the 2 cell types

The mean amplitude of the calcium peaks in the 2 cell types was higher in a medium with Ca^{2+} than in a medium without Ca^{2+} . The flux of external Ca^{2+} across the membrane is thus higher than the Ca^{2+} release from the ER. The mean concentration of the Ca^{2+} in the cytosol varies between 100 and 400 nM^{47,48}. The Ca^{2+} concentration in DMEM is 1.8 mM, near the one found in the body extracellular medium (around 2mM^{49,50}), (the free Ca^{2+} concentration in serum is between 1.2 and 1.5 mM (4.8 and 5.9 mg/dl)⁵¹) whereas it varies between 50 μM and 1 mM in the RE^{52,53}. Considering these concentrations and the fact that the Ca^{2+} reservoir in the DMEM (the extracellular medium) is larger

than the of Ca^{2+} reservoir in the vesicles, the different amplitude of the Ca^{2+} peaks can be easily understood.

Furthermore, the PM is more exposed to the fields than the ER membranes, which are encaged inside the cell. The electric field lines have to interact first with the PM, thus creating pores, and then, enter the cell inside and interact with the ER membrane. Hence the PM permeabilized areas PM should be greater in number or larger in size than those created in the ER. However the shape of the curves was the same in the two media: an exponential increase for the DC-3F cells and an exponential increase followed by a straight line for the haMSC. The second part of the haMSC response was not due to a limited access of Ca^{2+} ions but to a limitation in the fluo-4 as demonstrated by using higher external concentrations of fluo-4-AM (supplementary Fig. S6). A three times increase in fluo-4AM concentration did not modify the percentage of cells displaying a Ca^{2+} peak but caused a significant increase in the peaks mean amplitude. Furthermore, calcein-AM fluorescence in DC-3F cells was higher than in haMSC demonstrating that DC-3F have a larger capacity to load the fluophores than haMSC (the calcein-AM uses the same strategy as fluo-4-AM to enter the cell - that is the presence of the acetoxymethyl hydrophobic group - but once in the cell, its fluorescence depends (between others) on the acetylsterases activity – the enzymes that cut the AM group - and not on the Ca^{2+} presence).

Cell Viability under the pulse conditions

Since massive Ca^{2+} entry into cell cytoplasm can cause apoptosis ⁵⁴, it was expected that cell viability would be lower when cells were pulsed in the presence of Ca^{2+} or eventually that the viability would be the same in the 2 media. Actually, the results with DC-3F cells were the opposite since at all the field amplitudes, their viability in SMEM-EGTA was apparently lower than in DMEM. haMSC viability was not significantly affected after the delivery of one 100 μs pulse in the presence or absence of calcium. Even at 2000 V/cm (where the internal Ca^{2+} stores were permeabilized in all the haMSC cells), the percentage of haMSC viability was about 85%.

To understand these results, microscopic observations of the DC-3F cells were performed for 20 min directly after the pulses. In SMEM-EGTA, the videos showed rapid movements of the cells and polykaryons began to be observed at short times (even 5 minutes) after the pulse delivery (supplementary Fig. S7). When cells were pulsed in DMEM, no cell fusion was observed within the first 20 minutes. The generation of polykaryons in SMEM-EGTA could explain, in part, the decrease in the number of colonies (that is the number of cells able to still replicate for several generations), and thus the apparent loss of viability, which was actually due to the cells electrofusion. The role of Ca^{2+} in the cell fusion procedure is controversial. Whereas some studies evocate a positive role in enhancing cell fusion ⁵⁵, another shows an inhibiting one ⁵⁶. Actually, fusion is a cell type dependent event, maybe related to differences in the extracellular matrix of the cells ⁵⁷: the fusogenicity of the DC-3F cells in SMEM-EGTA was not found with the haMSC.

Conclusion

The present study shows, for the first time, the electroporeabilization of the ER membrane by μsPEF , experimentally, and with cell viability assessments. It also demonstrates that one single micropulse with a low field amplitude is sufficient to permeabilize the cells PM to Ca^{2+} ions, a small size

permeability marker. The importance of the ER size, distribution and architecture in the field amplitude needed to permeabilize the ER was revealed. This study brings the experimental evidence to previous simulation studies on the interaction of μ sPEF with the internal membranes and establishes thresholds of permeabilization between PM and ER membrane, which are highly dependent on the cell type. It is also possible to conclude that the use of μ sPEF is an efficient tool to modulate calcium concentration, through the interaction with the cell or the ER membranes. Since the Ca^{2+} signalization in the cell always implicate the ER, and since the Ca^{2+} is implicated in key cellular functions, the ER permeabilization could be an effective tool to study the role of Ca^{2+} in such functions and cellular physiology without a chemical stimulation and in a receptor-independent manner. This study demonstrates that, in some cases, μ sPEF can be used to permeabilize internal membranes instead of nsPEF, with the interest that the μ sPEF generation is cheaper, easier to control and more accessible to a large number of teams than the nsPEF technology.

Materials and methods

Cells and cell culture conditions

haMSC (Human adipose-derived mesenchymal stem cells), isolated from lipoaspirates (a plastic surgery waste) of individuals that volunteered and gave informed and written consent for the use of the lipoaspirates, were grown in DMEM (Dulbecco's Modified Eagle Medium). DC-3F cells (Chinese hamster lung fibroblast cells) were grown in MEM (Minimum Essential Medium). Both media were supplemented with 10% fetal bovine serum, 100 U/mL penicillin and 100 mg/mL streptomycin. The cell culture chemicals were purchased from Fischer Scientific (Parc d'innovation Illkirch, France). Cells were propagated at 37°C in a humidified 5% CO_2 atmosphere.

haMSC were passed every 3-4 days (one passage corresponding to one doubling time of the population). The multipotency capabilities of the cells were assessed by submitting them to differentiation conditions as previously reported by our group in André *et al.*¹². DC-3F were routinely passed every 2 days.

During the experiments, two different media were used: DMEM and SMEM (Suspension Minimal Essential Medium) supplemented with 2mM (final concentration) of EGTA (*ethylene glycol tetraacetic acid* – a calcium chelator). DMEM contained 1.8 mM CaCl_2 whereas SMEM did not contain CaCl_2 .

Cell staining

Cells were seeded in 24 well plates at a density of $5 \cdot 10^4$ cells/cm² (DC-3F cells) or $20 \cdot 10^3$ cells/cm² (haMSC) one day before the experiments. In order to visualize the effect of the μ sPEF on living cells, the cells were incubated with 5 μ M of Fluo-4 AM (Fischer Scientific), a fluorescent Ca^{2+} marker, for 30 min in a humidified 5% CO_2 atmosphere at 37 °C in complete DMEM (haMSC) or MEM (DC-3F). To easily localize the cells, the incubation buffer also contained 375 nM of the nuclear fluorescent dye Hoechst 33342 (Fischer Scientific). After incubation, the wells were washed three times with PBS (Phosphate Buffered Saline) and then 500 μ l of either DMEM or SMEM-EGTA were added.

Inhibition of calcium channels and receptors

In order to inhibit the Voltage-Operated Calcium Channels (VOCCs), 10 μ M verapamil (L-type VOCC inhibitor) and 5 μ M of mibefradil (T-type VOCC inhibitor) were added to a final volume of 500 μ l of DMEM (in addition to Fluo-4 AM and Hoechst 33342) and incubated with the cells for 30 min. Then, the incubation medium was removed, the cells were washed 3 times with PBS and a fresh DMEM medium containing the same concentration of the inhibitors was added to the cells.

In experiments devoted to inhibit the inositol trisphosphate receptors (IP3R) and ryanodine receptors (RyR), 50 μ M of 2-aminoethoxydiphenyl borate (2-APB – an IP3R inhibitor), 50 μ M of dantrolene sodium salt (a RyR1 and 3 inhibitor) and 25 μ M flecainide acetate salt (a RyR2 inhibitor) were added to a final volume of 500 μ l of SMEM-EGTA (in addition to Fluo-4 AM and Hoechst 33342) and incubated with the cells for 30 minutes. Then, the incubation medium was removed, the cells were washed 3 times with PBS and a fresh SMEM-EGTA medium containing the same concentration of the inhibitors was added to the cells.

In order to empty the endoplasmic reticulum from calcium, 2 μ M (final concentration) of thapsigargin, an inhibitor of the sarco/endoplasmic reticulum calcium ATPase (SERCA) were added to the cells. All drugs were purchased from Sigma Aldrich (St Quentin Fallavier, France).

Microsecond pulse generator and electrodes

μ sPEF were generated by a CliniporatorTM (Igea, Carpi, Italy). For the treatment of the cells under the microscope, the pulse generator was connected to two parallel stainless steel rods of 1.2 mm diameter used as electrodes. They were shaped to enter a 24 plate well and touch the bottom of the dish. The distance between the electrodes was always 5 mm, except when very high fields (> 2000 V/cm) were applied. In this latter case the distance was 2 mm between the electrodes. The whole system was set under a Zeiss Axiovert S100 epifluorescence inverted microscope. One single micropulse of 100 μ s was delivered in all the experiments.

For cell viability assessment, we designed a new model of electrodes. In this system, a thick cover of 10 cm² was designed to fit in a Petri dish of the same dimensions. This cover contained 2 slots in which 2 plate electrodes of 2 mm thickness and 2 cm length could fit in: the electrodes were slipped into the slots until they touched the bottom of the Petri dish.

Image analysis

Images of the cells were taken every 10 s for 10 to 20 min with a Zeiss AxioCam Hrc camera controlled by the Axio Vision 4.6 software (Carl Zeiss, Germany). The pulses were always delivered after at least 2 minutes of recording and 2 seconds before the next image. The excitation and emission wavelengths used for Fluo-4 were 496 nm and 515 nm respectively. The nuclear dye Hoechst 33342 (λ_{ex} = 350 nm, λ_{em} = 461 nm) was used to track the cells during the videomicroscopy recording. There was no interference between Fluo-4 and Hoechst 33342 fluorescence because their emission wavelengths are separated enough. In this way, nuclei were recognized and the individual cells tracked using the Cell Profiler (version 2.0) software (Broad Institute, Cambridge, USA), allowing the automatic measurement of the fluorescence intensity signal of each cell on every image. Curves were plotted with a MATLAB program (version 7.8.0). All the observations were done at room temperature. The minimum opening

time of the shutter for the fluorescent light was about 500 ms. To decrease the light energy applied on the cells, a 90% density Filter NE110B (Thorlabs, Maisons-Lafitte, France) was used.

Transfection of the cells with the pcDNA-D1ER and endoplasmic reticulum imaging

pcDNA-D1ER was a gift from Amy Palmer & Roger Tsien (Addgene plasmid # 36325). This plasmid is coding for an endoplasmic reticulum (ER) marker fluorescing in green (535 nm) ⁵⁸. Cells were transfected with pcDNA-D1ER using 8 electric pulses of 100 μ s and 1500 V/cm or 1200 V/cm (for the haMSC and DC-3F cells respectively) delivered at a repetition frequency of 1 Hz by the CliniporatorTM (Igea, Carpi, Italy). We used 50 μ g or 20 μ g plasmid (for the haMSC and DC-3F cells respectively) in 100 μ l, for $5 \cdot 10^5$ cells in a cuvette of 1mm distance between the electrodes. D1ER is retained in the ER lumen through its C-terminal KDEL (lysine, aspartic acid, glutamic acid, leucine) sequence ⁵⁹.

A confocal microscope Leica TCS SPE with an objective HC PL APO CS2 63x, 1.30 NA oil and the LAS AF software version 3.3 (Leica, Germany) was used to visualize the endoplasmic reticulum, labelled by the ER marker. Excitation of the marker was done at 480 nm and emission captured at 535 nm. Cells nuclei were marked with Hoechst 33342 (excitation and emission at 405 and 486 nm respectively). The images were taken without electronic zooming for the haMSC and using a $\times 2$ zoom for the DC-3F cells.

The area of ER has been identified and reconstructed on the basis of the green fluorescence by using a custom semi-automated MATLABTM routine, obtained adapting the procedure of Joensuu *et al.* ⁶⁰. For each cell the algorithm elaborates together all the images taken, considering only the green channel. The preliminary choice of which pixel is reticulum was taken on the basis of a threshold set by means of the specific procedure. In particular, the green value attributable to the background noise was chosen, by taking the 99.9% value of the distribution of the areas without cells, and subtracted to the images. Successively the final threshold, interpreted as the green value attributable to the presence of the cells, was identified by taking the 95 % value of the areas with not transfected cells (called for simplicity negative cells). After the threshold identification, a clusterization of the images was carried out. Finally, on this binary matrix, extraction of the edges was performed resulting in the identification of the ER boundaries in the images.

Microscopic observations of the DC-3F cells

In experiments devoted to detect cell fusion events in the electric pulse treated DC-3F cells, the Petri dish was transferred after the pulse delivery in a chamber set on the microscope stage to maintain the cells at 37° C and 5% CO₂, and a video of the cells was recorded for 20 min, with an image taken every 15 s.

Cell viability assessment

Cells were seeded in 10 cm² Petri dishes containing one 12 \times 32 mm cover slide, at a density of 10⁵ cells/cm² (DC-3F) or 20.10³ cells/cm² (haMSC) one day prior to the experiments. After one day, medium was removed, cells were washed with PBS, and 1 ml of treatment medium (SMEM-EGTA, without Ca²⁺, or DMEM, with Ca²⁺) was added to the cells. The Petri dish cover with slots and the electrodes were placed and the pulse was delivered. After the pulse, the Petri dish was transferred into the incubator

for 10 (DC-3F) or 20 minutes (haMSC). The placement of the electrodes causes the loss of cells beneath the electrodes. Interestingly, this allows recognizing the area covered by the pulsed cells after the removal of the electrodes. Then, the non-pulsed cells on the cover slides were scratched under the sterile hood, and the cover slide with the pulsed cells only was transferred to a fresh medium and put in the incubator for 10 min (DC-3F) or 2 hours (haMSC). The use of short incubation times (two times 10 min) in the case of the DC-3F cells was mandatory to prevent difficulty in cell trypsinization.

The DC-3F cells were counted in one or two trypsinized non-pulsed controls. The other controls and treated (pulsed) samples were then trypsinized and diluted in complete medium (according to the number of cells in the controls) in order to obtain a final number of 1000 cells/8ml, later on distributed in 3 wells of a 6 wells plate (250 cells or 2ml/plate). The surviving cells formed colonies which were counted after 5 days.

Because haMSC do not form colonies, the assessment of haMSC viability could not be performed using the precise clonogenic assay test like in the case of the DC-3F cells. Therefore, pulsed haMSC cells were trypsinized, centrifuged, resuspended in 300µl of fresh medium, and distributed in 2 wells of an opaque-walled 96 multiwell plate. After 24 hours in the incubator, 150 µl of Cell-Titer Glo Reagent (Promega) were added to each well according to manufacturer's protocol. This caused cell lysis and generation of a luminescence signal proportional to the amount of ATP. The amount of ATP was directly proportional to the number of cells present in culture ⁶¹. The luminescence was read on a GloMax luminometer (Promega).

Calculation of the mean diameter of the cells and the endoplasmic reticulum

50 cells from each cell type were chosen randomly in photos taken under the Zeiss Axiovert microscope. The larger diameter and a perpendicular diameter to it were measured, then the mean diameter of the two were calculated for each cell. The mean diameter for a cell type was calculated as the mean of the mean diameter of 50 cells. The ER mean diameter of each cell type was measured in the same manner.

Statistical analysis

All the experiments were done at least 3 times. Data are presented as means and standard deviations (except where indicated). To compare the effect of the VOCCs inhibitors, Mann-Whitney test was used. For the experiments using haMSC in a medium without calcium and with inhibitors of calcium channels, two-way ANOVA followed by Turkey multiple comparisons test was used. To compare the results of DC-3F viability, Kruskal-Wallis test was used.

References

1. Sale, A. J. & Hamilton, W. A. Effects of high electric fields on micro-organisms. 3. Lysis of erythrocytes and protoplasts. *Biochim. Biophys. Acta* **163**, 37–43 (1968).
2. Mir, L. M., Banoun, H. & Paoletti, C. Introduction of definite amounts of nonpermeant molecules into living cells after electroporabilization: direct access to the cytosol. *Exp. Cell Res.* **175**, 15–25 (1988).

3. Neumann, E., Schaefer-Ridder, M., Wang, Y. & Hofschneider, P. H. Gene transfer into mouse lyoma cells by electroporation in high electric fields. *EMBO J.* **1**, 841–845 (1982).
4. Belehradek, M. *et al.* Electrochemotherapy, a new antitumor treatment. First clinical phase I-II trial. *Cancer* **72**, 3694–3700 (1993).
5. Sersa, G., Kranjc, S., Scancar, J., Krzan, M. & Cemazar, M. Electrochemotherapy of mouse sarcoma tumors using electric pulse trains with repetition frequencies of 1 Hz and 5 kHz. *J. Membr. Biol.* **236**, 155–162 (2010).
6. Al-Sakere, B. *et al.* Tumor ablation with irreversible electroporation. *PloS One* **2**, e1135 (2007).
7. Scheffer, H. J. *et al.* Irreversible electroporation for nonthermal tumor ablation in the clinical setting: a systematic review of safety and efficacy. *J. Vasc. Interv. Radiol. JVIR* **25**, 997–1011; quiz 1011 (2014).
8. Potter, H. & Heller, R. Transfection by electroporation. *Curr. Protoc. Cell Biol. Editor. Board Juan Bonifacino Al Chapter 20*, Unit20.5 (2011).
9. Mir, L. M., Moller, P. H., André, F. & Gehl, J. Electric pulse-mediated gene delivery to various animal tissues. *Adv. Genet.* **54**, 83–114 (2005).
10. Satkauskas, S. *et al.* Mechanisms of in vivo DNA electrotransfer: respective contributions of cell electropermeabilization and DNA electrophoresis. *Mol. Ther. J. Am. Soc. Gene Ther.* **5**, 133–140 (2002).
11. Poddevin, B., Orłowski, S., Belehradek, J. & Mir, L. M. Very high cytotoxicity of bleomycin introduced into the cytosol of cells in culture. *Biochem. Pharmacol.* **42 Suppl**, S67-75 (1991).
12. Liew, A. *et al.* Robust, efficient, and practical electrogene transfer method for human mesenchymal stem cells using square electric pulses. *Hum. Gene Ther. Methods* **24**, 289–297 (2013).
13. Finaz, C., Lefevre, A. & Teissié, J. Electrofusion. A new, highly efficient technique for generating somatic cell hybrids. *Exp. Cell Res.* **150**, 477–482 (1984).
14. Davalos, R. V., Mir, I. L. M. & Rubinsky, B. Tissue ablation with irreversible electroporation. *Ann. Biomed. Eng.* **33**, 223–231 (2005).
15. Beebe, S. J. *et al.* Diverse effects of nanosecond pulsed electric fields on cells and tissues. *DNA Cell Biol.* **22**, 785–796 (2003).
16. Vernier, P. T. *et al.* Calcium bursts induced by nanosecond electric pulses. *Biochem. Biophys. Res. Commun.* **310**, 286–295 (2003).
17. Vernier, P. T., Sun, Y. & Gundersen, M. A. Nanoelectropulse-driven membrane perturbation and small molecule permeabilization. *BMC Cell Biol.* **7**, 37 (2006).
18. Hockerman, G. H., Peterson, B. Z., Johnson, B. D. & Catterall, W. A. Molecular determinants of drug binding and action on L-type calcium channels. *Annu. Rev. Pharmacol. Toxicol.* **37**, 361–396 (1997).
19. Martin, R. L., Lee, J. H., Cribbs, L. L., Perez-Reyes, E. & Hanck, D. A. Mibefradil block of cloned T-type calcium channels. *J. Pharmacol. Exp. Ther.* **295**, 302–308 (2000).
20. Lytton, J., Westlin, M. & Hanley, M. R. Thapsigargin inhibits the sarcoplasmic or endoplasmic reticulum Ca-ATPase family of calcium pumps. *J. Biol. Chem.* **266**, 17067–17071 (1991).
21. Thastrup, O., Cullen, P. J., Drøbak, B. K., Hanley, M. R. & Dawson, A. P. Thapsigargin, a tumor promoter, discharges intracellular Ca²⁺ stores by specific inhibition of the endoplasmic reticulum Ca²⁺(+)-ATPase. *Proc. Natl. Acad. Sci. U. S. A.* **87**, 2466–2470 (1990).

22. Bootman, M. D. *et al.* 2-Aminoethoxydiphenyl borate (2-APB) is a reliable blocker of store-operated Ca^{2+} entry but an inconsistent inhibitor of InsP_3 -induced Ca^{2+} release. *FASEB J.* **16**, 1145–1150 (2002).
23. Zhao, F., Li, P., Chen, S. R., Louis, C. F. & Fruen, B. R. Dantrolene inhibition of ryanodine receptor Ca^{2+} release channels. Molecular mechanism and isoform selectivity. *J. Biol. Chem.* **276**, 13810–13816 (2001).
24. Hilliard, F. A. *et al.* Flecainide inhibits arrhythmogenic Ca^{2+} waves by open state block of ryanodine receptor Ca^{2+} release channels and reduction of Ca^{2+} spark mass. *J. Mol. Cell. Cardiol.* **48**, 293–301 (2010).
25. Schoenbach, K. H., Beebe, S. J. & Buescher, E. S. Intracellular effect of ultrashort electrical pulses. *Bioelectromagnetics* **22**, 440–448 (2001).
26. Tekle, E. *et al.* Selective field effects on intracellular vacuoles and vesicle membranes with nanosecond electric pulses. *Biophys. J.* **89**, 274–284 (2005).
27. Batista Napotnik, T., Wu, Y.-H., Gundersen, M. A., Miklavčič, D. & Vernier, P. T. Nanosecond electric pulses cause mitochondrial membrane permeabilization in Jurkat cells. *Bioelectromagnetics* **33**, 257–264 (2012).
28. Salomone, F. *et al.* High-yield nontoxic gene transfer through conjugation of the CM_{18} -Tat₁₁ chimeric peptide with nanosecond electric pulses. *Mol. Pharm.* **11**, 2466–2474 (2014).
29. Esser, A. T., Smith, K. C., Gowrishankar, T. R., Vasilkoski, Z. & Weaver, J. C. Mechanisms for the intracellular manipulation of organelles by conventional electroporation. *Biophys. J.* **98**, 2506–2514 (2010).
30. Weaver, J. C., Smith, K. C., Esser, A. T., Son, R. S. & Gowrishankar, T. R. A brief overview of electroporation pulse strength-duration space: a region where additional intracellular effects are expected. *Bioelectrochemistry Amst. Neth.* **87**, 236–243 (2012).
31. Silve, A., Guimerà Brunet, A., Al-Sakere, B., Ivorra, A. & Mir, L. M. Comparison of the effects of the repetition rate between microsecond and nanosecond pulses: electroporeabilization-induced electro-desensitization? *Biochim. Biophys. Acta* **1840**, 2139–2151 (2014).
32. Teissié, J. & Rols, M. P. An experimental evaluation of the critical potential difference inducing cell membrane electroporeabilization. *Biophys. J.* **65**, 409–413 (1993).
33. Fox, A. P., Nowycky, M. C. & Tsien, R. W. Kinetic and pharmacological properties distinguishing three types of calcium currents in chick sensory neurones. *J. Physiol.* **394**, 149–172 (1987).
34. Craviso, G. L., Choe, S., Chatterjee, P., Chatterjee, I. & Vernier, P. T. Nanosecond electric pulses: a novel stimulus for triggering Ca^{2+} influx into chromaffin cells via voltage-gated Ca^{2+} channels. *Cell. Mol. Neurobiol.* **30**, 1259–1265 (2010).
35. Heubach, J. F. *et al.* Electrophysiological properties of human mesenchymal stem cells. *J. Physiol.* **554**, 659–672 (2004).
36. Zahanich, I. *et al.* Molecular and functional expression of voltage-operated calcium channels during osteogenic differentiation of human mesenchymal stem cells. *J. Bone Miner. Res. Off. J. Am. Soc. Bone Miner. Res.* **20**, 1637–1646 (2005).
37. Frandsen, S. K. *et al.* Direct therapeutic applications of calcium electroporation to effectively induce tumor necrosis. *Cancer Res.* **72**, 1336–1341 (2012).
38. Ashby, M. C. & Tepikin, A. V. ER calcium and the functions of intracellular organelles. *Semin. Cell Dev. Biol.* **12**, 11–17 (2001).
39. Semenov, I., Xiao, S. & Pakhomov, A. G. Primary pathways of intracellular Ca^{2+} mobilization by nanosecond pulsed electric field. *Biochim. Biophys. Acta* **1828**, 981–989 (2013).

40. Berridge, M. J., Bootman, M. D. & Roderick, H. L. Calcium: Calcium signalling: dynamics, homeostasis and remodelling. *Nat. Rev. Mol. Cell Biol.* **4**, 517–529 (2003).
41. Patel, S. & Docampo, R. Acidic calcium stores open for business: expanding the potential for intracellular Ca²⁺ signaling. *Trends Cell Biol.* **20**, 277–286 (2010).
42. Schwan, H. P. Electrical properties of tissue and cell suspensions. *Adv. Biol. Med. Phys.* **5**, 147–209 (1957).
43. Kotnik, T. & Miklavcic, D. Analytical description of transmembrane voltage induced by electric fields on spheroidal cells. *Biophys. J.* **79**, 670–679 (2000).
44. Kotnik, T., Pucihar, G. & Miklavcic, D. Induced transmembrane voltage and its correlation with electroporation-mediated molecular transport. *J. Membr. Biol.* **236**, 3–13 (2010).
45. Chen, M.-T., Jiang, C., Vernier, P. T., Wu, Y.-H. & Gundersen, M. A. Two-dimensional nanosecond electric field mapping based on cell electroporation. *PMC Biophys.* **2**, 9 (2009).
46. Gowrishankar, T. R. & Weaver, J. C. Electrical behavior and pore accumulation in a multicellular model for conventional and supra-electroporation. *Biochem. Biophys. Res. Commun.* **349**, 643–653 (2006).
47. Schantz, A. R. Cytosolic free calcium-ion concentration in cleaving embryonic cells of *Oryzias latipes* measured with calcium-selective microelectrodes. *J. Cell Biol.* **100**, 947–954 (1985).
48. Ratto, G. M., Payne, R., Owen, W. G. & Tsien, R. Y. The concentration of cytosolic free calcium in vertebrate rod outer segments measured with fura-2. *J. Neurosci. Off. J. Soc. Neurosci.* **8**, 3240–3246 (1988).
49. Larsson, L. & Ohman, S. Serum ionized calcium and corrected total calcium in borderline hyperparathyroidism. *Clin. Chem.* **24**, 1962–1965 (1978).
50. Goldstein, D. A. in *Clinical Methods: The History, Physical, and Laboratory Examinations* (eds. Walker, H. K., Hall, W. D. & Hurst, J. W.) (Butterworths, 1990).
51. Sofronescu, A. G. Serum Calcium: Reference Range, Interpretation, Collection and Panels. (2016).
52. Hofer, A. M. & Machen, T. E. Technique for in situ measurement of calcium in intracellular inositol 1,4,5-trisphosphate-sensitive stores using the fluorescent indicator mag-fura-2. *Proc. Natl. Acad. Sci. U. S. A.* **90**, 2598–2602 (1993).
53. Chatton, J. Y., Liu, H. & Stucki, J. W. Simultaneous measurements of Ca²⁺ in the intracellular stores and the cytosol of hepatocytes during hormone-induced Ca²⁺ oscillations. *FEBS Lett.* **368**, 165–168 (1995).
54. Orrenius, S., Zhivotovsky, B. & Nicotera, P. Regulation of cell death: the calcium-apoptosis link. *Nat. Rev. Mol. Cell Biol.* **4**, 552–565 (2003).
55. Suo, L. *et al.* Optimal concentration of calcium and electric field levels improve tetraploid embryo production by electrofusion in mice. *J. Reprod. Dev.* **55**, 383–385 (2009).
56. Zheng, Q. & Zhao, N. M. Electrofusion of IBRS2 cells and the study of their fusion process. *Sci. China B* **32**, 303–313 (1989).
57. Salomskaitė-Davalgienė, S., Čepurnienė, K., Satkauskas, S., Venslauskas, M. S. & Mir, L. M. Extent of Cell Electrofusion In Vitro and In Vivo Is Cell Line Dependent. *Anticancer Res.* **29**, 3125–3130 (2009).
58. Palmer, A. E., Jin, C., Reed, J. C. & Tsien, R. Y. Bcl-2-mediated alterations in endoplasmic reticulum Ca²⁺ analyzed with an improved genetically encoded fluorescent sensor. *Proc. Natl. Acad. Sci. U. S. A.* **101**, 17404–17409 (2004).

59. Munro, S. & Pelham, H. R. A C-terminal signal prevents secretion of luminal ER proteins. *Cell* **48**, 899–907 (1987).
60. Joensuu, M. *et al.* ER sheet persistence is coupled to myosin 1c-regulated dynamic actin filament arrays. *Mol. Biol. Cell* **25**, 1111–1126 (2014).
61. Crouch, S. P., Kozlowski, R., Slater, K. J. & Fletcher, J. The use of ATP bioluminescence as a measure of cell proliferation and cytotoxicity. *J. Immunol. Methods* **160**, 81–88 (1993).

Acknowledgements

This work has been supported by CNRS, Gustave Roussy and Université Paris XI. The research was also conducted in the scope of the EBAM European Associated Laboratory (LEA) and of the COST action BM 1309 EMF-MED. This project received support within the framework of the Joint IIT-Sapienza LAB on Life-NanoScience Project (81/13 16-04-2013). Authors want to thank Sophie Salome from the PFIC of Gustave Roussy for her precious help in acquiring the ER photos, Paola Camilleri and Mattia Corradini for their contribution to the setup of the ER images extraction procedure and Francesca Apollonio and Thierry Ragot for scientific discussions.

Author contributions

H.H, F.M.A and L.M.M.: Conception and design of the study, H.H: performance of biological experiments, A.D and M.L: performance of numerical research, H.H, A.D, M.L, F.M.A and L.M.M.: data analysis and interpretation, writing and final approval of manuscript.

Competing Financial Interests Statement

The authors declare no competing financial interests.

Figures

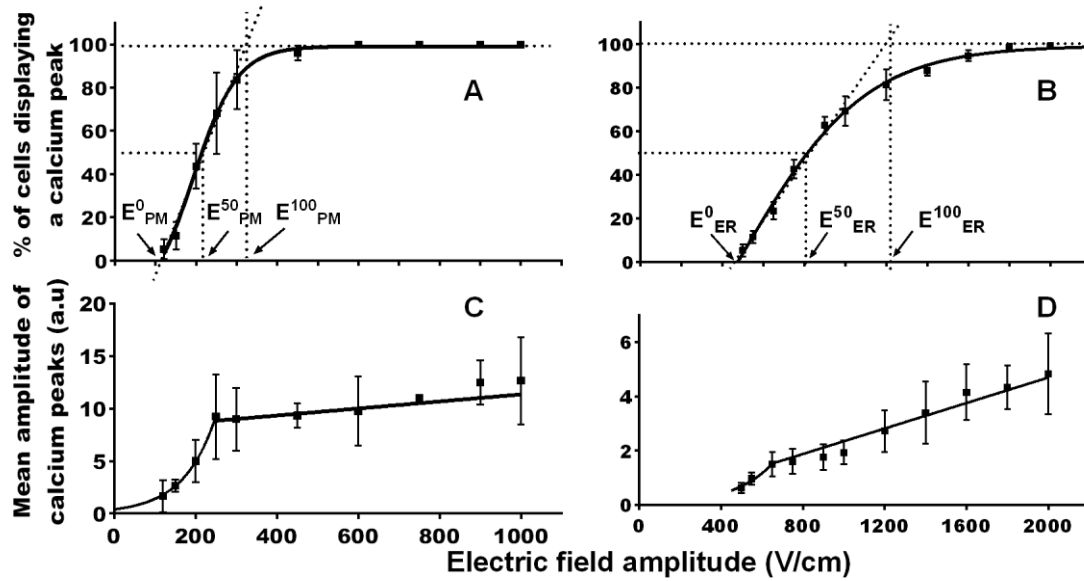


Figure 1. Response of the haMSC exposed to one pulse of 100 μ s in DMEM (panels A and C) or in SMEM-EGTA (panels B and D). (A and B): Percentage of cells displaying calcium peaks. (C and D): Mean amplitude of the calcium peaks. E^0 , E^{50} , and E^{100} are the values of the electric field amplitudes needed to respectively start to permeabilize the cells, and for the permeabilization of 50% and 100% of the cells.

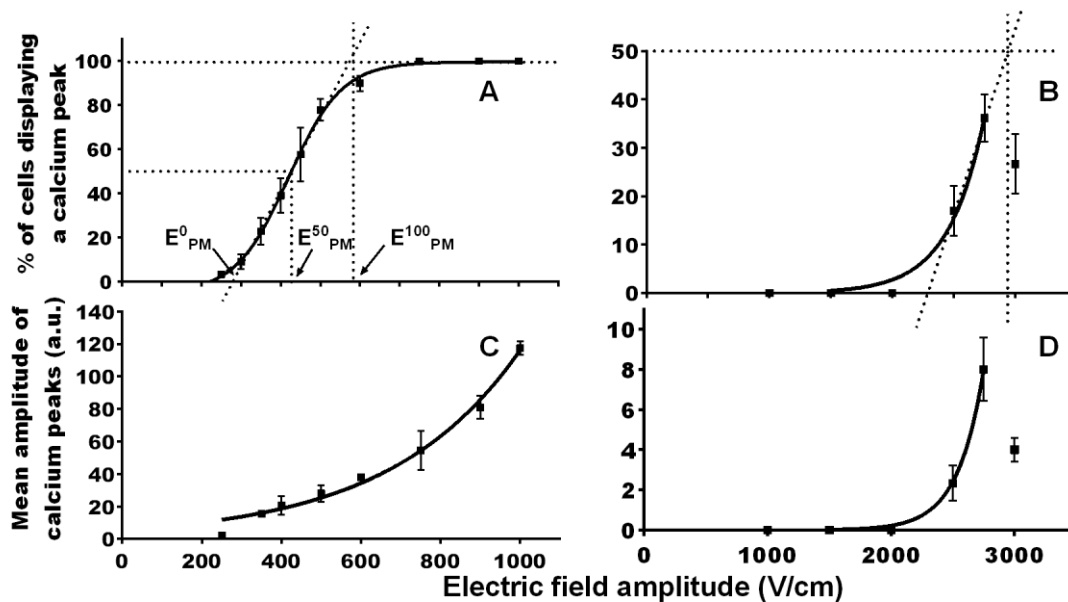


Figure 2. Response of the DC-3F cells exposed to one pulse of 100 μ s in DMEM (panels A and C) or in SMEM-EGTA (panels b and d). (A and B): Percentage of cells displaying calcium peaks. (C and D): Mean amplitude of the calcium peaks. For E^0 , E^{50} , and E^{100} , refer to Fig. 1.

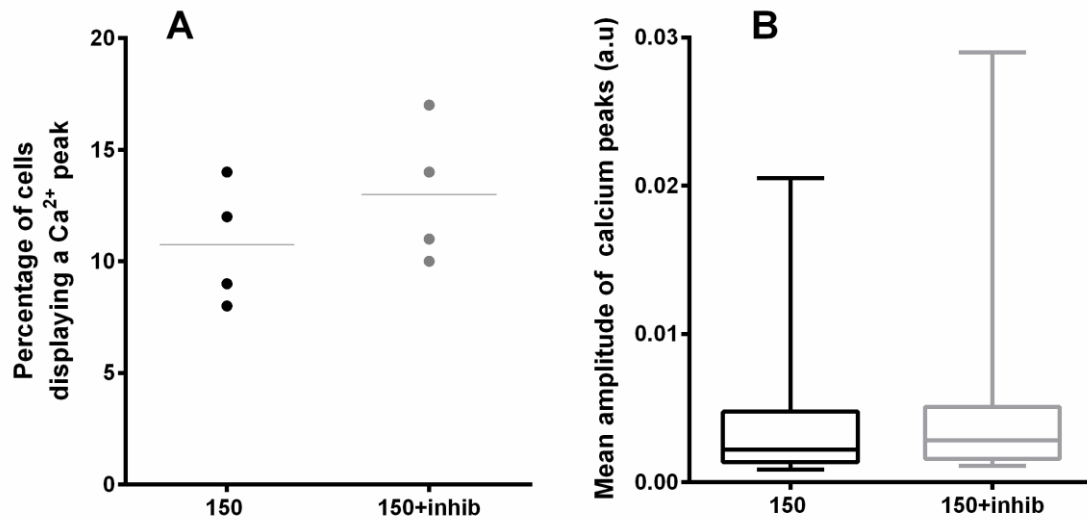


Figure 3. Response of haMSC in DMEM in the presence of VOCCs inhibitors. (A) Percentage of cells presenting a Ca²⁺ peak (n=4 experiments), the line represents the mean, P = 0.4. (B) Mean amplitude of Ca²⁺ peaks (n=39 cells for 150 and 49 cells for 150+inhib), boxes and whiskers representing 5-95 percentile are shown, P = 0.828. 150: one pulse of 150 V/cm (100 μ s), inhib: in the presence of 10 μ M verapamil and 5 μ M mibefradil.

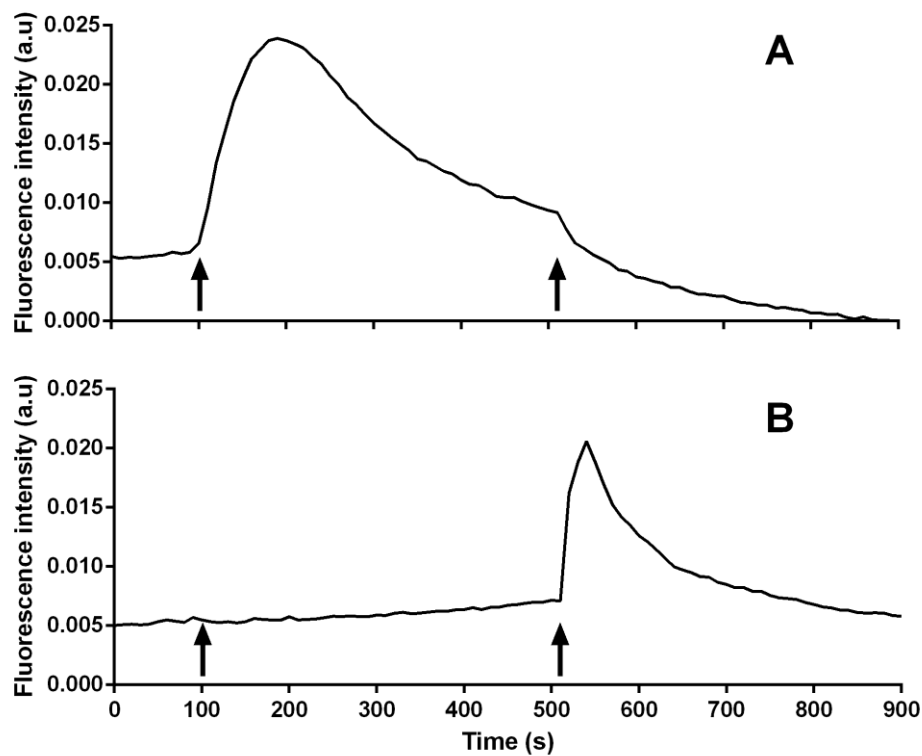


Figure 4. Application of 2000 V/cm in haMSC in SMEM-EGTA with or without thapsigargin. First arrow: (A) 2 μ M thapsigargin, (B) control. Second arrow: 2000 V/cm (A and B).

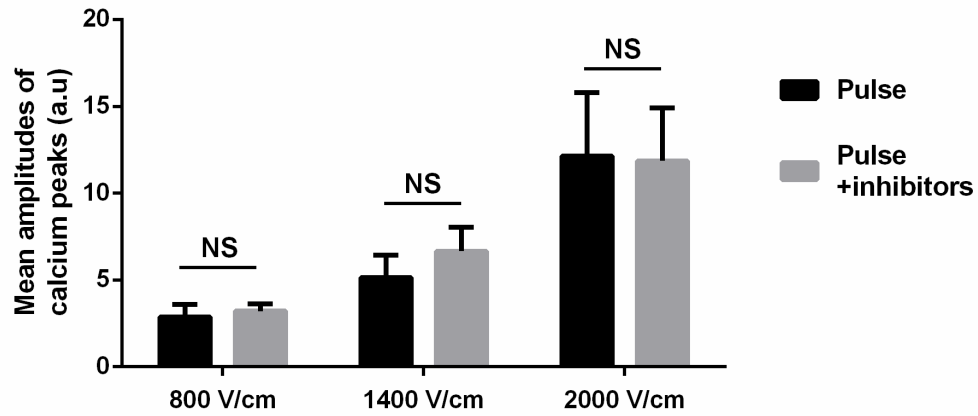


Figure 5. haMSC electropulsed in a medium without calcium (SMEM-EGTA): mean amplitude of the calcium peaks in the presence or the absence of 50 μ M of 2-APB, 50 μ M of Dantrolene and 25 μ M of Flecainide. Data are mean \pm SD.

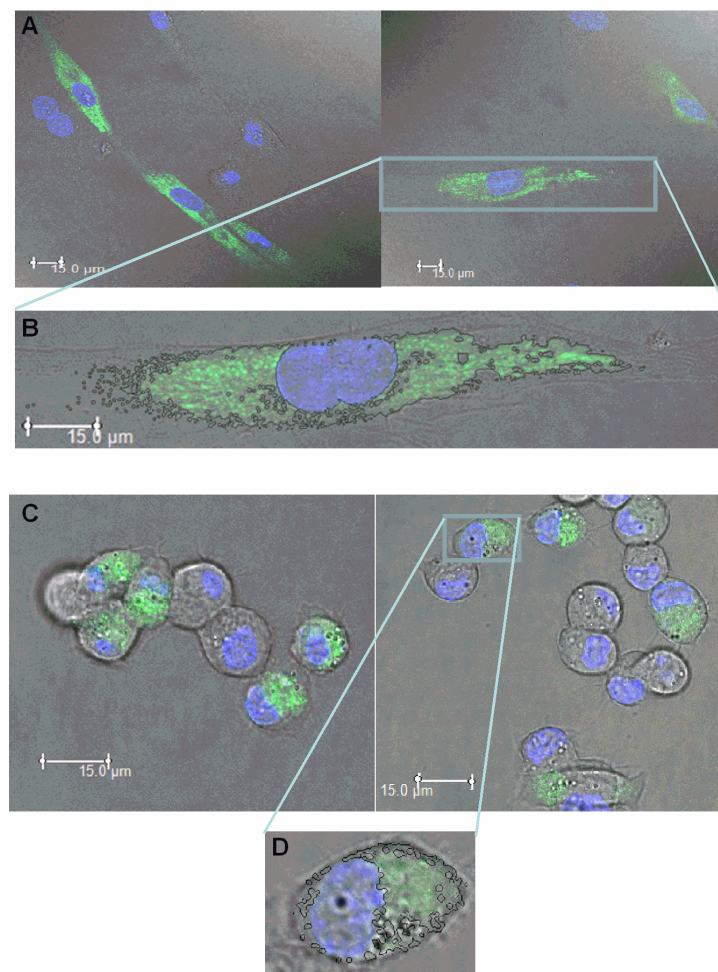


Figure 6. Endoplasmic reticulum of the 2 cell types labelled by the protein D1ER ($\times 63$). (A and B): haMSC; (C and D): DC-3F cells. The images were taken without zooming for the haMSC and using a $\times 2$

zoom for the DC-3F cells (Nuclei were labelled with by Hoechst 33342). (A and C): confocal pictures. (B and D): examples of ER identification and reconstruction.

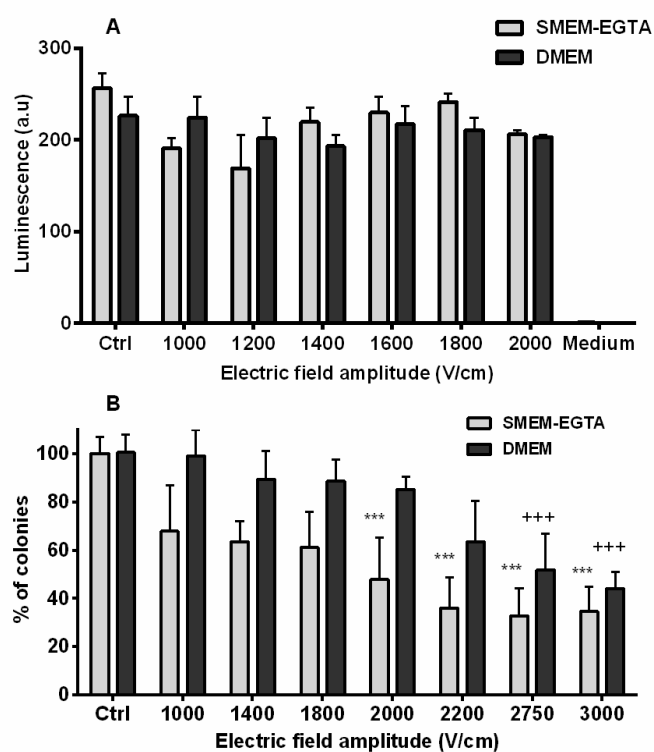


Figure 7. Cells viability after exposure to one 100 μ s pulse in a medium with calcium (DMEM) or without calcium (SMEM-EGTA). (A) haMSC. (B) DC-3F cells. Data are means \pm SD. +++ and *** p < 0.001 compared respectively to the DMEM and SMEM-EGTA controls (Ctrl).

Supplementary figures:

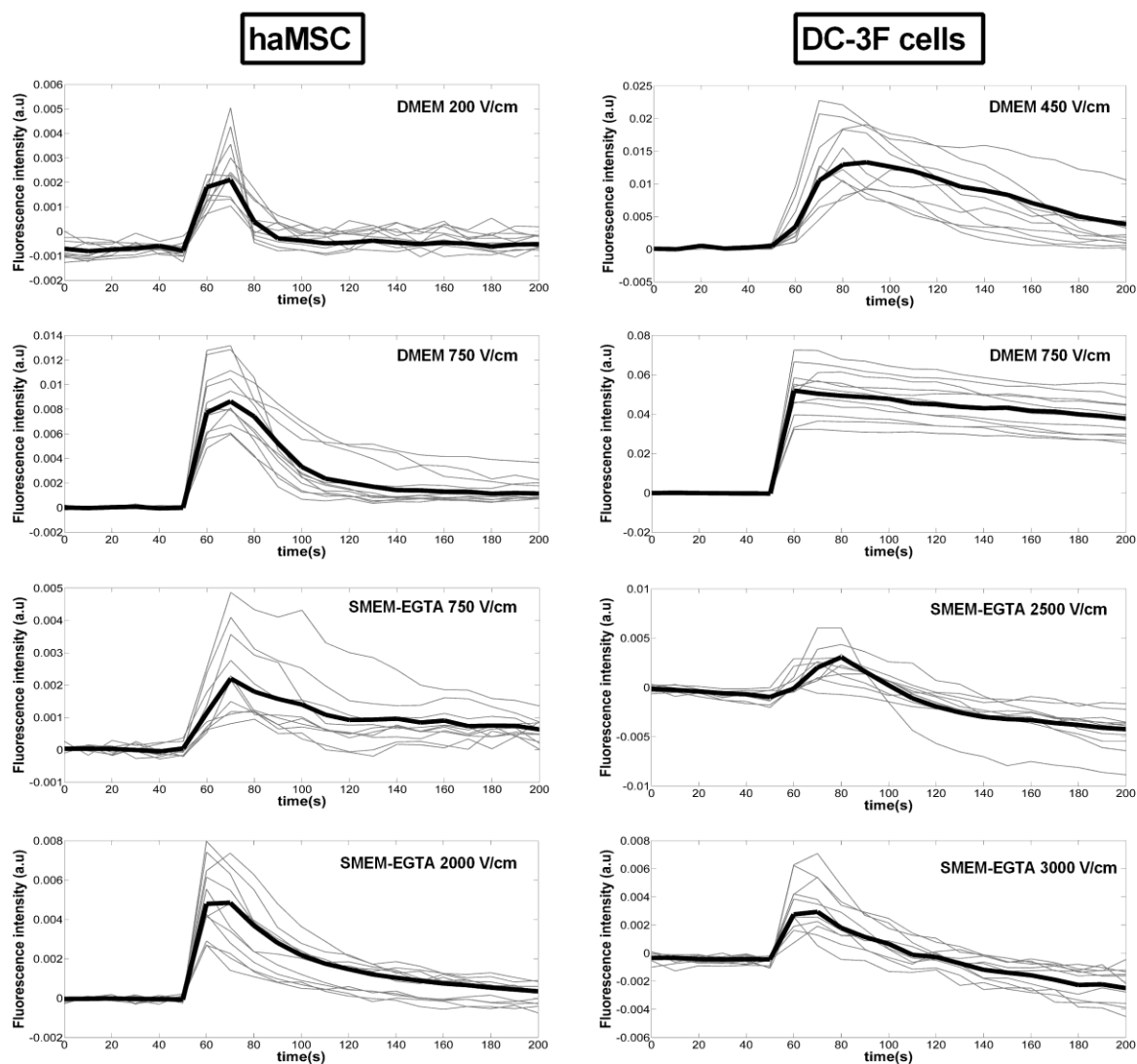


Figure S1. Typical traces of Ca^{2+} peaks for the haMSC and the DC-3F cells in a medium with (DMEM) or without Ca^{2+} (SMEM-AGTA). The rigid line represents the average. The optimal scale plotted by Matlab was shown.

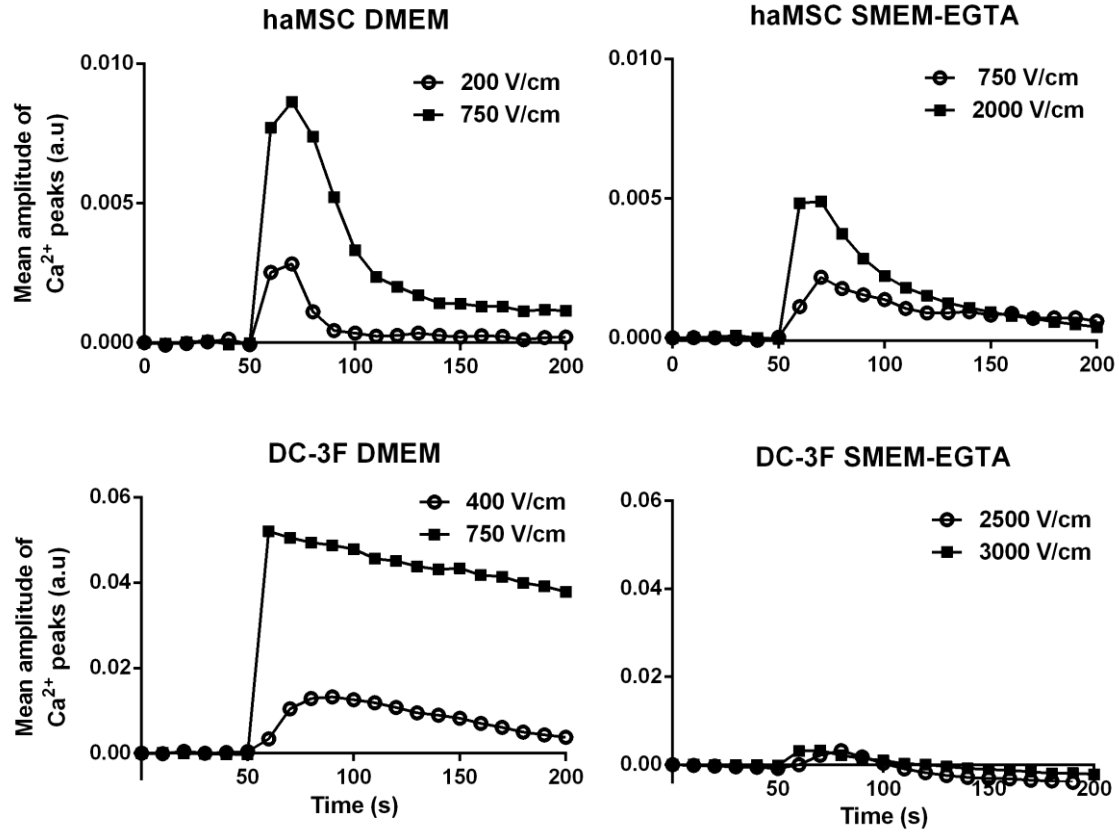


Figure S2. The average of Ca^{2+} peaks presented in Fig. S1 plotted on the same scale.

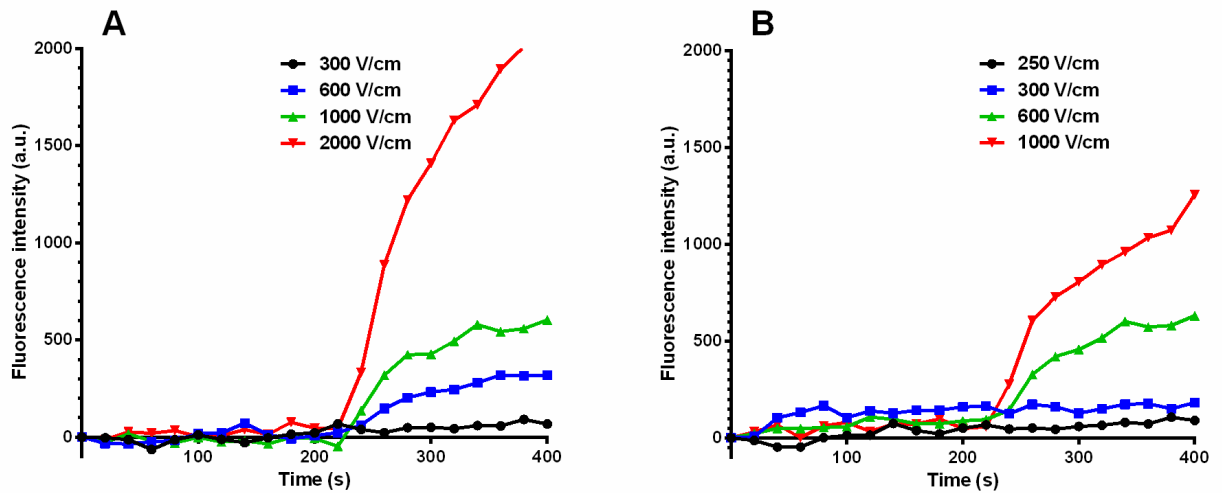


Figure S3. Evolution of the fluorescence intensity of the cells electroporated in the presence of $5\ \mu\text{M}$ yo-pro-1 iodide as a function of the pulse electric field amplitude. (A) haMSC. (B) DC-3F cells. Photos were taken every 20s. Pulse was delivered at $t=230$ seconds. The initial auto fluorescence of the cells at time 0 was subtracted from all the measurements.

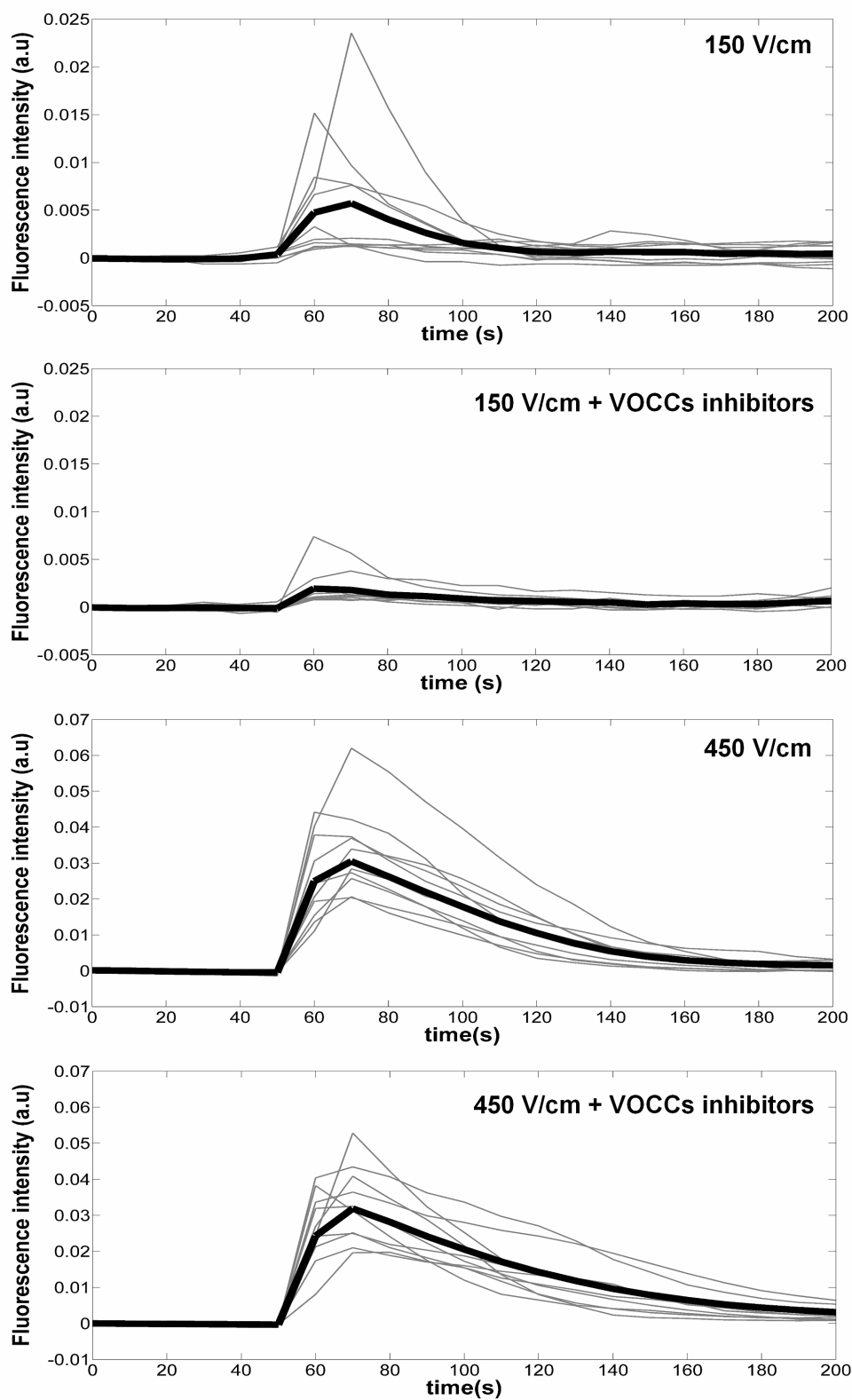


Figure S4. Typical traces of Ca^{2+} peaks for the haMSC in DMEM with or without VOCCs inhibitors.

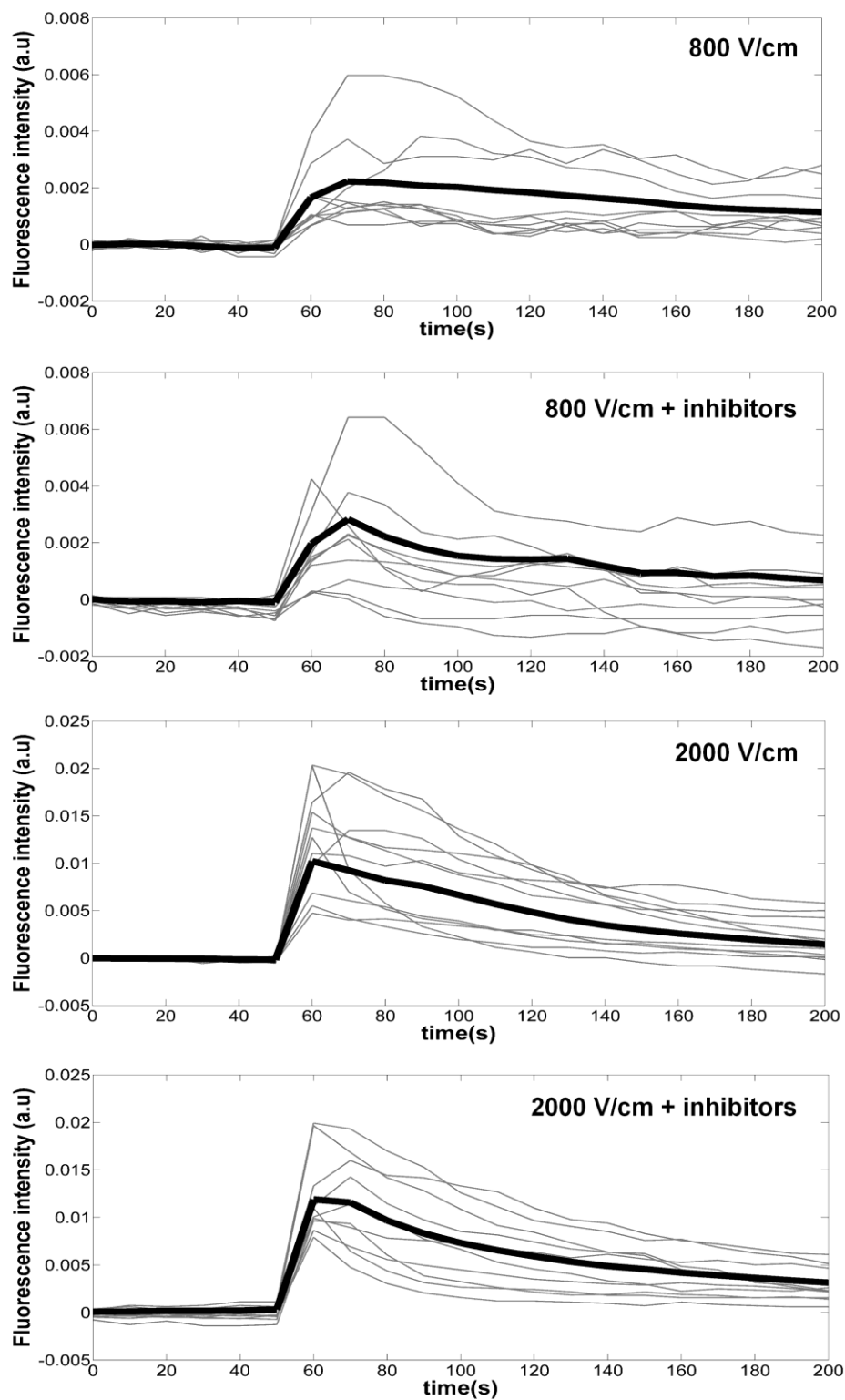


Figure S5. typical traces of Ca^{2+} peaks for the haMSC in SMEM-EGTA with or without IP3R and RyR inhibitors.

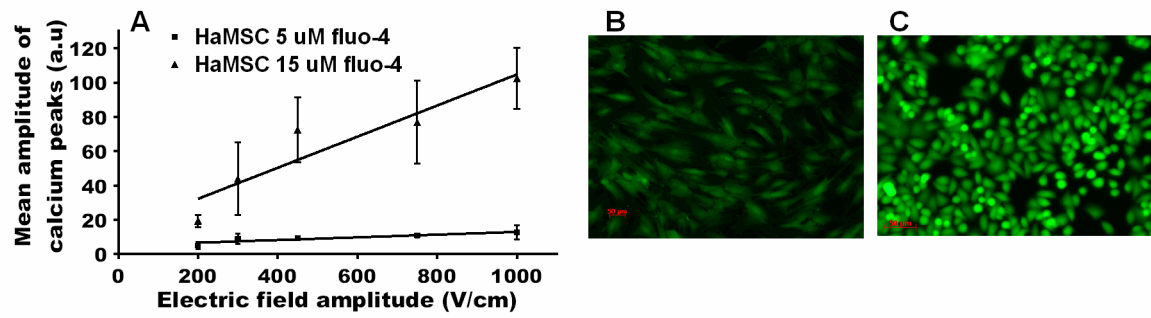


Figure S6. (A) Mean amplitude of the calcium peaks in haMSC after previous incubation of the cells in 5 or 15 μ M fluo-4 AM; (B and C): loading of respectively haMSC and DC-3F cells incubated in the presence of 5 μ M calcein AM for 30 minutes at 37°C.\

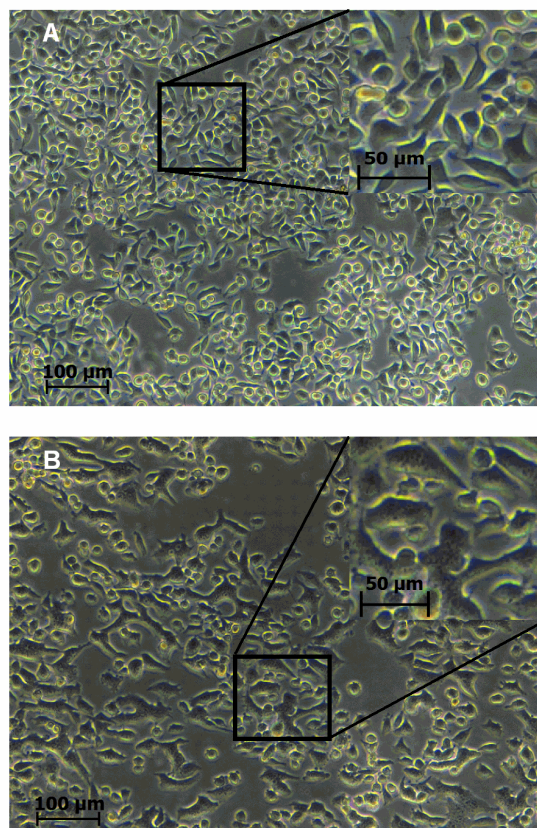


Figure S7. DC-3F cells electrofusion after one pulse in SMEM-EGTA. (A) control, (B) 20 min after a pulse of 2000 V/cm.

2 ELECTRICAL CONTROL OF CALCIUM OSCILLATIONS IN MESENCHYMAL STEM CELLS USING MICROSECOND PULSED ELECTRIC FIELDS (ARTICLE N°2)

The mesenchymal stem cells (MSCs) are promising candidates for the regenerative medicine and the cell therapy. These multipotent stem cells can differentiate into many cell types such as osteoblasts, chondrocytes, myoblasts and neuronal cells. These cells present spontaneous Ca^{2+} oscillations related to their differentiated state. Many studies demonstrated that the frequency of these oscillations differ according to the stemness or differentiated state of the MSCs. The team of Shan Sun (Sun et al. 2007) showed that the MSCs undergoing an osteoblastic differentiation for example have their Ca^{2+} oscillations frequency decreased, and that this frequency reached its minimal value in the finally differentiated osteoblasts. The team of Igor Titushkin (Titushkin et al. 2010) showed that the Ca^{2+} oscillations frequency differed between MSCs undergoing neurodifferentiation and MSCs undergoing osteo or myodifferentiation.

The first part of this thesis reports that one 100 μs pulse is able to induce cytosolic Ca^{2+} spikes originated from the extracellular medium or both the extracellular medium and the ER, depending on the electric field amplitude. Hence, we decided to use 100 μs pulse to create electro-induced Ca^{2+} spikes in the human adipose mesenchymal stem cells (haMSCs), to assess the effect of this pulse on the Ca^{2+} oscillations in the haMSCs. Our aim was to manipulate these oscillations by one or several 100 μs pulse. The results obtained in this second part of the thesis will help us to know how one 100 μs pulse can control the Ca^{2+} oscillations in MSCs. Since the Ca^{2+} oscillations are implicated in MSCs proliferation and differentiation, the control of these oscillations by an electric pulse could have an impact on MSCs differentiation. If one 100 μs pulse would give us positive results, we will use it later with haMSCs undergoing an osteogenic differentiation in order to evaluate its effect on this differentiation. These results have been submitted to “Stem Cell Research and Therapy” in September 2016.

Electrical control of calcium oscillations in mesenchymal stem cells using microsecond pulsed electric fields

Authors and affiliations

Hanna Hanna¹, Franck M. Andre¹, Lluís M. Mir^{1,*}

¹ Vectorology and Anticancer Therapies, UMR 8203, CNRS, Univ. Paris-Sud, Gustave Roussy, Université Paris-Saclay, 94 805 Villejuif, France.

Hanna.hanna@gustaveroussy.fr

franck.andre@cnrs.fr

luís.mir@cnrs.fr

* Correspondence should be addressed to Dr. Lluís M. Mir

E-mail address: luís.mir@cnrs.fr

Tel. : +33 1 42 11 47 92

UMR 8203 CNRS
Gustave Roussy, PR2
114 rue Edouard Vaillant
94805 VILLEJUIF Cédex
FRANCE

Abstract

Background

Human mesenchymal stem cells are promising tools for regenerative medicine due to their ability to differentiate into many cellular types such as osteocytes, chondrocytes and adipocytes amongst many other cell types. These cells present spontaneous calcium oscillations implicating calcium channels and pumps of the plasma membrane and the endoplasmic reticulum. These oscillations regulate many basic functions in the cell such as proliferation and differentiation. Therefore, the possibility to mimic or regulate these oscillations might be useful to regulate mesenchymal stem cells biological functions.

Methods

One or several electric pulses of 100 μ s were used to induce Ca^{2+} spikes caused by the penetration of Ca^{2+} from the extracellular medium, through the transiently electroporabilized plasma membrane, in human adipose mesenchymal stem cells from several donors. Attached cells were preloaded with

Fluo-4 AM and exposed to the electric pulse(s) under the fluorescence microscope. Viability was also checked.

Results

According to the pulse(s) electric field amplitude, it is possible to generate a supplementary calcium spike with properties close to those of calcium spontaneous oscillations, or, on the contrary, to inhibit the spontaneous calcium oscillations for a very long time compared to the pulses duration. Through that inhibition of the oscillations, Ca^{2+} oscillations of desired amplitude and frequency could then be imposed to the cells using subsequent electric pulses. None of the pulses used here, even those with the highest amplitude, caused a loss of cell viability.

Conclusions

An easy way to control Ca^{2+} oscillations in mesenchymal stem cells, through their cancellation or the addition of supplementary Ca^{2+} spikes, is reported here. Indeed, the direct link between the microsecond electric pulse(s) delivery and the occurrence/cancellation of cytosolic Ca^{2+} spikes allowed us to mimic and regulate the Ca^{2+} oscillations in these cells. Since microsecond electric pulses delivery constitutes a simple technology available in many laboratories, this new tool might be useful to investigate deeply the role of Ca^{2+} in human mesenchymal stem cells biological processes such as proliferation and differentiation.

Keywords

Mesenchymal stem cells - Calcium oscillations - Calcium spikes – Electroporation - Electric pulses – Electropermeabilization – Electropulsation

Background

Mesenchymal stem cells (MSCs) are multipotent stromal cells [1] originated from the embryonic mesoderm (mesenchyme) and present in many adult tissues such as bone marrow (bMSC), adipose tissue (aMSC), muscle, dermis, umbilical cord... [2,3]. These cells gained a lot of momentum in the last decade due to their ability to differentiate into a wide variety of cells including osteoblasts, myoblasts, fibroblasts and chondrocytes. They also express key markers of cardiomyocytes, neuronal and endothelial cells [4]. This ability makes them a very promising candidate for cell therapy and regenerative medicine in order to heal damaged tissues and organs. However, MSCs from different tissues are not the same. They have different differentiation capacities and transcriptomic signatures [5].

Human-adipose MSCs (haMSCs) that derived from the adipose tissue, are amongst the most easily accessible MSCs, in high quantities and without aggressive extraction procedures. They are more available than other MSCs as, for example, the human bMSCs (hbMSCs). In addition, they have a phenotype, surface markers [6] and gene expression profile similar to those of the hbMSC, and they are easier to maintain and proliferate [3], which make them ideal MSCs to use [7].

These cells present spontaneous Ca^{2+} oscillations implicating Ca^{2+} channels and pumps of the plasma membrane (PM) and the endoplasmic reticulum (ER) [8]. These oscillations seem to start by an ATP

autocrine/paracrine signaling [9] followed by Inositol triphosphate (IP3)-induced Ca^{2+} release from the ER and further amplification from plasma membrane store-operated Ca^{2+} channels (SOCCs). Afterward, the excess of Ca^{2+} is removed from the cytosol by the sarco/endoplasmic reticulum Ca^{2+} ATPase (SERCA), the plasma membrane Ca^{2+} ATPase (PMCA) and the $\text{Na}^+/\text{Ca}^{2+}$ exchanger (NCX) [10]. Ca^{2+} is the most important second messenger in the cell, and it regulates many important cellular processes such as ATP synthesis, apoptosis, cellular motility, growth, proliferation and gene expression. Hence, Ca^{2+} oscillations contain embedded information that have to be decoded by the cell, and Ca^{2+} signaling pathways play a key role in controlling cell behavior and differentiation processes of MSCs.

It was shown that the Ca^{2+} oscillations frequency is different between undifferentiated MSCs and MSCs on route of differentiation and it differs between the various outcomes of the differentiation process (the level of differentiation and the differentiated cell type). While the MSCs exhibit regularly repeated Ca^{2+} oscillations, MSCs undergoing osteodifferentiation display a decrease in the frequency of their spontaneous Ca^{2+} oscillations while primary myoblasts present still another pattern of oscillations [11]. This shows that each cell type possesses its own pattern of Ca^{2+} oscillations frequency and shape, but the exact correlation between Ca^{2+} oscillations and MSC differentiation is still unclear.

Presently, pulsed electric fields (PEF) are widely used in research as a non-invasive physical means to permeabilise cellular membranes. Using one or several pulses of ultrashort duration cause changes in the cell membrane structure that permits the access to the cell cytosol to molecules that cannot cross the plasma membrane under normal conditions [12]. Normally, Ca^{2+} is an ion that only crosses the plasma and ER membranes through channel proteins. Applying a PEF to cells in a medium containing Ca^{2+} (amongst other compounds) allows Ca^{2+} entry from the cell outside, and, if the electric field amplitude and pulse duration are high enough, Ca^{2+} is released from the cell inner stores [13]. The electromagnetic fields (EMF) have been already applied to hbMSCs to test their effect on the differentiation of these latters. Those EMF were either direct current of very low electric field amplitude (0.1 V/cm) and a long time exposition (30 min) [14] or biphasic electric current (1.5 $\mu\text{A}/\text{cm}^2$ for 250 μs) [15]. These fields either activate VOCCs if their amplitude is large enough or do not alter the membrane potential if the electric field is too low. None of the electromagnetic fields used was permeabilizing the cell PM.

The novelty of our study is the use of PEFs of a high field amplitude that are capable to permeabilize the cells PM or both the PM and the ER. Our objectives was to test the effect of these pulses on the Ca^{2+} oscillations of the cells. Attached haMSC presenting normal spontaneous Ca^{2+} oscillations were exposed to one single pulse of a duration of 100 μs and different electric field amplitudes. At low and moderate electric field amplitudes, the Ca^{2+} spike induced by such a PEF can be very similar to a spontaneous oscillation. At high electric field amplitudes, the electrically induced Ca^{2+} spikes inhibit the spontaneous oscillations occurrence for some time after which oscillations reappear. This inhibition allowed us to impose to the cells experimentally induced Ca^{2+} spikes at a desired frequency. Hence, we show here that it is possible to control haMSC spontaneous Ca^{2+} oscillations by microsecond pulsed electric field (μsPEF) with a complete preservation of the cell viability. The delivery of μsPEFs constitute an easy way to control Ca^{2+} oscillations in mesenchymal stem cells, through their cancellation or the addition of supplementary Ca^{2+} spikes. Indeed, unlike chemical factors which cause continuous effects, the direct link between the microsecond electric pulse(s) delivery and the ulterior occurrence/cancellation of the cytosolic Ca^{2+} spikes allowed us to mimic and regulate the Ca^{2+} oscillations in these cells. Since microsecond electric pulses delivery constitutes a simple technology

available in many laboratories, the electrical control of Ca^{2+} oscillations could be in the future a promising tool to further investigate the role of Ca^{2+} in MSC physiology and to better understand the correlation between the Ca^{2+} oscillations MSC biological processes such as proliferation and differentiation.

Methods

Cells and cell culture conditions

HaMSCs were isolated from surgical waste of individuals undergoing elective lipoaspiration. Samples were obtained after written informed consent from all the donors, in accordance with France and European legislations. The lipoaspirates were surgical waste and as such the French legislation (Art.L. 1245-2 du Code de la Santé Publique) establishes that the authorization from an ethics committee is not required. Every experiment was done on cells before passage 8 from, at least two donors (seven different donors in total). All haMSCs reacted similarly to the electric pulses, whatever the donor. The cells were grown in Dulbecco's Modified Eagle Medium (DMEM) with Glutamax and supplemented with 10% fetal bovine serum, 100 U/mL penicillin and 100 mg/mL streptomycin and were cultured at 37°C in a humidified incubator with 5% CO_2 . Cells were passed twice a week (every passage corresponds to one doubling time of the population). The multipotency capabilities of the cells were assessed by submitting them to differentiation conditions as previously reported in André *et al.* [16]. Cells from all the donors have thus been differentiated in osteoblasts, adipocytes and chondrocytes. The cell culture chemicals were purchased from Fischer Scientific (Parc d'innovation Illkirch, France).

Cell staining

One day prior to the experiments, cells were seeded in 24 well plates at a density of 20×10^3 cells/cm². After one day, the cells were incubated for 30 min with 5 μM of Fluo-4 AM (Fischer Scientific), a fluorescent Ca^{2+} marker, in a humidified 5% CO_2 atmosphere at 37°C in complete DMEM. The incubation buffer also contained 375 nM of the nuclear fluorescent dye Hoechst 33342. After incubation, the attached cells were rinsed three times with PBS (Phosphate Buffered Saline) and 500 μl of complete DMEM were added to the cells.

Microsecond pulse generator and electrodes

One single micropulse of 100 μs was delivered in all the experiments. A CliniporatorTM (Igea, Carpi, Italy) was used for the generation of the microsecond pulsed electric fields (μsPEFs). In order to treat the cells under the microscope, the pulse generator was connected to two parallel stainless steel rods of 1.2 mm diameter used as electrodes. The distance between them was 5 mm, and they were shaped to enter a 24 plate well and to reach the bottom of the dish. The whole system was set under a Zeiss Axiovert S100 epifluorescence inverted microscope.

In order to test the cell viability, another model of electrodes was designed. In this system, a thick cover of 10 cm² containing 2 slots was designed to fit in a Petri dish of the same dimensions. Two plate electrodes of 2 mm thickness and 2 cm length were slipped into the slots until they touched the bottom

of the Petri dish. This system does not permit to observe the cells under a microscope, it was used because it allows covering a larger surface (in order to have enough cells) than the system described above.

Images acquisition and analyses

Images of the cells were taken every 10 s for 10 to 20 min with a Zeiss AxioCam Hrc camera controlled by the Axio Vision 4.6 software (Carl Zeiss, Germany). The electric pulse was delivered after at least 2 minutes of recording, and 2 seconds before the next image. The excitation and emission wavelengths used for Fluo-4 were 496 nm and 515 nm respectively. The nuclear dye Hoechst 33342 (λ_{ex} = 350 nm, λ_{em} = 461 nm) was used to recognize the nuclei and to track the cells using the Cell Profiler (version 2.0) software (Broad Institute, Cambridge, USA). The software allowed the automatic measurement of the fluorescence intensity signal of each cell on every image. Curves were plotted using a Matlab program (version 7.8.0). All the observations were done at room temperature. The minimum opening time of the shutter for the fluorescent light was about 500 ms. To decrease the light energy applied on the cells, a 90% density Filter NE110B (Thorlabs, Maisons-Lafitte, France) was used.

Cell viability assessment

One day prior to the experiments, cells were seeded at a density of 20×10^3 cells/cm² in 10 cm² Petri dishes containing a 12×32 mm cover slide. After 24 hours, medium was removed, cells were washed with PBS, and 1 ml of fresh medium was added. The electrodes were placed on the cover slide using the Petri dish cover containing two slots and a 100 μ s pulse was delivered to the attached cells. After the pulse, the Petri dish was put in the incubator for 20 minutes. Then, the non- pulsed cells on the cover slides were scratched under a sterile hood. The area covered by the pulsed cells was recognised due to the loss of cells beneath the electrodes after the removal of these latter. The cover slide with the pulsed cells only was transferred to a Petri dish with fresh medium and placed for 2 hours in the incubator. Then medium was removed and the cells were trypsinised, centrifuged and resuspended in 300 μ l of a fresh medium. This volume was distributed in 2 wells of an opaque-walled 96 multiwell plate and put in the incubator for 24 hours. After 24 hours, cells were visualized on an epifluorescence microscope to compare their shape and level of confluence, and 150 μ l of Cell-Titer Glo Reagent (Promega) were added to each well according to manufacturer's protocol. The reagent caused cell lysis and the generation of a luminescent signal proportional to the amount of the ATP present in the medium. A GloMax luminometer (Promega) was used to read the luminescence. The ATP amount and therefore the luminescence intensity reflected the number of cells present in the culture [17].

Statistical analysis

All the experiments were done at least 3 times. Data are presented as means and standard deviations. The Spearman correlation was used to analyse data of Fig. 3 and Fig. 6.

Results

Spontaneous Ca^{2+} oscillations in haMSC in normal conditions and after one 100 μs electric pulse

Undifferentiated haMSC present asynchronous Ca^{2+} oscillations as seen in Fig. 1 (left column). The oscillations frequencies differed from cell to cell and not all of the cells displayed spontaneous Ca^{2+} oscillations (dire combien?). When one electric pulse of 100 μs was applied on haMSC, different situations could be observed. As shown in Fig. 1 (middle column), an electric pulse of 300 V/cm induced a Ca^{2+} spike in all the cells whatever the stage of their Ca^{2+} oscillation at the time the pulse was applied. After the pulse, the spontaneous Ca^{2+} oscillations returned to their original cell-dependent frequency and continued normally. When the electric pulse applied was 900 V/cm (Fig. 1, right), all the cells presented a Ca^{2+} spike with higher amplitude with respect to 300 V/cm. However, even 750 s after the pulse, the cells still presented a high cytosolic Ca^{2+} concentration (as shown by the persistent fluo-4 high fluorescence level) and the spontaneous Ca^{2+} oscillations did not yet resume.

Ca^{2+} spikes in response to different electric field amplitudes

The shapes of the electrically-induced Ca^{2+} spikes in response to a 100 μs duration pulse of different electric field amplitudes are represented in Fig. 2. At a very low electric field amplitude (100 V/cm), no Ca^{2+} spike was observed. At 150 V/cm, the Ca^{2+} spikes had a lower amplitude than the spontaneous oscillations and presented a relatively small slope. At moderate electric field amplitudes (200 to 450 V/cm), each electric pulse induced a Ca^{2+} spike. The Ca^{2+} spike displayed a higher slope than at 150 V/cm, then reached its maximal amplitude and came back to the normal Ca^{2+} amplitude as before the pulse. The electro-induced Ca^{2+} spikes had nearly the same shape and amplitude as the spontaneous oscillations at 200 and 300 V/cm. At 450 V/cm, their amplitudes were higher than the spontaneous ones, but they came back to the original baseline. When high electric field amplitudes were applied (600 to 900 V/cm), the electrically induced Ca^{2+} spike presented larger slopes (with different degree of sharpness depending on the electric field strength) and displayed a higher amplitude than the spontaneous oscillations; after the Ca^{2+} spike, the Ca^{2+} amplitude remained relatively high compared to the initial amplitude, and it took a longer time (several minutes) to come back to the normal depending also on the amplitude of the applied electric field.

According to Fig. 3, only 10% of the cells presented a Ca^{2+} spike in response to the electric pulse at 150 V/cm. This percentage increased proportionally to the electric field amplitude, mainly between 150 and 300 V/cm. 100% of the cells responded to the pulse at 450 V/cm. According to Spearman correlation analysis, there was a perfect correlation between the electric field amplitude and the percentage of cells displaying a Ca^{2+} spike ($r = 0.96$).

Different outcomes on Ca^{2+} oscillations according to the electric field amplitude

According to the electric field amplitude, the pulse-induced Ca^{2+} spike had different effects on Ca^{2+} oscillations. At a relatively low electric field amplitude (300 V/cm), the pulse-induced Ca^{2+} spike

displayed a very similar shape to the spontaneous Ca^{2+} oscillations (Fig. 4A), and it could be generated between two oscillations or during an oscillation. After the 100 μs pulse-induced Ca^{2+} spike, the spontaneous oscillations continued normally at their proper initial rhythm with no significant modification of the amplitude or duration of the oscillations. At relatively high electric field amplitude such as 600 V/cm, the pulse-induced Ca^{2+} spike displayed higher amplitude than the spontaneous oscillations and three different outcomes could be observed after the electro-induced spike. The oscillations could continue normally, with a minor change of the oscillation shape (Fig. 4B, upper trace). Or, secondly, a short inhibition of the spontaneous oscillations could be observed for some minutes, after which the oscillations reappeared (Fig. 4B, lower trace). The first oscillations that appeared after such an inhibition period did not displayed the same shape as the original ones. The third possible outcome was a longer inhibition of the Ca^{2+} oscillations, for a duration longer than 10 minutes (Fig. 4C). The application of higher electric field amplitude (750 and 900 V/cm) resulted in the inhibition of the spontaneous Ca^{2+} oscillations for longer times (depending on the amplitude of the electric field, even 45 to 60 minutes post pulses only some cells had recovered their oscillations). After 24 hours all cells recovered their oscillations whatever the electric field applied (data not shown).

The percentage of cells with no spontaneous oscillation for at least 10 minutes after the electric pulse delivery increased as a function of the electric field amplitude (Fig. 5). While no inhibition of the spontaneous oscillations was observed at 300 V/cm, 25% of the cells had their Ca^{2+} oscillations inhibited at 450 V/cm. Nearly all the cells had their Ca^{2+} oscillations inhibited after one electric pulse at 750 V/cm. 24 hours post pulses, the cells remained viable under all the conditions tested, even for the highest electric field amplitude (Fig. 6). Photos taken before the Cell-Titer Glo assay showed no difference in the shape and level of confluence of the cells between the pulsed and the control wells (data not shown). The Spearman correlation showed no effect of the electric field amplitude on the cell viability ($r = 0.43$).

Electrically-mediated Ca^{2+} spikes manipulation after the 900 V/cm inhibition

To test whether the cells were in a “refractory” state after the inhibition of their Ca^{2+} oscillations, or if they were still able to respond to the electric pulses, pulses of different field amplitudes were applied after a pulse of 900 V/cm (which provokes the absence of further spontaneous oscillations in 100% of the cells). For example (Fig. 7), a sequence of 3 pulses with descending electric field amplitudes (750 followed by 600 and 450 V/cm) were applied successively: the cells responded to the electric pulses as if each pulse would have been applied alone, or independently. The amplitude of the electrically-induced Ca^{2+} spike was again proportional to the electric field amplitude like in Fig. 2. Thus calibrated electric pulses allow to restore Ca^{2+} spikes at the time and with the amplitude chosen by the investigators.

Discussion

Mesenchymal stem cells (MSCs) are multipotent stromal cells that have the ability to self-renew and to differentiate into a wide variety of cells of the mesodermal, ectodermal, and endodermal lineages [18]. This is why they represent an important tool for cell therapy and regenerative medicine. However, the differentiation procedures may be long and not able to respond to the demand. The

improvement and optimization of these procedures is of a crucial importance to ensure the differentiated cells in a reasonable time. Many studies have tested the effects of physical stimuli on the differentiation outcomes. Altman *et al.* showed that the application of a cyclic mechanical stimulation (translational and rotational strain) to undifferentiated MSCs (embedded in a collagen gel) over a period of 21 days resulted in ligament cell lineage differentiation even without differentiation factors [19]. Ward and colleagues studied the effect of the application of a 3-5% tensile strain to a collagen I substrate and concluded that it stimulated osteogenesis of attached hMSCs [20]. Low intensity ultrasounds, another form of mechanical stress, have been shown to enhance the chondrogenic differentiation [21]. Sun *et al.* demonstrated that 0.1 V/cm electrical stimulation applied for 30 min per day for 10 days, on attached MSCs cultured with osteoinductive factors, accelerated their osteodifferentiation [14].

Ca²⁺ oscillations play an important role in the transduction of many physical stimuli in the cells. For example, tissue strain and shear stress on mouse tibia are transduced by repetitive Ca²⁺ spikes in the osteocytes. The spikes frequency and amplitude depend on the mechanical magnitude [22]. Electromagnetic fields (EMF) can also promote MSCs differentiation to osteoblasts through Ca²⁺-related mechanisms. The exposition of MSCs to pulsed EMF for 10 min every day results in the enhancement of osteogenesis early stages [23].

Ca²⁺ oscillations are a universal mode of Ca²⁺ signalling in both excitable [24,25], and non-excitable cells [26]. In non-excitable cells such as hMSC, Ca²⁺ oscillations are typically initiated by a receptor-triggered production of IP₃ (after the binding of an agonist to the receptor) [27] and the subsequent Ca²⁺ release from the ER [28] which stimulates the store-operated calcium entry (SOCE) via the SOCC [29]. It was shown that the Ca²⁺ oscillations frequency is different between undifferentiated MSC and MSC on routes of differentiation and it differs between the various differentiated cell types [11]. According to Titushkin *et al.*, the MSCs Ca²⁺ oscillations are suppressed after the addition of neuroinductive factors, but reappear in less than 7 days after neurodifferentiation [11]. Sun and colleagues observed that multipotent MSCs present 8.06 ± 2.64 Ca²⁺ spikes per 30 min of observation, and that this number decreases to 3.66 ± 2.42 after 28 days of incubation with osteoinductive factors [14].

In our study, we decided to analyse the effect of a type of short electric pulses termed microsecond pulsed electric fields (μ sPEF) on the spontaneous Ca²⁺ oscillations of haMSC because many of the physical stimuli are transduced by cytosolic Ca²⁺ concentration rapid changes (oscillations) in the cells. The ultrashort pulses (one thousandth to one ten thousandth shorter than the pulses of 100 μ s used in our study) called nanopulses or nanosecond pulsed electric fields (nsPEF) have been used already to induce Ca²⁺ bursts in the cell, which resulted from the electroporabilisation of the ER, the plasma membrane or both [13,30]. However, contrary to the 100 μ s electric pulses, the technology to deliver nanopulses is not yet spread in the laboratories and is not simple to use.

The haMSCs loaded with the fluorescent marker Fluo-4 asynchronously displayed periodic changes in their cytosolic Ca²⁺ concentration detected by the periodic increase of their fluorescence. The videos of the haMSCs showed that not all the cells presented Ca²⁺ oscillations at a specific time. Some of the cells never displayed oscillations during the recording time (20 minutes). This observation can be related to the fact that MSCs display Ca²⁺ oscillations only during the phases G1 and S of the cell cycle, and not all the cells in the visualisation area of an experiment were in those phases of the cell cycle. Ca²⁺ oscillations increase the levels of cell cycle regulators such as cyclins A and E and probably

control cell cycle progression and cell proliferation, via the regulation of cyclin levels (amongst other mechanisms) [31]. In addition, the haMSCs presenting Ca^{2+} oscillations displayed them at different rhythms and frequencies: the oscillations were asynchronous, and at a given time, each cell was in a different phase of a Ca^{2+} oscillation and the oscillations frequencies displayed wide variations between cells. The average duration of an oscillation was around two minutes.

Electric pulses of 100 μs duration are already applied in many biotechnological and medical applications, notably in anticancer electrochemotherapy [32], tumour ablation [33], and cell transfection [34]: by permeabilizing the plasma membrane temporally they allow the internalization of non-permeant molecules of interest like drugs or nucleic acids. Classically, 8 successive pulses of 100 μs are used in biomedical sciences. The technology is spread in many laboratories and is very simple to use. In our study, we applied a single electric pulse because, when several pulses are delivered, pulses repetition frequency may impact the efficacy of cell membrane permeabilisation as we have recently shown in our group [35]. When an electric pulse of 100 μs was applied to the cells, an electrically-induced Ca^{2+} spike was observed synchronously in a given percentage of the cells (as a function of the electric field amplitude). Moreover, the electric field amplitude should be enough to cause the transmembrane voltage to reach a permeabilization threshold. This threshold depends on the size of the molecule to be internalised. This is why, at 100 V/cm, which is a very low electric field amplitude, no Ca^{2+} spike was observed because there was no permeabilization and hence no Ca^{2+} entry. 120 V/cm was the lowest electric field amplitude at which some cells presented Ca^{2+} spikes. This threshold is very low compared to other ones previously reported, because the Ca^{2+} has a small size compared to other classical markers such as yo-pro-1 iodide, propidium iodide or bleomycin that are those frequently used (Hanna *et al.*, submitted). At 450 V/cm, 100% of the cells responded to the electric pulse. The origin of the Ca^{2+} causing the Ca^{2+} spike was not always the same: it could be the result of Ca^{2+} entry from the external medium only, or the combination of Ca^{2+} entry from cell outside and Ca^{2+} release from the ER. Our group demonstrated recently that the μsPEF could permeabilize not only the cell membrane (as usually observed and stated) but also the internal organelles membranes (Hanna *et al.*, submitted). The origin of the Ca^{2+} spike depends on the electric field amplitude. If this latter is below 500 V/cm, the pulse permeabilizes only the plasma membrane (Hanna *et al.*, submitted), and the Ca^{2+} spike is primarily the result of Ca^{2+} entry through the plasma membrane followed by an amplification due to Ca^{2+} entry from the voltage-operated Ca^{2+} channels (VOCC), activated by the membrane depolarization [36]. However, above 500 V/cm, the electric pulses will also affect the ER membranes, permeabilize them and cause Ca^{2+} release from the ER (Hanna *et al.*, submitted). Hence, the Ca^{2+} spike at high electric field amplitudes, resulted primarily of a massive Ca^{2+} entry through the plasma membrane (due to the generation of larger pores at the higher field amplitudes) also followed by the external Ca^{2+} entry through the VOCCs, the Ca^{2+} release from the ER and the subsequent stimulation of the store-operated Ca^{2+} channels (SOCC) [37]. This explains, why the Ca^{2+} spike induced by electric fields below 500 V/cm had a very similar shape to the spontaneous Ca^{2+} oscillations with a gradual increase and same amplitude, whereas the Ca^{2+} spike induced by electric fields above 500 V/cm had higher amplitude than the spontaneous oscillations, and presented a sharper rise (due to the abrupt penetration of Ca^{2+} through the permeabilized membranes). At 600 V/cm, three different outcomes were observed, mainly due to three factors: first the distribution of the electric field which results in field amplitude small differences in the area between the two electrodes; second, the cells are heterogeneous in size and according to Schwan equation [38], the electric field impact will be different between the smallest and the largest cells; third, the orientation of the cell with respect to

the electric field lines which has an impact on the induced transmembrane potential that will lead to the cell membrane permeabilization [39]; fourth, the position of the cells are in the cell cycle that could lead to different responses to the pulses. However, at 750 V/cm, it seems that the electric field has exceeded a certain threshold above which no more heterogeneity was observed and nearly all the cells had their Ca^{2+} oscillations inhibited.

The Ca^{2+} spikes obtained looked like the Ca^{2+} spikes induced by even shorter electric pulses (the so-called nanopulses, of a duration of e.g. 10 ns, that can directly affect the cell internal membranes such as those of the endoplasmic reticulum [30]). In our study, an electrically induced Ca^{2+} spike with properties very near to the oscillations did not inhibit these latter, could be applied at any time of an oscillation without interfering with this latter, and after the pulse, the oscillations continued normally at their own rhythm, and with their normal shape. Nevertheless, a high amplitude Ca^{2+} spike inhibited the Ca^{2+} oscillations. The percentage of cells that were unable to display further Ca^{2+} oscillations increased proportionally with the electric field amplitude of the inhibitory electric pulse. The Ca^{2+} oscillations inhibition could last some minutes or be longer, to reach tens of minutes, also depending on the electric field amplitude of the inhibitory electric pulse.

The inhibition of the Ca^{2+} oscillations for some time allowed us to study the state of the cell during this period, to determine whether the cell was in a “refractory state” or if it was still able to respond to an electric pulse. The application of several pulses after a 900 V/cm pulse inhibition showed that the cells could still react to the pulse and present Ca^{2+} spikes with different amplitudes depending on the applied electric field amplitude.

The electrically induced Ca^{2+} spikes can have wide effects on the Ca^{2+} oscillations frequency, amplitude and duration. Whereas the nanosecond pulses allowed only to add a Ca^{2+} spike to the oscillations [30], the microsecond pulses display more complex effects. The electric field amplitude allowed us either to induce a Ca^{2+} spike without affecting the oscillations, or to inhibit the Ca^{2+} oscillations and impose to the cell Ca^{2+} oscillations at a desired frequency and amplitude. It is worthy to note that the microsecond technology is cheaper than the nanosecond one, it is more available in the laboratories, and simple generators can deliver it. These considerations add further value to the observations reported here. Taking into account that each type of differentiated cell from MSC has its own Ca^{2+} oscillations characteristics, and that these oscillations may play an important role in the decision of MSC fate, the μsPEF constitutes a novel useful tool to control the oscillations and the differentiation of MSCs.

Conclusions

The hMSC present a big promise for the regenerative medicine. As a function of the pulse(s) electric field amplitude, we report here that it is possible to generate a supplementary calcium spike with properties close to those of calcium spontaneous oscillations, or, on the contrary, to inhibit the spontaneous calcium oscillations for a very long time compared to the pulses duration. Through that inhibition of the oscillations, Ca^{2+} oscillations of desired amplitude and frequency could then be imposed to the cells using subsequent electric pulses. The delivery of short PEF of 100 μs , a robust technology easy to apply, could be therefore a promising way to investigate the role of the Ca^{2+} in MSC physiology and biological processes such as proliferation and differentiation.

Abbreviations

aMSC: adipose tissue mesenchymal stem cells **bMSC:** bone marrow mesenchymal stem cells
DMEM: Dulbecco's Modified Eagle Medium **EMF:** Electromagnetic fields
ER: endoplasmic reticulum **haMSC:** human aMSC **hbMSC:** human bMSC
IP3: inositol triphosphate **MSC:** mesenchymal stem cells **NCX:** Na⁺/ Ca²⁺ exchanger
PBS: Phosphate Buffered Saline **PEF:** pulsed electric fields **PM:** plasma membrane
PMCA: plasma membrane Ca²⁺ ATPase **SERCA:** sarco/endoplasmic reticulum Ca²⁺ ATPase
SOCCs: store-operated Ca²⁺ channels **VOCC:** voltage-operated Ca²⁺ channels
µsPEF: microsecond pulsed electric field

Declarations

Acknowledgements

Authors would like to thank Dr. Bassim Al Sakere for the lipoaspirates.

Funding

This work was supported by CNRS, Gustave Roussy, Université Paris-Sud, the ITMO Cancer in the frame of the Plan Cancer 2015-2019 (project PC201517) and the Fondation EDF. The research was also conducted in the scope of the EBAM European Associated Laboratory (LEA) and of the COST action BM 1309 EMF-MED.

Author's contributions:

HH, FMA and LMM designed the study, contributed to data interpretation, analysed the data and drafted the manuscript. HH performed the experiments. All authors edited/approved the manuscript.

Competing interests

The authors indicate that they have no competing interests.

Consent for publication

All the authors have read and approved the manuscript for publication.

Ethics approval and consent to participate

HaMSCs were isolated from surgical waste of individuals undergoing elective lipoaspiration. Samples were obtained after written informed consent from all the donors, in accordance with France and

European legislations. The lipoaspirates were surgical waste and as such the French legislation (Art.L. 1245-2 du Code de la Santé Publique) establishes that the authorization from an ethics committee is not required.

References

1. Dominici M, Le Blanc K, Mueller I, Slaper-Cortenbach I, Marini F, Krause D, et al. Minimal criteria for defining multipotent mesenchymal stromal cells. The International Society for Cellular Therapy position statement. *Cytotherapy*. 2006;8:315–7.
2. Malgieri A, Kantzari E, Patrizi MP, Gambardella S. Bone marrow and umbilical cord blood human mesenchymal stem cells: state of the art. *Int. J. Clin. Exp. Med*. 2010;3:248–69.
3. Lee RH, Kim B, Choi I, Kim H, Choi HS, Suh K, et al. Characterization and expression analysis of mesenchymal stem cells from human bone marrow and adipose tissue. *Cell. Physiol. Biochem. Int. J. Exp. Cell. Physiol. Biochem. Pharmacol*. 2004;14:311–24.
4. Marion NW, Mao JJ. Mesenchymal stem cells and tissue engineering. *Methods Enzymol*. 2006;420:339–61.
5. Sacchetti B, Funari A, Remoli C, Giannicola G, Kogler G, Liedtke S, et al. No Identical “Mesenchymal Stem Cells” at Different Times and Sites: Human Committed Progenitors of Distinct Origin and Differentiation Potential Are Incorporated as Adventitial Cells in Microvessels. *Stem Cell Rep*. 2016;6:897–913.
6. Gronthos S, Franklin DM, Leddy HA, Robey PG, Storms RW, Gimble JM. Surface protein characterization of human adipose tissue-derived stromal cells. *J. Cell. Physiol*. 2001;189:54–63.
7. Lindroos B, Suuronen R, Miettinen S. The potential of adipose stem cells in regenerative medicine. *Stem Cell Rev*. 2011;7:269–91.
8. Kawano S, Shoji S, Ichinose S, Yamagata K, Tagami M, Hiraoka M. Characterization of Ca(2+) signaling pathways in human mesenchymal stem cells. *Cell Calcium*. 2002;32:165–74.
9. Kawano S, Otsu K, Kuruma A, Shoji S, Yanagida E, Muto Y, et al. ATP autocrine/paracrine signaling induces calcium oscillations and NFAT activation in human mesenchymal stem cells. *Cell Calcium*. 2006;39:313–24.
10. Kawano S, Otsu K, Shoji S, Yamagata K, Hiraoka M. Ca(2+) oscillations regulated by Na(+)-Ca(2+) exchanger and plasma membrane Ca(2+) pump induce fluctuations of membrane currents and potentials in human mesenchymal stem cells. *Cell Calcium*. 2003;34:145–56.
11. Titushkin I, Sun S, Shin J, Cho M. Physicochemical Control of Adult Stem Cell Differentiation: Shedding Light on Potential Molecular Mechanisms. *BioMed Res. Int*. 2010;2010:e743476.
12. Mir LM, Banoun H, Paoletti C. Introduction of definite amounts of nonpermeant molecules into living cells after electroporation: direct access to the cytosol. *Exp. Cell Res*. 1988;175:15–25.
13. Vernier PT, Sun Y, Marcu L, Salemi S, Craft CM, Gundersen MA. Calcium bursts induced by nanosecond electric pulses. *Biochem. Biophys. Res. Commun*. 2003;310:286–95.
14. Sun S, Liu Y, Lipsky S, Cho M. Physical manipulation of calcium oscillations facilitates osteodifferentiation of human mesenchymal stem cells. *FASEB J. Off. Publ. Fed. Am. Soc. Exp. Biol*. 2007;21:1472–80.

15. Kim IS, Song JK, Song YM, Cho TH, Lee TH, Lim SS, et al. Novel effect of biphasic electric current on in vitro osteogenesis and cytokine production in human mesenchymal stromal cells. *Tissue Eng. Part A*. 2009;15:2411–22.
16. Liew A, André FM, Lesueur LL, De Ménorval M-A, O'Brien T, Mir LM. Robust, efficient, and practical electrogene transfer method for human mesenchymal stem cells using square electric pulses. *Hum. Gene Ther. Methods*. 2013;24:289–97.
17. Crouch SP, Kozlowski R, Slater KJ, Fletcher J. The use of ATP bioluminescence as a measure of cell proliferation and cytotoxicity. *J. Immunol. Methods*. 1993;160:81–8.
18. Woodbury D, Reynolds K, Black IB. Adult bone marrow stromal stem cells express germline, ectodermal, endodermal, and mesodermal genes prior to neurogenesis. *J. Neurosci. Res*. 2002;69:908–17.
19. Altman GH, Horan RL, Martin I, Farhadi J, Stark PRH, Volloch V, et al. Cell differentiation by mechanical stress. *FASEB J. Off. Publ. Fed. Am. Soc. Exp. Biol.* 2002;16:270–2.
20. Ward DF, Salaszyk RM, Klees RF, Backiel J, Agius P, Bennett K, et al. Mechanical strain enhances extracellular matrix-induced gene focusing and promotes osteogenic differentiation of human mesenchymal stem cells through an extracellular-related kinase-dependent pathway. *Stem Cells Dev*. 2007;16:467–80.
21. Ebisawa K, Hata K-I, Okada K, Kimata K, Ueda M, Torii S, et al. Ultrasound enhances transforming growth factor beta-mediated chondrocyte differentiation of human mesenchymal stem cells. *Tissue Eng*. 2004;10:921–9.
22. Jing D, Baik AD, Lu XL, Zhou B, Lai X, Wang L, et al. In situ intracellular calcium oscillations in osteocytes in intact mouse long bones under dynamic mechanical loading. *FASEB J*. 2014;28:1582–92.
23. Petecchia L, Sbrana F, Utzeri R, Vercellino M, Usai C, Visai L, et al. Electro-magnetic field promotes osteogenic differentiation of BM-hMSCs through a selective action on Ca²⁺-related mechanisms. *Sci. Rep*. 2015; 5; 13856
24. Parri HR, Gould TM, Crunelli V. Spontaneous astrocytic Ca²⁺ oscillations in situ drive NMDAR-mediated neuronal excitation. *Nat. Neurosci*. 2001;4:803–12.
25. Tsien RW. Calcium Channels in Excitable Cell Membranes. *Annu. Rev. Physiol*. 1983;45:341–58.
26. Fewtrell C. Ca²⁺ Oscillations in Non-Excitable Cells. *Annu. Rev. Physiol*. 1993;55:427–54.
27. Nash MS, Young KW, John Challiss RA, Nahorski SR. Intracellular signalling: Receptor-specific messenger oscillations. *Nature*. 2001;413:381–2.
28. Liou J, Kim ML, Heo WD, Jones JT, Myers JW, Ferrell JE, et al. STIM is a Ca²⁺ sensor essential for Ca²⁺-store-depletion-triggered Ca²⁺ influx. *Curr. Biol. CB*. 2005;15:1235–41.
29. Parekh AB, Putney JW. Store-operated calcium channels. *Physiol. Rev*. 2005;85:757–810.
30. de Menorval M-A, Andre FM, Silve A, Dalmay C, Français O, Le Pioufle B, et al. Electric pulses: a flexible tool to manipulate cytosolic calcium concentrations and generate spontaneous-like calcium oscillations in mesenchymal stem cells. *Sci. Rep*. 2016;6:32331.
31. Resende RR, Adhikari A, da Costa JL, Lorençon E, Ladeira MS, Guatimosim S, et al. Influence of spontaneous calcium events on cell-cycle progression in embryonal carcinoma and adult stem cells. *Biochim. Biophys. Acta*. 2010;1803:246–60.
32. Belehradek M, Domenge C, Luboinski B, Orlowski S, Belehradek J, Mir LM. Electrochemotherapy, a new antitumor treatment. First clinical phase I-II trial. *Cancer*. 1993;72:3694–700.
33. Al-Sakere B, André F, Bernat C, Connault E, Opolon P, Davalos RV, et al. Tumor ablation with irreversible electroporation. *PLoS One*. 2007;2:e1135.

34. Potter H, Heller R. Transfection by electroporation. *Curr. Protoc. Cell Biol.* 2011;52:20.5.1-20.5.10.
35. Silve A, Guimerà Brunet A, Al-Sakere B, Ivorra A, Mir LM. Comparison of the effects of the repetition rate between microsecond and nanosecond pulses: electropermeabilization-induced electro-desensitization? *Biochim. Biophys. Acta.* 2014;1840:2139–51.
36. Catterall WA. Voltage-Gated Calcium Channels. *Cold Spring Harb. Perspect. Biol.* 2011;3:a003947.
37. Smyth JT, Hwang S-Y, Tomita T, DeHaven WI, Mercer JC, Putney JW. Activation and regulation of store-operated calcium entry. *J. Cell. Mol. Med.* 2010;14:2337–49.
38. Schwan HP. Electrical properties of tissue and cell suspensions. *Adv. Biol. Med. Phys.* 1957;5:147–209.
39. Kotnik T, Pucihar G, Miklavcic D. Induced transmembrane voltage and its correlation with electroporation-mediated molecular transport. *J. Membr. Biol.* 2010;236:3–13.

Figures:

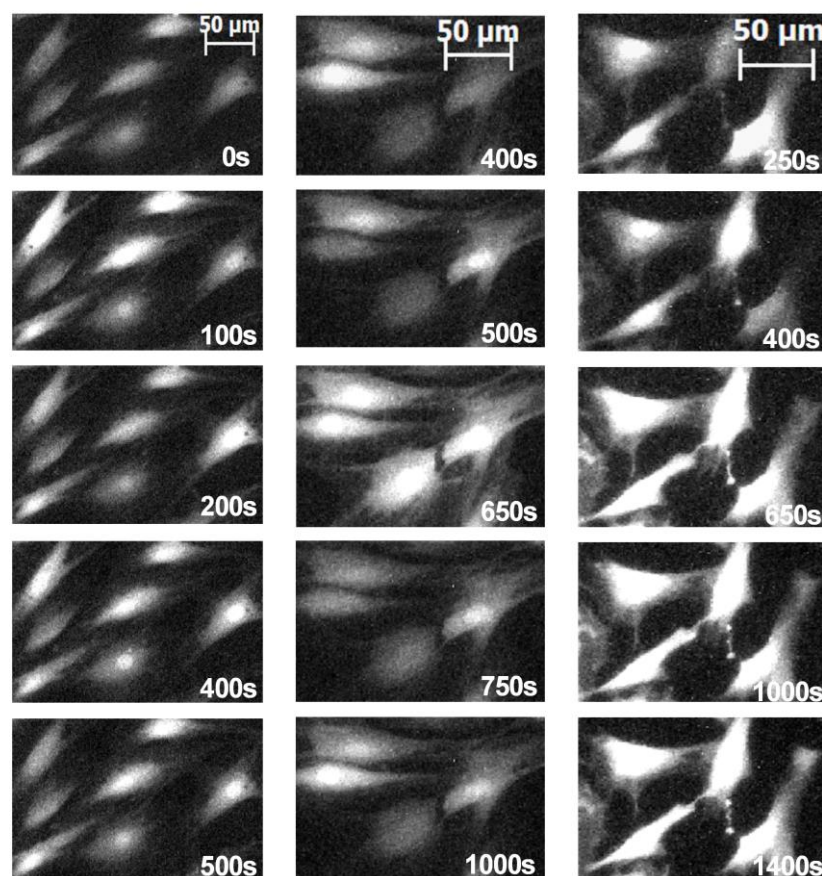


Figure 1. Time lapse follow-up of calcium oscillations and spikes in haMSC. Left: spontaneous calcium oscillations. Middle: spontaneous calcium oscillations before and after a 100 μs pulse of 300 V/cm (the pulse was applied at 630 s and a calcium spike in all the cells follows the pulse delivery at e.g. 650 s). Right: spontaneous calcium oscillations before a 100 μs pulse of 900 V/cm (applied at $t = 630$ s) followed by a non-oscillating increased calcium signal.

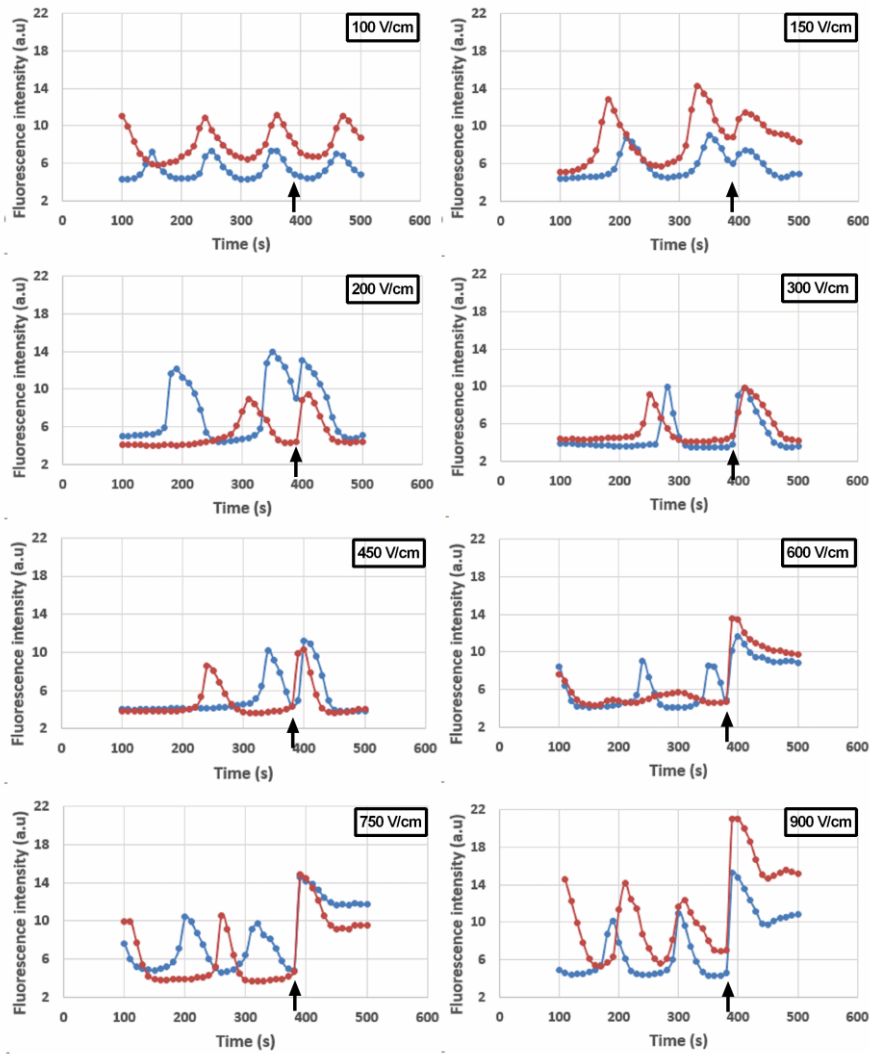


Figure 2. Calcium spikes in response to different electric field amplitudes. For each panel, two separate adherent cells, displaying the typical behavior of the cells after the delivery of one 100 μ s electric pulse, were chosen to illustrate that behavior. In all the cases, the pulse was applied at time = 390 s (black arrows).

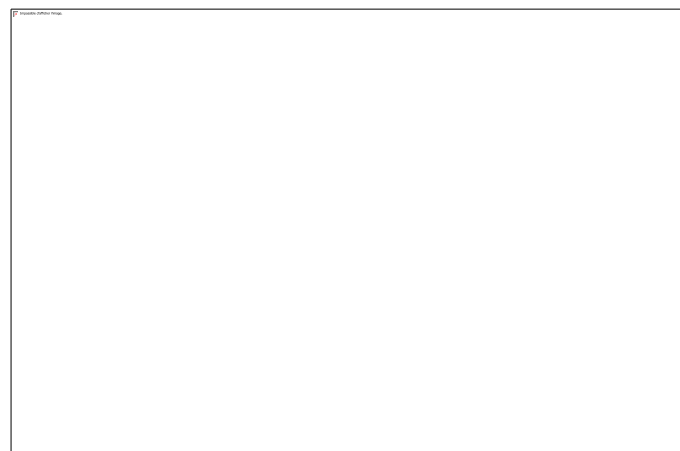


Figure 3. Percentage of cells presenting a calcium spike in response to one 100 μ s electric pulse as a function of the field amplitude. $r = 0.96$ according to Spearman correlation.

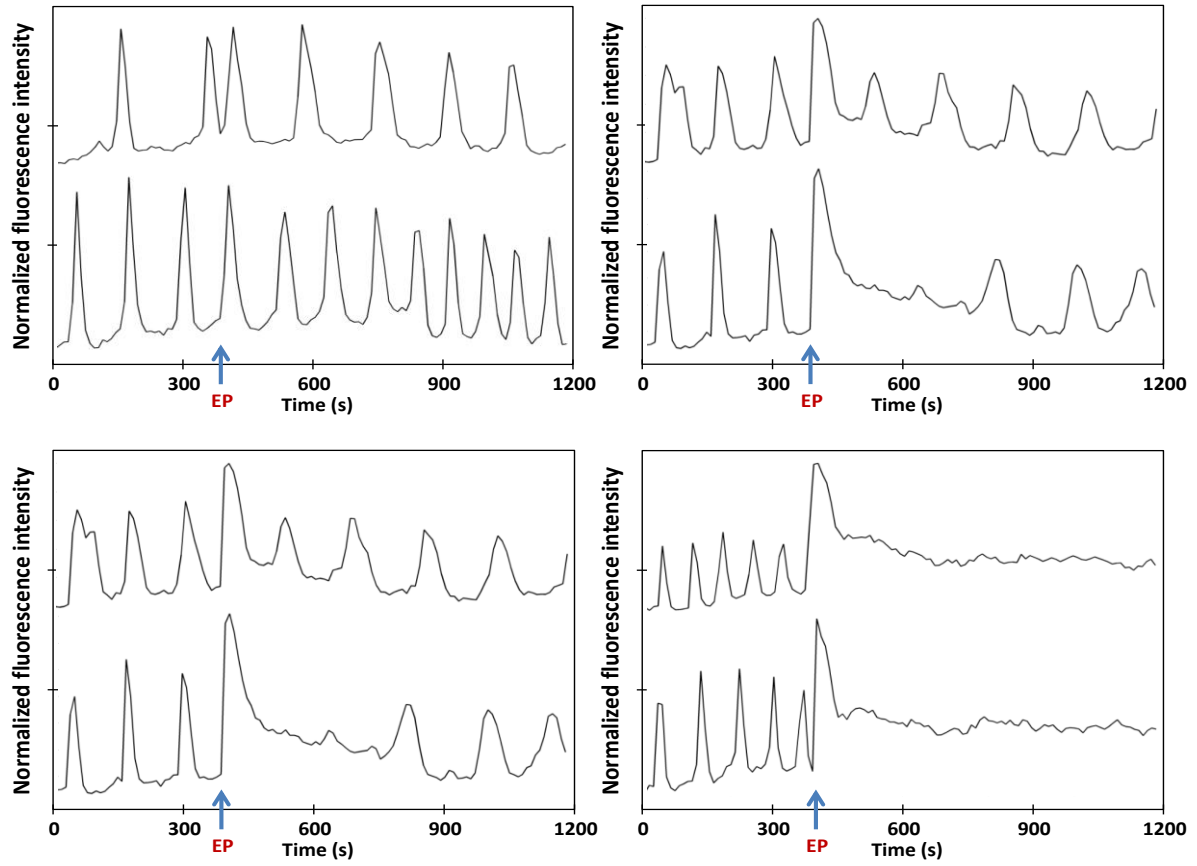


Figure 4. Examples of changes in the pattern of Ca^{2+} oscillations caused by the delivery of one $100\ \mu\text{s}$ electric pulse of different field amplitudes, a: $300\ \text{V/cm}$, b and c: $600\ \text{V/cm}$, d: $900\ \text{V/cm}$.

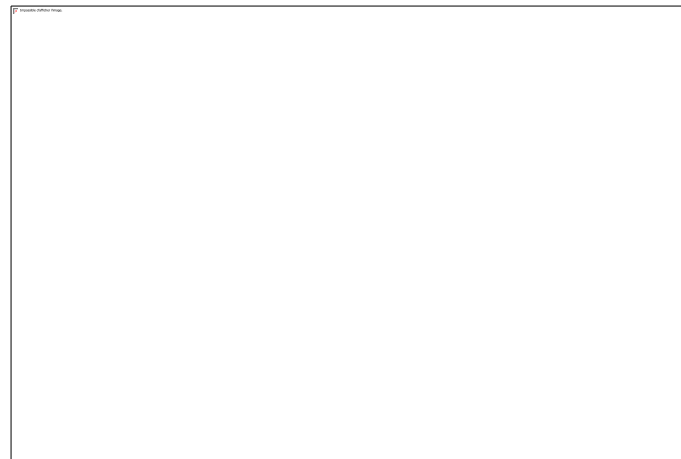


Figure 5. Percentage of cells displaying no Ca^{2+} oscillation within a period of at least 10 minutes after the delivery of one $100\ \mu\text{s}$ electric pulse of different field amplitudes.

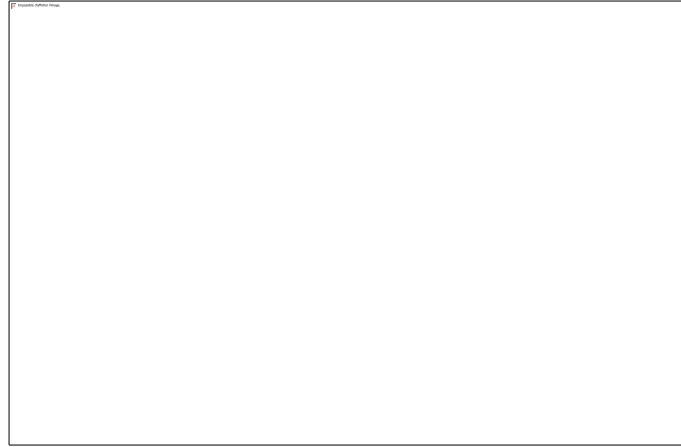


Figure 6. haMSC cell viability after the delivery of one 100 μ s electric pulse of different field amplitudes, $r = 0.43$ according to Spearman correlation.

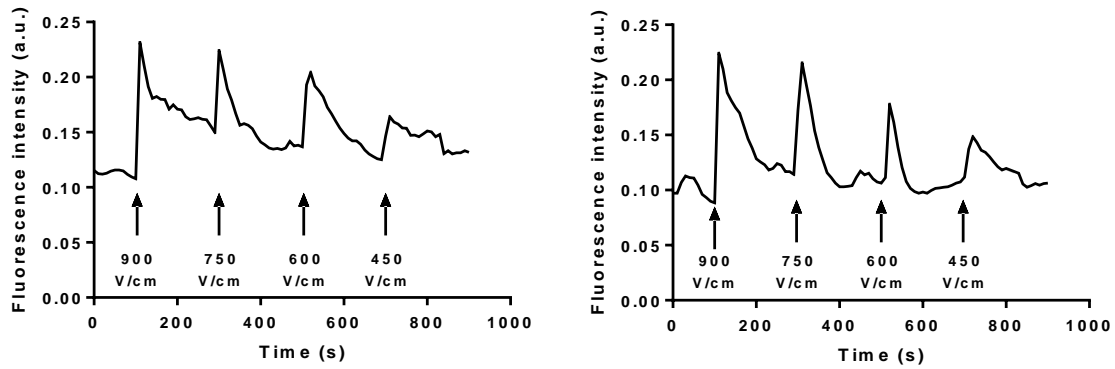


Figure 7. Two examples of calcium spikes manipulation in haMSC. After the delivery of one 100 μ s electric pulse at 900 V/cm (that abolishes the spontaneous Ca^{2+} oscillations), pulses of various field amplitudes were delivered to mimic Ca^{2+} oscillations at experimentally controlled times.

3 IN VITRO OSTEOBLASTIC DIFFERENTIATION OF MESENCHYMAL STEM CELLS GENERATES CELL LAYERS WITH DISTINCT PROPERTIES (ARTICLE N°3)

The mesenchymal stem cells undergoing an osteogenic differentiation form an extensive extracellular matrix connecting the cells. When we tried to trypsinise the cells in differentiation in order to study their Ca^{2+} oscillations, we found that these latter were not well dissociated. We decided to use the collagenase I to dissociate the cells since the ECM is mainly composed of collagen I. We found, after the use of the collagenase I, that an attached layer of cells remained at the bottom of the dish. This layer was not sensitive to the collagenase I but to the trypsin. This part of the thesis presents the observations done for the first time on the different layers of cells undergoing osteogenic differentiation. A characterization of the two different layers types was done. The comparison with an adipogenic and neurogenic differentiation was also assessed in order to compare the evolution of the cell monolayer during each differentiation. This work is related to a new observation that has been done on the osteogenic differentiation. This observation could be helpful for new applications and for obtaining osteoblasts in a shorter time in an electroporation-independent manner. In the next section of the thesis, the combination of an osteogenic differentiation with electroporation will be further evaluated. These results have been submitted to "FASEB Journal" in December 2016.

In vitro osteoblastic differentiation of mesenchymal stem cells generates cell layers with distinct properties

Short title:
Cell layers in MSC differentiation

Authors and affiliations

Hanna Hanna¹, Lluís M. Mir¹, Franck M. André^{1,*}

¹Vectorology and Anticancer Therapies, UMR 8203, CNRS, Univ. Paris-Sud, Gustave Roussy,
Université Paris-Saclay, 94 805 Villejuif, France.

* Correspondance should be addressed to Franck M. André

E-mail address: franck.andre@cnrs.fr

Tel. : +33 1 42 11 54 07

UMR 8203 CNRS
Gustave Roussy, PR2
114 rue Edouard Vaillant
94805 VILLEJUIF Cédex France

List of abbreviations:

ALP: alkaline phosphatase

CD: cluster of differentiation

DMEM: Dulbecco's Modified Eagle Medium

ECM: extracellular matrix

FABP4: fatty acid binding protein 4

haMSCs: human adipose mesenchymal stem cells

MAP2: microtubule-associated protein 2

MSCs: mesenchymal stem cells

pNPP: p-nitrophenyl phosphate

pNP: p-nitrophenol

Abstract

The differentiation of mesenchymal stem cells to osteoblasts is widely performed in research laboratories. Classical tests to prove this differentiation employ procedures such as cell fixation, cell lysis or cell scraping. Gentle dissociation of mesenchymal stem cells undergoing an osteodifferentiation is reported in very few studies. It reveals the presence of several cell layers in the culture dish. Through the sequential detachment of the cells, we confirm the presence of several layers of differentiated cells and we show that they have distinct properties. The upper layers, maintained by a collagen I extracellular matrix, can be dissociated using collagenase I, while the remaining lowest layer, attached to the bottom of the dish, is sensitive only to trypsin-versene. The action of collagenase I is more efficient before the mineralization of the extracellular matrix. The collagenase sensitive and trypsin sensitive layers differ in their cluster of differentiation expression. The dissociation of the cells on day 15 reveals that cells can resume their growth, while differentiating in osteoblasts in 2 weeks (instead of 4). Cells from the upper layers displayed a higher mineralization. This could allow the investigators to use upper layers to rapidly produce differentiated osteoblasts and the lowest layer to continue growth and differentiation until an ulterior dissociation.

Key Words: collagenase I, trypsin, extracellular matrix, multilayers, cluster of differentiations, calcium oscillations

Introduction

MSCs osteogenic differentiation was the first differentiation to be identified by Friedenstein and co-workers in the late 1960s – early 1970s (1, 2). As the MSCs (known then as marrow stromal cells) were extracted from the bone marrow, it was not surprising that they could give rise to osteoblasts. *In vitro*, osteogenic differentiation occurs on a period of one month and produces differentiated osteoblasts. Downregulation of DNA replication by the second week of differentiation is associated with expression of osteoblast markers (such as alkaline phosphatase, ALP), processing of type I procollagen to collagen I under the effect of ascorbic acid, and progressive deposition of a collagenous extracellular matrix (ECM) (3). Later on, other bone markers can be detected, such as osteocalcin, osteopontin, bone sialoprotein and osteonectin. Hydroxyapatite deposits mark the final phase of osteoblast phenotypic development (3). The ECM is an essential element for the osteogenic differentiation; it is secreted by the MSCs undergoing an osteogenic differentiation and contains growth factors and many proteins such as fibronectin, vitronectin, laminin, osteopontin and osteonectin (4). Osteoblasts must be in contact with a collagen I matrix before they can differentiate (5). ECM formation is a marker of MSC differentiation to osteoblast, and it accumulates maximally after one week of culture. After 2 weeks of culture, mineralization of ECM begins, which marks the final phase of the osteoblast phenotypic development (3). Cell proliferation before mineralization is a critical process for increasing bone mass. Because the cells are exposed to the differentiating agents when they form a more or less confluent monolayer in the culture dishes, the differentiated cells in 2D cultures are sometimes referred as « monolayers » (6), « confluent monolayers » (7) or « cells in monolayer » (8). The term « multilayer » was barely used (9). Zhu *et al.* showed that a weak osteogenesis is characterized by the formation of an ALP positive cell monolayer while a strong

osteogenesis is characterized by the presence of multilayered ALP positive nodular structures (10). To assess the differentiation potential, the investigators used many classical tests that label the cells or measure the osteogenic markers. In all of these methods there was no dissociation of the cells from the different layers. Indeed, the first step is often the fixation of the cells, for example to stain the cells with alizarin red that labels the deposits of calcium phosphate (hydroxyapatite $\text{Ca}_5(\text{PO}_4)_3(\text{OH})$) (11, 12). Other tests such as immunofluorescent labelling (13, 14), ECM protein production (4), external ALP measurement (12, 15) are performed without dissociation of the cells, just after their fixation. In other methods, the supernatant of the cells is taken, to measure osteocalcin (6, 16), type I procollagen (16), bone sialoprotein or different specific cytokines production (17, 18) by ELISA or other techniques. Finally, other methods starts by the scraping or the lysis of the cells using trichloroacetic acid and SDS (9), sonication (16), trizol (19), RIPA buffer (17) or many cycles of freeze-thaw (15) in order to perform DNA and calcium assays (16, 20, 21), to measure internal ALP by colorimetric assays (13, 15, 17, 20, 22) or to detect specific proteins by western blot or mRNA by RT-PCR (6, 8, 9, 12). All these techniques do not dissociate the living cells. Some studies (13, 23) used the trypsin alone (until day 14 of osteodifferentiation, before the mineralization occurred) or the trypsin-EDTA (24, 25) to harvest all the layers in 2D cultures.

In our study, we used human adipose mesenchymal stem cells (haMSCs) to perform osteogenic, adipogenic and neurogenic differentiations to assess the multipotency of the haMSCs and to compare the evolution of the cells in one or several layers during the differentiation. Confocal microscopy observations were performed in order to assess the evolution of the cells in one or many layers in the three differentiations. Furthermore, differential dissociation by collagenase I and trypsin was performed on the layers in osteogenic differentiation. The different layers were then characterized by their cluster of differentiation markers and their Ca^{2+} oscillations in order to evaluate if they were identical or not. The different cell populations resulting from differential dissociation at day 15 were also cultivated separately to evaluate their osteogenic potential. This study presents new observations on the cell layers in an *in vitro* osteogenic differentiation and proposes a new method to dissociate the cells which could expand their use and facilitate applications.

Materials and methods

Cell culture and differentiation

haMSCs (human adipose-derived mesenchymal stem cells) were isolated from lipoaspirates of individuals that gave informed and written consent for the use of the lipoaspirates. The cells were grown in Dulbecco's Modified Eagle Medium (DMEM) supplemented with 10% foetal bovine serum, 100 U/mL penicillin and 100 mg/mL streptomycin and were cultured at 37°C in a humidified incubator with 5% CO_2 . Cells were passed twice a week (every passage corresponded to one doubling time of the population). The multipotency capabilities of the cells were assessed by submitting them to differentiation conditions as previously reported in André *et al.* (26). The cell culture chemicals were purchased from Fischer Scientific (Parc d'innovation Illkirch, France). Prior to every differentiation, cells were seeded at a density of 15000 cells/cm² and let in culture for 2-3 days to attain confluence, after which the normal medium was removed and differentiation medium was added. This medium change corresponded to differentiation day 1. The osteogenic medium was composed of complete alpha MEM supplemented with 100 nM of dexamethasone, 200 µM of ascorbic acid and 10 mM of glycerol 2-

phosphate. Medium was changed twice a week. For the adipogenic differentiation, two media were consecutively used: an induction medium composed of complete DMEM supplemented with 1 μ M dexamethasone, 200 μ M indomethacin, 500 μ M 3-isobutyl-1-methylxanthine and 10 μ g/ml insulin for 2-3 days, and a maintenance medium composed of complete DMEM supplemented with 10 μ g/ml insulin renewed every 24 hours. For the neurogenic differentiation, a ready-to-use neurogenic induction medium was used from Promocell (C-28015), and was changed every 48 hours. The controls were haMSCs cultivated without passage in their normal medium, which was changed twice a week.

Cells dissociation and counting

For controls, adipogenic differentiation and neurogenic differentiation cells were simply trypsinised and counted 3 times at every time point. As described in this article, several layers of cells could be distinguished in osteogenic differentiation. To dissociate the upper layers before the calcium deposits begun to appear, 2mg/ml collagenase I (Fisher Scientific, Illkirch, France) diluted in PBS was added to the cells for 30 minutes. After collagenase I action, the cell cultures were pipetted gently to remove all the cells of the upper layers. The remaining layer was trypsinised. When the mineralization occurred, i.e. when Ca^{2+} deposits became apparent, the calcium deposits were removed using 20 to 40 mM of EDTA in PBS for 20 to 40 minutes, depending on the density of these deposits. Then the cells of the upper layers were detached using a higher concentration of collagenase (4 mg/ml) and the cells of the lowest layer using trypsin. The cells from all the layers were gathered together in one tube and counted 3 times at every time point.

Alkaline phosphatase assay and Alizarin Red staining

In order to test the ALP activity (osteogenic differentiation), cells were harvested by using collagenase I and trypsin, centrifuged at 1500 rpm for 5 min, resuspended in 1 ml of cold PBS (4°C) and counted. A volume corresponding to 300 000 cells was taken, centrifuged and suspended in 600 μ l of assay buffer (Abcam), and centrifuged at 13200 rpm for 5 minutes at 4°C. The supernatant was transferred to a new tube. 200 μ l of the supernatant were distributed in 4 wells of a 96 well plate (50 μ l/well). One of them served to determine the background through the simultaneous addition of 80 μ l p-nitrophenyl phosphate (pNPP) 1 mM and 20 μ l of stop solution. For the 3 remaining wells, 80 μ l of pNPP were added. After 60 minutes, 20 μ l of stop solution (Abcam) was added to the wells and the plate was read in a spectrophotometer (BioTek, Colmar, France) to measure the optical density at 405 nm. The quantity of p-nitrophenol (pNP) in each well was determined using a standard curve established using pNPP and purified ALP enzyme. 350 μ l of the remaining supernatant were incubated with 750 nM of Hoechst 33342 for 30 min and distributed in triplicate in an opaque 96 well plate to read the fluorescence at 365 nm excitation. Prior to AR staining, cells were washed in PBS and fixed in 95% methanol for 10 min. 2% Alizarin Red S solution was added for 5 min, then rinsed with water, and imaged under an epifluorescence microscope to visualize the Ca^{2+} deposits.

FABP4 and bodipy staining

To assess adipogenic differentiation, the attached cells were washed after medium removal, fixed in 10% formalin for 20 min and washed 3 times in PBS + 1% BSA. Then cells were permeabilized and

blocked with PBS containing 0.3% Triton X-100, 1% BSA and 10% universal blocking reagent. After blocking, the cells were incubated overnight at 4°C with an antibody (PA5-30591, Fisher scientific, Illkirch, France) against the fatty acid binding protein 4 (FABP4). Then the cells were washed 3 times in PBS + 1% BSA, incubated for 60 min in the dark with a secondary antibody coupled to alexa fluor 488 (A-11008, Fisher Scientific), washed 3 times in PBS + 1% BSA and visualized under an epifluorescence microscope (Zeiss Axiovert S100).

In order to stain the cells with Bodipy, the cell medium was removed and the cells were incubated for one hour with a fresh medium containing 100 µg/ml of Bodipy (Molecular Probes, Fisher Scientific), washed and imaged under the epifluorescence microscope.

MAP2 and cresyl violet staining

To assess neurogenic differentiation, cells were fixed and incubated with microtubule-associated protein 2 (MAP2) antibody (ref 4542, Cell signaling, Saint Quentin, France) following the same protocol as for the FABP4 antibody (see above).

In order to stain Nissl bodies, cells were washed and fixed with 10% formalin for 20 min. Then a 0.5% cresyl violet staining solution (Sigma Aldrich) was added to cells and incubated for 30 min at room temperature. Then the cells were washed 3 times in PBS and imaged under an epifluorescence microscope.

Living cells imaging

MSCs were seeded, prior to the differentiation, on a glass bottom µ-slide 4 well (ref 80447, Ibidi GMBH, Planegg, Germany). Prior to confocal imaging, cells were incubated for 30 min with 375 nM Hoechst 33342 (nuclei marker; λ_{exc} 480 nm; λ_{em} 535 nm) and 5 µM of fluorescein diacetate (FDA) (cytoplasm marker; λ_{exc} 405 nm; λ_{em} 486 nm). A confocal microscope Leica TCS SPE with an objective HC PL APO CS2 20x, and the LAS AF software version 3.3 (Leica, Germany) were used to visualize the mono/multilayers in osteogenic, adipogenic or neurogenic differentiation.

Calcium oscillations visualization and analysis

The upper layers in osteogenic differentiation were dissociated by collagenase I as described before, the lowest layer was trypsinized and the cells from each layer type were seeded apart at a density of 15 000 cells/cm² for 24 hours in an osteogenic differentiation medium. After 24 hours, medium was removed and the cells were incubated for 30 min with 5 µM of Fluo-4 AM (Fischer Scientific), a fluorescent Ca²⁺ marker, in a humidified 5% CO₂ atmosphere at 37°C in osteogenic medium. The incubation buffer also contained 375 nM of the nuclear fluorescent dye Hoechst 33342. After incubation, the attached cells were rinsed three times with PBS and 500 µl of fresh medium were added to the cells.

Immunofluorescent staining

Upper layers in osteogenic differentiation were dissociated with 2 mg/ml of collagenase I. The remaining layer was trypsinized. On day 22, the differentiating cell cultures were treated first by 20 mM EDTA in PBS before the collagenase addition. Cells were counted and centrifuged at 825 rpm for 10 min after which the supernatant was aspirated and the cells suspended in a buffer made of PBS, 0.5% BSA and 2mM EDTA (100 µl/100 000 cells). 10 µl of anti-CD44 APC, CD90 PE and CD105 FITC were added per 100 µl of cells. The cells were incubated with the antibodies for 10 minutes at 4°C in the dark. Then cells were washed with 1 ml of buffer and centrifuged. The pellet was resuspended in 300 µl of buffer for analysis by flow cytometry (Accuri C6 cytometer, BD Life Sciences, Le Pont de Claix, France). The antibodies were purchased from Miltenyi Biotec, Paris, France.

Statistical analysis

To compare the difference in immunofluorescent staining between the upper and lowest layers, unpaired t test was used. To analyse the influence of the layers and the number of days of differentiation on Ca^{2+} oscillations, two-way Anova with Tukey's multiple comparisons test was used. To compare the control to the other conditions, we used one-way Anova with Dunnett's multiple comparisons test. All the results are expressed as the mean and standard deviation from three different differentiations.

Results

Cells characterization

Characterization of osteodifferentiation was performed by the measure of ALP activity and the staining of the Ca^{2+} deposits using Alizarin Red. The control MSC (Fig. 1A) displayed no alizarin red labeling and no ALP activity. In osteogenic differentiation the Ca^{2+} deposits started to accumulate at the end of the second week and became more and more dense (Fig. 1B). These deposits were colored in red by the alizarin red staining (Fig. 2A). The ALP activity slightly increased at day 8 of osteodifferentiation and reached a peak on day 15 (Fig. 2B).

The adipodifferentiation was characterized by the FABP4 staining and the lipidic vacuoles formation. The lipidic vacuoles shown in Fig. 1 C are stained in green by bodipy staining in fig. 2 D. The adipose cells fluoresced in green after FABP4 labeling (fig. 2 C). The controls displayed no bodipy staining or FABP4 antibody labeling. The cresyl violet that stains the Nissl bodies specific of the neuronal cells labeled the haMSCs undergoing neurodifferentiation but not the controls (Fig. 2E). The MAP2 antibody interacted with neuronal cells but not with control, and this was revealed by the green fluorescence displayed by the neuronal cells (Fig. 2F).

Evolution of the cell number in the different differentiation pathways

When the cells were exposed to the neurodifferentiation medium, they showed no proliferation at all: the cell number remained nearly the same during all the differentiation process (Fig. 3). In adipogenic

differentiation, cell proliferation was maintained, only slightly reduced with respect to the proliferation in the controls (Fig. 3). On the contrary, in osteogenic differentiation there was a real stimulation of the cell proliferation: cells proliferated extensively between day 1 and 15 and faster than the control MSCs (Fig. 3). At days 8 and 15, there were nearly 4 and 6 times more cells than at day 1. After day 15, no further increase of the cell number was observed.

In osteogenic differentiation, due to the initial very rapid cell proliferation, cells started to accumulate in several layers in the first week of osteodifferentiation (Fig. 4). The number of layers stabilized at the end of the second week when the cells stopped proliferation. Four different layers of cells could be seen on day 22 of osteodifferentiation, every layer hiding the previous one. The layers were well separated, and almost no cell could be observed in between. In adipogenic differentiation (Fig. 5), above a first continuous layer, a discontinuous second layer of cells could also be observed in some parts of the dish. In neurogenic differentiation, even at day 22, cells remained always in one single layer in agreement with the total absence of cell proliferation. Furthermore, the cells shrank with time when they transformed from the mesenchymal fibroblastic shape to the neuronal one.

Characterization of the different cell layers in osteogenic differentiation

When 2mg/ml collagenase I were applied to the cells undergoing an osteogenic differentiation (before the Ca^{2+} deposits started to appear), only the cells of the upper cells layers dissociated. After the action of collagenase I, an attached cell layer remained intact at the bottom of the culture dishes (Fig. 6 A). This lowest layer was not sensitive to the collagenase. It could only be detached by trypsin.

When the mineralization occurred, collagenase I had no effect at all, even on the upper layers. The Ca^{2+} deposits had to be removed first. Prior EDTA treatment (20 to 40 mM for 20 to 40 minutes) was used to remove these deposits and collagenase concentration had to be increased from 2 to 4 mg/ml (Fig. 6 B).

The upper (collagenase sensitive) and lowest (trypsin sensitive) layers were labeled using MSC markers at days 1, 8, 15 and 22 (Fig. 7). As expected, the cells significantly lost the MSC markers (CD105, CD90 and CD44) when they progressed in the differentiation (****, $p < 0.0001$, two-way ANOVA). Unexpectedly, this immunostaining showed different evolutions between the upper and the lowest layers. The CD105 expression was the most rapidly lost among the three. At day 8, 60% of the cells had already significantly lost it (****, $p < 0.0001$, two-way ANOVA with Tukey's multiple comparisons test). At day 22, only 15 to 20% of the cells were still positive to the CD105 labeling. No significant differences between the upper and lowest layers was observed in terms of CD105 labeling ($p = 0.7081$, 0.8878 and 0.7531 , at days 8, 15 and 22, two-way ANOVA with Tukey's multiple comparisons test). The loss of the CD90 and CD44 positive labeling was slower and more progressive (Fig. 7). Moreover, a different evolution was found in the cells from the upper and lowest layers. Decrease was significantly faster in the trypsin-treated cells (lowest layer) than in the collagen-treated ones (upper layers) ($p < 0.05$ to $p < 0.001$, two-way ANOVA with Tukey's multiple comparisons test), except for day 8 for the CD44 ($p = 0.8376$, two-way ANOVA with Tukey's multiple comparisons test). The cells in the controls expressed their markers at high levels all the time.

The different layers were also compared in terms of Ca^{2+} oscillations. These oscillations significantly decreased when the hMSCs were put in the osteodifferentiation medium ($p < 0.0001$, one-way Anova

with Dunnett's multiple comparisons test) (the difference between MSC and cells under differentiation is shown in Fig. 8). At all the days observed, the mean Ca^{2+} oscillations were lower in number (per 30 min) in the lowest layer than in the upper layers, even though this is only significant at day 8 (**, $p < 0.01$, $p = 0.0038$, two-way ANOVA with Sidak's multiple comparisons test).

At day 15, cells from the upper layers (dissociated by collagenase) and the lowest layer (dissociated by trypsin) were put in culture separately in osteogenic medium. Both cell types recovered cell proliferation (supplementary data), and after 2 weeks, they formed 2 to 3 layers of cells with Ca^{2+} deposits (data not shown). The mineralization seemed to be more important in the cells differentiated from the upper layers (Fig. 9B) than in the cells differentiated from the lowest layer (Fig. 9A). The cells of the upper and lowest layers put in culture with a normal medium (without osteoinductive factors) did not form Ca^{2+} deposits (data not shown).

Discussion

Existence of distinct layers in MSCs osteogenic differentiation

In our study, we performed for the first time a sequential treatment to dissociate MSC cells undergoing osteogenic differentiation in 2D *in vitro* cultures, using collagenase I first and then trypsin. Collagenase I is used to dissociate cells from rodent or human bones in order to obtain primary osteoblasts (27, 28). Collagenase I, at a high concentration (20 mg/ml) and agitation at 37°C, is also used on 3D cultures *in vitro*, for example to harvest cells from microcarrier cultures, (24). Collagenase B was reported also to dissolve collagen scaffolds in *in vitro* 3D cultures (25). In the work here reported, human adipose-derived mesenchymal stem cells (haMSCs) were differentiated into osteoblasts. The multipotency of these cells was also assessed by their ability to differentiate into adipocytes and neuronal cells (as shown in Fig. 1 and 2). The use of collagenase I did not dissociate all the cells in the osteogenic differentiation since a cell layer remained attached to the bottom of the dish as shown in figure 6. To the best of our knowledge, only a single study, by Franceschi *et al.* (1994) mentioned a « remaining layer » (29). They used 0.15 M phosphate buffer containing 2 mM phenylmethylsulfonylfluoride and 2.5 mM N-ethylmaleimide to dissociate the cells (until day 7 of osteodifferentiation). After that, they collected the cells of the remaining layer separately. The remaining layer in our case had to be trypsinised. Our results demonstrate that there are two types of layers in osteogenic differentiation that have not been explored before: the upper layers which are collagenase I sensitive and the lowest layer, attached to the substrate, which is trypsin sensitive only. It must be noted that in our experiments the use of trypsin only (until day 15) showed an effect on all the layers and detached all the cells, but the cells were not as well dissociated as with the collagenase I (data not shown). We will thus refer to the upper layers as the collagenase-sensitive layers and to the lowest layer as a trypsin-sensitive layer.

As described in the results section, at day 22 the cells formed 4 layers in osteogenic differentiation, one layer in neurogenic differentiation and two layers, one continuous and one discontinuous, in adipogenic differentiation. Thus, only the cells in osteogenic differentiation form several layers. These observations correlate perfectly with the evolution of the cell number, since the cells proliferated massively for the first 15 days in osteogenic differentiation and this proliferation was higher than in

the adipogenic and neurogenic differentiations. After day 15, we observed no further proliferation of the cells as well as the beginning of the mineralization. The evolution of the cell number in osteogenic differentiation corroborates the observations in other studies showing also that cell proliferation stops by the second week of the osteogenic differentiation (3). Cells have to proliferate before mineralization in order to increase bone mass.

After mineralization started, the action of collagenase I was more difficult. This is why we treated first the cells with 20 mM EDTA to remove the Ca^{2+} deposits. EDTA is classically used during the osteoblasts isolation from rodent and human bones (27). EDTA is also used *in vitro* on fixed cells in order to remove Ca^{2+} deposits (9) or combined to trypsin for harvesting cells in osteogenic differentiation (24, 25). However, the EDTA concentrations used *in vitro* on fixed cells (about 350 mM) were 9 to 17 times higher than the concentrations that we used here on viable cells (9). The dissociation of the upper and lowest layers on day 29 required a higher EDTA concentration (40 mM) and a longer treatment time (40 minutes). After this intense EDTA treatment, collagenase I dissociated and detached all the cells from the dish, probably because EDTA weakened the bonds between the lowest layer and the bottom of the dish due to the chelation of the Ca^{2+} necessary to keep the cells attached to the culture substrate.

Differences between upper and lowest layers

The upper and lowest layers were characterized by cluster of differentiation (CD) expression and by Ca^{2+} oscillations. The MSCs express the CD105, CD90 and CD44 when they are multipotent (30, 31). As the cells progress in the differentiation process, they lose the multipotency markers compared to the control cells. The two types of layers showed no difference in losing the CD105 expression but showed a difference in the CD90 and CD44 evolution. This observation reveals that the cells in the two layers are not identical. Since decrease was probably faster in the cells of the upper layer, these latter could be considered as more differentiated than the cells of the lowest layer. The determination of the number of spontaneous Ca^{2+} oscillations during a given period of time confirmed previous results showing that the frequency of Ca^{2+} oscillations decreases progressively when MSCs undergo the osteogenic differentiation (32). It also revealed, again, that cells of the two layers behave differently. On day 8 of osteodifferentiation, the Ca^{2+} oscillations frequency was lower in the lowest layer than the upper layers which could indicate that the cells of the lowest layer could differentiate faster than the cells of the upper layer. However, no significant difference was observed on days 15 and 22.

To further investigate the osteogenic potential of the two layer types, cells from the upper layers and cells from the lowest one were taken at day 15 and separately put again in the osteogenic medium at the same confluency as at day 1 of osteodifferentiation. Cell growth resumed and after 2 weeks, cells had formed again multilayers as well as Ca^{2+} deposits. The Ca^{2+} deposits were more extensive in the cells from the upper layers. Moreover, cells originated from lowest layer proliferated more extensively than the cells originated from the upper layers. Three conclusions can be drawn from this experiment: the first one is that the cells, even on day 15, could proliferate again provide they are separated and cultured again. It is true that they did not form 4 layers as in the first two weeks of osteodifferentiation but they still formed 2 to 3 layers of cells, repetitively. On the contrary, if the layers had remained together, they would have stopped proliferation at day 15 (Fig. 3). The second conclusion is that this experiment confirmed our previous observations showing that the two cell layer types are different. It seems that the upper layers are slightly more differentiated than the lowest one. Indeed, the former

cells proliferated less than the cells originated from the lowest layer and they produced more Ca^{2+} deposits after two more weeks. Finally, the very important role of the osteogenic extracellular matrix is confirmed. As mentioned before, osteoblasts must be in contact with such a matrix to differentiate (4, 13, 33). When cells were dissociated and separated from the extracellular matrix as in our case, the cells presented again an ability to proliferate.

In conclusion, we show that MSC undergoing osteogenic differentiation form several layers. Collagenase I was used to dissociate the cells of the upper layers which gives access to a lowest attached layer sensitive to trypsin. The collagenase-sensitive upper layers and the trypsin-sensitive lowest layer showed differences in the expression of the MSC CDs. The characterization of these two types of layers that are not identical constitutes a new observation in osteogenic differentiation which offers new possibilities in the control of the number, the quality and the time to produce terminally differentiated osteoblasts. We can suggest that the investigators could indeed, on the one hand, dissociate the upper layers by collagenase I on day 15, expand them and use them rapidly (in 15 days) as terminally differentiated osteoblasts, and on the other hand, treat by trypsin the lowest layer, put the cells again in culture to keep them in proliferation, to dissociate them later, to continue the cycle of the production of differentiated osteoblast in only two weeks (instead of four) from a pool of rapidly growing cells in the middle of the differentiation process. This cycle should favor both the production of differentiated osteoblasts and the maintenance of a stock of cells undergoing the differentiation facilitating the application of these cells and spreading their uses.

References

1. Friedenstein, A. J., Petrakova, K. V., Kurolesova, A. I., and Frolova, G. P. (1968) Heterotopic of bone marrow. Analysis of precursor cells for osteogenic and hematopoietic tissues. *Transplantation* **6**, 230–247
2. Friedenstein, A. J., Chailakhjan, R. K., and Lalykina, K. S. (1970) The development of fibroblast colonies in monolayer cultures of guinea-pig bone marrow and spleen cells. *Cell Tissue Kinet.* **3**, 393–403
3. Quarles, L. D., Yohay, D. A., Lever, L. W., Caton, R., and Wenstrup, R. J. (1992) Distinct proliferative and differentiated stages of murine MC3T3-E1 cells in culture: an in vitro model of osteoblast development. *J. Bone Miner. Res. Off. J. Am. Soc. Bone Miner. Res.* **7**, 683–692
4. El-Amin, S. F., Lu, H. H., Khan, Y., Burems, J., Mitchell, J., Tuan, R. S., and Laurencin, C. T. (2003) Extracellular matrix production by human osteoblasts cultured on biodegradable polymers applicable for tissue engineering. *Biomaterials* **24**, 1213–1221
5. Vater, C., Kasten, P., and Stiehler, M. (2011) Culture media for the differentiation of mesenchymal stromal cells. *Acta Biomater.* **7**, 463–477
6. Aksu, A. E., Rubin, J. P., Dudas, J. R., and Marra, K. G. (2008) Role of gender and anatomical region on induction of osteogenic differentiation of human adipose-derived stem cells. *Ann. Plast. Surg.* **60**, 306–322

7. Langenbach, F. and Handschel, J. (2013) Effects of dexamethasone, ascorbic acid and β -glycerophosphate on the osteogenic differentiation of stem cells in vitro. *Stem Cell Res. Ther.* **4**, 117
8. Granéli, C., Thorfve, A., Ruetschi, U., Brisby, H., Thomsen, P., Lindahl, A., and Karlsson, C. (2014) Novel markers of osteogenic and adipogenic differentiation of human bone marrow stromal cells identified using a quantitative proteomics approach. *Stem Cell Res.* **12**, 153–165
9. Owen, T. A., Aronow, M., Shalhoub, V., Barone, L. M., Wilming, L., Tassinari, M. S., Kennedy, M. B., Pockwinse, S., Lian, J. B., and Stein, G. S. (1990) Progressive development of the rat osteoblast phenotype in vitro: reciprocal relationships in expression of genes associated with osteoblast proliferation and differentiation during formation of the bone extracellular matrix. *J. Cell. Physiol.* **143**, 420–430
10. Zhu, M., Kohan, E., Bradley, J., Hedrick, M., Benhaim, P., and Zuk, P. (2009) The effect of age on osteogenic, adipogenic and proliferative potential of female adipose-derived stem cells. *J. Tissue Eng. Regen. Med.* **3**, 290–301
11. Friedman, M. S., Long, M. W., and Hankenson, K. D. (2006) Osteogenic differentiation of human mesenchymal stem cells is regulated by bone morphogenetic protein-6. *J. Cell. Biochem.* **98**, 538–554
12. Song, I.-H., Caplan, A. I., and Dennis, J. E. (2009) In vitro dexamethasone pretreatment enhances bone formation of human mesenchymal stem cells in vivo. *J. Orthop. Res. Off. Publ. Orthop. Res. Soc.* **27**, 916–921
13. Kundu, A. K., Khatiwala, C. B., and Putnam, A. J. (2009) Extracellular matrix remodeling, integrin expression, and downstream signaling pathways influence the osteogenic differentiation of mesenchymal stem cells on poly(lactide-co-glycolide) substrates. *Tissue Eng. Part A* **15**, 273–283
14. Jaiswal, N., Haynesworth, S. E., Caplan, A. I., and Bruder, S. P. (1997) Osteogenic differentiation of purified, culture-expanded human mesenchymal stem cells in vitro. *J. Cell. Biochem.* **64**, 295–312
15. Birmingham, E., Niebur, G. L., McHugh, P. E., Shaw, G., Barry, F. P., and McNamara, L. M. (2012) Osteogenic differentiation of mesenchymal stem cells is regulated by osteocyte and osteoblast cells in a simplified bone niche. *Eur. Cell. Mater.* **23**, 13–27
16. Fromigué, O., Marie, P. J., and Lomri, A. (1997) Differential effects of transforming growth factor beta2, dexamethasone and 1,25-dihydroxyvitamin D on human bone marrow stromal cells. *Cytokine* **9**, 613–623
17. Kim, I. S., Song, J. K., Song, Y. M., Cho, T. H., Lee, T. H., Lim, S. S., Kim, S. J., and Hwang, S. J. (2009) Novel effect of biphasic electric current on in vitro osteogenesis and cytokine production in human mesenchymal stromal cells. *Tissue Eng. Part A* **15**, 2411–2422
18. Tada, H., Nemoto, E., Foster, B. L., Somerman, M. J., and Shimauchi, H. (2011) Phosphate increases bone morphogenetic protein-2 expression through cAMP-dependent protein kinase and ERK1/2 pathways in human dental pulp cells. *Bone* **48**, 1409–1416
19. Huang, Z., Nelson, E. R., Smith, R. L., and Goodman, S. B. (2007) The sequential expression profiles of growth factors from osteoprogenitors [correction of osteroprogenitors] to osteoblasts in vitro. *Tissue Eng.* **13**, 2311–2320
20. Li, Y. J., Batra, N. N., You, L., Meier, S. C., Coe, I. A., Yellowley, C. E., and Jacobs, C. R. (2004) Oscillatory fluid flow affects human marrow stromal cell proliferation and differentiation. *J. Orthop. Res. Off. Publ. Orthop. Res. Soc.* **22**, 1283–1289

21. Bruder, S. P., Jaiswal, N., and Haynesworth, S. E. (1997) Growth kinetics, self-renewal, and the osteogenic potential of purified human mesenchymal stem cells during extensive subcultivation and following cryopreservation. *J. Cell. Biochem.* **64**, 278–294
22. George, J., Kuboki, Y., and Miyata, T. (2006) Differentiation of mesenchymal stem cells into osteoblasts on honeycomb collagen scaffolds. *Biotechnol. Bioeng.* **95**, 404–411
23. Rickard, D. J., Sullivan, T. A., Shenker, B. J., Leboy, P. S., and Kazhdan, I. (1994) Induction of rapid osteoblast differentiation in rat bone marrow stromal cell cultures by dexamethasone and BMP-2. *Dev. Biol.* **161**, 218–228
24. Goh, T. K.-P., Zhang, Z.-Y., Chen, A. K.-L., Reuveny, S., Choolani, M., Chan, J. K. Y., and Oh, S. K.-W. (2013) Microcarrier culture for efficient expansion and osteogenic differentiation of human fetal mesenchymal stem cells. *BioResearch Open Access* **2**, 84–97
25. Castrén, E., Sillat, T., Oja, S., Noro, A., Laitinen, A., Konttinen, Y. T., Lehenkari, P., Hukkanen, M., and Korhonen, M. (2015) Osteogenic differentiation of mesenchymal stromal cells in two-dimensional and three-dimensional cultures without animal serum. *Stem Cell Res. Ther.* **6**, 167
26. Liew, A., André, F. M., Lesueur, L. L., De Ménorval, M.-A., O'Brien, T., and Mir, L. M. (2013) Robust, efficient, and practical electroporation method for human mesenchymal stem cells using square electric pulses. *Hum. Gene Ther. Methods* **24**, 289–297
27. Bakker, A. D. and Klein-Nulend, J. (2012) Osteoblast isolation from murine calvaria and long bones. *Methods Mol. Biol. Clifton NJ* **816**, 19–29
28. Taylor, S. E. B., Shah, M., and Orriss, I. R. (2014) Generation of rodent and human osteoblasts. *BoneKEy Rep.* **3**
29. Franceschi, R. T., Iyer, B. S., and Cui, Y. (1994) Effects of ascorbic acid on collagen matrix formation and osteoblast differentiation in murine MC3T3-E1 cells. *J. Bone Miner. Res. Off. J. Am. Soc. Bone Miner. Res.* **9**, 843–854
30. Lindroos, B., Suuronen, R., and Miettinen, S. (2011) The potential of adipose stem cells in regenerative medicine. *Stem Cell Rev.* **7**, 269–291
31. Ullah, I., Subbarao, R. B., and Rho, G. J. (2015) Human mesenchymal stem cells - current trends and future prospective. *Biosci. Rep.* **35**
32. Titushkin, I., Sun, S., Shin, J., and Cho, M. (2010) Physicochemical Control of Adult Stem Cell Differentiation: Shedding Light on Potential Molecular Mechanisms. *BioMed Res. Int.* **2010**, e743476
33. Xiao, J., Liang, D., Zhao, H., Liu, Y., Zhang, H., Lu, X., Liu, Y., Li, J., Peng, L., and Chen, Y.-H. (2010) 2-Aminoethoxydiphenyl borate, a inositol 1,4,5-triphosphate receptor inhibitor, prevents atrial fibrillation. *Exp. Biol. Med. Maywood NJ* **235**, 862–868

Author contributions:

Hanna Hanna, Franck M. Andre and Lluís M. Mir designed research, analysed data and wrote the paper; Hanna Hanna: performed research.

Acknowledgements

This work has been supported by CNRS, Gustave Roussy, Université Paris XI, Paris-Saclay, the ITMO Cancer and INSERM in the frame of the Plan Cancer 2015-2019 (project PC201517) and the Fondation EDF. The research was also conducted in the scope of the EBAM European Associated Laboratory (LEA) and of the COST action BM 1309 EMF-MED. Authors would like to thank Dr. Bassim Al Sakere for the lipoaspirates, and Sophie Salomé, from the PFIC of Gustave Roussy, for her precious help in acquiring the multilayers stacks under the confocal microscope.

Figures:

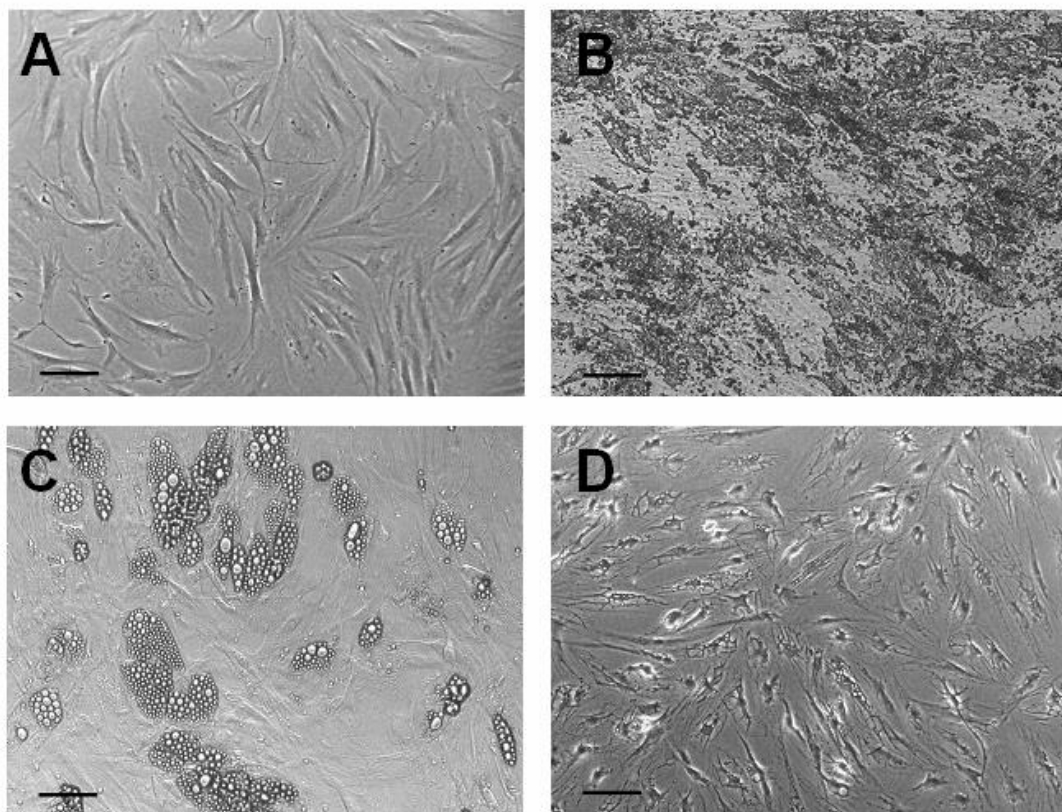


Figure 1. Morphological aspects of the cells. A: control haMSCs after three days of culture, B, C and D: haMSCs undergoing respectively osteogenic (day 29), adipogenic (day 15) and neurogenic (day 5) differentiation. The calibration bars correspond to 100 μm .

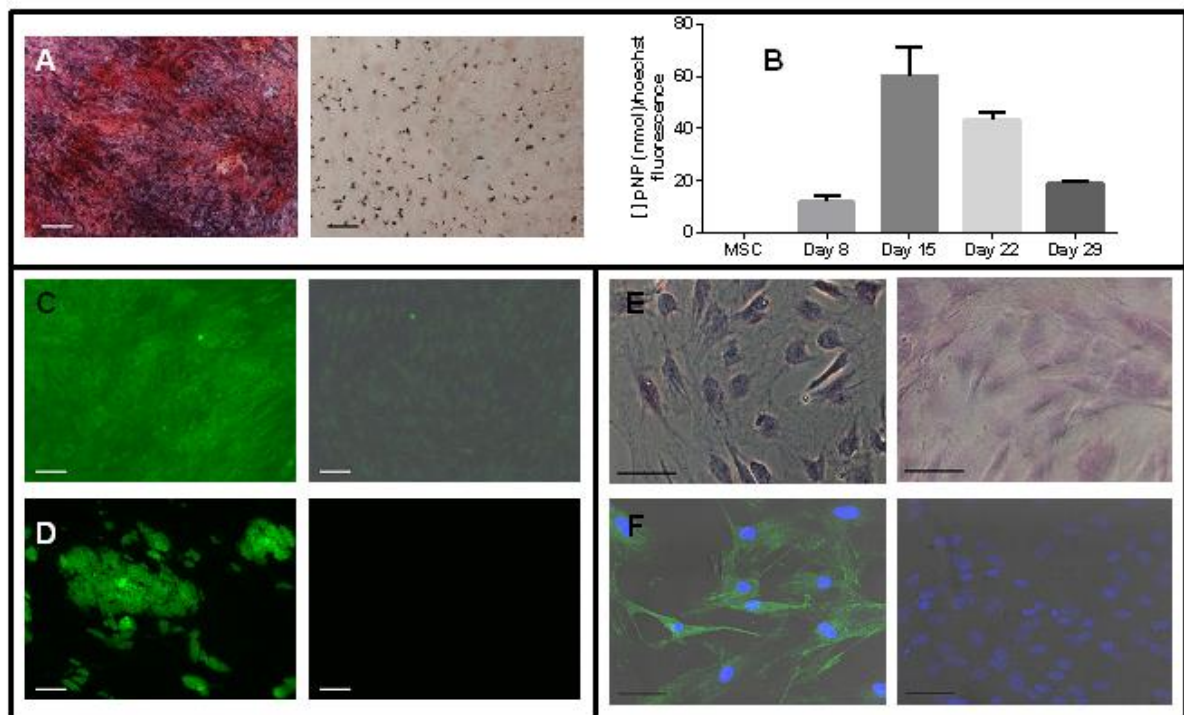


Figure 2. Characterization of the differentiated cells. A and B: osteogenic differentiation, C and D: adipogenic differentiation, E and F: neurogenic differentiation. A: alizarin red staining, B: alkaline phosphatase activity, C: labeling with FABP4 antibody, D: bodipy staining, E: cresyl violet staining, F: labeling with MAP2 antibody and Hoechst. In all pairs of photos, the right one is the control (undifferentiated) MSC. The calibration bars correspond to 100 μ m.

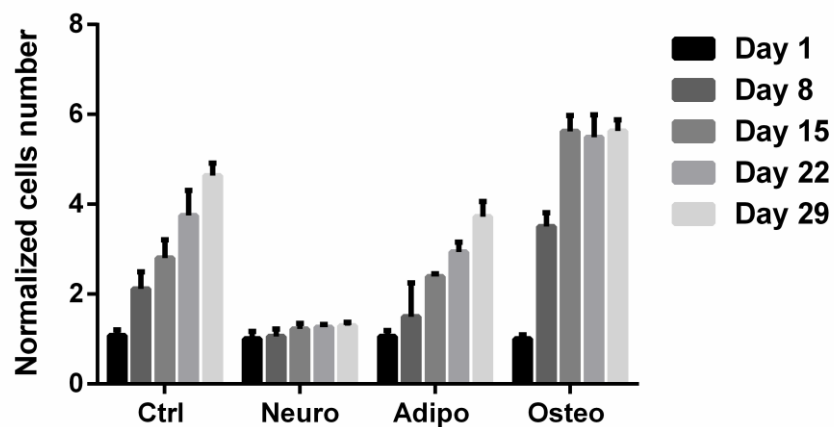


Figure 3. Evolution of the cell number between day 1 and day 29 in the different groups of cells.

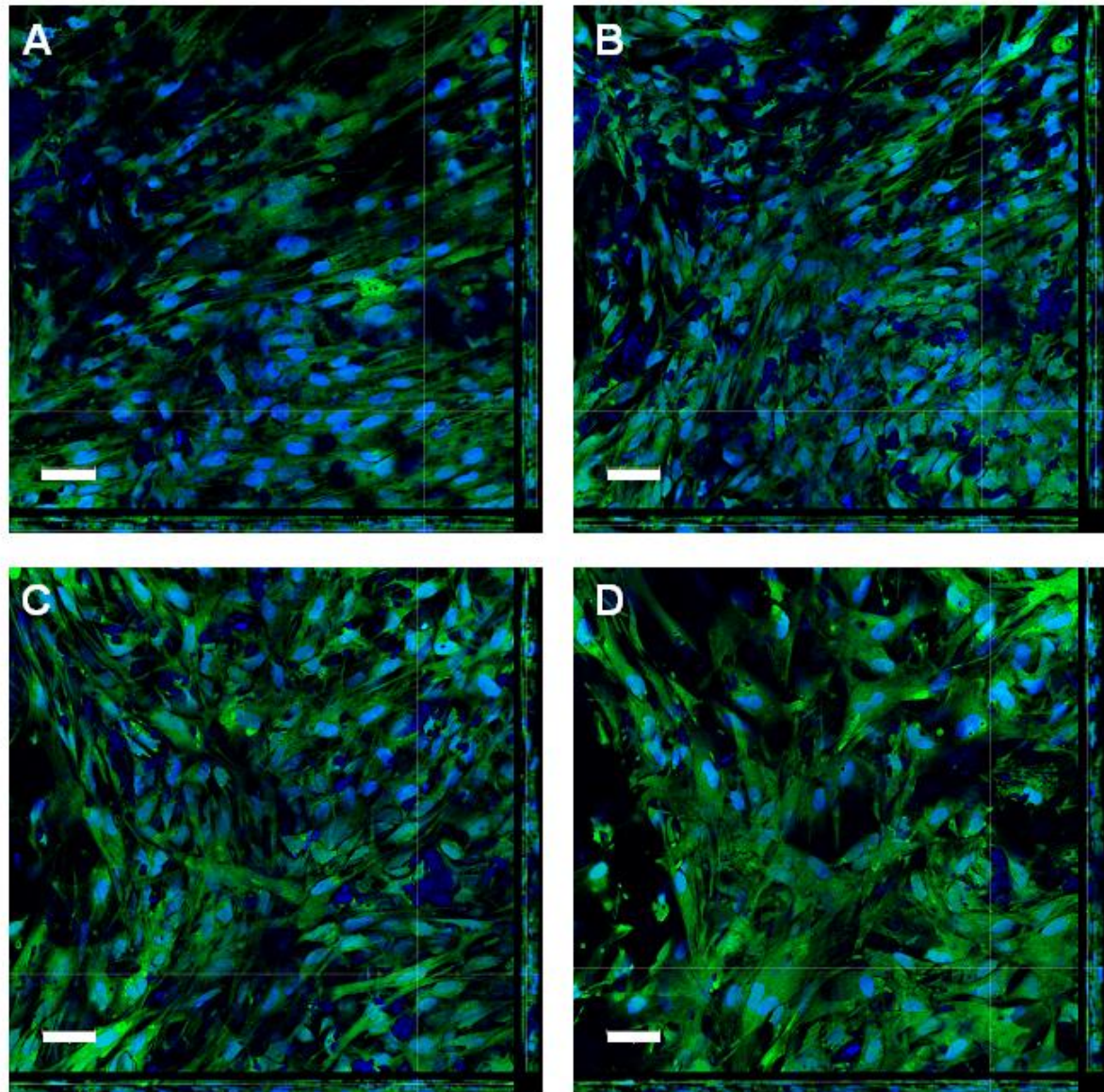


Figure 4. The different layers of an osteogenic differentiation day 22, stained with Hoechst and fluorescein diacetate. A: first layer (the layer in contact with the coverslide), B, C and D: second, third and fourth layer respectively. The grids to the right and below every photo represent the Z axis. The calibration bars correspond to 50 μm .

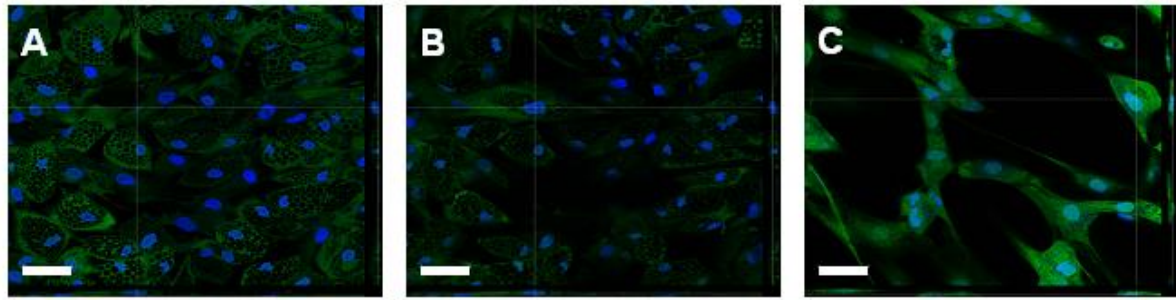


Figure 5. The different layers of an adipogenic (A and B) and neurogenic (C) differentiation day 22, stained with Hoechst and fluorescein diacetate. A: first layer (the layer in contact with the microslide), B: second layer. The grids to the right and below every photo represent the Z axis. The calibration bars correspond to 50 μm .

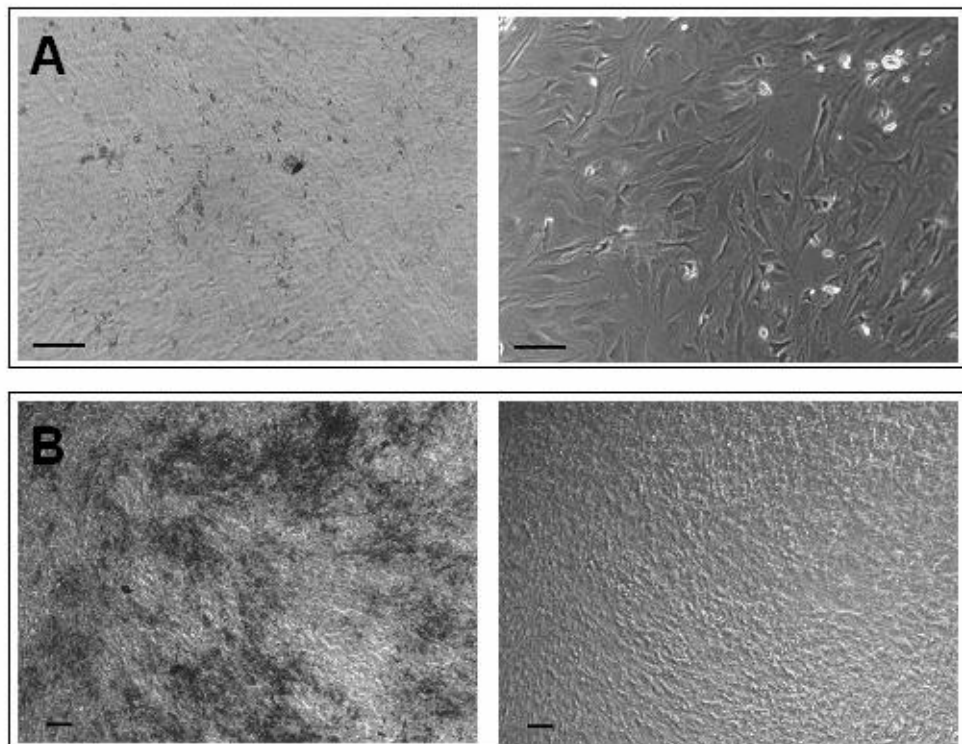


Figure 6. The action of collagenase I and EDTA on the osteogenic layers. A: the observation of the cells before (left) and after (right) the action of the collagenase I (2 mg/ml) on day 15 of osteodifferentiation. B: The Ca^{2+} deposits before (left) and after (right) the action of 40 mM of EDTA on day 29 of osteodifferentiation. The calibration bars correspond to 100 μm .

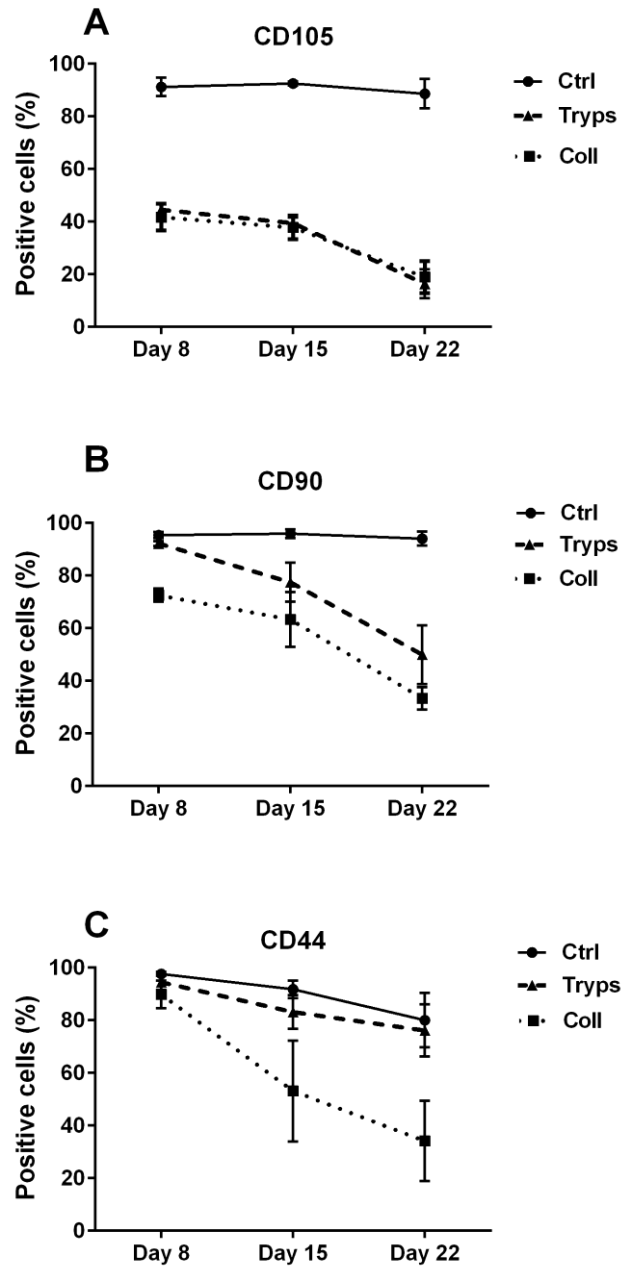


Figure 7. Immunostaining of the upper and lowest layers in an osteogenic differentiation. Coll: the upper layers dissociated with collagenase I; tryps: the lowest layer trypsinised.

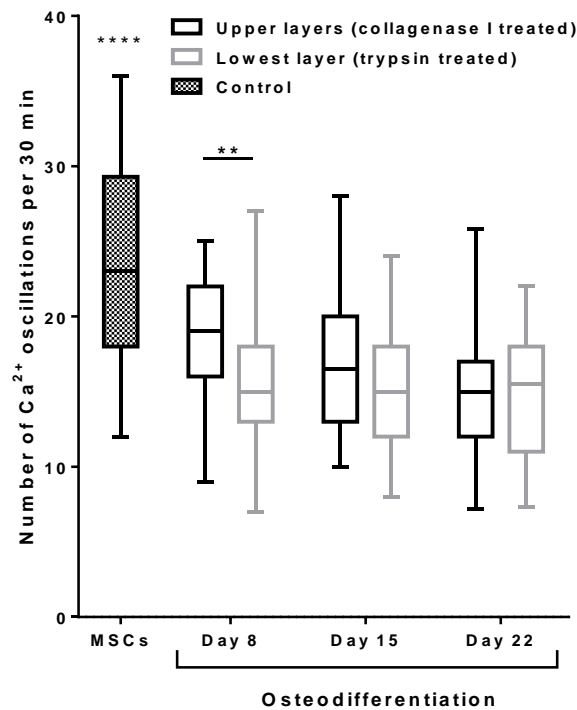


Figure 8. Comparison of the number of Ca^{2+} oscillations between upper and lowest layers on different days of an osteogenic differentiation. MSC controls have significantly more Ca^{2+} oscillations than the differentiated layers (****, $p < 0.0001$, one-way Anova with Dunnett's multiple comparisons test). At day 8 the Ca^{2+} oscillations were significantly lower in number in the lowest layer than in the upper layers (**, $p < 0.01$, $p = 0.0038$, two-way ANOVA with Sidak's multiple comparisons test). The whiskers represent the 95th and the 5th percentile.

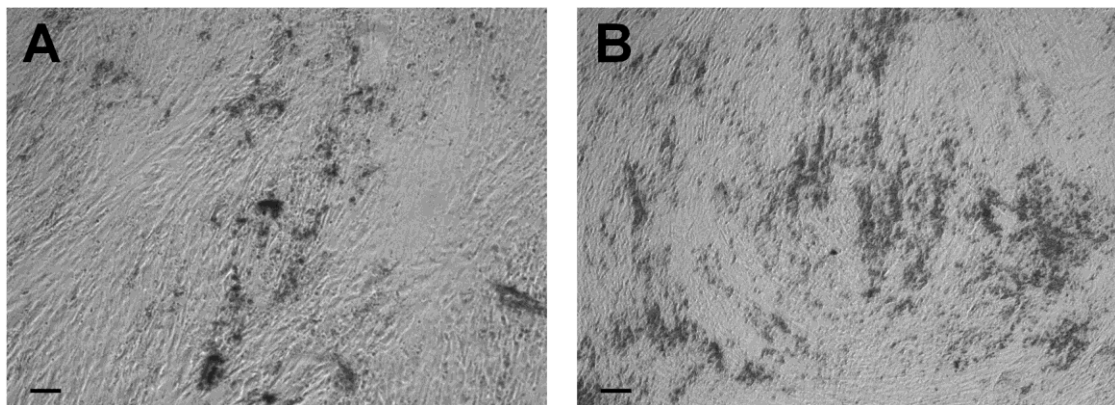


Figure 9. Cells from lowest (A) and upper (B) layers dissociated on day 15 and put in an osteogenic medium for 2 weeks. The black spots are the Ca^{2+} deposits. The calibration bars correspond to 100 μm .

Supplementary figure:

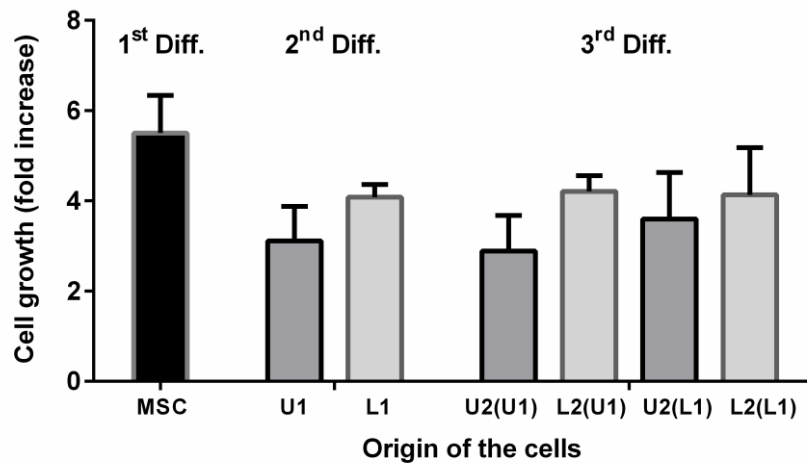


Figure 1. Cells growth in osteodifferentiation medium for three consecutive periods of 15 days. Culture dishes were seeded always with the same number of cells at day 1 and cells were counted after 15 days of culture. Growth is reported as the increase fold in the number of the cells at day 15. HaMSCs were put in cultured in osteodifferentiation medium for the “first differentiation”. After 15 days, the upper layers (U1) and the lowest layer (L1) were counted and seeded separately in osteodifferentiation medium (“second differentiation”). After 15 more days, the upper layers (U2 from U1 and U2 from L1) and the lowest layer (U2 from L1 and U2 from L1) were counted and seeded separately in osteodifferentiation medium (“third differentiation”). After 15 days, all the cells were counted for each condition that is U2(U1), L2(U1), U2(L1) and L2(L1). Each condition was counted three times in three independent repeats. Diff: differentiation.

4 SUPPLEMENTARY DATA

4.1 EFFECT OF A ONE 100 μ S PULSE APPLIED ONCE A DAY ON THE OSTEODIFFERENTIATION OF HUMAN-ADIPOSE MESENCHYMAL STEM CELLS

I. Introduction

In the first part of this thesis, we assessed the effect of 100 μ s pulse on the plasma membrane (PM) and the endoplasmic reticulum (ER) membranes of DC-3F cells and the human-adipose mesenchymal stem cells (haMSC). In the second part, we used the same pulse to induce cytosolic Ca^{2+} spikes in haMSC, and to see the effect of the pulse on the spontaneous Ca^{2+} oscillations in these latters. As shown, the 100 μ s pulse had different effects on the Ca^{2+} oscillations according to the electric field amplitude. In this last part of the thesis, we decided to apply the same type of pulses used before on haMSC undergoing osteogenic differentiation. The purpose was to combine the classical chemical factors used to induce an osteogenic differentiation with the delivery of 100 μ s pulses (a physical factor) and to evaluate the effect of the pulses on the speed of differentiation. Since 100 μ s pulses can create cytosolic Ca^{2+} spikes from different origins (the PM or the PM and the ER), and since they can control the Ca^{2+} oscillations in haMSC, it would be useful to use them with haMSC undergoing a differentiation. The team of Shan Sun (Sun et al. 2007) showed that the Ca^{2+} oscillations frequency decreased in MSCs undergoing an osteogenic differentiation. The final goal was to assess if, by controlling the Ca^{2+} oscillations frequency, and the PM permeability to the osteogenic factors, 100 μ s pulses could control an osteogenic differentiation.

II. Hypothesis

Two larges effects of the 100 μ s electric pulses could be expected:

- 1- The control of the Ca^{2+} oscillations:** we chose two different electric field amplitudes: 300 and 600 V/cm, because we reported in the second part of the thesis (article n° 2) that a pulse of 300 V/cm was able to induce additional oscillation(s) to the existing oscillations in nearly all the haMSC cells, and that a pulse of 600 V/cm induced a Ca^{2+} spike that inhibited the normal oscillations for some minutes. Hence, we intended to study the effect on MSCs differentiation of these two different outcomes on Ca^{2+} oscillations.
- 2- The enhancement of osteogenic factors entry into the cells:** As shown in fig. 1A, the osteogenic factors have a molecular weight smaller than the Yo-pro 1 iodide. Hence, if the cells were permeabilized to Yo-pro 1 iodide, they should also be permeabilized to the osteogenic factors. Fig. 1B shows that, with 300 V/cm in MEM α (conductive medium), there was a very little permeabilization to Yo-Pro 1. However, in a non-conductive medium such as STM, there was a little permeabilization at 300 V/cm and an obvious permeabilization at 600 V/cm. However it must be noted that dexamethasone (Dex) is a glucocorticoid steroid. Hence, it diffuses freely across the PM and has intracellular receptors. Ascorbic acid (Asc) enters the cells through the glucose transporters GLUT1. The glycerol-2-phosphate (G2P) plays a role at the outside of the cell since it provides the phosphate necessary for the mineralization. So, Dex and Asc can normally enter in the cells and G2P does not need to enter. The role of the electric

pulse could be just to enhance the entry of these factors in the cells, with probably very limited effects.

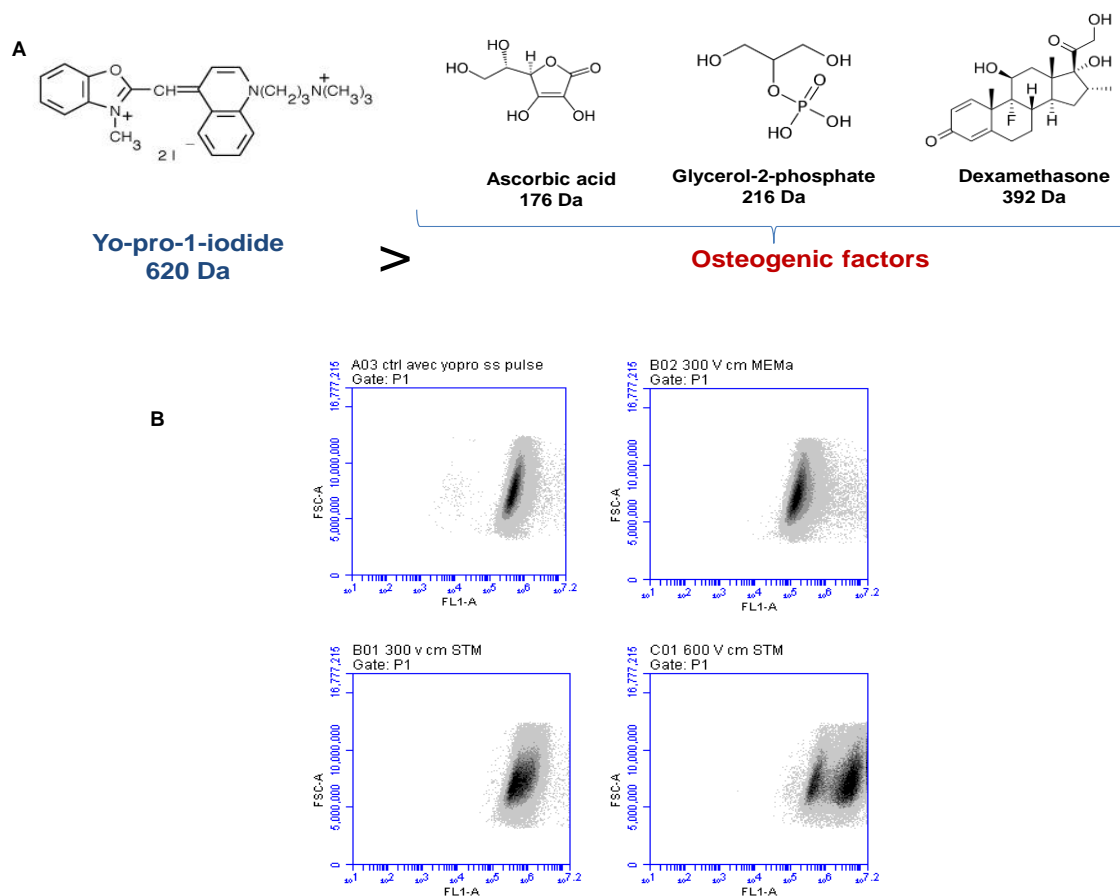


Figure 1. A: the relative size of Yo-pro 1 iodide and the osteogenic factors. B: FACS results on the permeabilization to Yo-pro 1 iodide according to the medium and the electric field amplitude

III. Limitations

The experimental design and the pulse conditions came after initial tests with the electrodes that could be used with the μ sPEFs generators available in our laboratory. The electrode used to deliver the pulse was finally a Petri PulserTM (BTX, UK) (Fig.2). It is composed of several gold plated electrodes distant of 2 mm. The electric pulse was delivered by a CliniporatorTM (Igea, Carpi, Italy).



Figure 2. The Petri pulser™

The Petri pulser™ electrode has advantages and inconvenient.

✓ **Advantages:**

- It is designed to fit into every single well of a 6 well plate or into individual 35 mm Petri dish (surface of 10 cm²).
- The thin electrodes composing the Petri pulser™ are designed to cover all the surface area of the well.

✓ **Drawbacks:**

- It could be used with 830 µl maximum of conductive medium and a maximum of 300 V/cm could be delivered, otherwise, the Cliniporator is saturated in the electric current (12 A).
- With a conductive medium, an electric current limitation (due to the pulse generator characteristics) occurred when a pulse of only 300 V/cm is delivered and with a volume of 830 µl (the normal volume to culture the cells in a 10 cm² dish/well is usually 2 ml). This is why we were limited by the electric field amplitude and medium volume when a conductive medium was to be used.

For the delivery of pulses of higher field amplitudes, non-conductive medium (containing or not Ca²⁺) was used. The non-conductive medium used was the STM, composed of 250 mM sucrose, 10 mM of Tris-HCl and 1 mM MgCl₂. It has a conductivity of 0.1 S/m and an osmolarity of 287 mOsmol/Kg. The conductive medium was the MEMα (the normal medium of the cells) which has a conductivity of 1.5 S/m and an osmolarity of 330 mOsmol/Kg.

IV. Experimental design

haMSCs were grown in 6 well plates and let to attain 90-100% confluence. Then the osteogenic medium was added. This medium change corresponds to day 1 of differentiation. Every day (from day 1 to day 29), the osteogenic medium was removed and 830 µl of pulsing medium was added to the cells in order to apply one single electric pulse. The pulsing medium was either MEMα (conductive medium) or STM (non-conductive medium without Ca²⁺) or STM+CaCl₂ (non-conductive medium with 1.8 mM of Ca²⁺). All the pulsing media contained the classical concentrations of osteogenic factors (100 nM Dex, 200 µM Asc and 10 mM G2P). One pulse of 100 µs was delivered by a Cliniporator™ (Igea, Carpi, Italy). After the pulse delivery, the pulsing medium was left for 30 min, after which it was removed and replaced by 2 ml of MEMα with the osteogenic factors. Fig. 3 shows the different conditions of pulse and medium; 830 µl of the pulsing medium was also added to the control but no pulse was delivered (sham treated).

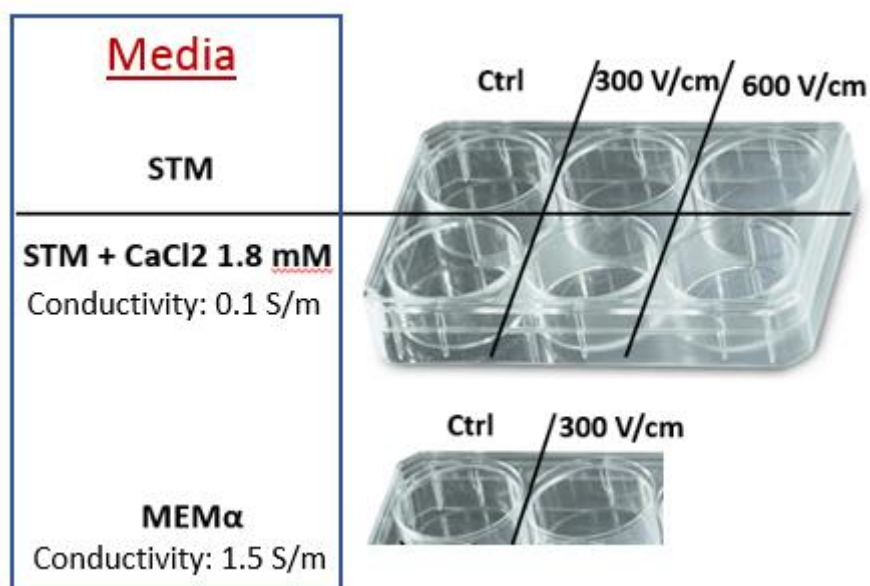


Figure 3. Experiment design; pulsing media and electric field conditions.

In the next section STM + CaCl₂ will be referred as STM+Ca²⁺ or STM+CaCl₂ or STM-CaCl₂. When a pulse was applied, it is referred with the name of the pulse medium and the field amplitude, for example: STM-Ca 600 means a pulse of 600 V/cm in STM+ CaCl₂, STM 300 means a pulse of 300 V/cm applied in STM.

V. Results

Cell counting

The cell number was determined in the same manner as in article 3.

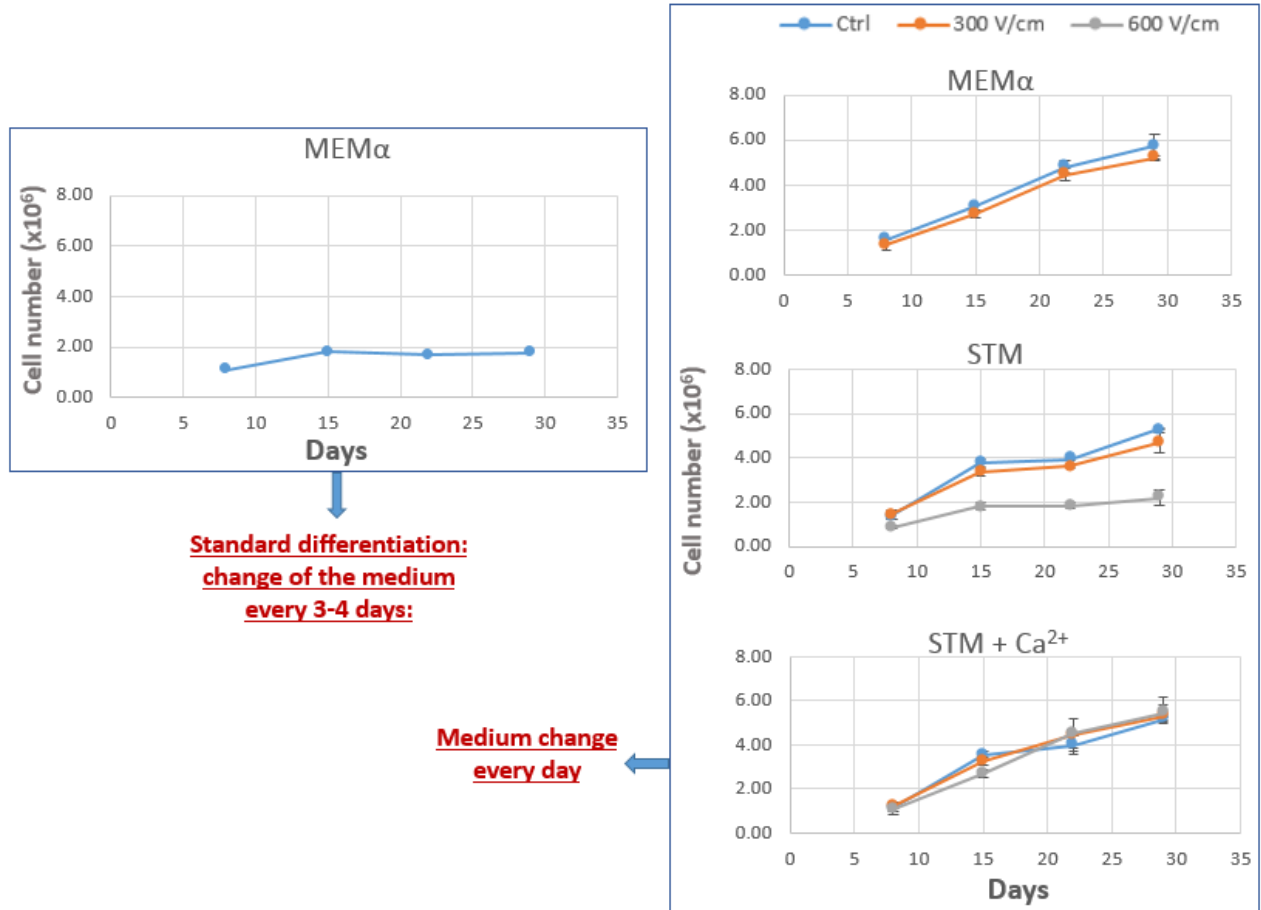


Figure 4. Evolution of the cell number during the different conditions. Data are represented as means and standard deviations of three different counting for every condition. Standard: haMSCs undergoing a normal differentiation with medium change twice a week.

Alkaline phosphatase assay and Alizarin Red staining

For internal ALP activity measurement (the cytoplasmic ALP), refer to article 3. To measure the external ALP activity (that is the ALP located on the cell membrane), medium was discarded and cells were washed with PBS and fixed with ethanol 95% for 10 minutes. After washing 3 times with PBS, a BCIP/NBT solution was added (Sigma Aldrich) (1ml for 4 cm²) and cells were put for 10 minutes at 37°C. After discarding the solution, cells were washed 3 times with sterile water (protected from light) and observed under a microscope.

Prior to Alizarin Red S staining, cells were washed in PBS and fixed in 95% methanol for 10 min. 2% Alizarin Red S solution was added for 5 min, then rinsed with water. To quantify the alizarin red staining, 1ml of 10% cetylperidinium chloride (Sigma Aldrich) was added to each well, and cells were

incubated for 20 min to elute the stain. After that, 100 μ l of the eluted stain were put in a 96 well plate and read on the spectrophotometer at 570 nm.

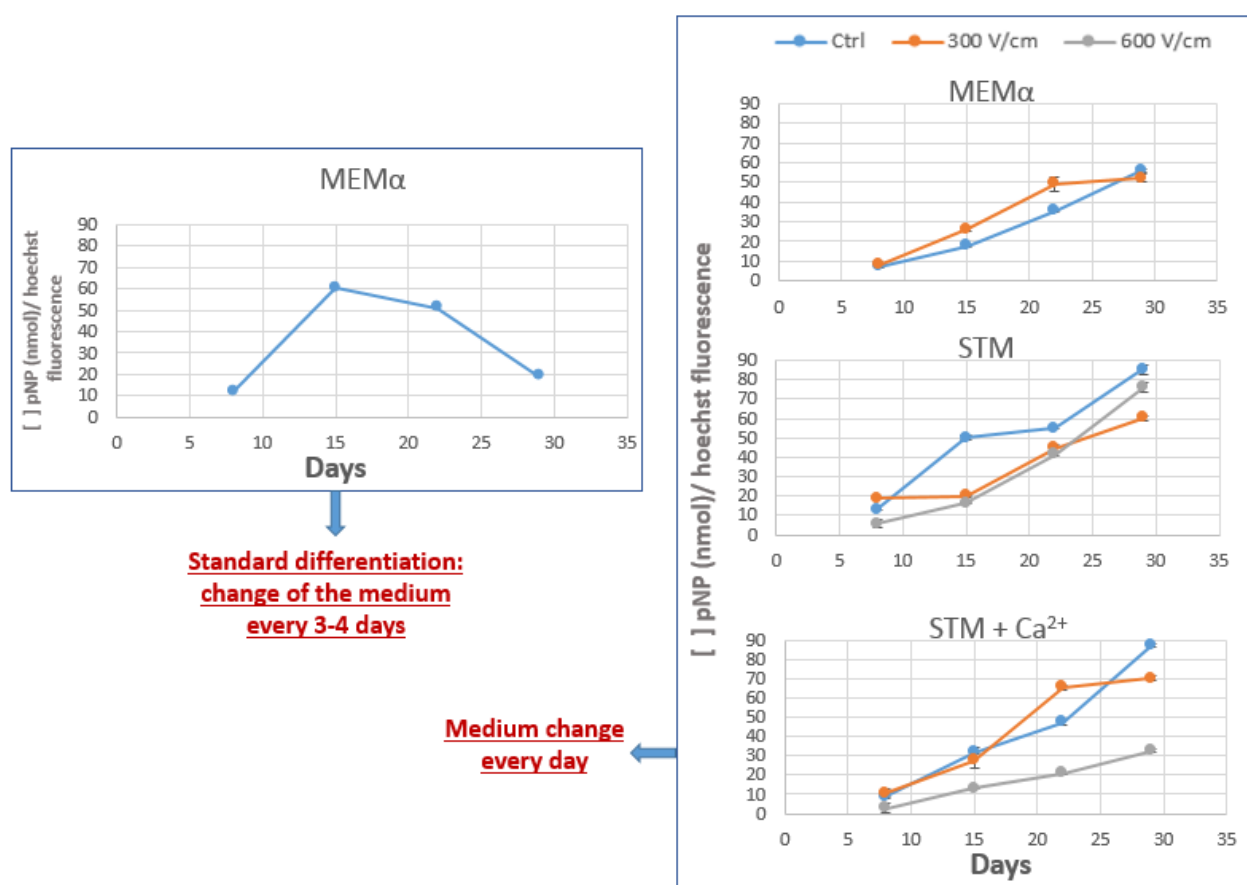


Figure 5. The evolution of internal ALP activity. Data are represented as means and standard deviations of three different values for every condition.

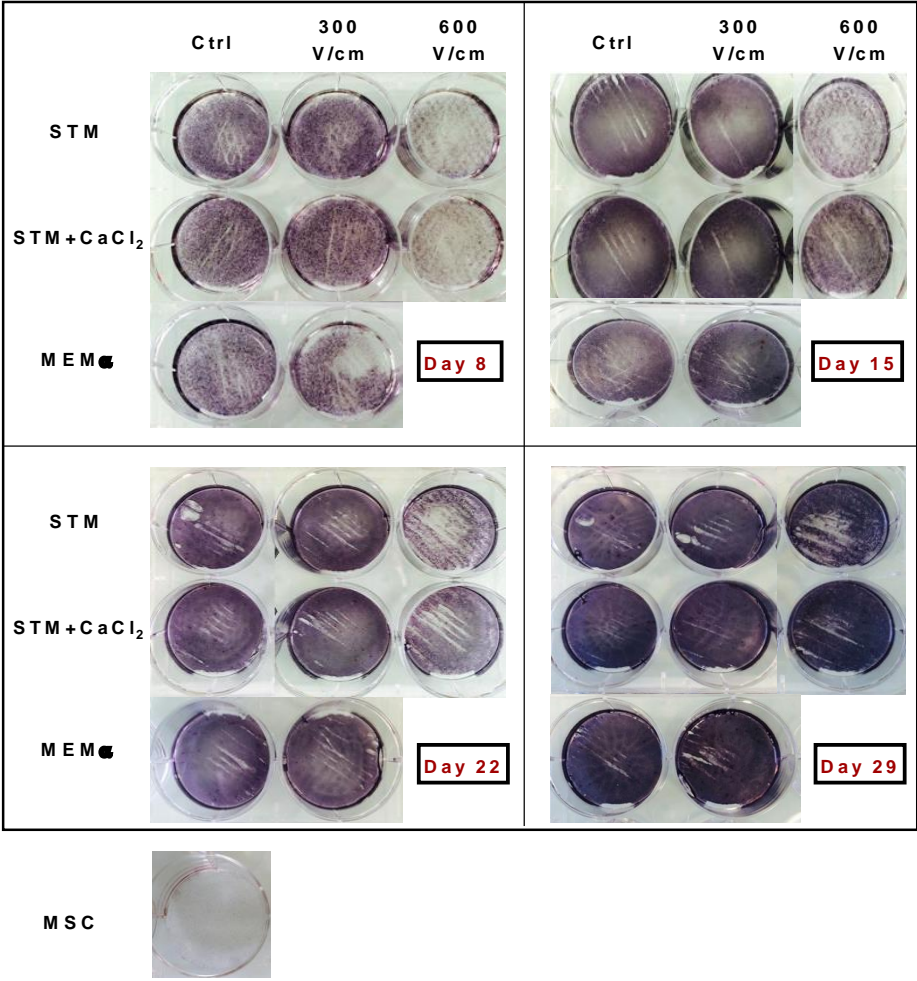


Figure 6. External ALP staining.

Alizarin red staining

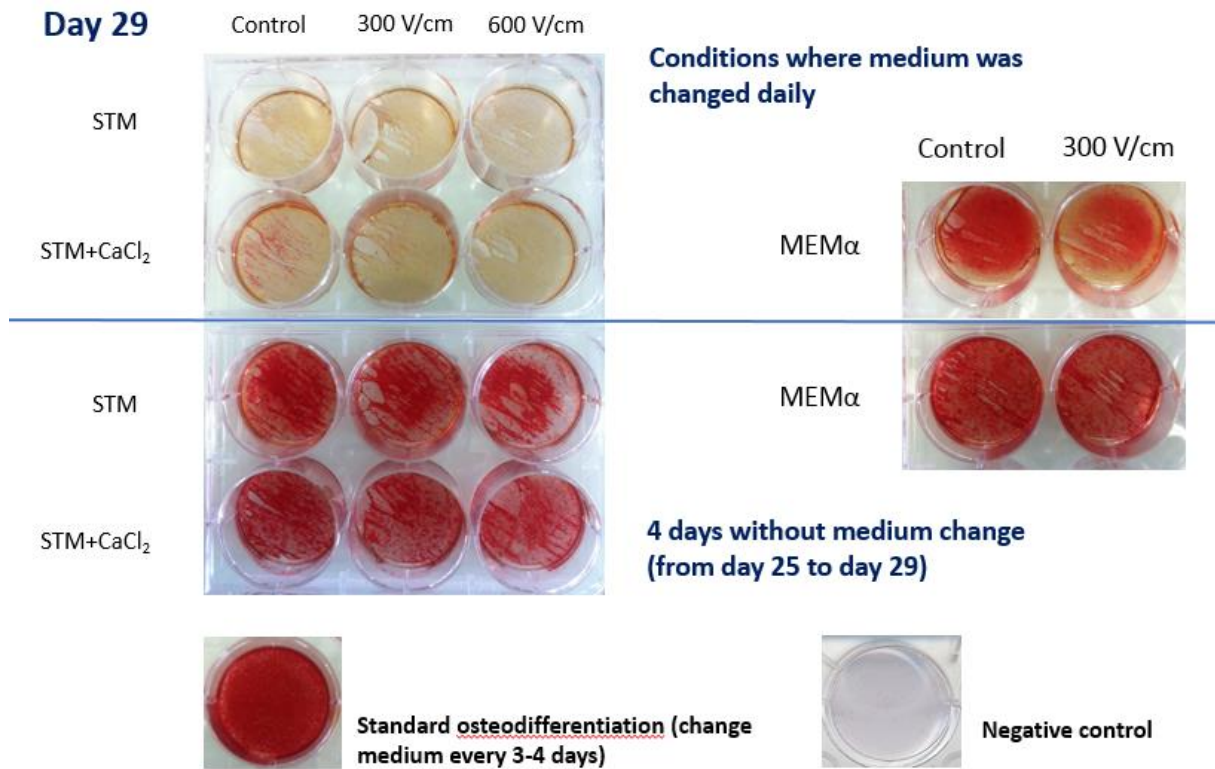
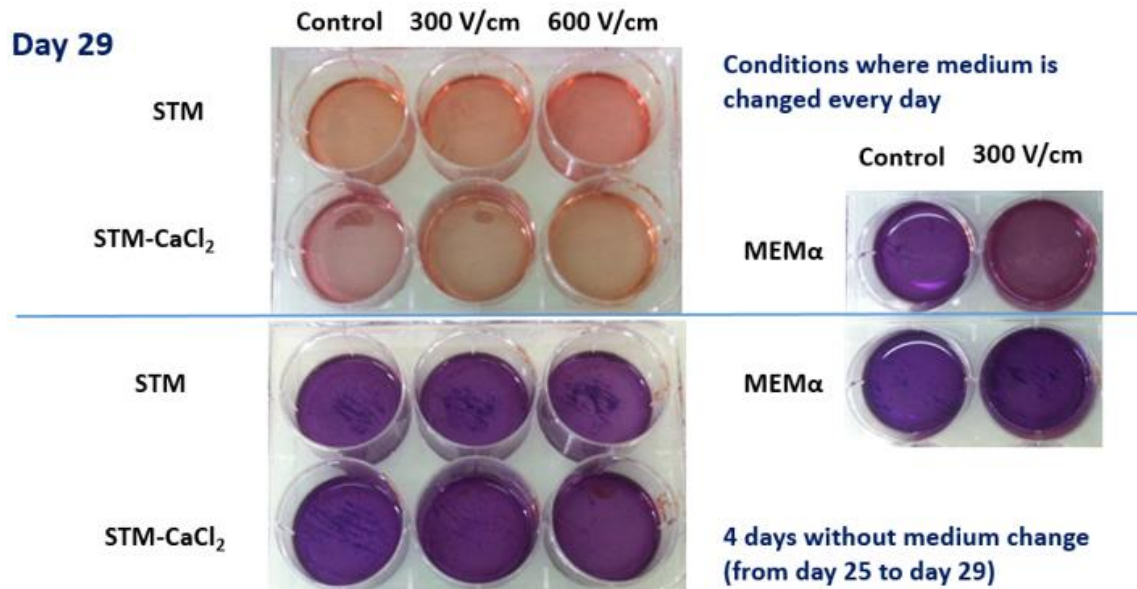


Figure 7. Alizarin red staining.

Cetylperidinium Chloride



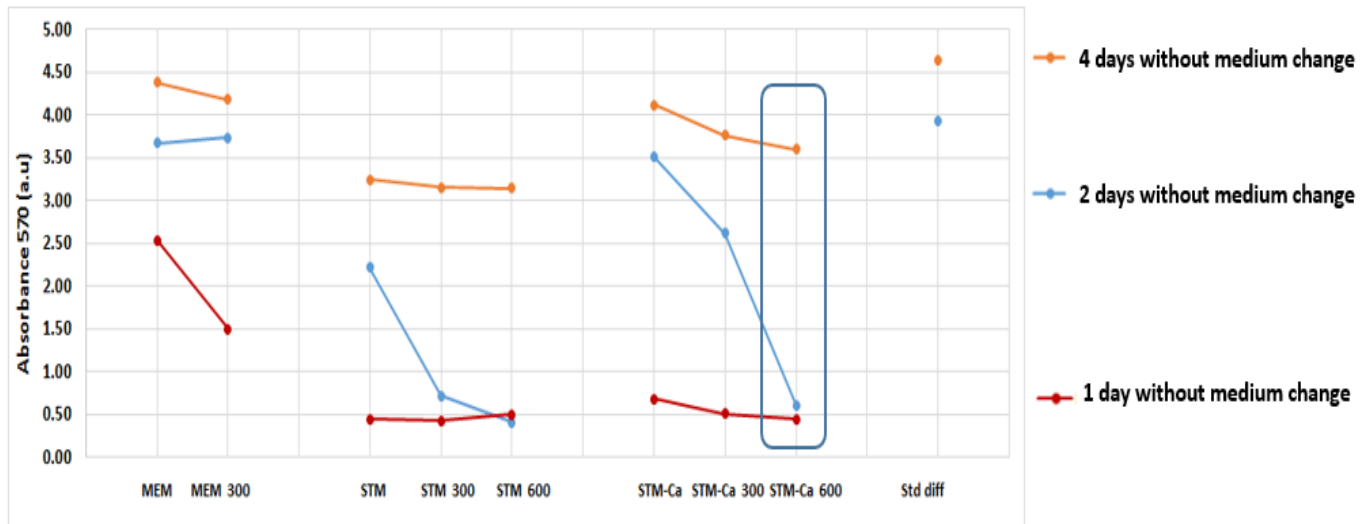


Figure 8. Quantification of the Ca^{2+} deposits after elution with cetylperidinium chloride.

Calcium oscillations visualization and analysis

For the methods, refer to article 3.

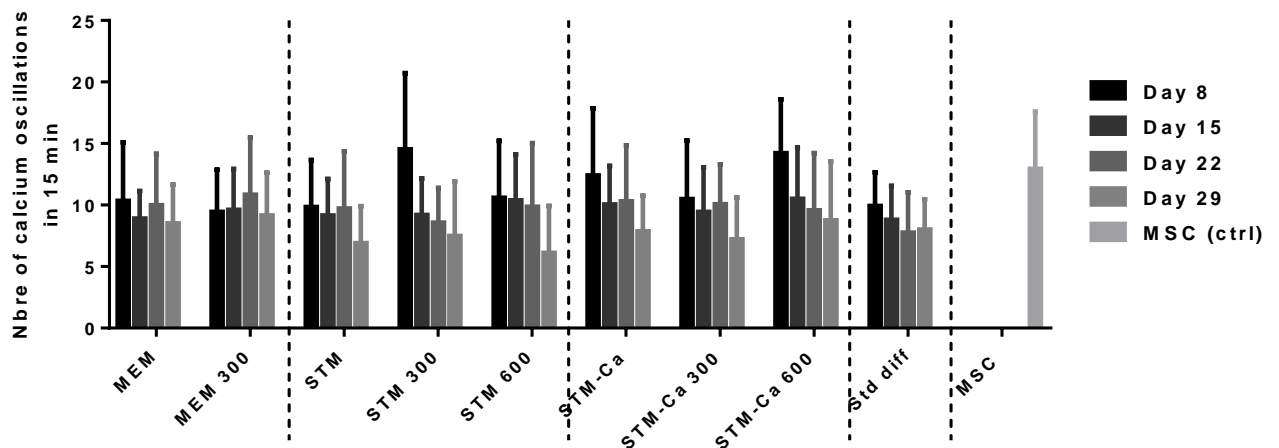


Figure 9. Comparison of calcium oscillations number in 15 min between the different conditions. Data are represented as means and standard deviations of at least 30 cells per condition. According to two way Anova, the condition and the day have a significant effect (**** $p < 0.0001$).

VI. Discussion of the results

The evolution in the cell number during the different conditions of our experiment, except for the standard differentiation, showed that the number of the cells continued to increase during the differentiation process in all the conditions including those receiving or not a pulse (Fig. 4). In a standard differentiation the number of cells increased during the first two weeks then it was stabilized as it was reported also in article 3. The ALP is an osteodifferentiation marker and its expression increase

demonstrates that the MSCs are on the osteogenic route. A normal cycle of internal ALP activity included an increase on day 8 and a peak on day 15, then a decrease as it was observed in the standard differentiation (Fig. 5) and in other studies (Quarles et al. 1992, Birmingham et al. 2012, Frohbergh et al. 2012). However in all the other conditions, the internal ALP activity continued to increase during all the differentiation process. The cell number and the ALP activity had the same tendency: a tendency to increase continuously during the differentiation in all the conditions where the medium was daily changed, unlike the standard differentiation where the cell number was stabilized at the end of the second week and the ALP activity reached its maximum.

As shown in figure 7, no Ca^{2+} deposit was observed even at day 29 of osteodifferentiation in all the conditions where the medium was changed every day. The absence of Ca^{2+} deposits on cells supposedly being differentiated in osteoblasts was not expected. However, in a standard differentiation, the Ca^{2+} deposits were extremely high, as they should be normally at this level of differentiation (Langenbach & Handschel 2013). These observations demonstrate that the medium change every day probably prevented the Ca^{2+} deposits to occur. This was also corroborated in figure 7; the cells let in their osteogenic medium for 2 days without changing this medium (from day 20 to day 22) exhibited Ca^{2+} deposits, and if they were left more days without medium change (from day 25 to day 29), even more Ca^{2+} deposits were observed. These mineralization problems can explain why the cell number and the ALP activity increased during all the differentiation process when the medium was changed every day; in a standard differentiation, when the Ca^{2+} deposits began to occur, the cell number stopped increasing and the ALP reached its maximal value. When the medium was changed every day (in order to apply the pulse, or not for the controls), the mineralization did not occur. This is why the cell number and the ALP activity continued to increase. During a normal osteogenic differentiation, the cells undergo first an extensive proliferation followed by the differentiation (Huang et al. 2007), and the ALP reaches an initial peak followed by a subsequent decrease (Aubin 2001, Huang et al. 2007). The more the ALP peak occurs rapidly, the more the differentiation is fast (Birmingham et al. 2012). Hence, in our conditions where the medium was changed every day, the differentiation was delayed as demonstrated by the ALP cycle which did not reach its maximal value and did not start to decrease.

However, even though the general observation was a delay in the differentiation under the conditions where the medium was changed every day, there were further differences when an electric pulse was applied daily. The application of an electric pulse in STM or STM-Ca induced a decrease in the internal ALP activity (Fig. 5). At all the days, the intracellular ALP activity was lower when a pulse of 600 V/cm was applied (except at day 29 in STM). When a pulse of 300 V/cm was applied daily, no difference in the external ALP staining was observed compared to the control (Fig. 6). However, when a 600 V/cm electric pulse was applied every day, the external ALP staining was lower at days 8, 15 and 22.

The medium change prevented the mineralization, therefore no analysis of the alizarin red staining could be done in this case. To compare the Ca^{2+} deposits, we had to evaluate them when the medium was not removed for two or four days (from day 20 to 22 and from day 25 to 29 respectively). When the cells remained 2 days with the osteogenic medium, there were less Ca^{2+} deposits in STM 300, STM 600 and STM-Ca 600. The observations with 600 V/cm corroborated the results obtained in internal and external ALP activity. The cetylperidinium chloride elution permitted to evaluate

quantitatively the Ca^{2+} deposits. As it can be seen in figure 8, when the medium was changed every day, a very little absorbance was detected in all the conditions of STM and STM-Ca. However, the absorbance was higher (reflecting higher mineralization) when the pulse medium was the MEM α . The fact that medium was not changed daily allowed to observe more relevant differences between the conditions. In STM and STM-Ca, when an electric pulse was applied, the mineralization was lower, and the more the electric field was higher (600 V/cm), the more the mineralization was smaller. After 4 days without medium change, there were little differences between the conditions of each group. However, in STM-Ca, there was always less mineralization when an electric pulse was applied. These results corroborated the previous ones: the differentiation was delayed by the application of an electric pulse and this is proportional to the electric field amplitude. Note that, when the pulse medium did not contain Ca^{2+} (the STM medium), the mineralization was always lower than when the cells were pulsed in a Ca^{2+} containing medium.

Even though there were significant differences between the conditions and the days, the Ca^{2+} oscillations did not contradict the previous results. When an electric pulse was applied, the Ca^{2+} oscillations were either higher than in the control or they were nearly equal, especially when a 600 V/cm electric pulse was applied.

VII. Conclusion

The first objective of this work was to study the effect of an electric pulse applied once a day on the progress of an osteodifferentiation. Due to many limitations caused by the electrodes and the generator and the obligation to change the medium every day, the results were not comparable to a standard differentiation. However, there was an effect of the electric pulse on the retardation of the differentiation, and the more the electric field amplitude was higher, the more the differentiation was delayed. Even though this effect was different of what we were expecting when experiment was designed, a 600 V/cm pulse for example could be used to delay a differentiation when the medium is changed every day. This effect could be useful to keep the cells in a half differentiated state for, as long as possible, and to obtain differentiated cells in 4 days only, just by keeping the osteogenic medium without change.

4.2 EXAMPLES OF ELECTRO-INDUCED CALCIUM SPIKES AND SPONTANEOUS CALCIUM OSCILLATIONS

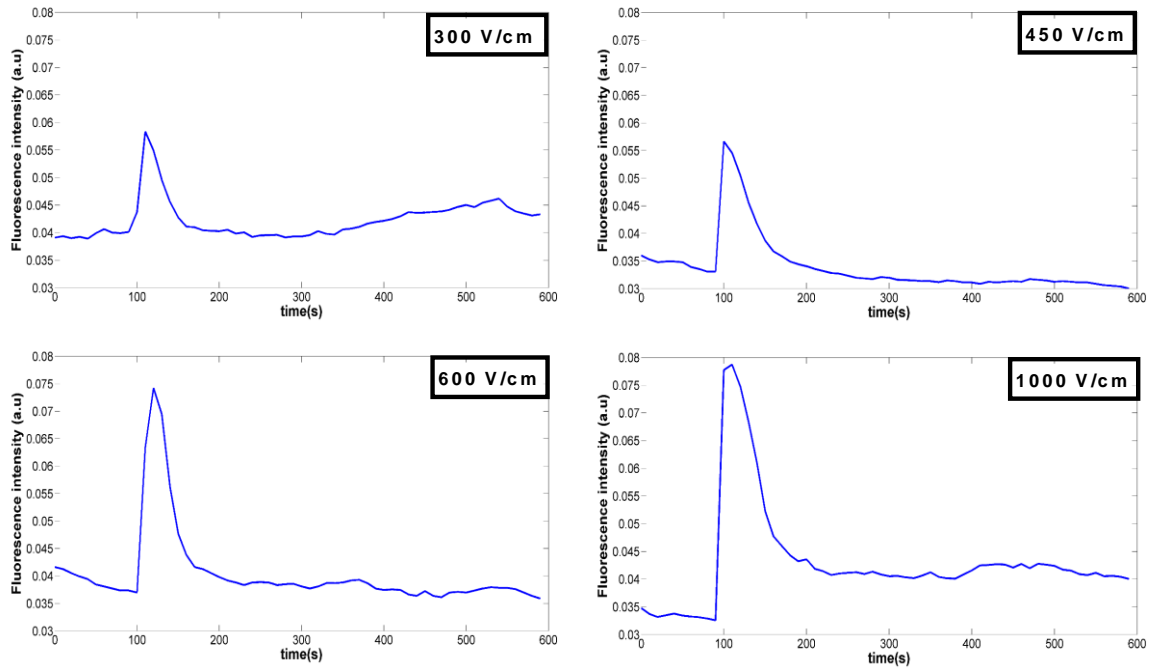
The two different cell types used in the first part of the thesis (DC-3F and haMSCs) displayed different shapes of electro-induced Ca^{2+} spikes in a medium with or without Ca^{2+} . The Ca^{2+} oscillations studied in the second and third part of the thesis showed also significant difference in shape and frequency between pluripotent haMSCs, haMSCs undergoing different differentiations and primary osteoblasts.

The aim of this part is to elucidate the different shapes of spontaneous Ca^{2+} oscillations and electro-induced Ca^{2+} spikes.

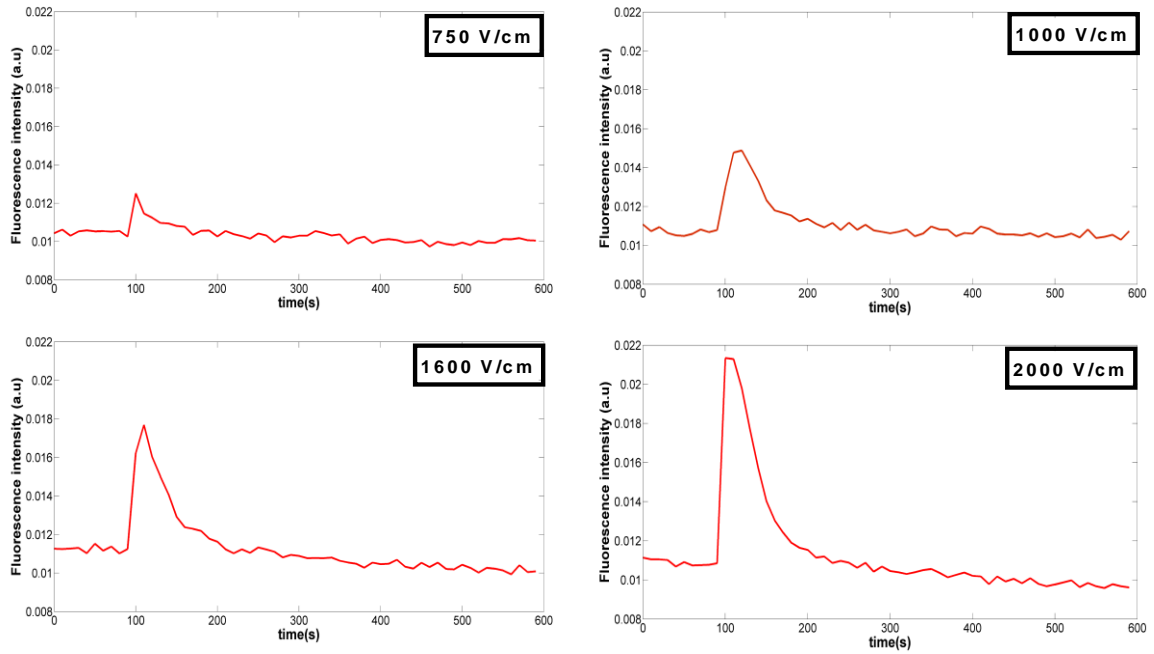
A) Examples of electro-induced Ca^{2+} spikes:

In the shapes of the Ca^{2+} spikes presented below, the scales are not the same under the different conditions, because the small spikes would not be observable using a single scale. The medium containing Ca^{2+} was the DMEM without serum. In the absence of serum, the haMSCs rapidly lose their Ca^{2+} oscillations. This is why the electro-induced Ca^{2+} spikes were mainly observed in DMEM alone. In complete DMEM, the haMSCs presented the spontaneous Ca^{2+} oscillations normally for at least 30 minutes (duration of the video recordings). In this medium, the oscillations were observed either before or before and after the delivery of the electric pulse (depending on the electric field amplitude). Under all the conditions, except for DC-3F in SMEM-EGTA, the higher the electric field strength, the larger the duration, sharpness and amplitude of the Ca^{2+} spikes. On the contrary, when a very high electric field was applied to DC-3F cells in SMEM-EGTA, the Ca^{2+} spikes were smaller due to the leakage of fluo-4 from the large pores of the PM created by the electric field. At 3000 V/cm for example, the fluorescence level of fluo-4 after the Ca^{2+} spike decreased below its basic level before the pulse. The electro-induced Ca^{2+} spike amplitude was higher in the DC-3F cells than in the haMSCs because there is a limitation in the fluo-4 content in the latter (already reported in article 1). Moreover, the Ca^{2+} spike was longer in the DC-3F cells, either in DMEM or in SMEM-EGTA, probably because the DC-3F cells do not have the same Ca^{2+} machinery as the haMSCs. DC-3F cells do not have Ca^{2+} oscillations and therefore do not possess the powerful Ca^{2+} pumps that are found in haMSCs, and that serve to rapidly restore the normal Ca^{2+} level in the cytoplasm after Ca^{2+} concentration increased during the spontaneous Ca^{2+} oscillation.

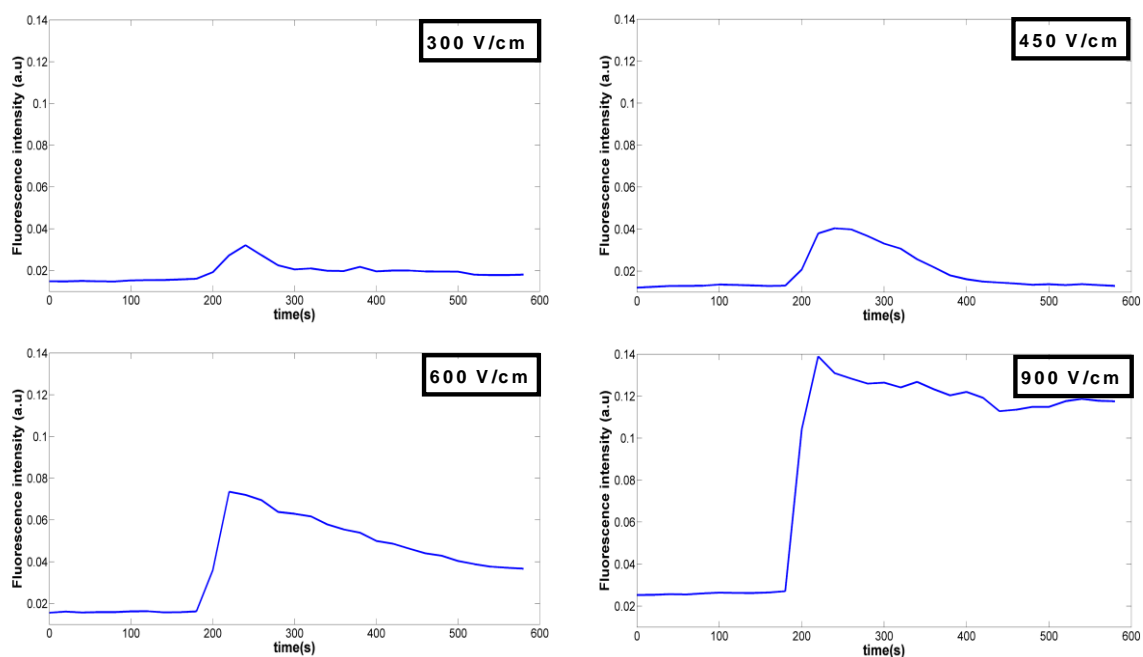
haMSC in DMEM



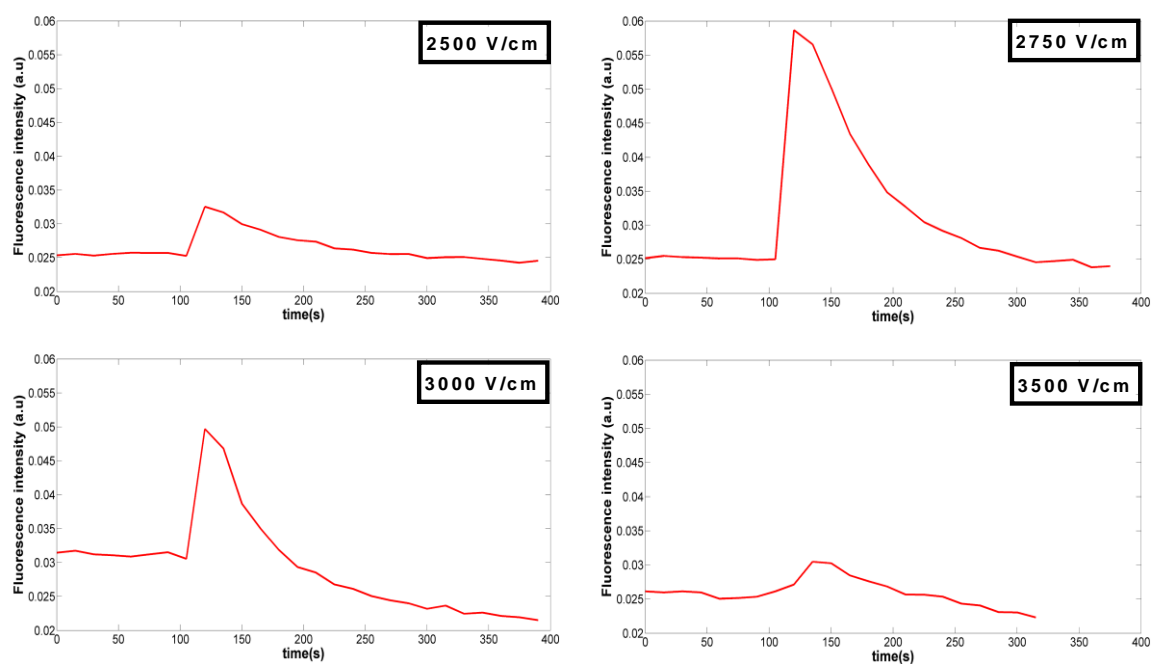
haMSC in SMEM-EGTA



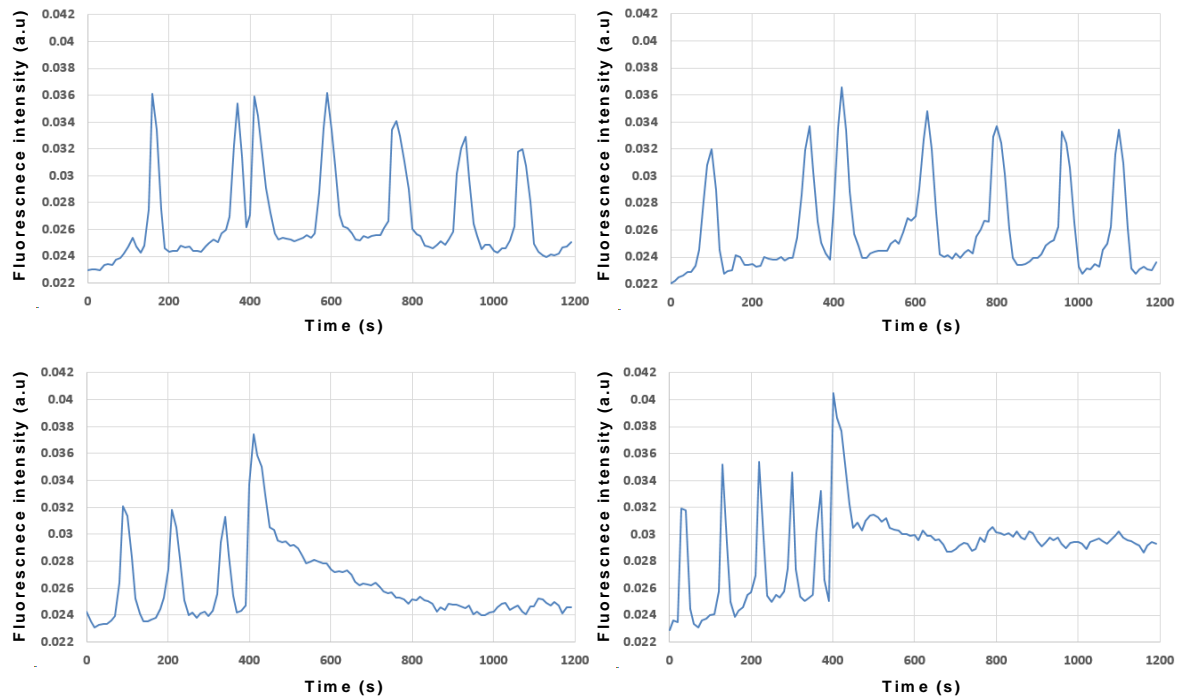
DC-3F in a DMEM



DC-3F in SMEM-EGTA



**haMSCs spontaneous oscillations in complete DMEM.
100 μ s electric pulse delivered at t = 390s**



B) Examples of spontaneous Ca^{2+} oscillations:

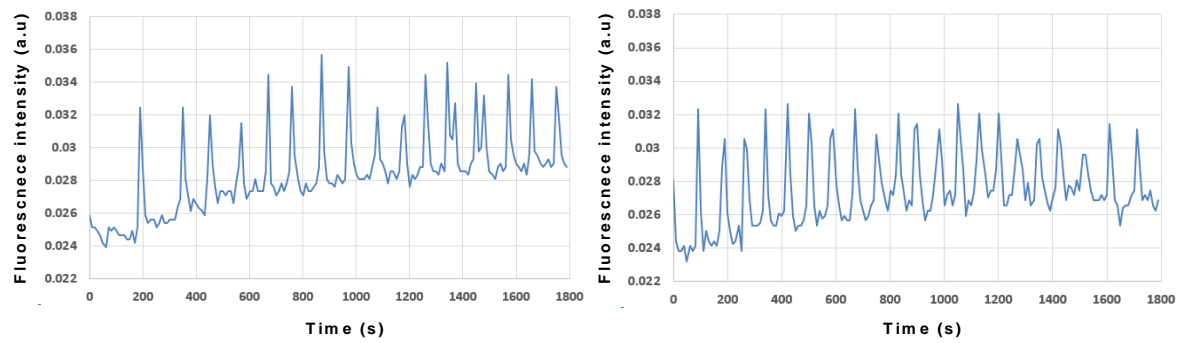
The graphs here below represent typical Ca^{2+} oscillations in different cells. Examples from haMSCs, haMSCs undergoing osteo, adipo or neurodifferentiation and primary osteoblasts are given. The scales are the same for all the conditions, except for the neuronal cells which had oscillations of high amplitude. The average number of Ca^{2+} oscillations per 30 minutes is also reported in the titles of the graphs.

Note that, when the haMSCs underwent a neuronal differentiation, they do not display independent and frequent Ca^{2+} oscillations. Actually, they display a wave propagating from cell to cell. In most of cases, this intercellular Ca^{2+} wave was observed only once in a period of 30 minutes for each well. This wave seemed to start in one or two cells (in comparison with cardiac Ca^{2+} waves, we might call them “batteries” because they initiate from their own) and propagated to the entire population. Hence, every cell presented only one single oscillation or a maximum of two in the 30 minutes observation period, and in this last case, the second oscillation had lower amplitude than the first one.

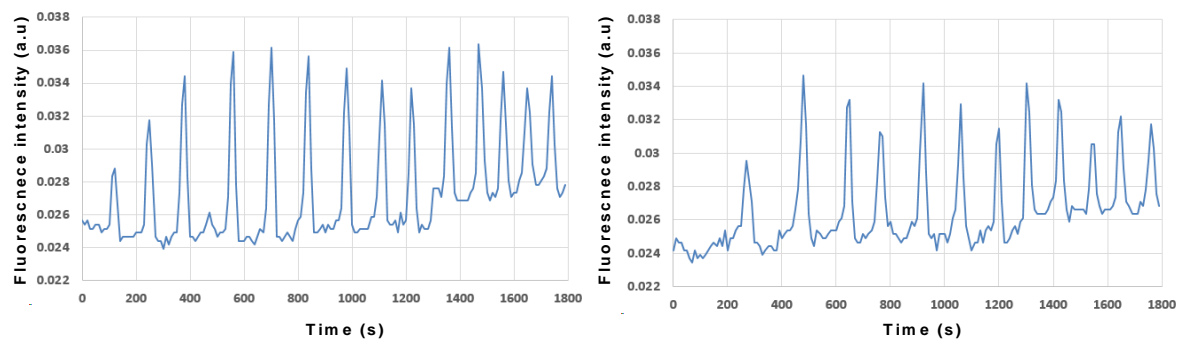
When haMSCs were in a pluripotent state and until day 15 of osteodifferentiation, each cell displayed ordered Ca^{2+} oscillations. At day 29 of osteodifferentiation, the oscillations were less ordered and started to resemble to those observed in primary osteoblasts. The Ca^{2+} oscillations frequency decreased during the osteodifferentiation.

On the contrary, during adipodifferentiation, the oscillations frequency increased and the cells presented less ordered oscillations.

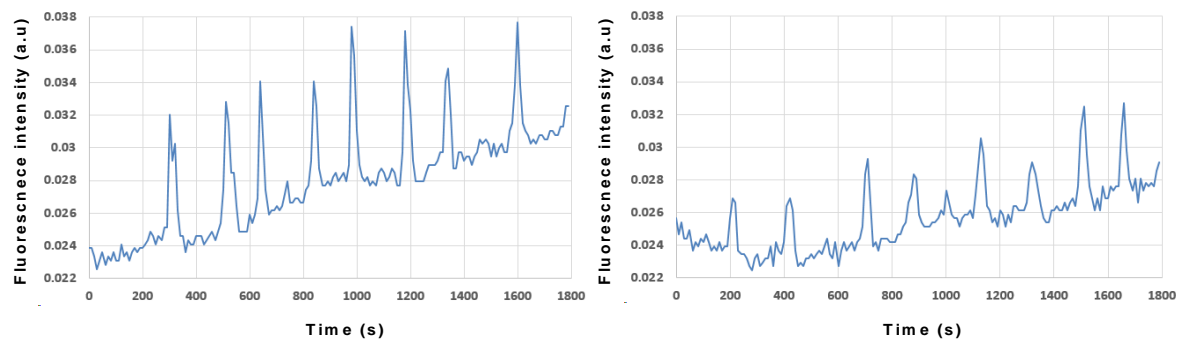
Pluripotent haMSCs (21 oscillations/30 min)



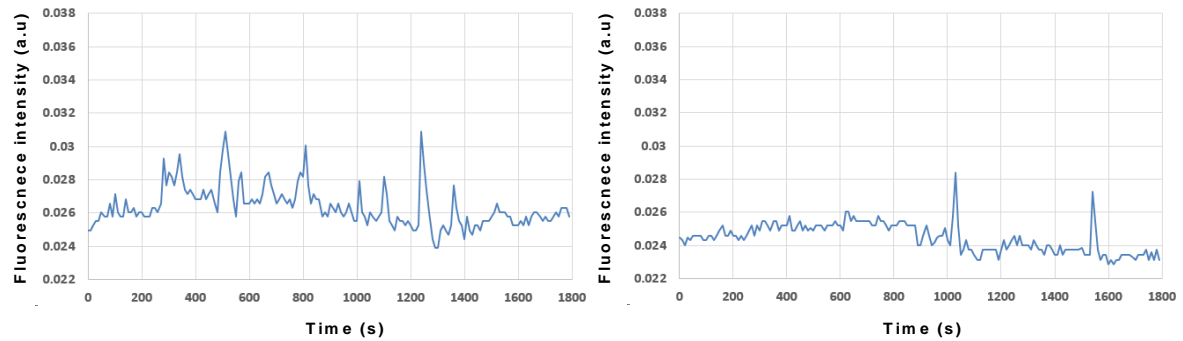
haMSCs undergoing osteodifferentiation, day 15 (16 oscillations/30 min)



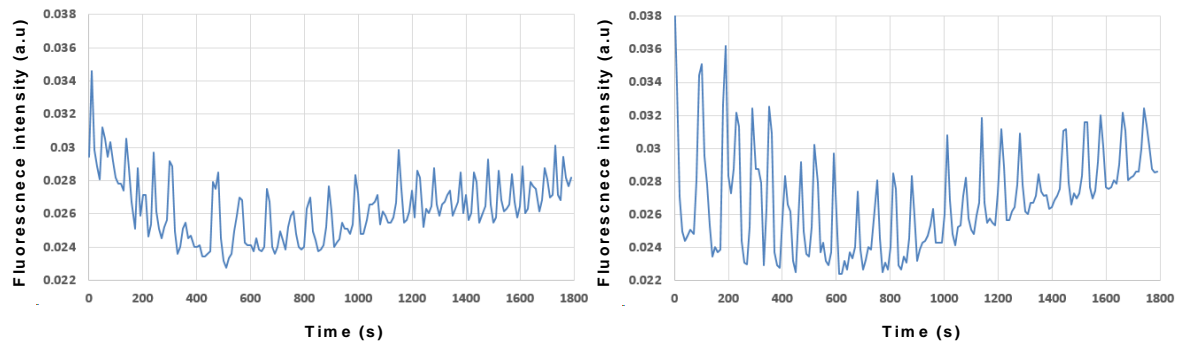
haMSCs undergoing osteodifferentiation, day 29 (12 oscillations/30 min)



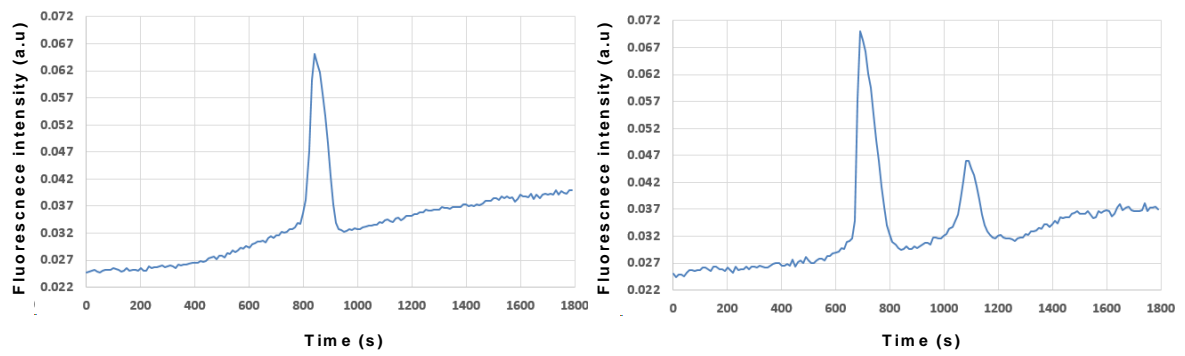
Primary osteoblasts (8 oscillations/30 min)



haMSCs undergoing adipodifferentiation, day 15 (25 oscillations/30 min)



haMSCs undergoing neurodifferentiation, day 5 (1.2 oscillations/30 min)



IV. DISCUSSION AND PERSPECTIVES

This thesis aimed to study the generation, control and consequences of electro-induced calcium (Ca^{2+}) spikes in the cells by using 100 μs pulses. A one 100 μs pulse was chosen because one pulse allows us to avoid the study of the repetition frequency of the pulses. Moreover, 100 μs is a classical pulse duration used in many electroporation applications *in vitro* and *in vivo*. In the first part of the thesis, we aimed to study the interaction of the 100 μs pulse with the PM and ER of two cell lines: the DC-3F cells and the human-adipose mesenchymal stem cells (hAMSC). The DC-3F cells are a hamster cell line whereas the hAMSC are human primary cells. Moreover, the DC-3F cells are small cells whereas the hAMSC are large ones. The origin and size difference was important for us in order to have two models of cells and to study the interaction of the electric field with their PM and ER. First, we hypothesized that even with μsPEF , there is an intracellular electric field that is permitted to flow after the electroporation of the PM and that this field could be intense enough to permeabilize the cell organelles. Interestingly, two theoretical studies of Weaver *et al.* showed that *in silico* it is possible to permeabilize the cell organelles using μsPEF (Esser *et al.* 2010, Weaver *et al.* 2012). However, no experimental study had demonstrated this effect. Thus, this was a first track to discover in the first part of the thesis and to demonstrate such an effect experimentally on living cells. The results obtained confirmed our expectations. The electro-induced Ca^{2+} spikes in the hAMSCs and DC-3F cells in a medium without Ca^{2+} demonstrated that these spikes were originated from the Ca^{2+} inner stores of the cells. We also assessed the PM and ER permeabilization thresholds in the two cell types. The difference in ER architecture and distribution led to different proportionalities between the two cell types. This first study of the thesis presents an importance on 2 levels: electrically and biologically. Electrically, the demonstration of the permeabilization of inner cellular membranes by μsPEFs was identified for the first time experimentally. This achievement allows the use of this technology by a large number of laboratories for the manipulation of not only the PM but also the organelles membranes. Biologically, the creation of Ca^{2+} spikes in the cell is a very interesting way to study the effect of the Ca^{2+} in many cellular functions. The μsPEFs present a powerful tool to modulate the Ca^{2+} level in the cell. Since a large number of laboratories are equipped with the μsPEF technology but not with the nsPEF one, which is more expensive and sophisticated, these laboratories are no more limited in their applications on the cells because they can use the μsPEF technology to manipulate the PM and organelles membranes permeability. Depending on the electric field amplitude and the medium used, the investigator can choose the Ca^{2+} spike amplitude to impose to the cell, and the origin of the Ca^{2+} spike (the extracellular medium or the ER or both). Since the Ca^{2+} constitutes a universal mode of signaling and it is implicated in nearly every cellular process, the μsPEFs can be used to control key functions in the cell such as proliferation, differentiation, senescence and apoptosis by controlling Ca^{2+} levels in a receptor-independent manner.

We used, in this first part of the thesis one electric pulse of 100 μs and two different cell types. Further investigations of the μsPEF interaction with the organelles membranes could be done on other cell types and by using many pulses or by modulating the electric field intensity, the pulse duration, the number of pulses and their repetition frequency. The optimal combination of electric pulse parameters is to be determined by the investigator depending on the cell type to be used, in order to obtain optimal efficiency outcomes with minimal cell viability loss. The ER imaging and the calculation of its dimensions with the cell diameter is of primordial importance to set the right electric parameters and to understand the results. In our case, the decorating of the ER and the segmentation of the images to reconstruct the ER geometry revealed large differences between the two cell types and demonstrated a collective electrical behavior of the ER.

In the second part of the thesis, we decided to use the same 100 μ s pulse on the haMSC to see whether this pulse can control the Ca^{2+} oscillations in the latter. The first part permitted to have an idea on the origin of the Ca^{2+} spike (whereas an entry from the external medium or an entry from the external medium and a release from the ER) according to the electric field amplitude. The Ca^{2+} is a universal mode of signaling, and it is implicated in many key cellular functions such as motility, vesicular transport, proliferation, differentiation and apoptosis (Berridge et al. 2003). The Ca^{2+} oscillations in the mesenchymal stem cells control the multipotency of these latter. The frequency of such oscillations is interpreted by the cell by different transcription factors expression (De Koninck & Schulman 1998), thus controlling the proliferation and the differentiation of the stem cells. The MSCs are very interesting candidates for cell therapy and regenerative medicine. The differentiation of the MSCs have been already performed in many laboratories in order to obtain a large palette of specialized cells such as osteoblasts, adipocytes, myoblasts, chondrocytes or neuronal cells (Pittenger et al. 1999). Different chemical factors formulas have been used for every differentiation. Few studies used the electromagnetic fields alone or combined with the chemical factors to enhance a differentiation. The electromagnetic fields that have been used include direct current of a very low electric field and a long time exposition (Sun et al. 2007) or biphasic electric current (Kim et al. 2009a). These fields either alter the membrane potential and activate VOCCs if they are large enough or do not alter the membrane potential if the electric field is too low. None of the electromagnetic fields used in the bibliography was permeabilizing the cell PM. The novelty of our study is the use of a pulsed electric field of a high intensity capable to permeabilize the cells PM or both the PM and the ER. Indeed, there is a contribution of the VOCCs due to the induced transmembrane potential, and of the SOCCs due to ER Ca^{2+} release, and consequently an activation of the CICR process. The contribution of all these mechanisms to the electroinduced Ca^{2+} spike varies depending on the electric field amplitude and hence the number and diameter of the electropores and the relative increase of Ca^{++} concentration in the cytoplasm. The Ca^{2+} spikes induced by a 100 μ s pulse showed a high capacity to modulate the Ca^{2+} oscillations in the haMSC. The advantage of such a technique is that the investigator can choose the electric field amplitude in order to obtain different outcomes: either add a further oscillation (thus increasing the frequency) or inhibit the oscillations for a time proportional to the electric field amplitude (thus decreasing their frequency), or impose to the cell Ca^{2+} oscillations of controlled frequency by applying many 100 μ s electric pulses.

The control of Ca^{2+} oscillations by a pulsed electric field can have large applications on many cell types presenting or not Ca^{2+} oscillations. In polarized pancreatic acinar cells for example, an electric pulse can control enzyme secretion or gene transcription by the creation of Ca^{2+} spikes of different strength (Thorn et al. 1993, Lee et al. 1997). If the Ca^{2+} spike is small, it will be localized in specific subcellular regions and activate digestive enzymes secretion, but if it is sufficiently large, it will spread as a wave to the entire cell and controls other cell functions. An electro-induced Ca^{2+} spike in pancreatic β cells could control ATP synthesis and insulin secretion (Tsuboi et al. 2003). Therefore, such an application could present a hope to get larger insulin quantity by pancreatic cells in order to heal diabetes. Another example is the T lymphocytes which present Ca^{2+} oscillations that play a crucial role in the activation of these cells after an antigen binding to T-cell receptor (Lewis 2003). A μ sPEF could be used to activate T lymphocytes without an antigen binding and to induce their proliferation by controlling their Ca^{2+} oscillations, which present an important application for active immunotherapy (Perica et al. 2015). In cardiomyocytes, Ca^{2+} spikes can induce an action potential (Stuyvers et al. 2000), thus a contraction. Hence, an electro-induced Ca^{2+} spike could control the cardiomyocytes excitation-

contraction frequency. Furthermore, by controlling the electric field amplitude (hence the amplitude of the Ca^{2+} spike), the action potential propagation velocity could be controlled since the velocity of Ca^{2+} waves in the heart depends on localized Ca^{2+} concentration (Kaneko et al. 2000). The excitation-contraction control by an electric pulse can also be applied on skeletal muscle. In neurons, Ca^{2+} mediates synaptic transmission (Catterall & Few 2008). A pulsed electric field could be applied to cause neurotransmitters secretion even without a physiological action potential.

All the interesting applications cited above can be applied *in vitro* as well as *in vivo*. The existence of a variety of electrodes shapes, suitable for different organs makes this possible. From the plate and needles electrodes (for the superficial organs and the skin) to expandable electrodes (for the brain), endoscopes (intraluminal) and finger electrodes (for oral and anal cavities), the application of μPEF in order to control/heal disorders *in vivo* could be possible.

The μPEF showed a high capacity to control the Ca^{2+} oscillations in the MSCs and could be a very useful tool to control the MSCs differentiation route and level (since the control of intracellular Ca^{2+} levels and oscillations have an impact on cell proliferation and differentiation) or to modulate many cellular functions related to the Ca^{2+} in different cell types. In the next part of the thesis, we aimed to study the Ca^{2+} oscillations in haMSC undergoing osteo, adipo and neurodifferentiation to evaluate, under our conditions, if there is a fingerprint of Ca^{2+} oscillations according to the differentiation type and level. When we tried to dissociate the cells in osteodifferentiation, we found a difficulty to have fully dissociated cells by using the trypsin only. Since the extracellular matrix in osteogenic differentiation is known to be rich in collagen I (Franceschi & Iyer 1992, Vater et al. 2011a), we decided to use the collagenase I in order to dissociate the cells. We observed, after the collagenase I action, that a cell layer remained in the bottom of the dish. This remaining bottom layer was sensitive to trypsin. Then, the characterization of the two types of cell layers (the upper layers – collagenase sensitive, and the lower layer – trypsin sensitive) gave some differences in the stemness markers and the Ca^{2+} oscillations. However, the cells of the two cell layers can be put separately in culture to give terminally differentiated osteoblast. This observation was new in the osteogenic differentiation since no other study had mentioned yet two types of layers. This new observation was worth to continue it until the end. The presence of two cell layers type permits to use one cell layer to follow the differentiation and another one to keep cells in differentiation in order to dissociate them later and have again many layers. The use of a layer already kept in differentiation permits to obtain mature osteoblasts in a reduced period of time.

Indeed, the time required for an osteogenic differentiation is normally long (one month) even with an optimal concentration of the differentiation chemical factors. This time of MSC differentiation could be a drawback for the cell therapy or the regenerative medicine because in these fields, a large quantity of differentiated cells is needed in a short time. Many studies tried to combine a physical factor with the classical chemical factors used for MSC differentiation in order to enhance the differentiation and to obtain differentiated cells in less time. Such physical factors may be a mechanical stimulation such as translational or rotational strain (Altman et al. 2002) or tensile strain (Ward et al. 2007), low intensity ultrasounds (Ebisawa et al. 2004), or an electromagnetic field (Sun et al. 2007). Nearly all the studies that showed a positive effect of a mechanical factor alone or its combination with chemical factors, demonstrated that there is an implication of the Ca^{2+} in the transduction of the physical signal, by changes in the Ca^{2+} oscillations frequency (Jing et al. 2014), or through the activation of voltage operated Ca^{2+} channels (VOCCs) and the increase of intracellular Ca^{2+} concentrations (Khatib et al. 2004, Petecchia et al. 2015). The last part of the thesis was to combine the electric pulse, already

used to induce cytosolic Ca^{2+} spikes from different origins and to control the haMSC Ca^{2+} oscillations, in haMSC undergoing an osteogenic differentiation. The purpose was to assess, whether by controlling the Ca^{2+} oscillations frequency and the permeability of the PM to the osteogenic factors, one 100 μs electric pulse can modulate an osteogenic differentiation. In the third part of the thesis, after the observation of the presence of several cell layers in the osteogenic differentiation, we proposed a new technique in order to obtain mature osteoblasts in 2 weeks instead of four. In this part, we tried to do the same but in an electroporation-dependent manner. However, due to the electrodes used in order to cover the whole cell surface of a dish (the Petri Pulser) we were limited by the electric field amplitude and the volume of the medium because of an electric current limitation. This limitation came from the generator used that delivers a maximum of 16 A in current. A second limitation of this study was the time consumption. The investigator had to remove the medium of the cells every day, replace it with a pulsing (non-conductive) medium, apply the pulse, then put back the osteogenic medium half an hour later, and this for tens to hundreds of wells every day. This operation took a long time and could be done only once a day by an investigator. Furthermore, the renewal of the medium every day in order to apply the pulse prevented the mineralization to occur and resulted in the fact that the cells continued to proliferate indefinitely. Due to all these limitations and to the lack of time, the experiment was done only once. However, interesting conclusions were drawn from this last part, even though the final purpose, which is the achievement of mature osteoblasts in a small period of time, was not reached. For future experiments, an adapted generator should be used, especially in term of electric current delivery. Secondly, the generator could be programmed to deliver a pulse (or many) every hour (or for a period determined by the investigator) without changing the medium. By this way, the mineralization could occur normally and the comparison of a standard differentiation (where the medium is changed every 3-4 days) could be done with the differentiation receiving one (or several) pulse(s) per day. The electric pulse could also be applied with a neurogenic or adipogenic differentiation in order to study its effect on the evolution of these latter and the time to achieve terminally differentiated cells. Finally, many combinations of pulses could be done on MSCs in their stem state in order to see if a pulse (or a set of several pulses with precise frequency and amplitude) can engage the MSCs in a route of differentiation or another.

V.DISCUSSION EN LANGUE FRANÇAISE

Durant cette thèse, nous avons visé à étudier la production, le contrôle et les conséquences de pics calciques électro-induits dans les cellules en utilisant une impulsion électrique de 100 μ s. Une impulsion de 100 μ s a été choisie car l'étude d'une impulsion nous délivre de l'étude de la fréquence des impulsions quand plusieurs impulsions seront délivrées, et de plus car 100 μ s est une durée classique utilisée dans de nombreuses applications liées à l'électroporation. Dans la première partie de la thèse, nous avons cherché à étudier l'interaction d'une impulsion 100 μ s avec la membrane plasmique (MP) et le réticulum endoplasmique (RE) de deux types de cellules: les cellules DC-3F qui sont des fibroblastes pulmonaires de hamster chinois, et les cellules souches mésenchymateuses humaines issues du tissu adipeux (haMSCs). Les cellules DC-3F sont une lignée de cellules de hamster chinois alors que les haMSCs sont des cellules primaires humaines. De plus, les cellules DC-3F sont des cellules de petite taille alors que les haMSCs sont des cellules de grande taille. La différence d'origine et de la taille était importante pour nous afin d'avoir deux modèles de cellules différents et d'étudier l'interaction du champ électrique avec leur MP et leur RE. Tout d'abord, nous avons émis l'hypothèse que, même avec les champs électriques pulsés microsecondes (μ sPEFs), il existe un champ électrique intracellulaire pendant l'application du pulse. Ce champ provient du champ externe, qui peut pénétrer dans la cellule par suite de l'électroporation de la MP. Nous avons fait aussi l'hypothèse que ce champ pourrait être suffisamment intense pour perméabiliser les organites cellulaires. Fait intéressant, deux études théoriques de Weaver *et al.* ont montré que, *in silico*, il est possible de perméabiliser les organites cellulaires en utilisant des μ sPEFs (Esser et al. 2010, Weaver et al. 2012). Cependant, aucune étude expérimentale n'a démontré cet effet. Ainsi, ce fut une première piste à découvrir dans la première partie de la thèse et de démontrer un tel effet expérimentalement sur des cellules vivantes. Les résultats obtenus ont confirmé nos attentes. Les pics calciques électro-induits dans les cellules haMSCs et DC-3F dans un milieu externe sans calcium (Ca^{2+}) démontrent que ces pics ont pour origine le calcium libéré par la perméabilisation des organites cellulaires stockant le Ca^{2+} surtout le RE. Nous avons également évalué les seuils de perméabilisation de la MP et des membranes du RE dans les deux types cellulaires. La différence dans l'architecture et la distribution du RE a abouti à des proportionnalités différentes entre les deux types de cellules. Cette première étude de la thèse présente une importance sur deux niveaux: électriquement et biologiquement. Sur le plan électrique, la démonstration de la perméabilisation des membranes cellulaires internes par les μ sPEFs a ainsi été identifiée pour la première fois expérimentalement au cours de cette thèse. Cette réalisation permet l'utilisation de cette technologie par un grand nombre de laboratoires pour le but de manipuler, non seulement la MP, mais aussi les organites cellulaires. Biologiquement, l'induction de pics calciques dans la cellule est un moyen très intéressant d'étudier l'effet du Ca^{2+} dans de nombreuses fonctions cellulaires. Les μ sPEFs présentent un outil puissant pour moduler le Ca^{2+} au niveau de la cellule. Étant donné qu'un grand nombre de laboratoires est équipé de la technologie microseconde (mais pas de la technologie nanoseconde, car étant plus coûteuse et sophistiquée), ces laboratoires ne seront plus limités dans leurs applications sur les cellules, et ils pourront utiliser la technologie μ sPEFs pour manipuler la perméabilité de la MP et les membranes internes. En fonction de l'amplitude du champ électrique et du milieu utilisé (avec ou sans Ca^{2+}), l'investigateur pourrait choisir l'amplitude du pic calcique à imposer à la cellule, et l'origine de ce pic (le milieu extracellulaire ou bien le RE ou bien les deux). Étant donné que le Ca^{2+} constitue un mode universel de signalisation et qu'il est impliqué dans presque tous les processus cellulaires, les μ sPEFs peuvent être utilisés pour contrôler des fonctions principales dans la cellule telles que la prolifération, la différenciation, l'apoptose et la sénescence. Nous avons utilisé dans cette première partie de la thèse une seule impulsion électrique de 100 μ s et deux différents types de cellules. D'autres études visant à étudier l'interaction des μ sPEFs avec les

membranes des organelles pourraient être effectuées sur d'autres types cellulaires, et en utilisant plusieurs pulses, ou en modulant l'intensité du champ électrique, la durée, le nombre et la fréquence de répétition des impulsions. La combinaison optimale des paramètres d'impulsions électriques est à déterminer par le manipulateur en fonction du type de cellule à utiliser, afin d'obtenir des résultats en matière d'efficacité optimale et avec un minimum de perte de viabilité cellulaire. L'imagerie confocale du RE et le calcul de ses dimensions avec le diamètre de la cellule est d'une importance primordiale pour définir les bons paramètres électriques et pour comprendre les résultats. Dans notre cas, la décoration du RE et la segmentation des images afin de reconstruire la géométrie du RE ont révélé de grandes différences entre les deux types de cellules utilisées et ont démontré un comportement électrique collectif du RE.

Dans la deuxième partie de la thèse, nous avons décidé d'utiliser la même impulsion de 100 μ s avec les haMSCs pour voir si cette impulsion pourrait contrôler les oscillations calciques spontanées dans ces dernières. La première partie de la thèse a permis d'avoir une idée sur l'origine d'un pic calcique (si c'est une entrée du Ca^{2+} du milieu extracellulaire ou bien une entrée du milieu extérieur et un relargage du RE) selon l'amplitude du champ électrique. Les cellules souches mésenchymateuses sont parmi les cellules souches les plus utilisées dans la thérapie cellulaire afin de restaurer la fonction d'un tissu. Les oscillations calciques dans ces cellules contrôlent leur pluripotence et leur différenciation. La fréquence de ces oscillations est interprétée par la cellule à travers l'expression de différents facteurs de transcription (Koninck & Schulman 1998), contrôlant ainsi la prolifération et la différenciation des cellules souches. La différenciation des cellules souches mésenchymateuses a déjà été effectuée dans de nombreux laboratoires afin d'obtenir une large palette de cellules spécialisées telles que les ostéoblastes, les adipocytes, les myoblastes, les chondrocytes ou les cellules neuronales (Pittenger et al. 1999). Différents cocktails de facteurs chimiques sont utilisés dans chaque cas pour induire la différenciation. Parfois, des facteurs physiques, comme les champs électromagnétiques, ont été utilisés pour favoriser une différenciation. Les champs électromagnétiques utilisés étaient une exposition de longue durée à un courant continu d'une amplitude de champ électrique très faible (Sun et al. 2007) ou bien à un courant électrique biphasique (Kim et al. 2009a). Ces champs soit modifient le potentiel de la membrane et activent les canaux Ca^{2+} voltage-dépendants (VOCCs) s'ils sont assez élevés, ou bien ne modifient pas le potentiel membranaire dans le cas où le champ électrique est trop faible. Aucun des champs électromagnétiques utilisés dans la bibliographie ne perméabilisait la MP. La nouveauté de notre étude est l'utilisation d'un champ électrique pulsé d'une haute amplitude de champ capable de perméabiliser la MP des cellules ou bien à la fois la PM et le RE. En effet, avec l'impulsion qu'on utilise, il y a aussi une contribution des VOCCs en raison du potentiel transmembranaire induit, et à cause de la libération du Ca^{2+} du RE, les canaux calciques dépendant des stores internes (SOCCs) seront aussi activés. En raison de l'entrée massive du Ca^{2+} dans le cytosol, « la libération du Ca^{2+} induite par le Ca^{2+} » (LCIC) est donc déclenchée. La contribution de tous ces mécanismes au pic calcique induit par l'impulsion varie en fonction de l'amplitude du champ électrique, et donc en fonction du nombre et du diamètre des parties perméabilisées de la membrane. Les pics calciques induits par une impulsion de 100 μ s ont montré une forte capacité à moduler les oscillations calciques dans les haMSCs. L'avantage d'une telle technique est que l'investigateur pourrait choisir l'amplitude du champ électrique afin d'obtenir des résultats différents: soit ajouter une nouvelle oscillation (augmentant ainsi la fréquence des oscillations) ou inhiber les oscillations pendant un temps d'autant plus long que l'amplitude du champ électrique est forte (diminuant ainsi leur

fréquence), ou bien d'imposer à la cellule des oscillations de fréquence contrôlée en utilisant plusieurs impulsions de 100 μ s.

Le contrôle des oscillations calciques spontanées par un champ électrique pulsé pourrait avoir plusieurs applications sur de nombreux types cellulaires présentant ou non des oscillations calciques. Dans les cellules acineuses polarisées du pancréas par exemple, une impulsion électrique permettrait de contrôler la sécrétion d'enzymes ou la transcription de gènes par la création de pics calciques d'amplitudes différentes (Thorn et al. 1993, Lee et al. 1997). Si le pic calcique est d'une faible amplitude, il sera localisé dans des régions cellulaires spécifiques et activer la sécrétion d'enzymes digestives, mais s'il est suffisamment grand, il se répandra comme une vague calcique dans la cellule entière et activera d'autres fonctions cellulaires. Un pic calcique électro-induit dans les cellules pancréatiques β pourrait contrôler la synthèse d'ATP et la sécrétion d'insuline (Tsuboi et al. 2003). Par conséquent, une telle application pourrait présenter un espoir de libérer une plus grande quantité d'insuline par les cellules pancréatiques afin de traiter le diabète. Un autre exemple sont les lymphocytes T qui présentent des oscillations calciques jouant un rôle essentiel dans l'activation de ces cellules après la liaison d'un antigène à leur récepteur (TCR) (Lewis 2003). Un pulse microseconde pourrait être utilisé pour activer les lymphocytes T sans liaison à l'antigène et induire leur prolifération en contrôlant les oscillations calciques, ce qui pourrait présenter une application importante pour l'immunothérapie active (Perica et al. 2015). Dans les cardiomyocytes, les pics calciques induits pourraient créer un potentiel d'action (Stuyvers et al. 2000), et par suite une contraction. Par conséquent, un pic calcique induit par une impulsion électrique pourrait contrôler la fréquence d'excitation et de contraction des cardiomyocytes. De plus, en contrôlant l'amplitude du champ électrique (et par suite l'amplitude du pic calcique), la vitesse de propagation du potentiel d'action pourrait être contrôlée car la vitesse des vagues calciques dans le cœur dépend de la concentration calcique locale (Kaneko et al. 2000). Le contrôle du couplage excitation-contraction par une impulsion électrique pourrait également être appliqué sur le muscle squelettique. Dans les neurones, le Ca^{2+} initie la transmission synaptique (Catterall & Few 2008). Un champ électrique pulsé pourrait être appliqué pour provoquer la sécrétion de neurotransmetteurs, même en absence d'un potentiel d'action physiologique.

Toutes les applications intéressantes mentionnées ci-dessus pourraient être appliquées *in vitro* ainsi que *in vivo*. L'existence d'une variété de formes d'électrodes, adaptées aux différents organes le permet. Des électrodes en plaques ou en aiguilles (pour les organes superficiels et la peau) à des électrodes expansibles (pour le cerveau), endoscopiques (intraluminaux) et des électrodes en doigts (pour les cavités orales et anales), l'application des μ sPEFs afin de contrôler/guérir des troubles *in vivo* pourrait être possible.

Les impulsions électriques microsecondes ont montré une grande capacité à contrôler les oscillations calciques dans les MSCs. Le contrôle des niveaux du Ca^{2+} intracellulaire et des oscillations calciques a un impact sur la prolifération et la différenciation cellulaire. Par conséquent, ces impulsions pourraient être un outil très utile pour contrôler la voie de différenciation de ces cellules ainsi que le niveau de cette différenciation ou bien pour moduler de nombreuses fonctions cellulaires en relation avec le Ca^{2+} dans différents types cellulaires. Dans la partie suivante de la thèse, nous avons cherché à étudier les oscillations calciques dans les haMSCs subissant des différenciations osseuse, adipeuse et neuronale afin d'évaluer, dans nos conditions, s'il y a une empreinte d'oscillations calciques en fonction du type de différenciation et de son niveau. Lorsque nous avons essayé de dissocier les cellules au

cours de la différenciation osseuse, nous avons trouvé une difficulté à avoir des cellules totalement dissociées en utilisant la trypsine seule. Vu que la matrice extracellulaire dans la différenciation osseuse est connue pour être riche en collagène I (Franceschi & Iyer 1992, Vater et al. 2011a), nous avons décidé d'utiliser la collagénase I afin de dissocier les cellules. Nous avons observé, après l'action de la collagénase I, une couche intacte de cellules qui sont restées au fond du puits. Cette couche inférieure restante était sensible à la trypsine. La caractérisation des deux types de couches cellulaires (les couches supérieures sensibles à la collagénase, et la couche inférieure sensible à la trypsine) a montré des différences en ce qui concerne les marqueurs de cellules souches et les oscillations calciques. Cependant, les cellules des deux couches de cellules peuvent être mises en culture séparément pour donner des ostéoblastes en différenciation terminale, les cellules des couches supérieures donnant relativement plus de dépôts calciques au bout de 15 jours par rapport aux cellules de la couche inférieure. Cette observation était nouvelle dans la différenciation osseuse des haMSC car aucune autre étude n'a encore mentionné deux types de couches aux propriétés différentes. Les nombreuses différenciations effectuées pour analyser les différentes couches dans la différenciation ostéogénique et les comparer avec l'évolution des couches dans la différenciation adipeuse et neuronale. La présence de deux types de couches permet d'utiliser une couche de cellules pour continuer la différenciation et une autre pour maintenir les cellules en différenciation afin de les dissocier plus tard et avoir de nouveau plusieurs couches. L'utilisation d'une couche déjà conservée en état de différenciation permet d'obtenir des ostéoblastes matures dans une période de temps relativement réduite.

En effet, le temps requis pour une différenciation osseuse est normalement long (un mois), même avec une concentration optimale des facteurs chimiques de différenciation. Cette période de différenciation des MSCs pourrait être un inconvénient pour la thérapie cellulaire ou la médecine régénérative, car dans ces domaines, une grande quantité de cellules différenciées peut être nécessaire dans un court laps de temps. Peu d'études ont tenté de combiner un facteur physique avec les facteurs chimiques classiques utilisés pour la différenciation des MSCs afin d'améliorer cette différenciation et pour obtenir des cellules différenciées en moins de temps. Ces facteurs physiques peuvent être une stimulation mécanique, comme une tension translationnelle ou rotationnelle (Altman et al. 2002), une traction (Ward et al. 2007), des ultrasons de faible intensité (Ebisawa et al. 2004), ou un champ électromagnétique (Sun et al. 2007). Presque toutes les études qui ont montré un effet positif d'un facteur mécanique que ce soit seul ou en combinaison avec des facteurs chimiques, ont démontré qu'il existe une implication du Ca^{2+} dans la transduction du signal physique, par des changements dans la fréquence des oscillations calciques (Jing et al. 2014), ou par l'activation des VOCCs et l'augmentation de la concentration du Ca^{2+} intracellulaire (Khatib et al. 2004, Petecchia et al. 2015). La dernière partie de la thèse consistait à combiner l'impulsion électrique, déjà utilisé pour induire des pics calciques cytosoliques de différentes origines et pour contrôler les oscillations calciques dans les haMSCs, avec des haMSCs en voie de différenciation osseuse. Le but était d'investiguer si, en contrôlant la fréquence des oscillations calciques et la perméabilité de la MP aux facteurs ostéogéniques, une impulsion électrique de 100 μs appliquée une fois par jour pourrait moduler une différenciation osseuse. Dans la troisième partie de la thèse, après l'observation de la présence de plusieurs couches de cellules dans la différenciation osseuse, nous avons proposé une nouvelle technique non basée sur l'électroporation, afin d'obtenir des ostéoblastes matures en moins de temps que la normale. Dans cette quatrième et dernière partie, nous avons essayé de faire la même chose, mais d'une manière électroporation-dépendante. Cependant, en raison des électrodes utilisées

pour couvrir la totalité de la surface cellulaire d'un puits (le petri pulser TM), il a fallu faire face à une limitation de l'amplitude du champ électrique applicable et du volume du milieu traitable en raison d'une limitation en courant électrique. Cette limitation était due au générateur utilisé qui offre un maximum de 16 A en courant. Une deuxième limite de cette étude était la consommation de temps. Il fallait enlever le milieu des cellules chaque jour, le remplacer par un milieu (non-conducteur) afin d'appliquer l'impulsion électrique, puis remettre le milieu ostéogénique une demi-heure plus tard, et cela pour des dizaines à une centaine de puits tous les jours. Cette opération a pris beaucoup de temps et ne pourrait se faire qu'une seule fois par jour par une personne. En outre, le renouvellement du milieu tous les jours afin d'appliquer l'impulsion a empêché la minéralisation de se produire et a entraîné le fait que les cellules ont continué à proliférer indéfiniment. En raison de toutes ces limitations, l'expérience a été effectuée une seule fois. Cependant, des conclusions intéressantes ont été tirées de cette dernière partie, même si le but final, qui est l'obtention d'ostéoblastes matures dans une petite période de temps, n'a pas été atteint. Pour les expériences futures, un générateur adapté doit être utilisé, en particulier en termes de livraison de courant électrique. De plus, le générateur pourrait être programmé pour délivrer une impulsion (ou plusieurs) toutes les heures (ou pendant une période déterminée par l'investigateur) sans changer le milieu. De cette manière, la minéralisation devrait pouvoir se produire normalement, et la comparaison d'une différenciation normale (où le milieu est changé tous les 3-4 jours) pourrait être faite avec la différenciation qui reçoit une (ou plusieurs) impulsion(s) électriques par jour. L'impulsion électrique pourrait également être appliquée avec une différenciation neuronale ou adipeuse afin d'étudier son effet sur l'évolution de celles-ci et le temps pour atteindre des cellules différenciées. Enfin, de nombreuses combinaisons d'impulsions pourraient être faites sur des MSCs dans leur état souche afin de voir si une impulsion (ou un ensemble de plusieurs impulsions avec une fréquence et une amplitude précises) pourraient engager les MSCs dans une voie de différenciation ou une autre.

VI. REFERENCES

- Abidor IG, Arakelyan VB, Chernomordik LV, Chizmadzhev YA, Pastushenko VF and Tarasevich MR** 1979 246 - Electric breakdown of bilayer lipid membranes I. The main experimental facts and their qualitative discussion. *Bioelectrochemistry and Bioenergetics* 6: 37–52.
- Aksu AE, Rubin JP, Dudas JR and Marra KG** 2008 Role of gender and anatomical region on induction of osteogenic differentiation of human adipose-derived stem cells. *Annals of Plastic Surgery* 60: 306–322.
- Alberts B, Bray D, Hopkin K, Johnson AD, Johnson A, Lewis J, Raff M, Roberts K and Walter P** 2009 Essential Cell Biology, 3rd edition.. Garland Science
- Alberts B, Johnson A, Lewis J, Morgan D, Raff M, Roberts K and Walter P** 2014 Molecular Biology of the Cell, Sixth Edition. Garland Science
- Alberts B, Johnson A, Lewis J, Raff M, Roberts K and Walter P** 2002a Molecular Biology of the Cell, 4th edition.. Garland Science
- Alberts B, Johnson A, Lewis J, Raff M, Roberts K and Walter P** 2002b Membrane Proteins
- Aldridge A, Kouroupis D, Churchman S, English A, Ingham E and Jones E** 2013 Assay validation for the assessment of adipogenesis of multipotential stromal cells—a direct comparison of four different methods. *Cytotherapy* 15: 89–101.
- Allbritton NL and Meyer T** 1993 Localized calcium spikes and propagating calcium waves. *Cell Calcium* 14: 691–697.
- Almeida PFF** 2009 Thermodynamics of lipid interactions in complex bilayers. *Biochimica Et Biophysica Acta* 1788: 72–85.
- Al-Sakere B, André F, Bernat C, Connault E, Opolon P, Davalos RV, Rubinsky B and Mir LM** 2007 Tumor ablation with irreversible electroporation. *PLoS One* 2: e1135.
- Altman GH, Horan RL, Martin I, Farhadi J, Stark PRH, Volloch V, Richmond JC, Vunjak-Novakovic G and Kaplan DL** 2002 Cell differentiation by mechanical stress. *FASEB journal: official publication of the Federation of American Societies for Experimental Biology* 16: 270–272.
- Andrae J, Gallini R and Betsholtz C** 2008 Role of platelet-derived growth factors in physiology and medicine. *Genes & Development* 22: 1276–1312.
- André FM, Gehl J, Sersa G, Prétat V, Hojman P, Eriksen J, Golzio M, Cemazar M, Pavselj N, Rols M-P, Miklavcic D, Neumann E, Teissié J and Mir LM** 2008a Efficiency of high- and low-voltage pulse combinations for gene electrotransfer in muscle, liver, tumor, and skin. *Human Gene Therapy* 19: 1261–1271.
- André FM, Gehl J, Sersa G, Prétat V, Hojman P, Eriksen J, Golzio M, Cemazar M, Pavselj N, Rols M-P, Miklavcic D, Neumann E, Teissié J and Mir LM** 2008b Efficiency of high- and low-voltage pulse combinations for gene electrotransfer in muscle, liver, tumor, and skin. *Human Gene Therapy* 19: 1261–1271.
- Artman M, Ichikawa H, Avkiran M and Coetzee WA** 1995 Na⁺/Ca²⁺ exchange current density in cardiac myocytes from rabbits and guinea pigs during postnatal development. *The American Journal of Physiology* 268: H1714-1722.
- Asavasanti S, Ristenpart W, Stroeve P and Barrett DM** 2011 Permeabilization of plant tissues by monopolar pulsed electric fields: effect of frequency. *Journal of Food Science* 76: E98-111.
- Ashby MC and Tepikin AV** 2001 ER calcium and the functions of intracellular organelles. *Seminars in Cell & Developmental Biology* 12: 11–17.
- Ashton Acton** 2012 Issues in Life Sciences: Muscle, Membrane, and General Microbiology: 2011 Edition. ScholarlyEditions
- Aubin JE** 1998 Bone stem cells. *Journal of Cellular Biochemistry. Supplement* 30–31: 73–82.

- Aubin JE** 2001 Regulation of osteoblast formation and function. *Reviews in Endocrine & Metabolic Disorders* 2: 81–94.
- Bae JH, Park J-W and Kwon TK** 2003 Ruthenium red, inhibitor of mitochondrial Ca^{2+} uniporter, inhibits curcumin-induced apoptosis via the prevention of intracellular Ca^{2+} depletion and cytochrome c release. *Biochemical and Biophysical Research Communications* 303: 1073–1079.
- Baird GS, Zacharias DA and Tsien RY** 1999 Circular permutation and receptor insertion within green fluorescent proteins. *Proceedings of the National Academy of Sciences of the United States of America* 96: 11241–11246.
- Beebe SJ, Fox PM, Rec LJ, Somers K, Stark RH and Schoenbach KH** 2002 Nanosecond pulsed electric field (nsPEF) effects on cells and tissues: apoptosis induction and tumor growth inhibition. *IEEE Transactions on Plasma Science* 30: 286–292.
- Beebe SJ, Fox PM, Rec LJ, Willis ELK and Schoenbach KH** 2003 Nanosecond, high-intensity pulsed electric fields induce apoptosis in human cells. *FASEB journal: official publication of the Federation of American Societies for Experimental Biology* 17: 1493–1495.
- Belehradek J, Orlowski S, Poddevin B, Paoletti C and Mir LM** 1991 Electrochemotherapy of spontaneous mammary tumours in mice. *European Journal of Cancer (Oxford, England: 1990)* 27: 73–76.
- Bennett J and Weeds A** 1986 Calcium and the cytoskeleton. *British Medical Bulletin* 42: 385–390.
- Benz R and Zimmermann U** 1980 Pulse-length dependence of the electrical breakdown in lipid bilayer membranes. *Biochimica Et Biophysica Acta* 597: 637–642.
- Berg JM, Tymoczko JL and Stryer L** 2002a Lipids and Many Membrane Proteins Diffuse Rapidly in the Plane of the Membrane
- Berg JM, Tymoczko JL and Stryer L** 2002b There Are Three Common Types of Membrane Lipids
- Berridge MJ** 1990 Calcium oscillations. *The Journal of Biological Chemistry* 265: 9583–9586.
- Berridge MJ** 1997a Elementary and global aspects of calcium signalling. *The Journal of Physiology* 499 (Pt 2): 291–306.
- Berridge MJ** 1997b Elementary and global aspects of calcium signalling.. *The Journal of Physiology* 499: 291–306.
- Berridge MJ, Bootman MD and Roderick HL** 2003 Calcium: Calcium signalling: dynamics, homeostasis and remodelling. *Nature Reviews Molecular Cell Biology* 4: 517–529.
- Berridge MJ, Lipp P and Bootman MD** 2000 The versatility and universality of calcium signalling. *Nature Reviews. Molecular Cell Biology* 1: 11–21.
- Bers DM** 2002 Cardiac excitation–contraction coupling. *Nature* 415: 198–205.
- Bibb MJ, Ward JM and Hopwood DA** 1978 Transformation of plasmid DNA into *Streptomyces* at high frequency. *Nature* 274: 398–400.
- Binggeli R and Weinstein RC** 1986 Membrane potentials and sodium channels: hypotheses for growth regulation and cancer formation based on changes in sodium channels and gap junctions. *Journal of Theoretical Biology* 123: 377–401.
- Bird GS, Hwang S-Y, Smyth JT, Fukushima M, Boyles RR and Putney JW** 2009 STIM1 is a calcium sensor specialized for digital signaling. *Current biology: CB* 19: 1724–1729.
- Birmingham E, Niebur GL, McHugh PE, Shaw G, Barry FP and McNamara LM** 2012 Osteogenic differentiation of mesenchymal stem cells is regulated by osteocyte and osteoblast cells in a simplified bone niche. *European Cells & Materials* 23: 13–27.

- Black IB and Woodbury D** 2001 Adult Rat and Human Bone Marrow Stromal Stem Cells Differentiate into Neurons. *Blood Cells, Molecules, and Diseases* 27: 632–636.
- Bootman MD and Berridge MJ** 1996 Subcellular Ca²⁺ signals underlying waves and graded responses in HeLa cells. *Current biology: CB* 6: 855–865.
- Bouzzara H and Vorobiev E** 2000 Beet juice extraction by pressing and pulsed electric fields.. *International Sugar Journal* 102: 194–200.
- Brandman O, Liou J, Park WS and Meyer T** 2007 STIM2 is a feedback regulator that stabilizes basal cytosolic and endoplasmic reticulum Ca²⁺ levels. *Cell* 131: 1327–1339.
- Brenner R, Pérez GJ, Bonev AD, Eckman DM, Kosek JC, Wiler SW, Patterson AJ, Nelson MT and Aldrich RW** 2000 Vasoregulation by the beta1 subunit of the calcium-activated potassium channel. *Nature* 407: 870–876.
- Breton M and Mir LM** 2012 Microsecond and nanosecond electric pulses in cancer treatments. *Bioelectromagnetics* 33: 106–123.
- Breton M, Silve A and Mir LM** 2016 Cell electropulsation Induces Phospholipid Oxidation: the Membrane Impermeability Rupture Model Reconciles Electroporation and Electropermeabilization at the Molecular Level. *Submitted*
- Brigger I, Morizet J, Aubert G, Chacun H, Terrier-Lacombe M-J, Couvreur P and Vassal G** 2002 Poly(ethylene glycol)-coated hexadecylcyanoacrylate nanospheres display a combined effect for brain tumor targeting. *The Journal of Pharmacology and Experimental Therapeutics* 303: 928–936.
- Brighton CT, Wang W, Seldes R, Zhang G and Pollack SR** 2001 Signal transduction in electrically stimulated bone cells. *The Journal of Bone and Joint Surgery. American Volume* 83–A: 1514–1523.
- Brini M and Carafoli E** 2011 The Plasma Membrane Ca²⁺ ATPase and the Plasma Membrane Sodium Calcium Exchanger Cooperate in the Regulation of Cell Calcium. *Cold Spring Harbor Perspectives in Biology* 3: a004168.
- van den Brink-van der Laan E, Antoinette Killian J and de Kruijff B** 2004 Nonbilayer lipids affect peripheral and integral membrane proteins via changes in the lateral pressure profile. *Biochimica et Biophysica Acta (BBA) - Biomembranes* 1666: 275–288.
- Bround MJ, Wambolt R, Luciani DS, Kulpa JE, Rodrigues B, Brownsey RW, Allard MF and Johnson JD** 2013 Cardiomyocyte ATP production, metabolic flexibility, and survival require calcium flux through cardiac ryanodine receptors in vivo. *The Journal of Biological Chemistry* 288: 18975–18986.
- Bruder SP, Jaiswal N and Haynesworth SE** 1997 Growth kinetics, self-renewal, and the osteogenic potential of purified human mesenchymal stem cells during extensive subcultivation and following cryopreservation. *Journal of Cellular Biochemistry* 64: 278–294.
- Burdon T, Smith A and Savatier P** 2002 Signalling, cell cycle and pluripotency in embryonic stem cells. *Trends in Cell Biology* 12: 432–438.
- Burgain-Chain A and Scherm D** 2013 DNA Electrotransfer: An Effective Tool for Gene Therapy. In Martin F (ed.) *Gene Therapy - Tools and Potential Applications* p.. InTech
- Burnstock G** 2006 Historical review: ATP as a neurotransmitter. *Trends in Pharmacological Sciences* 27: 166–176.
- Cahalan MD, Wulff H and Chandy KG** 2001 Molecular properties and physiological roles of ion channels in the immune system. *Journal of Clinical Immunology* 21: 235–252.

- Callamaras N, Marchant JS, Sun XP and Parker I** 1998 Activation and co-ordination of InsP3-mediated elementary Ca^{2+} events during global Ca^{2+} signals in *Xenopus* oocytes. *The Journal of Physiology* 509 (Pt 1): 81–91.
- Calvet CY, Famin D, André FM and Mir LM** 2014a Electrochemotherapy with bleomycin induces hallmarks of immunogenic cell death in murine colon cancer cells. *Oncoimmunology* 3
- Calvet CY, Thalmensi J, Liard C, Pliquet E, Bestetti T, Huet T, Langlade-Demoyen P and Mir LM** 2014b Optimization of a gene electrotransfer procedure for efficient intradermal immunization with an hTERT-based DNA vaccine in mice. *Molecular Therapy. Methods & Clinical Development* 1: 14045.
- Campbell JBR Lisa A Urry, Michael L Ca Neil A** (n.d.) Biology, 8th Edition by Neil A. Campbell, Jane B. Reece, Lisa A. Urry, Michael L. Ca (2008) Hardcover, **8th edition**.. Pearson Benjamin Cummings
- Campbell NA and Reece JB** 2007 Biology: International Edition, **8th edition**.. Pearson
- Canut H, Carrasco A, Rossignol M and Ranjeva R** 1993 Is vacuole the richest store of IP3-mobilizable calcium in plant cells?. *Plant Science* 90: 135–143.
- Cao Z, Umek RM and McKnight SL** 1991 Regulated expression of three C/EBP isoforms during adipose conversion of 3T3-L1 cells. *Genes & Development* 5: 1538–1552.
- Capes Em, Loaiza R and Valdivia HH** 2011 Ryanodine receptors. *Skeletal Muscle* 1: 18.
- Caplan AI** 1991 Mesenchymal stem cells. *Journal of Orthopaedic Research: Official Publication of the Orthopaedic Research Society* 9: 641–650.
- Caplan AI and Bruder SP** 2001 Mesenchymal stem cells: building blocks for molecular medicine in the 21st century. *Trends in Molecular Medicine* 7: 259–264.
- Carafoli E, Santella L, Branca D and Brini M** 2001 Generation, control, and processing of cellular calcium signals. *Critical Reviews in Biochemistry and Molecular Biology* 36: 107–260.
- Caride AJ, Filoteo AG, Penheiter AR, Pászty K, Enyedi A and Penniston JT** 2001 Delayed activation of the plasma membrane calcium pump by a sudden increase in Ca^{2+} : fast pumps reside in fast cells. *Cell Calcium* 30: 49–57.
- Catterall WA** 2011 Voltage-Gated Calcium Channels. *Cold Spring Harbor Perspectives in Biology* 3
- Catterall WA and Few AP** 2008 Calcium channel regulation and presynaptic plasticity. *Neuron* 59: 882–901.
- Celsi F, Pizzo P, Brini M, Leo S, Fotino C, Pinton P and Rizzuto R** 2009 Mitochondria, calcium and cell death: A deadly triad in neurodegeneration. *Biochimica et biophysica acta* 1787: 335–344.
- Cemazar M, Parkins CS, Holder AL, Chaplin DJ, Tozer GM and Sersa G** 2001 Electroporation of human microvascular endothelial cells: evidence for an anti-vascular mechanism of electrochemotherapy. *British Journal of Cancer* 84: 565–570.
- Cha J, Zhang J, Gurbani S, Cheon GW, Li M and Kang JU** 2013 Gene transfection efficacy assessment of human cervical cancer cells using dual-mode fluorescence microendoscopy. *Biomedical Optics Express* 4: 151–159.
- Chang S and Cohen SN** 1979 High frequency transformation of *Bacillus subtilis* protoplasts by plasmid DNA. *Molecular and General Genetics MGG* 168: 111–115.
- Chatton JY, Liu H and Stucki JW** 1995 Simultaneous measurements of Ca^{2+} in the intracellular stores and the cytosol of hepatocytes during hormone-induced Ca^{2+} oscillations. *FEBS letters* 368: 165–168.
- Chen N, Schoenbach KH, Kolb JF, James Swanson R, Garner AL, Yang J, Joshi RP and Beebe SJ** 2004 Leukemic cell intracellular responses to nanosecond electric fields. *Biochemical and Biophysical Research Communications* 317: 421–427.

- Cheng H, Lederer MR, Lederer WJ and Cannell MB** 1996 Calcium sparks and $[Ca^{2+}]_i$ waves in cardiac myocytes. *The American Journal of Physiology* 270: C148-159.
- Cho MR** 2002 A review of electrocoupling mechanisms mediating facilitated wound healing. *IEEE Transactions on Plasma Science* 30: 1504–1515.
- Choi JW, Choi BH, Park S-H, Pai KS, Li TZ, Min B-H and Park SR** 2013 Mechanical stimulation by ultrasound enhances chondrogenic differentiation of mesenchymal stem cells in a fibrin-hyaluronic acid hydrogel. *Artificial Organs* 37: 648–655.
- Claude B and Justin T** 1983 Homokaryon production by electrofusion: A convenient way to produce a large number of viable mammalian fused cells. *Biochemical and Biophysical Research Communications* 114: 663–669.
- Cole KS** 1937 Electric impedance of marine egg membranes. *Transactions of the Faraday Society* 33: 966–972.
- Cone CD and Tongier M** 1971 Control of somatic cell mitosis by simulated changes in the transmembrane potential level. *Oncology* 25: 168–182.
- Cone, Jr. CD** 1970 Variation of the Transmembrane Potential Level as a Basic Mechanism of Mitosis Control. *Oncology* 24: 438–470.
- Cooper GM** 2000a Cell Membranes
- Cooper GM** 2000b The Cell, **2nd edition**.. Sinauer Associates
- Cooper RA** 1978 Influence of increased membrane cholesterol on membrane fluidity and cell function in human red blood cells. *Journal of Supramolecular Structure* 8: 413–430.
- Coster HG and Simmermann U** 1975 The mechanism of electrical breakdown in the membranes of Valonai utricularis. *The Journal of Membrane Biology* 22: 73–90.
- Coustets M, Al-Karablieh N, Thomsen C and Teissié J** 2013 Flow process for electroextraction of total proteins from microalgae. *The Journal of Membrane Biology* 246: 751–760.
- Coutifarís C, Kao LC, Sehdev HM, Chin U, Babalola GO, Blaschuk OW and Strauss JF** 1991 E-cadherin expression during the differentiation of human trophoblasts. *Development (Cambridge, England)* 113: 767–777.
- Crowley JM** 1973 Electrical Breakdown of Bimolecular Lipid Membranes as an Electromechanical Instability. *Biophysical Journal* 13: 711–724.
- Csala M, Bánhegyi G and Benedetti A** 2006a Endoplasmic reticulum: A metabolic compartment. *FEBS Letters* 580: 2160–2165.
- Csala M, Bánhegyi G and Benedetti A** 2006b Endoplasmic reticulum: a metabolic compartment. *FEBS letters* 580: 2160–2165.
- Curie T, Rogers KL, Colasante C and Brûlet P** 2007 Red-shifted aequorin-based bioluminescent reporters for in vivo imaging of Ca^{2+} signaling. *Molecular Imaging* 6: 30–42.
- Cyranoski D** 2008 Stem cells: 5 things to know before jumping on the iPS bandwagon. *Nature News* 452: 406–408.
- Daleke DL** 2007 Phospholipid Flippases. *Journal of Biological Chemistry* 282: 821–825.
- Danielli JF and Davson H** 1935 A contribution to the theory of permeability of thin films. *Journal of Cellular and Comparative Physiology* 5: 495–508.
- Danielsen EM** 1995 Involvement of detergent-insoluble complexes in the intracellular transport of intestinal brush border enzymes. *Biochemistry* 34: 1596–1605.
- Datta N, Pham QP, Sharma U, Sikavitsas VI, Jansen JA and Mikos AG** 2006 In vitro generated extracellular matrix and fluid shear stress synergistically enhance 3D osteoblastic

- differentiation. *Proceedings of the National Academy of Sciences of the United States of America* 103: 2488–2493.
- Davalos RV, Mir ILM and Rubinsky B** 2005 Tissue ablation with irreversible electroporation. *Annals of Biomedical Engineering* 33: 223–231.
- Dawson SP, Keizer J and Pearson JE** 1999 Fire-diffuse-fire model of dynamics of intracellular calcium waves. *Proceedings of the National Academy of Sciences of the United States of America* 96: 6060–6063.
- Dayel MJ, Hom EF and Verkman AS** 1999 Diffusion of green fluorescent protein in the aqueous-phase lumen of endoplasmic reticulum. *Biophysical Journal* 76: 2843–2851.
- De Francesco F, Tirino V, Desiderio V, Ferraro G, D'Andrea F, Giuliano M, Libondi G, Pirozzi G, De Rosa A and Papaccio G** 2009 Human CD34/CD90 ASCs are capable of growing as sphere clusters, producing high levels of VEGF and forming capillaries. *PloS One* 4: e6537.
- De Koninck P and Schulman H** 1998 Sensitivity of CaM kinase II to the frequency of Ca²⁺ oscillations. *Science (New York, N.Y.)* 279: 227–230.
- DeBruin KA and Krassowska W** 1999 Modeling electroporation in a single cell. II. Effects Of ionic concentrations.. *Biophysical Journal* 77: 1225–1233.
- Decuypere J-P, Monaco G, Missiaen L, De Smedt H, Parys JB and Bultynck G** 2011 IP₃ Receptors, Mitochondria, and Ca²⁺ Signaling: Implications for Aging. *Journal of Aging Research* 2011
- Denecke J** 2001 Plant Endoplasmic Reticulum. *eLS* p.. John Wiley & Sons, Ltd
- Deng J, Schoenbach KH, Buescher ES, Hair PS, Fox PM and Beebe SJ** 2003 The Effects of Intense Submicrosecond Electrical Pulses on Cells. *Biophysical Journal* 84: 2709–2714.
- Deng W, Obrocka M, Fischer I and Prockop DJ** 2001 In Vitro Differentiation of Human Marrow Stromal Cells into Early Progenitors of Neural Cells by Conditions That Increase Intracellular Cyclic AMP. *Biochemical and Biophysical Research Communications* 282: 148–152.
- Deshpande DA, White TA, Dogan S, Walseth TF, Panettieri RA and Kannan MS** 2005 CD38/cyclic ADP-ribose signaling: role in the regulation of calcium homeostasis in airway smooth muscle. *American Journal of Physiology - Lung Cellular and Molecular Physiology* 288: L773–L788.
- Devaux PF and Morris R** 2004 Transmembrane asymmetry and lateral domains in biological membranes. *Traffic (Copenhagen, Denmark)* 5: 241–246.
- Díaz R and Rubinsky B** 2004 A Single Cell Study on the Temperature Effects of Electroporation: 755–761.
- van Dijk A, Niessen HWM, Zandieh Doulabi B, Visser FC and van Milligen FJ** 2008 Differentiation of human adipose-derived stem cells towards cardiomyocytes is facilitated by laminin. *Cell and Tissue Research* 334: 457–467.
- Dimitrov DS** 1984 Electric field-induced breakdown of lipid bilayers and cell membranes: a thin viscoelastic film model. *The Journal of Membrane Biology* 78: 53–60.
- Dityatev A and El-Husseini A** 2006 Molecular Mechanisms of Synaptogenesis. Springer Science & Business Media
- Dolmetsch RE, Xu K and Lewis RS** 1998 Calcium oscillations increase the efficiency and specificity of gene expression. *Nature* 392: 933–936.
- Dominici M, Le Blanc K, Mueller I, Slaper-Cortenbach I, Marini F, Krause D, Deans R, Keating A, Prockop D and Horwitz E** 2006 Minimal criteria for defining multipotent mesenchymal stromal cells. The International Society for Cellular Therapy position statement. *Cytotherapy* 8: 315–317.

- Dupré DJ, Hébert TE and Jockers R** 2012 GPCR Signalling Complexes – Synthesis, Assembly, Trafficking and Specificity. Springer Science & Business Media
- Dushek O, Mueller S, Soubies S, Depoil D, Caramalho I, Coombs D and Valitutti S** 2008 Effects of Intracellular Calcium and Actin Cytoskeleton on TCR Mobility Measured by Fluorescence Recovery. *PLOS ONE* 3: e3913.
- Eberhard M and Erne P** 1991 Calcium binding to fluorescent calcium indicators: calcium green, calcium orange and calcium crimson. *Biochemical and Biophysical Research Communications* 180: 209–215.
- Ebisawa K, Hata K-I, Okada K, Kimata K, Ueda M, Torii S and Watanabe H** 2004 Ultrasound enhances transforming growth factor beta-mediated chondrocyte differentiation of human mesenchymal stem cells. *Tissue Engineering* 10: 921–929.
- El-Amin SF, Lu HH, Khan Y, Burems J, Mitchell J, Tuan RS and Laurencin CT** 2003 Extracellular matrix production by human osteoblasts cultured on biodegradable polymers applicable for tissue engineering. *Biomaterials* 24: 1213–1221.
- Ellis C** 2004 The state of GPCR research in 2004. *Nature Reviews Drug Discovery* 3: 577–626.
- Engler AJ, Sen S, Sweeney HL and Discher DE** 2006 Matrix elasticity directs stem cell lineage specification. *Cell* 126: 677–689.
- Escoffre J-M, Portet T, Wasungu L, Teissié J, Dean D and Rols M-P** 2009 What is (still not) known of the mechanism by which electroporation mediates gene transfer and expression in cells and tissues. *Molecular Biotechnology* 41: 286–295.
- Escoffre J-M and Rols M-P** 2012 Electrochemotherapy: Progress and Prospects. *Current Pharmaceutical Design* 18: 3406–3415.
- Esser AT, Smith KC, Gowrishankar TR, Vasilkoski Z and Weaver JC** 2010 Mechanisms for the intracellular manipulation of organelles by conventional electroporation. *Biophysical Journal* 98: 2506–2514.
- Europe-Finner GN and Newell PC** 1986 Inositol 1,4,5-trisphosphate and calcium stimulate actin polymerization in Dictyostelium discoideum. *Journal of Cell Science* 82: 41–51.
- Falkenburger BH, Dickson EJ and Hille B** 2013 Quantitative properties and receptor reserve of the DAG and PKC branch of G(q)-coupled receptor signaling. *The Journal of General Physiology* 141: 537–555.
- Fatherazi S, Matsa-Dunn D, Foster BL, Rutherford RB, Somerman MJ and Presland RB** 2009 Phosphate regulates osteopontin gene transcription. *Journal of Dental Research* 88: 39–44.
- Fedida D, Noble D, Rankin AC and Spindler AJ** 1987 The arrhythmogenic transient inward current *i*T₁ and related contraction in isolated guinea-pig ventricular myocytes. *The Journal of Physiology* 392: 523–542.
- Felizola SJA, Maekawa T, Nakamura Y, Satoh F, Ono Y, Kikuchi K, Aritomi S, Ikeda K, Yoshimura M, Tojo K and Sasano H** 2014 Voltage-gated calcium channels in the human adrenal and primary aldosteronism. *The Journal of Steroid Biochemistry and Molecular Biology* 144 Pt B: 410–416.
- Fewtrell C** 1993 Ca²⁺ Oscillations in Non-Excitable Cells. *Annual Review of Physiology* 55: 427–454.
- Fill M and Copello JA** 2002 Ryanodine Receptor Calcium Release Channels. *Physiological Reviews* 82: 893–922.
- Flavell SW and Greenberg ME** 2008 Signaling mechanisms linking neuronal activity to gene expression and plasticity of the nervous system. *Annual Review of Neuroscience* 31: 563–590.
- FOSKETT JK, WHITE C, CHEUNG K-H and MAK D-OD** 2007 Inositol Trisphosphate Receptor Ca²⁺ Release Channels. *Physiological reviews* 87: 593–658.

- Foundation N** 2003 Role of the Sarcoplasmic Reticulum in Smooth Muscle. John Wiley & Sons
- Franceschi RT and Iyer BS** 1992 Relationship between collagen synthesis and expression of the osteoblast phenotype in MC3T3-E1 cells. *Journal of Bone and Mineral Research: The Official Journal of the American Society for Bone and Mineral Research* 7: 235–246.
- Franceschi RT, Iyer BS and Cui Y** 1994 Effects of ascorbic acid on collagen matrix formation and osteoblast differentiation in murine MC3T3-E1 cells. *Journal of Bone and Mineral Research: The Official Journal of the American Society for Bone and Mineral Research* 9: 843–854.
- Franzini-Armstrong C and Jorgensen AO** 1994 Structure and development of E-C coupling units in skeletal muscle. *Annual Review of Physiology* 56: 509–534.
- Freeman SA, Wang MA and Weaver JC** 1994 Theory of electroporation of planar bilayer membranes: predictions of the aqueous area, change in capacitance, and pore-pore separation.. *Biophysical Journal* 67: 42–56.
- Frendo JL, Xiao G, Fuchs S, Franceschi RT, Karsenty G and Ducy P** 1998 Functional hierarchy between two OSE2 elements in the control of osteocalcin gene expression in vivo. *The Journal of Biological Chemistry* 273: 30509–30516.
- Frey W, White JA, Price RO, Blackmore PF, Joshi RP, Nuccitelli R, Beebe SJ, Schoenbach KH and Kolb JF** 2006 Plasma Membrane Voltage Changes during Nanosecond Pulsed Electric Field Exposure. *Biophysical Journal* 90: 3608–3615.
- Friedenstein AJ, Chailakhjan RK and Lalykina KS** 1970 The development of fibroblast colonies in monolayer cultures of guinea-pig bone marrow and spleen cells. *Cell and Tissue Kinetics* 3: 393–403.
- Friedenstein AJ, Chailakhyan RK, Latsinik NV, Panasyuk AF and Keiliss-Borok IV** 1974 Stromal cells responsible for transferring the microenvironment of the hemopoietic tissues. Cloning in vitro and retransplantation in vivo. *Transplantation* 17: 331–340.
- Friedenstein AJ, Petrakova KV, Kurolesova AI and Frolova GP** 1968 Heterotopic of bone marrow. Analysis of precursor cells for osteogenic and hematopoietic tissues. *Transplantation* 6: 230–247.
- Friedman MH** 2008 Principles and Models of Biological Transport. Springer Science & Business Media
- Friel DD** 1995 Calcium oscillations in neurons. *Ciba Foundation Symposium* 188: 210–223–234.
- Frohbergh ME, Katsman A, Botta GP, Lazarovici P, Schauer CL, Wegst UGK and Lelkes PI** 2012 Electrospun Hydroxyapatite-Containing Chitosan Nanofibers Crosslinked with Genipin for Bone Tissue Engineering. *Biomaterials* 33: 9167–9178.
- Frye LD and Edidin M** 1970 The Rapid Intermixing of Cell Surface Antigens After Formation of Mouse-Human Heterokaryons. *Journal of Cell Science* 7: 319–335.
- Futerman AH and Riezman H** 2005 The ins and outs of sphingolipid synthesis. *Trends in Cell Biology* 15: 312–318.
- Gaigg B, Simbeni R, Hrastnik C, Paltauf F and Daum G** 1995 Characterization of a microsomal subfraction associated with mitochondria of the yeast, *Saccharomyces cerevisiae*. Involvement in synthesis and import of phospholipids into mitochondria. *Biochimica Et Biophysica Acta* 1234: 214–220.
- Garrett RH and Grisham CM** 2000 Biochimie. De Boeck Supérieur
- Gehl J, Skovsgaard T and Mir LM** 1998 Enhancement of cytotoxicity by electroporation: an improved method for screening drugs. *Anti-Cancer Drugs* 9: 319–325.
- George J, Kuboki Y and Miyata T** 2006 Differentiation of mesenchymal stem cells into osteoblasts on honeycomb collagen scaffolds. *Biotechnology and Bioengineering* 95: 404–411.

- Gimble JM, Katz AJ and Bunnell BA** 2007 Adipose-Derived Stem Cells for Regenerative Medicine. *Circulation Research* 100: 1249–1260.
- Golzio M, Teissié J and Rols M-P** 2002 Direct visualization at the single-cell level of electrically mediated gene delivery. *Proceedings of the National Academy of Sciences* 99: 1292–1297.
- Gorter E and Grendel F** 1925 ON BIMOLECULAR LAYERS OF LIPOIDS ON THE CHROMOCYTES OF THE BLOOD. *The Journal of Experimental Medicine* 41: 439–443.
- Gowrishankar TR and Weaver JC** 2006 Electrical behavior and pore accumulation in a multicellular model for conventional and supra-electroporation. *Biochemical and biophysical research communications* 349: 643–653.
- Gregoire FM, Smas CM and Sul HS** 1998 Understanding Adipocyte Differentiation. *Physiological Reviews* 78: 783–809.
- Gregory CA, Prockop DJ and Spees JL** 2005 Non-hematopoietic bone marrow stem cells: Molecular control of expansion and differentiation. *Experimental Cell Research* 306: 330–335.
- Gronthos S, Franklin DM, Leddy HA, Robey PG, Storms RW and Gimble JM** 2001 Surface protein characterization of human adipose tissue-derived stromal cells. *Journal of Cellular Physiology* 189: 54–63.
- Gruber SJ, Cornea RL, Li J, Peterson KC, Schaaf TM, Gillispie GD, Dahl R, Zsebo KM, Robia SL and Thomas DD** 2014 Discovery of enzyme modulators via high-throughput time-resolved FRET in living cells. *Journal of biomolecular screening* 19: 215–222.
- Guo D-P, Li X-Y, Sun P, Wang Z-G, Chen X-Y, Chen Q, Fan L-M, Zhang B, Shao L-Z and Li X-R** 2004 Ultrasound/microbubble enhances foreign gene expression in ECV304 cells and murine myocardium. *Acta Biochimica Et Biophysica Sinica* 36: 824–831.
- Harris EH, Boynton JE and Gillham NW** 1994 Chloroplast ribosomes and protein synthesis.. *Microbiological Reviews* 58: 700–754.
- Hartzell C, Putzier I and Arreola J** 2005 Calcium-activated chloride channels. *Annual Review of Physiology* 67: 719–758.
- Haudenschild AK, Hsieh AH, Kapila S and Lotz JC** 2009 Pressure and distortion regulate human mesenchymal stem cell gene expression. *Annals of Biomedical Engineering* 37: 492–502.
- Hauner H, Entenmann G, Wabitsch M, Gaillard D, Ailhaud G, Negrel R and Pfeiffer EF** 1989 Promoting effect of glucocorticoids on the differentiation of human adipocyte precursor cells cultured in a chemically defined medium.. *Journal of Clinical Investigation* 84: 1663–1670.
- Hay E** 2012 *Macromolecules Regulating Growth and Development*. Elsevier
- von Heijne G** 2007 The membrane protein universe: what's out there and why bother?. *Journal of Internal Medicine* 261: 543–557.
- Hempling HG and White S** 1984 Permeability of cultured megakaryocytopoietic cells of the rat to dimethyl sulfoxide. *Cryobiology* 21: 133–143.
- Hepler PK** 2016 The Cytoskeleton and Its Regulation by Calcium and Protons. *Plant Physiology* 170: 3–22.
- Hertwig O, Campbell HJ and Cornell University. College of Veterinary Medicine. Flower-Sprecher Veterinary Library. fmo** 1895 *The cell; outlines of general anatomy and physiology* .. London, Sonnenschein and Co., New York, Macmillan and Co.
- Hibino M, Itoh H and Kinoshita K** 1993 Time courses of cell electroporation as revealed by submicrosecond imaging of transmembrane potential.. *Biophysical Journal* 64: 1789–1800.
- Hille B** 2001 *Ionic channels of excitable membranes*. Second edition. *Sinauer Associates, Inc: Sunderland, MA, USA*: 814,818.

- Hiller S, Abramson J, Mannella C, Wagner G and Zeth K** 2010 The 3D structures of VDAC represent a native conformation. *Trends in biochemical sciences* 35: 514–521.
- Hirano S, Nose A, Hatta K, Kawakami A and Takeichi M** 1987 Calcium-dependent cell-cell adhesion molecules (cadherins): subclass specificities and possible involvement of actin bundles. *The Journal of Cell Biology* 105: 2501–2510.
- Ho IC, Kim JH, Rooney JW, Spiegelman BM and Glimcher LH** 1998 A potential role for the nuclear factor of activated T cells family of transcriptional regulatory proteins in adipogenesis. *Proceedings of the National Academy of Sciences of the United States of America* 95: 15537–15541.
- Hofer AM and Machen TE** 1993 Technique for in situ measurement of calcium in intracellular inositol 1,4,5-trisphosphate-sensitive stores using the fluorescent indicator mag-fura-2. *Proceedings of the National Academy of Sciences of the United States of America* 90: 2598–2602.
- Hofmann GA, Dev SB, Nanda GS and Rabussay D** 1999 Electroporation therapy of solid tumors. *Critical Reviews in Therapeutic Drug Carrier Systems* 16: 523–569.
- Hojman P, Gissel H, Andre FM, Cournil-Henrionnet C, Eriksen J, Gehl J and Mir LM** 2008 Physiological effects of high- and low-voltage pulse combinations for gene electrotransfer in muscle. *Human Gene Therapy* 19: 1249–1260.
- Holthuis JC, Pomorski T, Riggers RJ, Sprong H and Van Meer G** 2001 The organizing potential of sphingolipids in intracellular membrane transport. *Physiological Reviews* 81: 1689–1723.
- Holthuis JCM and Menon AK** 2014 Lipid landscapes and pipelines in membrane homeostasis. *Nature* 510: 48–57.
- Hu Q, Viswanadham S, Joshi RP, Schoenbach KH, Beebe SJ and Blackmore PF** 2005 Simulations of transient membrane behavior in cells subjected to a high-intensity ultrashort electric pulse. *Physical Review E* 71
- Huang J, Hove-Madsen L and Tibbits GF** 2005 Na⁺/Ca²⁺ exchange activity in neonatal rabbit ventricular myocytes. *American Journal of Physiology. Cell Physiology* 288: C195–203.
- Huang Z, Nelson ER, Smith RL and Goodman SB** 2007a The sequential expression profiles of growth factors from osteoprogenitors [correction of osteoprogenitors] to osteoblasts in vitro. *Tissue Engineering* 13: 2311–2320.
- Huang Z, Nelson ER, Smith RL and Goodman SB** 2007b The sequential expression profiles of growth factors from osteoprogenitors [correction of osteoprogenitors] to osteoblasts in vitro. *Tissue Engineering* 13: 2311–2320.
- Ikonen E** 2008 Cellular cholesterol trafficking and compartmentalization. *Nature Reviews Molecular Cell Biology* 9: 125–138.
- Iwamoto T, Watanabe Y, Kita S and Blaustein MP** 2007 Na⁺/Ca²⁺ exchange inhibitors: a new class of calcium regulators. *Cardiovascular & Hematological Disorders Drug Targets* 7: 188–198.
- Izadpanah R, Trygg C, Patel B, Kriedt C, Dufour J, Gimble JM and Bunnell BA** 2006 Biologic properties of mesenchymal stem cells derived from bone marrow and adipose tissue. *Journal of Cellular Biochemistry* 99: 1285–1297.
- Jacobson K, Sheets ED and Simson R** 1995 Revisiting the fluid mosaic model of membranes. *Science (New York, N.Y.)* 268: 1441–1442.
- Jaffe LA and Terasaki M** 1994 Structural changes in the endoplasmic reticulum of starfish oocytes during meiotic maturation and fertilization. *Developmental Biology* 164: 579–587.

- Jaiswal N, Haynesworth SE, Caplan AI and Bruder SP** 1997 Osteogenic differentiation of purified, culture-expanded human mesenchymal stem cells in vitro. *Journal of Cellular Biochemistry* 64: 295–312.
- Jensen TP, Filoteo AG, Knopfel T and Empson RM** 2007 Presynaptic plasma membrane Ca²⁺ ATPase isoform 2a regulates excitatory synaptic transmission in rat hippocampal CA3. *The Journal of Physiology* 579: 85–99.
- Jing D, Baik AD, Lu XL, Zhou B, Lai X, Wang L, Luo E and Guo XE** 2014 In situ intracellular calcium oscillations in osteocytes in intact mouse long bones under dynamic mechanical loading. *The FASEB Journal* 28: 1582–1592.
- Jokerst JV, Lobovkina T, Zare RN and Gambhir SS** 2011 Nanoparticle PEGylation for imaging and therapy. *Nanomedicine (London, England)* 6: 715–728.
- Jori FP, Napolitano MA, Melone MAB, Cipollaro M, Cascino A, Altucci L, Peluso G, Giordano A and Galderisi U** 2005 Molecular pathways involved in neural in vitro differentiation of marrow stromal stem cells. *Journal of Cellular Biochemistry* 94: 645–655.
- Kandel ER, Schwartz JH and Jessel TM** 2000 Principles of Neural Science **4** edition.. McGraw-Hill Medical
- Kaneko T, Tanaka H, Oyamada M, Kawata S and Takamatsu T** 2000 Three distinct types of Ca(2+) waves in Langendorff-perfused rat heart revealed by real-time confocal microscopy. *Circulation Research* 86: 1093–1099.
- Kao JPY, Li G and Auston DA** 2010 Practical aspects of measuring intracellular calcium signals with fluorescent indicators. *Methods in Cell Biology* 99: 113–152.
- Karp G** 2010 Biologie cellulaire et moléculaire: Concepts and experiments. De Boeck Supérieur
- Kawano S, Otsu K, Kuruma A, Shoji S, Yanagida E, Muto Y, Yoshikawa F, Hirayama Y, Mikoshiba K and Furuichi T** 2006 ATP autocrine/paracrine signaling induces calcium oscillations and NFAT activation in human mesenchymal stem cells. *Cell Calcium* 39: 313–324.
- Kawano S, Otsu K, Shoji S, Yamagata K and Hiraoka M** 2003a Ca(2+) oscillations regulated by Na(+)-Ca(2+) exchanger and plasma membrane Ca(2+) pump induce fluctuations of membrane currents and potentials in human mesenchymal stem cells. *Cell Calcium* 34: 145–156.
- Kawano S, Otsu K, Shoji S, Yamagata K and Hiraoka M** 2003b Ca(2+) oscillations regulated by Na(+)-Ca(2+) exchanger and plasma membrane Ca(2+) pump induce fluctuations of membrane currents and potentials in human mesenchymal stem cells. *Cell Calcium* 34: 145–156.
- Kawano S, Shoji S, Ichinose S, Yamagata K, Tagami M and Hiraoka M** 2002 Characterization of Ca(2+) signaling pathways in human mesenchymal stem cells. *Cell Calcium* 32: 165–174.
- Kew JNC and Davies CH** 2010 Ion Channels: From Structure to Function. Oxford University Press
- Khan H, Metra M, Blair JEA, Vogel M, Harinstein ME, Filippatos GS, Sabbah HN, Porchet H, Valentini G and Gheorghiade M** 2009 Istaroxime, a first in class new chemical entity exhibiting SERCA-2 activation and Na-K-ATPase inhibition: a new promising treatment for acute heart failure syndromes?. *Heart Failure Reviews* 14: 277–287.
- Khatib L, Golan DE and Cho M** 2004 Physiologic electrical stimulation provokes intracellular calcium increase mediated by phospholipase C activation in human osteoblasts. *The FASEB Journal*
- Kim IS, Song JK, Song YM, Cho TH, Lee TH, Lim SS, Kim SJ and Hwang SJ** 2009a Novel effect of biphasic electric current on in vitro osteogenesis and cytokine production in human mesenchymal stromal cells. *Tissue Engineering. Part A* 15: 2411–2422.

- Kim T-J, Seong J, Ouyang M, Sun J, Lu S, Hong JP, Wang N and Wang Y** 2009b Substrate rigidity regulates Ca²⁺ oscillation via RhoA pathway in stem cells. *Journal of cellular physiology* 218: 285–293.
- Kinosita K, Ashikawa I, Saita N, Yoshimura H, Itoh H, Nagayama K and Ikegami A** 1988 Electroporation of cell membrane visualized under a pulsed-laser fluorescence microscope.. *Biophysical Journal* 53: 1015–1019.
- Kinosita K and Tsong TY** 1977 Formation and resealing of pores of controlled sizes in human erythrocyte membrane. *Nature* 268: 438–441.
- Klemm DJ, Leitner JW, Watson P, Nesterova A, Reusch JE-B, Goalstone ML and Draznin B** 2001 Insulin-induced Adipocyte Differentiation ACTIVATION OF CREB RESCUES ADIPOGENESIS FROM THE ARREST CAUSED BY INHIBITION OF PRENYLATION. *Journal of Biological Chemistry* 276: 28430–28435.
- Koch GL** 1987 Reticuloplasmins: a novel group of proteins in the endoplasmic reticulum. *Journal of Cell Science* 87 (Pt 4): 491–492.
- Koshimizu TA, Van Goor F, Tomić M, Wong AO, Tanoue A, Tsujimoto G and Stojilkovic SS** 2000 Characterization of calcium signaling by purinergic receptor-channels expressed in excitable cells. *Molecular Pharmacology* 58: 936–945.
- Kotnik T, Bobanović F and Miklavc̃ić D** 1997 Sensitivity of transmembrane voltage induced by applied electric fields—A theoretical analysis. *Bioelectrochemistry and Bioenergetics* 43: 285–291.
- Kotnik T and Miklavcic D** 2000 Analytical description of transmembrane voltage induced by electric fields on spheroidal cells. *Biophysical Journal* 79: 670–679.
- Kotnik T, Pucihar G and Miklavcic D** 2010 Induced transmembrane voltage and its correlation with electroporation-mediated molecular transport. *The Journal of Membrane Biology* 236: 3–13.
- Kreke MR, Sharp LA, Lee YW and Goldstein AS** 2008 Effect of intermittent shear stress on mechanotransductive signaling and osteoblastic differentiation of bone marrow stromal cells. *Tissue Engineering. Part A* 14: 529–537.
- Kriegelstein J, Lippert K and Pösch G** 1996 Apparent independent action of nimodipine and glutamate antagonists to protect cultured neurons against glutamate-induced damage. *Neuropharmacology* 35: 1737–1742.
- Krutovskikh VA, Piccoli C, Yamasaki H and Yamasaki H** 2002 Gap junction intercellular communication propagates cell death in cancerous cells. *Oncogene* 21: 1989–1999.
- Lan HY, Mu W, Tomita N, Huang XR, Li JH, Zhu H-J, Morishita R and Johnson RJ** 2003 Inhibition of renal fibrosis by gene transfer of inducible Smad7 using ultrasound-microbubble system in rat UUO model. *Journal of the American Society of Nephrology: JASN* 14: 1535–1548.
- Langenbach F and Handschel J** 2013 Effects of dexamethasone, ascorbic acid and β -glycerophosphate on the osteogenic differentiation of stem cells in vitro. *Stem Cell Research & Therapy* 4: 117.
- Le Gall S, Neuhofer A and Rapoport T** 2004 The Endoplasmic Reticulum Membrane Is Permeable to Small Molecules. *Molecular Biology of the Cell* 15: 447–455.
- Lebovka NI, Bazhal MI and Vorobiev E** 2001 Pulsed electric field breakage of cellular tissues: visualisation of percolative properties. *Innovative Food Science & Emerging Technologies* 2: 113–125.
- Lee HC** 1993 Potentiation of calcium- and caffeine-induced calcium release by cyclic ADP-ribose. *The Journal of Biological Chemistry* 268: 293–299.

- Lee HC, Aarhus R, Graeff R, Gurnack ME and Walseth TF** 1994 Cyclic ADP ribose activation of the ryanodine receptor is mediated by calmodulin. *Nature* 370: 307–309.
- Lee MG, Xu X, Zeng W, Diaz J, Kuo TH, Wuytack F, Racymaekers L and Muallem S** 1997 Polarized expression of Ca²⁺ pumps in pancreatic and salivary gland cells. Role in initiation and propagation of [Ca²⁺]_i waves. *The Journal of Biological Chemistry* 272: 15771–15776.
- Lee RH, Kim B, Choi I, Kim H, Choi HS, Suh K, Bae YC and Jung JS** 2004 Characterization and expression analysis of mesenchymal stem cells from human bone marrow and adipose tissue. *Cellular Physiology and Biochemistry: International Journal of Experimental Cellular Physiology, Biochemistry, and Pharmacology* 14: 311–324.
- Lefkimmiatis K, Srikanthan M, Maiellaro I, Moyer MP, Curci S and Hofer AM** 2009 Store-operated cyclic AMP signalling mediated by STIM1. *Nature Cell Biology* 11: 433–442.
- Levin M** 2007 Large-scale biophysics: ion flows and regeneration. *Trends in Cell Biology* 17: 261–270.
- Levine ZA and Vernier PT** 2010 Life cycle of an electropore: field-dependent and field-independent steps in pore creation and annihilation. *The Journal of Membrane Biology* 236: 27–36.
- Lewis RS** 2003 Calcium oscillations in T-cells: mechanisms and consequences for gene expression. *Biochemical Society Transactions* 31: 925–929.
- Li L, Bennett SAL and Wang L** 2012 Role of E-cadherin and other cell adhesion molecules in survival and differentiation of human pluripotent stem cells. *Cell Adhesion & Migration* 6: 59–70.
- Li YJ, Batra NN, You L, Meier SC, Coe IA, Yellowley CE and Jacobs CR** 2004 Oscillatory fluid flow affects human marrow stromal cell proliferation and differentiation. *Journal of Orthopaedic Research: Official Publication of the Orthopaedic Research Society* 22: 1283–1289.
- Lindenburg L and Merckx M** 2014 Engineering genetically encoded FRET sensors. *Sensors (Basel, Switzerland)* 14: 11691–11713.
- Lindroos B, Suuronen R and Miettinen S** 2011 The potential of adipose stem cells in regenerative medicine. *Stem Cell Reviews* 7: 269–291.
- Liou J, Kim ML, Heo WD, Jones JT, Myers JW, Ferrell JE and Meyer T** 2005 STIM is a Ca²⁺ sensor essential for Ca²⁺-store-depletion-triggered Ca²⁺ influx. *Current biology: CB* 15: 1235–1241.
- Lipp P and Niggli E** 1996 A hierarchical concept of cellular and subcellular Ca²⁺-signalling. *Progress in Biophysics and Molecular Biology* 65: 265–296.
- Litsky ML and Pfeiffer DR** 1997 Regulation of the mitochondrial Ca²⁺ uniporter by external adenine nucleotides: the uniporter behaves like a gated channel which is regulated by nucleotides and divalent cations. *Biochemistry* 36: 7071–7080.
- Liu LH, Paul RJ, Sutliff RL, Miller ML, Lorenz JN, Pun RY, Duffy JJ, Doetschman T, Kimura Y, MacLennan DH, Hoving JB and Shull GE** 1997 Defective endothelium-dependent relaxation of vascular smooth muscle and endothelial cell Ca²⁺ signaling in mice lacking sarco(endo)plasmic reticulum Ca²⁺-ATPase isoform 3. *The Journal of Biological Chemistry* 272: 30538–30545.
- Liu Q, Cheng G, Wang Z, Zhan S, Xiong B and Zhao X** 2015 Bone marrow-derived mesenchymal stem cells differentiate into nerve-like cells in vitro after transfection with brain-derived neurotrophic factor gene. *In Vitro Cellular & Developmental Biology. Animal* 51: 319–327.
- Lo MMS and Tsong TY** 1989 Producing Monoclonal Antibodies by Electroporation. In Neumann E, Sowers AE, and Jordan CA (eds.) *Electroporation and Electroporation in Cell Biology* pp. 259–270. Springer US, Boston, MA
- Lodish H, Berk A, Kaiser CA, Krieger M, Scott MP, Bretscher A, Ploegh H and Matsudaira P** 2007 Molecular Cell Biology 6th edition.. W. H. Freeman, New York

- Lodish H, Berk A, Zipursky SL, Matsudaira P, Baltimore D and Darnell J** 2000a Biomembranes: Structural Organization and Basic Functions
- Lodish H, Berk A, Zipursky SL, Matsudaira P, Baltimore D and Darnell J** 2000b Molecular Cell Biology, 4th edition.. W. H. Freeman
- Loeb J** 1904 The Recent Development of Biology. *Science* 20: 777–786.
- Lorich DG, Brighton CT, Gupta R, Corsetti JR, Levine SE, Gelb ID, Seldes R and Pollack SR** 1998 Biochemical pathway mediating the response of bone cells to capacitive coupling. *Clinical Orthopaedics and Related Research*: 246–256.
- Lucas ML and Heller R** 2003 IL-12 gene therapy using an electrically mediated nonviral approach reduces metastatic growth of melanoma. *DNA and cell biology* 22: 755–763.
- Luengo E, Martínez JM, Coustets M, Álvarez I, Teissié J, Rols M-P and Raso J** 2015 A Comparative Study on the Effects of Millisecond- and Microsecond-Pulsed Electric Field Treatments on the Permeabilization and Extraction of Pigments from *Chlorella vulgaris*. *The Journal of Membrane Biology* 248: 883–891.
- Luttrell LM** 2002 Activation and targeting of mitogen-activated protein kinases by G-protein-coupled receptors. *Canadian Journal of Physiology and Pharmacology* 80: 375–382.
- Lytton J** 2007 Na⁺/Ca²⁺ exchangers: three mammalian gene families control Ca²⁺ transport. *Biochemical Journal* 406: 365–382.
- MacLennan DH, Rice WJ and Green NM** 1997 The Mechanism of Ca²⁺ Transport by Sarco(Endo)plasmic Reticulum Ca²⁺-ATPases. *Journal of Biological Chemistry* 272: 28815–28818.
- Malaval L, Liu F, Roche P and Aubin JE** 1999 Kinetics of osteoprogenitor proliferation and osteoblast differentiation in vitro. *Journal of Cellular Biochemistry* 74: 616–627.
- Malgieri A, Kantzari E, Patrizi MP and Gambardella S** 2010 Bone marrow and umbilical cord blood human mesenchymal stem cells: state of the art. *International Journal of Clinical and Experimental Medicine* 3: 248–269.
- Maltman DJ, Hardy SA and Przyborski SA** 2011 Role of mesenchymal stem cells in neurogenesis and nervous system repair. *Neurochemistry International* 59: 347–356.
- Mank M, Reiff DF, Heim N, Friedrich MW, Borst A and Griesbeck O** 2006 A FRET-based calcium biosensor with fast signal kinetics and high fluorescence change. *Biophysical Journal* 90: 1790–1796.
- Mansilla MC, Cybulski LE, Albanesi D and de Mendoza D** 2004 Control of Membrane Lipid Fluidity by Molecular Thermosensors. *Journal of Bacteriology* 186: 6681–6688.
- Marcum JM, Dedman JR, Brinkley BR and Means AR** 1978 Control of microtubule assembly-disassembly by calcium-dependent regulator protein. *Proceedings of the National Academy of Sciences of the United States of America* 75: 3771–3775.
- Mareschi K, Novara M, Rustichelli D, Ferrero I, Guido D, Carbone E, Medico E, Madon E, Vercelli A and Fagioli F** 2006 Neural differentiation of human mesenchymal stem cells: Evidence for expression of neural markers and eag K⁺ channel types. *Experimental Hematology* 34: 1563–1572.
- Marieb EN and Hoehn K** 2006 Human Anatomy And Physiology7 Pck edition.. Pearson Prentice Hall
- Marion NW and Mao JJ** 2006 Mesenchymal stem cells and tissue engineering. *Methods in Enzymology* 420: 339–361.
- Mark MD and Herlitze S** 2000 G-protein mediated gating of inward-rectifier K⁺ channels. *European Journal of Biochemistry* 267: 5830–5836.

- Marsh D** 2007 Lateral pressure profile, spontaneous curvature frustration, and the incorporation and conformation of proteins in membranes. *Biophysical Journal* 93: 3884–3899.
- Marshall CJ** 1995 Specificity of receptor tyrosine kinase signaling: Transient versus sustained extracellular signal-regulated kinase activation. *Cell* 80: 179–185.
- Mauroy C, Portet T, Winterhalder M, Bellard E, Blache M-C, Teissié J, Zumbusch A and Rols M-P** 2012 Giant lipid vesicles under electric field pulses assessed by non invasive imaging. *Bioelectrochemistry (Amsterdam, Netherlands)* 87: 253–259.
- Maxfield FR and Tabas I** 2005 Role of cholesterol and lipid organization in disease. *Nature* 438: 612–621.
- McCormack JG, Halestrap AP and Denton RM** 1990 Role of calcium ions in regulation of mammalian intramitochondrial metabolism. *Physiological Reviews* 70: 391–425.
- Meer G van and Lisman Q** 2002 Sphingolipid Transport: Rafts and Translocators. *Journal of Biological Chemistry* 277: 25855–25858.
- van Meer G, Voelker DR and Feigenson GW** 2008 Membrane lipids: where they are and how they behave. *Nature Reviews Molecular Cell Biology* 9: 112–124.
- Meglić SH, Levičnik E, Luengo E, Raso J and Miklavčič D** 2016 The Effect of Temperature on Protein Extraction by Electroporation and on Bacterial Viability. In Jarm T and Kramar P (eds.) *1st World Congress on Electroporation and Pulsed Electric Fields in Biology, Medicine and Food & Environmental Technologies* pp. 175–178. Springer Singapore, Singapore
- Mehlmann LM, Terasaki M, Jaffe LA and Kline D** 1995 Reorganization of the endoplasmic reticulum during meiotic maturation of the mouse oocyte. *Developmental Biology* 170: 607–615.
- Mekid H and Mir LM** 2000 In vivo cell electrofusion. *Biochimica et Biophysica Acta (BBA) - General Subjects* 1524: 118–130.
- Meldolesi J and Pozzan T** 1998 The endoplasmic reticulum Ca²⁺ store: a view from the lumen. *Trends in Biochemical Sciences* 23: 10–14.
- Menick DR, Renaud L, Buchholz A, Müller JG, Zhou H, Kappler CS, Kubalak SW, Conway SJ and Xu L** 2007 Regulation of Ncx1 gene expression in the normal and hypertrophic heart. *Annals of the New York Academy of Sciences* 1099: 195–203.
- Ménorval M-A de, Mir LM, Fernández ML and Reigada R** 2012 Effects of Dimethyl Sulfoxide in Cholesterol-Containing Lipid Membranes: A Comparative Study of Experiments In Silico and with Cells. *PLOS ONE* 7: e41733.
- Metuzals J, Chang D, Hammar K and Reese TS** 1997 Organization of the cortical endoplasmic reticulum in the squid giant axon. *Journal of Neurocytology* 26: 529–539.
- Michael DH and O'Neill ME** 1970 Electrohydrodynamic instability in plane layers of fluid. *Journal of Fluid Mechanics* 41: 571–580.
- Michelangeli F and East JM** 2011 A diversity of SERCA Ca²⁺ pump inhibitors. *Biochemical Society Transactions* 39: 789–797.
- Miklavčič D, Mali B, Kos B, Heller R and Serša G** 2014 Electrochemotherapy: from the drawing board into medical practice. *BioMedical Engineering OnLine* 13: 29.
- Mir LM, Banoun H and Paoletti C** 1988 Introduction of definite amounts of nonpermeant molecules into living cells after electropermeabilization: direct access to the cytosol. *Experimental Cell Research* 175: 15–25.
- Mir LM, Belehradek M, Domenge C, Orlowski S, Poddevin B, Belehradek J, Schwaab G, Luboinski B and Paoletti C** 1991 [Electrochemotherapy, a new antitumor treatment: first clinical trial]. *Comptes rendus de l'Académie des sciences. Série III, Sciences de la vie* 313: 613–618.

- Mir LM, Bureau MF, Gehl J, Rangara R, Rouy D, Caillaud J-M, Delaere P, Branellec D, Schwartz B and Scherman D** 1999 High-efficiency gene transfer into skeletal muscle mediated by electric pulses. *Proceedings of the National Academy of Sciences of the United States of America* 96: 4262–4267.
- Mir LM, Gehl J, Sersa G, Collins CG, Garbay J-R, Billard V, Geertsens PF, Rudolf Z, O'Sullivan GC and Marty M** 2006 Standard operating procedures of the electrochemotherapy: Instructions for the use of bleomycin or cisplatin administered either systemically or locally and electric pulses delivered by the CliniporatorTM by means of invasive or non-invasive electrodes. *European Journal of Cancer Supplements* 4: 14–25.
- Mir LM, Moller PH, André F and Gehl J** 2005 Electric pulse-mediated gene delivery to various animal tissues. *Advances in Genetics* 54: 83–114.
- Mir LM, Orlowski S, Poddevin B and Belehradek J** 1992 Electrochemotherapy tumor treatment is improved by interleukin-2 stimulation of the host's defenses. *European Cytokine Network* 3: 331–334.
- Miranti CK and Brugge JS** 2002 Sensing the environment: a historical perspective on integrin signal transduction. *Nature Cell Biology* 4: E83–90.
- Miranville A, Heeschen C, Sengenès C, Curat CA, Busse R and Bouloumié A** 2004 Improvement of postnatal neovascularization by human adipose tissue-derived stem cells. *Circulation* 110: 349–355.
- Miyawaki A, Llopis J, Heim R, McCaffery JM, Adams JA, Ikura M and Tsien RY** 1997 Fluorescent indicators for Ca²⁺ based on green fluorescent proteins and calmodulin. *Nature* 388: 882–887.
- Mohr JC, de Pablo JJ and Palecek SP** 2006 Electroporation of human embryonic stem cells: Small and macromolecule loading and DNA transfection. *Biotechnology Progress* 22: 825–834.
- Montel-Hagen A, Kinet S, Manel N, Mongellaz C, Prohaska R, Battini J-L, Delaunay J, Sitbon M and Taylor N** 2008 Erythrocyte Glut1 Triggers Dehydroascorbic Acid Uptake in Mammals Unable to Synthesize Vitamin C. *Cell* 132: 1039–1048.
- Montero M, Lobatón CD, Hernández-Sanmiguel E, Santodomingo J, Vay L, Moreno A and Alvarez J** 2004 Direct activation of the mitochondrial calcium uniporter by natural plant flavonoids. *The Biochemical Journal* 384: 19–24.
- Moreau B, Nelson C and Parekh AB** 2006 Biphasic regulation of mitochondrial Ca²⁺ uptake by cytosolic Ca²⁺ concentration. *Current biology: CB* 16: 1672–1677.
- Morth JP, Pedersen BP, Buch-Pedersen MJ, Andersen JP, Vilsen B, Palmgren MG and Nissen P** 2011 A structural overview of the plasma membrane Na⁺,K⁺-ATPase and H⁺-ATPase ion pumps. *Nature Reviews Molecular Cell Biology* 12: 60–70.
- MÜLLER DJ, WU N and PALCZEWSKI K** 2008 Vertebrate Membrane Proteins: Structure, Function, and Insights from Biophysical Approaches. *Pharmacological reviews* 60: 43–78.
- Munro S and Pelham HR** 1987 A C-terminal signal prevents secretion of luminal ER proteins. *Cell* 48: 899–907.
- Nagai T, Sawano A, Park ES and Miyawaki A** 2001 Circularly permuted green fluorescent proteins engineered to sense Ca²⁺. *Proceedings of the National Academy of Sciences of the United States of America* 98: 3197–3202.
- Nagayama M, Uchida T and Gohara K** 2007 Temporal and spatial variations of lipid droplets during adipocyte division and differentiation. *Journal of Lipid Research* 48: 9–18.
- Nakai J, Ohkura M and Imoto K** 2001 A high signal-to-noise Ca(2+) probe composed of a single green fluorescent protein. *Nature Biotechnology* 19: 137–141.

- Nash MS, Young KW, John Challiss RA and Nahorski SR** 2001 Intracellular signalling: Receptor-specific messenger oscillations. *Nature* 413: 381–382.
- Neher E and Sakmann B** 1976 Single-channel currents recorded from membrane of denervated frog muscle fibres. *Nature* 260: 799–802.
- Nehls S, Snapp EL, Cole NB, Zaal KJ, Kenworthy AK, Roberts TH, Ellenberg J, Presley JF, Siggia E and Lippincott-Schwartz J** 2000 Dynamics and retention of misfolded proteins in native ER membranes. *Nature Cell Biology* 2: 288–295.
- Neumann E, Kakorin S and Toensing K** 1999 Fundamentals of electroporative delivery of drugs and genes. *Bioelectrochemistry and Bioenergetics (Lausanne, Switzerland)* 48: 3–16.
- Neumann E and Rosenheck K** 1972 Permeability changes induced by electric impulses in vesicular membranes. *The Journal of Membrane Biology* 10: 279–290.
- Neumann E, Schaefer-Ridder M, Wang Y and Hofschneider PH** 1982 Gene transfer into mouse lyoma cells by electroporation in high electric fields. *The EMBO journal* 1: 841–845.
- Newman CMH and Bettinger T** 2007 Gene therapy progress and prospects: Ultrasound for gene transfer. *Gene Therapy* 14: 465–475.
- Nicolson GL** 2014 The Fluid—Mosaic Model of Membrane Structure: Still relevant to understanding the structure, function and dynamics of biological membranes after more than 40 years. *Biochimica et Biophysica Acta (BBA) - Biomembranes* 1838: 1451–1466.
- Niemelä PS, Ollila S, Hyvönen MT, Karttunen M and Vattulainen I** 2007 Assessing the Nature of Lipid Raft Membranes. *PLoS Computational Biology* 3
- Noguchi N, Takasawa S, Nata K, Tohgo A, Kato I, Ikehata F, Yonekura H and Okamoto H** 1997 Cyclic ADP-ribose binds to FK506-binding protein 12.6 to release Ca²⁺ from islet microsomes. *The Journal of Biological Chemistry* 272: 3133–3136.
- Nordenfelt P and Tapper H** 2011 Phagosome dynamics during phagocytosis by neutrophils. *Journal of Leukocyte Biology* 90: 271–284.
- Norton WT and Cammer W** 1984 Isolation and Characterization of Myelin. In Morell P (ed.) *Myelin* pp. 147–195. Springer US
- O'Brien TW** 2003 Properties of human mitochondrial ribosomes. *IUBMB life* 55: 505–513.
- Odermatt A, Barton K, Khanna VK, Mathieu J, Escolar D, Kuntzer T, Karpati G and MacLennan DH** 2000 The mutation of Pro789 to Leu reduces the activity of the fast-twitch skeletal muscle sarco(endo)plasmic reticulum Ca²⁺ ATPase (SERCA1) and is associated with Brody disease. *Human Genetics* 106: 482–491.
- Odermatt A, Taschner PE, Khanna VK, Busch HF, Karpati G, Jablecki CK, Breuning MH and MacLennan DH** 1996 Mutations in the gene-encoding SERCA1, the fast-twitch skeletal muscle sarcoplasmic reticulum Ca²⁺ ATPase, are associated with Brody disease. *Nature Genetics* 14: 191–194.
- Ohvo-Rekilä H, Ramstedt B, Leppimäki P and Slotte JP** 2002 Cholesterol interactions with phospholipids in membranes. *Progress in Lipid Research* 41: 66–97.
- Olivotto M, Arcangeli A, Carlà M and Wanke E** 1996 Electric fields at the plasma membrane level: A neglected element in the mechanisms of cell signalling. *BioEssays* 18: 495–504.
- Orlowski S, Belehradek J, Paoletti C and Mir LM** 1988 Transient electropermeabilization of cells in culture. Increase of the cytotoxicity of anticancer drugs. *Biochemical Pharmacology* 37: 4727–4733.
- Ortiz-Gonzalez XR, Keene CD, Verfaillie CM and Low WC** 2004 Neural induction of adult bone marrow and umbilical cord stem cells. *Current Neurovascular Research* 1: 207–213.

- Ostrovskaya O, Goyal R, Osman N, McAllister CE, Pessah IN, Hume JR and Wilson SM** 2007 Inhibition of ryanodine receptors by 4-(2-aminopropyl)-3,5-dichloro-N,N-dimethylaniline (FLA 365) in canine pulmonary arterial smooth muscle cells. *The Journal of Pharmacology and Experimental Therapeutics* 323: 381–390.
- Overton CE** 1895 Ueber die osmotischen eigenschaften der lebenden pflanzen- und tierzelle. Fäsi & Beer
- Owen TA, Aronow M, Shalhoub V, Barone LM, Wilming L, Tassinari MS, Kennedy MB, Pockwinse S, Lian JB and Stein GS** 1990 Progressive development of the rat osteoblast phenotype in vitro: reciprocal relationships in expression of genes associated with osteoblast proliferation and differentiation during formation of the bone extracellular matrix. *Journal of Cellular Physiology* 143: 420–430.
- Pairault J and Green H** 1979 A study of the adipose conversion of suspended 3T3 cells by using glycerophosphate dehydrogenase as differentiation marker. *Proceedings of the National Academy of Sciences of the United States of America* 76: 5138–5142.
- Pakhomov AG, Gianulis E, Vernier PT, Semenov I, Xiao S and Pakhomova ON** 2015 Multiple nanosecond electric pulses increase the number but not the size of long-lived nanopores in the cell membrane. *Biochimica Et Biophysica Acta* 1848: 958–966.
- Pakhomov AG, Shevin R, White JA, Kolb JF, Pakhomova ON, Joshi RP and Schoenbach KH** 2007 Membrane permeabilization and cell damage by ultrashort electric field shocks. *Archives of Biochemistry and Biophysics* 465: 109–118.
- Palecek J, Lips MB and Keller BU** 1999 Calcium dynamics and buffering in motoneurons of the mouse spinal cord. *The Journal of Physiology* 520: 485–502.
- Pall ML** 2013 Electromagnetic fields act via activation of voltage-gated calcium channels to produce beneficial or adverse effects. *Journal of Cellular and Molecular Medicine* 17: 958–965.
- Palmer AE, Giacomello M, Kortemme T, Hires SA, Lev-Ram V, Baker D and Tsien RY** 2006 Ca²⁺ indicators based on computationally redesigned calmodulin-peptide pairs. *Chemistry & Biology* 13: 521–530.
- Palmer AE, Jin C, Reed JC and Tsien RY** 2004 Bcl-2-mediated alterations in endoplasmic reticulum Ca²⁺ analyzed with an improved genetically encoded fluorescent sensor. *Proceedings of the National Academy of Sciences of the United States of America* 101: 17404–17409.
- Papahadjopoulos D, Nir S and Ohki S** 1972 Permeability properties of phospholipid membranes: Effect of cholesterol and temperature. *Biochimica et Biophysica Acta (BBA) - Biomembranes* 266: 561–583.
- Paredes RM, Etzler JC, Watts LT and Lechleiter JD** 2008 Chemical Calcium Indicators. *Methods (San Diego, Calif.)* 46: 143–151.
- Parekh AB and Putney JW** 2005 Store-operated calcium channels. *Physiological Reviews* 85: 757–810.
- Parker I, Choi J and Yao Y** 1996 Elementary events of InsP₃-induced Ca²⁺ liberation in *Xenopus* oocytes: hot spots, puffs and blips. *Cell Calcium* 20: 105–121.
- Parri HR, Gould TM and Crunelli V** 2001 Spontaneous astrocytic Ca²⁺ oscillations in situ drive NMDAR-mediated neuronal excitation. *Nature Neuroscience* 4: 803–812.
- Parsegian VA** 1975 Ion-Membrane Interactions as Structural Forces. *Annals of the New York Academy of Sciences* 264: 161–174.
- Patel S and Docampo R** 2010 Acidic calcium stores open for business: expanding the potential for intracellular Ca²⁺ signaling. *Trends in Cell Biology* 20: 277–286.

- Patergnani S, Suski JM, Agnoletto C, Bononi A, Bonora M, De Marchi E, Giorgi C, Marchi S, Missiroli S, Poletti F, Rimessi A, Duszynski J, Wieckowski MR and Pinton P** 2011 Calcium signaling around Mitochondria Associated Membranes (MAMs). *Cell Communication and Signaling* 9: 19.
- Pauly H and Schwan HP** 1959 [Impedance of a suspension of ball-shaped particles with a shell; a model for the dielectric behavior of cell suspensions and protein solutions]. *Zeitschrift Für Naturforschung. Teil B: Chemie, Biochemie, Biophysik, Biologie* 14B: 125–131.
- Pavlin M, Pavselj N and Miklavcic D** 2002 Dependence of induced transmembrane potential on cell density, arrangement, and cell position inside a cell system. *IEEE transactions on bio-medical engineering* 49: 605–612.
- Pérez Koldenkova V and Nagai T** 2013 Genetically encoded Ca(2+) indicators: properties and evaluation. *Biochimica Et Biophysica Acta* 1833: 1787–1797.
- Perez-Reyes E and Lory P** 2006 Molecular biology of T-type calcium channels. *CNS & neurological disorders drug targets* 5: 605–609.
- Perica K, Varela JC, Oelke M and Schneck J** 2015 Adoptive T Cell Immunotherapy for Cancer. *Rambam Maimonides Medical Journal* 6
- Perkins G, Renken C, Martone ME, Young SJ, Ellisman M and Frey T** 1997 Electron tomography of neuronal mitochondria: three-dimensional structure and organization of cristae and membrane contacts. *Journal of Structural Biology* 119: 260–272.
- Petecchia L, Sbrana F, Utzeri R, Vercellino M, Usai C, Visai L, Vassalli M and Gavazzo P** 2015 Electro-magnetic field promotes osteogenic differentiation of BM-hMSCs through a selective action on Ca2+-related mechanisms. *Scientific Reports* 5
- Peters MA, Teramoto T, White JQ, Iwasaki K and Jorgensen EM** 2007 A Calcium Wave Mediated by Gap Junctions Coordinates a Rhythmic Behavior in *C. elegans*. *Current Biology* 17: 1601–1608.
- Petersen OH, Michalak M and Verkhratsky A** 2005 Calcium signalling: past, present and future. *Cell Calcium* 38: 161–169.
- Philipson KD, Longoni S and Ward R** 1988 Purification of the cardiac Na⁺-Ca²⁺ exchange protein. *Biochimica Et Biophysica Acta* 945: 298–306.
- Piersma AH, Brockbank KG, Ploemacher RE, van Vliet E, Brakel-van Peer KM and Visser PJ** 1985 Characterization of fibroblastic stromal cells from murine bone marrow. *Experimental Hematology* 13: 237–243.
- Pike LJ** 2003 Lipid rafts bringing order to chaos. *Journal of Lipid Research* 44: 655–667.
- Pinton P, Pozzan T and Rizzuto R** 1998 The Golgi apparatus is an inositol 1,4,5-trisphosphate-sensitive Ca²⁺ store, with functional properties distinct from those of the endoplasmic reticulum.. *The EMBO Journal* 17: 5298–5308.
- Pittenger MF, Mackay AM, Beck SC, Jaiswal RK, Douglas R, Mosca JD, Moorman MA, Simonetti DW, Craig S and Marshak DR** 1999 Multilineage Potential of Adult Human Mesenchymal Stem Cells. *Science* 284: 143–147.
- Poddevin B, Orlowski S, Belehradek J and Mir LM** 1991 Very high cytotoxicity of bleomycin introduced into the cytosol of cells in culture. *Biochemical Pharmacology* 42 Suppl: S67-75.
- Polak A, Bonhenry D, Dehez F, Kramar P, Miklavčič D and Tarek M** 2013 On the electroporation thresholds of lipid bilayers: molecular dynamics simulation investigations. *The Journal of Membrane Biology* 246: 843–850.
- Porumb T, Yau P, Harvey TS and Ikura M** 1994 A calmodulin-target peptide hybrid molecule with unique calcium-binding properties. *Protein Engineering* 7: 109–115.

- Potter H and Heller R** 2011 Transfection by electroporation. *Current Protocols in Cell Biology / Editorial Board, Juan S. Bonifacino ... [et Al.]* Chapter 20: Unit20.5.
- Prins D and Michalak M** 2011 Organellar Calcium Buffers. *Cold Spring Harbor Perspectives in Biology* 3: a004069.
- Pucihar G, Kotnik T, Teissié J and Miklavčič D** 2007 Electroporabilization of dense cell suspensions. *European Biophysics Journal* 36: 173–185.
- Pullar CE** 2011 The Physiology of Bioelectricity in Development, Tissue Regeneration and Cancer. CRC Press
- Purves D, Augustine GJ, Fitzpatrick D, Katz LC, LaMantia A-S, McNamara JO and Williams SM** 2001 Ligand-Gated Ion Channels
- Putney JW** 2009 SOC: now also store-operated cyclase. *Nature Cell Biology* 11: 381–382.
- Qu B, Al-Ansary D, Kummerow C, Hoth M and Schwarz EC** 2011 ORAI-mediated calcium influx in T cell proliferation, apoptosis and tolerance. *Cell Calcium* 50: 261–269.
- Quarles LD, Yohay DA, Lever LW, Caton R and Wenstrup RJ** 1992 Distinct proliferative and differentiated stages of murine MC3T3-E1 cells in culture: an in vitro model of osteoblast development. *Journal of Bone and Mineral Research: The Official Journal of the American Society for Bone and Mineral Research* 7: 683–692.
- Ratto GM, Payne R, Owen WG and Tsien RY** 1988 The concentration of cytosolic free calcium in vertebrate rod outer segments measured with fura-2. *The Journal of Neuroscience: The Official Journal of the Society for Neuroscience* 8: 3240–3246.
- Reddy A, Caler EV and Andrews NW** 2001 Plasma membrane repair is mediated by Ca(2+)-regulated exocytosis of lysosomes. *Cell* 106: 157–169.
- Remm M and Sonnhammer E** 2000 Classification of Transmembrane Protein Families in the Caenorhabditis elegans Genome and Identification of Human Orthologs. *Genome Research* 10: 1679–1689.
- Rems L, Ušaj M, Kandušer M, Reberšek M, Miklavčič D and Pucihar G** 2013 Cell electrofusion using nanosecond electric pulses. *Scientific Reports* 3
- Resende RR, Adhikari A, da Costa JL, Lorençon E, Ladeira MS, Guatimosim S, Kihara AH and Ladeira LO** 2010 Influence of spontaneous calcium events on cell-cycle progression in embryonal carcinoma and adult stem cells. *Biochimica Et Biophysica Acta* 1803: 246–260.
- Resh MD** 1999 Fatty acylation of proteins: new insights into membrane targeting of myristoylated and palmitoylated proteins. *Biochimica et Biophysica Acta (BBA) - Molecular Cell Research* 1451: 1–16.
- Ridgway EB and Ashley CC** 1967 Calcium transients in single muscle fibers. *Biochemical and Biophysical Research Communications* 29: 229–234.
- Riley RT, Enongene E, Voss KA, Norred WP, Meredith FI, Sharma RP, Spitsbergen J, Williams DE, Carlson DB and Merrill AH** 2001 Sphingolipid perturbations as mechanisms for fumonisins carcinogenesis.. *Environmental Health Perspectives* 109: 301–308.
- Rizzuto R, Marchi S, Bonora M, Aguiari P, Bononi A, De Stefani D, Giorgi C, Leo S, Rimessi A, Siviero R, Zecchini E and Pinton P** 2009 Ca²⁺ transfer from the ER to mitochondria: When, how and why. *Biochimica et Biophysica Acta (BBA) - Bioenergetics* 1787: 1342–1351.
- Robb-Gaspers LD, Rutter GA, Burnett P, Hajnóczky G, Denton RM and Thomas AP** 1998 Coupling between cytosolic and mitochondrial calcium oscillations: role in the regulation of hepatic metabolism. *Biochimica Et Biophysica Acta* 1366: 17–32.

- Robertson JD** 1959 The ultrastructure of cell membranes and their derivatives. *Biochemical Society Symposium* 16: 3–43.
- Robertson JD** 1960 The molecular structure and contact relationships of cell membranes. *Progress in Biophysics and Molecular Biology* 10: 343–418.
- Rodan GA and Noda M** 1991 Gene expression in osteoblastic cells. *Critical Reviews in Eukaryotic Gene Expression* 1: 85–98.
- Rodney GG, Wilson GM and Schneider MF** 2005 A Calmodulin Binding Domain of RyR Increases Activation of Spontaneous Ca²⁺ Sparks in Frog Skeletal Muscle. *Journal of Biological Chemistry* 280: 11713–11722.
- Rols MP, Delteil C, Serin G and Teissié J** 1994 Temperature effects on electrotransfection of mammalian cells.. *Nucleic Acids Research* 22: 540.
- Rols MP and Teissié J** 1990 Electroporation of mammalian cells. Quantitative analysis of the phenomenon.. *Biophysical Journal* 58: 1089–1098.
- Rooney TA and Thomas AP** 1993 Intracellular calcium waves generated by ins(1,4,5)P₃-dependent mechanisms. *Cell Calcium* 14: 674–690.
- Rosen D and Sutton AM** 1968 The effects of a direct current potential bias on the electrical properties of bimolecular lipid membranes. *Biochimica et Biophysica Acta (BBA) - Biomembranes* 163: 226–233.
- Rosen ED and Spiegelman BM** 2000 Molecular Regulation of Adipogenesis. *Annual Review of Cell and Developmental Biology* 16: 145–171.
- Roux S, Bernat C, Al-Sakere B, Ghiringhelli F, Opolon P, Carpentier AF, Zitvogel L, Mir LM and Robert C** 2008 Tumor destruction using electrochemotherapy followed by CpG oligodeoxynucleotide injection induces distant tumor responses. *Cancer immunology, immunotherapy: CII* 57: 1291–1300.
- Roy A and Wonderlin WF** 2003 The permeability of the endoplasmic reticulum is dynamically coupled to protein synthesis. *The Journal of Biological Chemistry* 278: 4397–4403.
- Saito K, Chang Y-F, Horikawa K, Hatsugai N, Higuchi Y, Hashida M, Yoshida Y, Matsuda T, Arai Y and Nagai T** 2012 Luminescent proteins for high-speed single-cell and whole-body imaging. *Nature Communications* 3: 1262.
- Saito K, Hatsugai N, Horikawa K, Kobayashi K, Matsu-Ura T, Mikoshiba K and Nagai T** 2010 Auto-luminescent genetically-encoded ratiometric indicator for real-time Ca²⁺ imaging at the single cell level. *PLoS One* 5: e9935.
- Saitoh N, Oritani K, Saito K, Yokota T, Ichii M, Sudo T, Fujita N, Nakajima K, Okada M and Kanakura Y** 2011 Identification of functional domains and novel binding partners of STIM proteins. *Journal of Cellular Biochemistry* 112: 147–156.
- Sale AJ and Hamilton WA** 1968 Effects of high electric fields on micro-organisms. 3. Lysis of erythrocytes and protoplasts. *Biochimica Et Biophysica Acta* 163: 37–43.
- Santo-Domingo J and Demarex N** 2010 Calcium uptake mechanisms of mitochondria. *Biochimica Et Biophysica Acta* 1797: 907–912.
- Satkauskas S, Bureau MF, Puc M, Mahfoudi A, Scherman D, Miklavcic D and Mir LM** 2002 Mechanisms of in vivo DNA electrotransfer: respective contributions of cell electroporation and DNA electrophoresis. *Molecular Therapy: The Journal of the American Society of Gene Therapy* 5: 133–140.

- Saunders CM, Larman MG, Parrington J, Cox LJ, Royse J, Blayney LM, Swann K and Lai FA** 2002 PLC ζ : a sperm-specific trigger of Ca²⁺ oscillations in eggs and embryo development. *Development* 129: 3533–3544.
- Schantz AR** 1985 Cytosolic free calcium-ion concentration in cleaving embryonic cells of *Oryzias latipes* measured with calcium-selective microelectrodes. *The Journal of Cell Biology* 100: 947–954.
- Scheurich P, Zimmermann U, Mischel M and Lamprecht I** 1980 Membrane fusion and deformation of red blood cells by electric fields. *Zeitschrift Für Naturforschung. Section C: Biosciences* 35: 1081–1085.
- Scheurich P, Zimmermann U and Schnabl H** 1981 Electrically Stimulated Fusion of Different Plant Cell Protoplasts 12. *Plant Physiology* 67: 849–853.
- Schnitzer JE, McIntosh DP, Dvorak AM, Liu J and Oh P** 1995 Separation of caveolae from associated microdomains of GPI-anchored proteins. *Science (New York, N.Y.)* 269: 1435–1439.
- Schoenbach KH, Beebe SJ and Buescher ES** 2001a Intracellular effect of ultrashort electrical pulses. *Bioelectromagnetics* 22: 440–448.
- Schoenbach KH, Beebe SJ and Buescher ES** 2001b Intracellular effect of ultrashort electrical pulses. *Bioelectromagnetics* 22: 440–448.
- Schoenbach KH, Joshi RP, Kolb JF, Chen N, Stacey M, Blackmore PF, Buescher ES and Beebe SJ** 2004 Ultrashort electrical pulses open a new gateway into biological cells. *Proceedings of the IEEE* 92: 1122–1137.
- Schoenbach KH, Joshi RP, Stark RH, Dobbs FC and Beebe SJ** 2000 Bacterial decontamination of liquids with pulsed electric fields. *IEEE Transactions on Dielectrics and Electrical Insulation* 7: 637–645.
- Schultheiss C, Bluhm H, Mayer H-G, Kern M, Michelberger T and Witte G** 2002 Processing of sugar beets with pulsed-electric fields. *IEEE Transactions on Plasma Science* 30: 1547–1551.
- Schwan HP** 1957 Electrical properties of tissue and cell suspensions. *Advances in Biological and Medical Physics* 5: 147–209.
- Scott MA, Nguyen VT, Levi B and James AW** 2011 Current Methods of Adipogenic Differentiation of Mesenchymal Stem Cells. *Stem Cells and Development* 20: 1793–1804.
- Sekiya I, Larson BL, Vuoristo JT, Cui J-G and Prockop DJ** 2004 Adipogenic differentiation of human adult stem cells from bone marrow stroma (MSCs). *Journal of Bone and Mineral Research: The Official Journal of the American Society for Bone and Mineral Research* 19: 256–264.
- Seo MJ, Suh SY, Bae YC and Jung JS** 2005 Differentiation of human adipose stromal cells into hepatic lineage in vitro and in vivo. *Biochemical and Biophysical Research Communications* 328: 258–264.
- Serhan CN, Haeggström JZ and Leslie CC** 1996 Lipid mediator networks in cell signaling: update and impact of cytokines. *FASEB journal: official publication of the Federation of American Societies for Experimental Biology* 10: 1147–1158.
- Sersa G, Kranjc S, Scancar J, Krzan M and Cemazar M** 2010 Electrochemotherapy of mouse sarcoma tumors using electric pulse trains with repetition frequencies of 1 Hz and 5 kHz. *The Journal of Membrane Biology* 236: 155–162.
- Sharon N** 1987 Bacterial lectins, cell-cell recognition and infectious disease. *FEBS Letters* 217: 145–157.
- Sharp LA, Lee YW and Goldstein AS** 2009 Effect of low-frequency pulsatile flow on expression of osteoblastic genes by bone marrow stromal cells. *Annals of Biomedical Engineering* 37: 445–453.
- Shenoda B** 2015 The role of Na⁺/Ca²⁺ exchanger subtypes in neuronal ischemic injury. *Translational Stroke Research* 6: 181–190.

- Shibata Y, Voeltz GK and Rapoport TA** 2006 Rough Sheets and Smooth Tubules. *Cell* 126: 435–439.
- Shimomura O, Johnson FH and Saiga Y** 1962 Extraction, Purification and Properties of Aequorin, a Bioluminescent Protein from the Luminous Hydromedusan, Aequorea. *Journal of Cellular and Comparative Physiology* 59: 223–239.
- Shoshan-Barmatz V and Gincel D** 2003 The voltage-dependent anion channel: characterization, modulation, and role in mitochondrial function in cell life and death. *Cell Biochemistry and Biophysics* 39: 279–292.
- Silve A, Guimerà Brunet A, Al-Sakere B, Ivorra A and Mir LM** 2014 Comparison of the effects of the repetition rate between microsecond and nanosecond pulses: electroporation-induced electro-desensitization?. *Biochimica Et Biophysica Acta* 1840: 2139–2151.
- Silve A, Leray I and Mir LM** 2012 Demonstration of cell membrane permeabilization to medium-sized molecules caused by a single 10 ns electric pulse. *Bioelectrochemistry (Amsterdam, Netherlands)* 87: 260–264.
- Silve A, Leray I, Poignard C and Mir LM** 2016 Impact of external medium conductivity on cell membrane electroporation by microsecond and nanosecond electric pulses. *Scientific Reports* 6: 19957.
- Simmons CA, Matlis S, Thornton AJ, Chen S, Wang CY and Mooney DJ** 2003 Cyclic strain enhances matrix mineralization by adult human mesenchymal stem cells via the extracellular signal-regulated kinase (ERK1/2) signaling pathway. *Journal of Biomechanics* 36: 1087–1096.
- Simons K and Ikonen E** 1997 Functional rafts in cell membranes. *Nature* 387: 569–572.
- Singer SJ and Nicolson GL** 1972 The fluid mosaic model of the structure of cell membranes. *Science (New York, N.Y.)* 175: 720–731.
- Sisalli MJ, Secondo A, Esposito A, Valsecchi V, Savoia C, Di Renzo GF, Annunziato L and Scorziello A** 2014 Endoplasmic reticulum refilling and mitochondrial calcium extrusion promoted in neurons by NCX1 and NCX3 in ischemic preconditioning are determinant for neuroprotection. *Cell Death & Differentiation* 21: 1142–1149.
- Snutch TP, Peloquin J, Mathews E and McRory JE** 2013 Molecular Properties of Voltage-Gated Calcium Channels
- Sperelakis N** 2012 Cell Physiology Source Book: Essentials of Membrane Biophysics. Elsevier
- Strehler EE and Zacharias DA** 2001 Role of alternative splicing in generating isoform diversity among plasma membrane calcium pumps. *Physiological Reviews* 81: 21–50.
- Stuyvers BD, Boyden PA and Keurs HEDJ ter** 2000 Calcium Waves Physiological Relevance in Cardiac Function. *Circulation Research* 86: 1016–1018.
- Styner M, Sen B, Xie Z, Case N and Rubin J** 2010 Indomethacin Promotes Adipogenesis of Mesenchymal Stem Cells Through a Cyclooxygenase Independent Mechanism. *Journal of cellular biochemistry* 111: 1042–1050.
- Subhra T, Wang P-C and Gang F** 2013 Electroporation Based Drug Delivery and Its Applications. In Takahata K (ed.) *Advances in Micro/Nano Electromechanical Systems and Fabrication Technologies* p.. InTech
- Subramanian K and Meyer T** 1997 Calcium-induced restructuring of nuclear envelope and endoplasmic reticulum calcium stores. *Cell* 89: 963–971.
- Sugar IP and Neumann E** 1984 Stochastic model for electric field-induced membrane pores. Electroporation. *Biophysical Chemistry* 19: 211–225.

- Sumanasinghe RD, Bernacki SH and Lobo EG** 2006 Osteogenic differentiation of human mesenchymal stem cells in collagen matrices: effect of uniaxial cyclic tensile strain on bone morphogenetic protein (BMP-2) mRNA expression. *Tissue Engineering* 12: 3459–3465.
- Sun S, Liu Y, Lipsky S and Cho M** 2007 Physical manipulation of calcium oscillations facilitates osteodifferentiation of human mesenchymal stem cells. *FASEB journal: official publication of the Federation of American Societies for Experimental Biology* 21: 1472–1480.
- Sundelacruz S, Levin M and Kaplan DL** 2008 Membrane Potential Controls Adipogenic and Osteogenic Differentiation of Mesenchymal Stem Cells. *PLOS ONE* 3: e3737.
- Susil R, Šemrov D and Miklavčič D** 1998 Electric Field-Induced Transmembrane Potential Depends on Cell Density and Organization. *Electro- and Magnetobiology* 17: 391–399.
- Szabadkai G, Bianchi K, Várnai P, De Stefani D, Wieckowski MR, Cavagna D, Nagy AI, Balla T and Rizzuto R** 2006 Chaperone-mediated coupling of endoplasmic reticulum and mitochondrial Ca^{2+} channels. *The Journal of Cell Biology* 175: 901–911.
- Szewczyk MM, Pande J and Grover AK** 2008 Caloxins: a novel class of selective plasma membrane Ca^{2+} pump inhibitors obtained using biotechnology. *Pflügers Archiv: European Journal of Physiology* 456: 255–266.
- Tada H, Nemoto E, Foster BL, Somerman MJ and Shimauchi H** 2011 Phosphate increases bone morphogenetic protein-2 expression through cAMP-dependent protein kinase and ERK1/2 pathways in human dental pulp cells. *Bone* 48: 1409–1416.
- Takahashi A, Camacho P, Lechleiter JD and Herman B** 1999 Measurement of intracellular calcium. *Physiological Reviews* 79: 1089–1125.
- Takasawa S, Ishida A, Nata K, Nakagawa K, Noguchi N, Tohgo A, Kato I, Yonekura H, Fujisawa H and Okamoto H** 1995 Requirement of calmodulin-dependent protein kinase II in cyclic ADP-ribose-mediated intracellular Ca^{2+} mobilization. *The Journal of Biological Chemistry* 270: 30257–30259.
- Takei K, Mignery GA, Mugnaini E, Südhof TC and De Camilli P** 1994 Inositol 1,4,5-trisphosphate receptor causes formation of ER cisternal stacks in transfected fibroblasts and in cerebellar Purkinje cells. *Neuron* 12: 327–342.
- Takekura H, Takeshima H, Nishimura S, Takahashi M, Tanabe T, Flockerzi V, Hofmann F and Franzini-Armstrong C** 1995 Co-expression in CHO cells of two muscle proteins involved in excitation-contraction coupling. *Journal of Muscle Research and Cell Motility* 16: 465–480.
- Tang QQ, Jiang MS and Lane MD** 1999 Repressive effect of Sp1 on the C/EBP α gene promoter: role in adipocyte differentiation. *Molecular and Cellular Biology* 19: 4855–4865.
- Tarek M** 2005 Membrane Electroporation: A Molecular Dynamics Simulation. *Biophysical Journal* 88: 4045–4053.
- Teissie J and Rols MP** 1986 Fusion of mammalian cells in culture is obtained by creating the contact between cells after their electroporation. *Biochemical and Biophysical Research Communications* 140: 258–266.
- Teissie J and Rols MP** 1993 An experimental evaluation of the critical potential difference inducing cell membrane electroporation. *Biophysical Journal* 65: 409–413.
- Teissie J and Tsong TY** 1981 Electric field induced transient pores in phospholipid bilayer vesicles. *Biochemistry* 20: 1548–1554.
- Tekle E, Wolfe MD, Oubrahim H and Chock PB** 2008 Phagocytic clearance of electric field induced ‘apoptosis-mimetic’ cells. *Biochemical and Biophysical Research Communications* 376: 256–260.

- Teramoto T and Iwasaki K** 2006 Intestinal calcium waves coordinate a behavioral motor program in *C. elegans*. *Cell Calcium* 40: 319–327.
- Terasaki M, Jaffe LA, Hunnicutt GR and Hammer JA** 1996 Structural change of the endoplasmic reticulum during fertilization: evidence for loss of membrane continuity using the green fluorescent protein. *Developmental Biology* 179: 320–328.
- Thomson JA, Itskovitz-Eldor J, Shapiro SS, Waknitz MA, Swiergiel JJ, Marshall VS and Jones JM** 1998 Embryonic stem cell lines derived from human blastocysts. *Science (New York, N.Y.)* 282: 1145–1147.
- Thorn P, Lawrie AM, Smith PM, Gallacher DV and Petersen OH** 1993 Local and global cytosolic Ca^{2+} oscillations in exocrine cells evoked by agonists and inositol trisphosphate. *Cell* 74: 661–668.
- Thurneysen T, Nicoll DA, Philipson KD and Porzig H** 2002 Sodium/calcium exchanger subtypes NCX1, NCX2 and NCX3 show cell-specific expression in rat hippocampus cultures. *Brain Research. Molecular Brain Research* 107: 145–156.
- Tieleman DP** 2004 The molecular basis of electroporation. *BMC Biochemistry* 5: 10.
- Tien HT and Diana AL** 1967 Black lipid membranes in aqueous media: The effect of salts on electrical properties. *Journal of Colloid and Interface Science* 24: 287–296.
- Timper K, Seboek D, Eberhardt M, Linscheid P, Christ-Crain M, Keller U, Müller B and Zulewski H** 2006 Human adipose tissue-derived mesenchymal stem cells differentiate into insulin, somatostatin, and glucagon expressing cells. *Biochemical and Biophysical Research Communications* 341: 1135–1140.
- Titushkin I, Sun S, Shin J and Cho M** 2010 Physicochemical Control of Adult Stem Cell Differentiation: Shedding Light on Potential Molecular Mechanisms. *BioMed Research International* 2010: e743476.
- Tokman M, Lee JH, Levine ZA, Ho M-C, Colvin ME and Vernier PT** 2013 Electric Field-Driven Water Dipoles: Nanoscale Architecture of Electroporation. *PLOS ONE* 8: e61111.
- Toyoshima C, Nakasako M, Nomura H and Ogawa H** 2000 Crystal structure of the calcium pump of sarcoplasmic reticulum at 2.6 [Å] resolution. *Nature* 405: 647–655.
- Trevor KT, Cover C, Ruiz YW, Akporiaye ET, Hersh EM, Landais D, Taylor RR, King AD and Walters RE** 2004 Generation of dendritic cell-tumor cell hybrids by electrofusion for clinical vaccine application. *Cancer immunology, immunotherapy: CII* 53: 705–714.
- Trombetta ES and Parodi AJ** 2003 Quality control and protein folding in the secretory pathway. *Annual Review of Cell and Developmental Biology* 19: 649–676.
- Tsien JZ, Huerta PT and Tonegawa S** 1996 The Essential Role of Hippocampal CA1 NMDA Receptor-Dependent Synaptic Plasticity in Spatial Memory. *Cell* 87: 1327–1338.
- Tsien RW** 1983 Calcium Channels in Excitable Cell Membranes. *Annual Review of Physiology* 45: 341–358.
- Tsien RY** 1980 New calcium indicators and buffers with high selectivity against magnesium and protons: design, synthesis, and properties of prototype structures. *Biochemistry* 19: 2396–2404.
- Tsien RY** 1998 The green fluorescent protein. *Annual Review of Biochemistry* 67: 509–544.
- Tsuboi T, da Silva Xavier G, Holz GG, Jouaville LS, Thomas AP and Rutter GA** 2003 Glucagon-like peptide-1 mobilizes intracellular Ca^{2+} and stimulates mitochondrial ATP synthesis in pancreatic MIN6 beta-cells. *Biochemical Journal* 369: 287–299.

- Turovsky EA, Kaimachnikov NP, Turovskaya MV, Berezhnov AV, Dynnik VV and Zinchenko VP** 2012 Two mechanisms of calcium oscillations in adipocytes. *Biochemistry (Moscow) Supplement Series A: Membrane and Cell Biology* 6: 26–34.
- Uccelli A, Moretta L and Pistoia V** 2008 Mesenchymal stem cells in health and disease. *Nature Reviews Immunology* 8: 726–736.
- Ullah I, Subbarao RB and Rho GJ** 2015 Human mesenchymal stem cells - current trends and future prospective. *Bioscience Reports* 35
- Unwin N and Henderson R** 1984 The structure of proteins in biological membranes. *Scientific American* 250: 78–94.
- Uzman A** 2003 Molecular biology of the cell (4th ed.): Alberts, B., Johnson, A., Lewis, J., Raff, M., Roberts, K., and Walter, P.. *Biochemistry and Molecular Biology Education* 31: 212–214.
- Vance JE and Vance DE** 2008 Biochemistry of Lipids, Lipoproteins and Membranes. Elsevier
- VanHouten J, Sullivan C, Bazinet C, Ryoo T, Camp R, Rimm DL, Chung G and Wysolmerski J** 2010 PMCA2 regulates apoptosis during mammary gland involution and predicts outcome in breast cancer. *Proceedings of the National Academy of Sciences of the United States of America* 107: 11405–11410.
- Vassart G and Costagliola S** 2011 G protein-coupled receptors: mutations and endocrine diseases. *Nature Reviews Endocrinology* 7: 362–372.
- Vater C, Kasten P and Stiehler M** 2011a Culture media for the differentiation of mesenchymal stromal cells. *Acta Biomaterialia* 7: 463–477.
- Vater C, Kasten P and Stiehler M** 2011b Culture media for the differentiation of mesenchymal stromal cells. *Acta Biomaterialia* 7: 463–477.
- Veech RL, Kashiwaya Y and King MT** 1995 The resting membrane potential of cells are measures of electrical work, not of ionic currents. *Integrative Physiological and Behavioral Science: The Official Journal of the Pavlovian Society* 30: 283–307.
- Vernier PT, Levine ZA, Wu Y-H, Joubert V, Ziegler MJ, Mir LM and Tieleman DP** 2009 Electroporating Fields Target Oxidatively Damaged Areas in the Cell Membrane. *PLoS ONE* 4
- Vernier PT, Sun Y and Gundersen MA** 2006 Nanoelectropulse-driven membrane perturbation and small molecule permeabilization. *BMC Cell Biology* 7: 37.
- Vernier PT, Sun Y, Marcu L, Craft CM and Gundersen MA** 2004 Nanosecond pulsed electric fields perturb membrane phospholipids in T lymphoblasts. *FEBS letters* 572: 103–108.
- Vernier PT, Sun Y, Marcu L, Salemi S, Craft CM and Gundersen MA** 2003 Calcium bursts induced by nanosecond electric pulses. *Biochemical and Biophysical Research Communications* 310: 286–295.
- Viana F, Van den Bosch L, Missiaen L, Vandenberghe W, Droogmans G, Nilius B and Robberecht W** 1997 Mibefradil (Ro 40-5967) blocks multiple types of voltage-gated calcium channels in cultured rat spinal motoneurons. *Cell Calcium* 22: 299–311.
- Vlahovska PM** 2015 Voltage-morphology coupling in biomimetic membranes: dynamics of giant vesicles in applied electric fields. *Soft Matter* 11: 7232–7236.
- Voelker DR** 2005 Bridging gaps in phospholipid transport. *Trends in Biochemical Sciences* 30: 396–404.
- Wal J van der, Habets R, Várnai P, Balla T and Jalink K** 2001 Monitoring Agonist-induced Phospholipase C Activation in Live Cells by Fluorescence Resonance Energy Transfer. *Journal of Biological Chemistry* 276: 15337–15344.
- Ward DF, Salaszyk RM, Klees RF, Backiel J, Agius P, Bennett K, Boskey A and Plopper GE** 2007 Mechanical strain enhances extracellular matrix-induced gene focusing and promotes

- osteogenic differentiation of human mesenchymal stem cells through an extracellular-related kinase-dependent pathway. *Stem Cells and Development* 16: 467–480.
- Weaver JC and Chizmadzhev YA** 1996 Theory of electroporation: A review. *Bioelectrochemistry and Bioenergetics* 41: 135–160.
- Weaver JC, Smith KC, Esser AT, Son RS and Gowrishankar TR** 2012 A brief overview of electroporation pulse strength-duration space: a region where additional intracellular effects are expected. *Bioelectrochemistry (Amsterdam, Netherlands)* 87: 236–243.
- Wegner LH, Flickinger B, Eing C, Berghöfer T, Hohenberger P, Frey W and Nick P** 2011 A patch clamp study on the electro-permeabilization of higher plant cells: Supra-physiological voltages induce a high-conductance, K⁺ selective state of the plasma membrane. *Biochimica Et Biophysica Acta* 1808: 1728–1736.
- White JA, Blackmore PF, Schoenbach KH and Beebe SJ** 2004 Stimulation of capacitative calcium entry in HL-60 cells by nanosecond pulsed electric fields. *The Journal of Biological Chemistry* 279: 22964–22972.
- Widera G, Austin M, Rabussay D, Goldbeck C, Barnett SW, Chen M, Leung L, Otten GR, Thudium K, Selby MJ and Ulmer JB** 2000 Increased DNA vaccine delivery and immunogenicity by electroporation in vivo. *Journal of Immunology (Baltimore, Md.: 1950)* 164: 4635–4640.
- Wier WG, ter Keurs HE, Marban E, Gao WD and Balke CW** 1997 Ca²⁺ ‘sparks’ and waves in intact ventricular muscle resolved by confocal imaging. *Circulation Research* 81: 462–469.
- Wilhelm C, Winterhalter M, Zimmermann U and Benz R** 1993 Kinetics of pore size during irreversible electrical breakdown of lipid bilayer membranes.. *Biophysical Journal* 64: 121–128.
- Wislet-Gendebien S, Hans G, Leprince P, Rigo J-M, Moonen G and Rogister B** 2005 Plasticity of cultured mesenchymal stem cells: switch from nestin-positive to excitable neuron-like phenotype. *Stem Cells (Dayton, Ohio)* 23: 392–402.
- Wonderlin WF and Strobl JS** 1996 Potassium channels, proliferation and G1 progression. *The Journal of Membrane Biology* 154: 91–107.
- Woodbury D, Reynolds K and Black IB** 2002 Adult bone marrow stromal stem cells express germline, ectodermal, endodermal, and mesodermal genes prior to neurogenesis. *Journal of Neuroscience Research* 69: 908–917.
- Woodbury D, Schwarz EJ, Prockop DJ and Black IB** 2000 Adult rat and human bone marrow stromal cells differentiate into neurons. *Journal of Neuroscience Research* 61: 364–370.
- Woods NM, Cuthbertson KS and Cobbold PH** 1986 Repetitive transient rises in cytoplasmic free calcium in hormone-stimulated hepatocytes. *Nature* 319: 600–602.
- Wozniak MA, Modzelewska K, Kwong L and Keely PJ** 2004 Focal adhesion regulation of cell behavior. *Biochimica Et Biophysica Acta* 1692: 103–119.
- Wu MM, Llopis J, Adams S, McCaffery JM, Kulomaa MS, Machen TE, Moore HP and Tsien RY** 2000 Organelle pH studies using targeted avidin and fluorescein-biotin. *Chemistry & Biology* 7: 197–209.
- Wuytack F, Dode L, Baba-Aissa F and Raeymaekers L** 1995 The SERCA3-type of organellar Ca²⁺pumps. *Bioscience Reports* 15: 299–306.
- Wuytack F, Raeymaekers L and Missiaen L** 2002 Molecular physiology of the SERCA and SPCA pumps. *Cell Calcium* 32: 279–305.
- Xiao J, Liang D, Zhao H, Liu Y, Zhang H, Lu X, Liu Y, Li J, Peng L and Chen Y-H** 2010 2-Aminoethoxydiphenyl borate, a inositol 1,4,5-triphosphate receptor inhibitor, prevents atrial fibrillation. *Experimental Biology and Medicine (Maywood, N.J.)* 235: 862–868.

- Yada T, Oiki S, Ueda S and Okada Y** 1986 Synchronous oscillation of the cytoplasmic Ca^{2+} concentration and membrane potential in cultured epithelial cells (Intestine 407). *Biochimica et Biophysica Acta (BBA) - Molecular Cell Research* 887: 105–112.
- Yamashita J, Kita S, Iwamoto T, Ogata M, Takaoka M, Tazawa N, Nishikawa M, Wakimoto K, Shigekawa M, Komuro I and Matsumura Y** 2003 Attenuation of ischemia/reperfusion-induced renal injury in mice deficient in $\text{Na}^{+}/\text{Ca}^{2+}$ exchanger. *The Journal of Pharmacology and Experimental Therapeutics* 304: 284–293.
- Yang S-N and Berggren P-O** 2006 The Role of Voltage-Gated Calcium Channels in Pancreatic β -Cell Physiology and Pathophysiology. *Endocrine Reviews* 27: 621–676.
- Yin L, Li Y and Wang Y** 2006 Dexamethasone-induced adipogenesis in primary marrow stromal cell cultures: mechanism of steroid-induced osteonecrosis. *Chinese Medical Journal* 119: 581–588.
- Yoshikawa T, Peel SA, Gladstone JR and Davies JE** 1997 Biochemical analysis of the response in rat bone marrow cell cultures to mechanical stimulation. *Bio-Medical Materials and Engineering* 7: 369–377.
- Zhang Y, Khan D, Delling J and Tobiasch E** 2012 Mechanisms Underlying the Osteo- and Adipo-Differentiation of Human Mesenchymal Stem Cells. *The Scientific World Journal* 2012
- Zhao F, Chella R and Ma T** 2007 Effects of shear stress on 3-D human mesenchymal stem cell construct development in a perfusion bioreactor system: Experiments and hydrodynamic modeling. *Biotechnology and Bioengineering* 96: 584–595.
- Zhao F, Li P, Chen SR, Louis CF and Fruen BR** 2001 Dantrolene inhibition of ryanodine receptor Ca^{2+} release channels. Molecular mechanism and isoform selectivity. *The Journal of Biological Chemistry* 276: 13810–13816.
- Zhao Y, Araki S, Wu J, Teramoto T, Chang Y-F, Nakano M, Abdelfattah AS, Fujiwara M, Ishihara T, Nagai T and Campbell RE** 2011 An expanded palette of genetically encoded Ca^{2+} indicators. *Science (New York, N.Y.)* 333: 1888–1891.
- Zhong J** 2011 From simple to complex: investigating the effects of lipid composition and phase on the membrane interactions of biomolecules using in situ atomic force microscopy. *Integrative Biology* 3: 632–644.
- Zhu M, Kohan E, Bradley J, Hedrick M, Benhaim P and Zuk P** 2009 The effect of age on osteogenic, adipogenic and proliferative potential of female adipose-derived stem cells. *Journal of Tissue Engineering and Regenerative Medicine* 3: 290–301.
- Zhu MX, Ma J, Parrington J, Calcraft PJ, Galione A and Evans AM** 2010 Calcium signaling via two-pore channels: local or global, that is the question. *American Journal of Physiology - Cell Physiology* 298: C430–C441.
- Ziegler MJ and Vernier PT** 2008 Interface Water Dynamics and Porating Electric Fields for Phospholipid Bilayers. *The Journal of Physical Chemistry B* 112: 13588–13596.
- Zilberfarb V, Siquier K, Strosberg AD and Issad T** 2001 Effect of dexamethasone on adipocyte differentiation markers and tumour necrosis factor- α expression in human PAZ6 cells. *Diabetologia* 44: 377–386.

Abstract

Pulsed electric fields are widely used in research, medicine, food industry and other biotechnological processes. The interaction of one 100 μ s pulse with the plasma membrane and the endoplasmic reticulum membrane was evaluated in two different cell types. Pulse amplitude ranged between 100 and 3 000 V/cm. Organelles membrane permeabilization using this kind of pulses was experimentally demonstrated for the first time. The use of such a pulse to control the spontaneous calcium oscillations in human-adipose mesenchymal stem cells was also assessed. By creating electro-induced calcium spikes of different amplitudes, the pulse can either add a supplementary spike, or, on the contrary, inhibit the spontaneous oscillations for some tens of minutes. During this inhibition period, the electric pulse-mediated addition of calcium spikes of desired amplitude and frequency is still possible. The delivery of 100 μ s pulses to stem cells undergoing osteodifferentiation was also performed. The electric pulse seemed to delay the differentiation. Moreover, during osteogenic differentiation, cells cultures displayed an organization in a few cell layers. The characterization of these layers gave results that may help to obtain mature osteoblast in less time than usual one. The use of the microsecond electric pulses technology to permeabilize the plasma and the internal cell membranes as well as to modulate internal calcium concentrations is therefore interesting to study the role of calcium in many physiological processes and to manipulate the cell calcium dynamics (oscillations, waves, spikes) in different cell types. Doing so, this available, simple and easy to apply technology could be used for the modulation and the control of basic cellular functions such as proliferation, differentiation and apoptosis.

Keywords: microsecond pulsed electric field, electroporation, electropermeabilization, plasma membrane, endoplasmic reticulum, calcium spikes, mesenchymal stem cells, calcium oscillations, osteogenic differentiation.

Résumé

Les champs électriques pulsés sont largement utilisés dans la recherche, la médecine, l'industrie alimentaire et d'autres procédés biotechnologiques. L'interaction d'une impulsion de 100 μ s avec la membrane plasmique et la membrane du réticulum endoplasmique a été évaluée dans deux types cellulaires différents. La perméabilisation des organites cellulaires avec ce type d'impulsions est démontrée expérimentalement pour la première fois. L'utilisation d'une telle impulsion afin de contrôler les oscillations calciques spontanées dans les cellules souches mésenchymateuses humaines issues du tissu adipeux a été évaluée. En créant des pics calciques électro-induits d'amplitudes différentes, l'impulsion peut ou bien induire un pic calcique supplémentaire ou bien inhiber les oscillations spontanées pour quelques dizaines de minutes. Cette inhibition rend possible d'imposer à la cellule des pics d'amplitude et de fréquence désirés. Un essai d'application de l'impulsion 100 μ s à des cellules souches subissant une différenciation osseuse a aussi été réalisé. Une impulsion électrique semble retarder la différenciation. Lors d'une différenciation osseuse, plusieurs couches cellulaires ont été observées. La caractérisation de ces couches a donné des résultats qui pourraient aider à obtenir des ostéoblastes matures dans un temps moindre que la normale. L'utilisation des champs électriques pulsés microsecondes, pour perméabiliser la membrane plasmique et les membranes internes des cellules, ainsi que pour moduler les concentrations du calcium intracellulaire, semble donc très intéressante pour étudier le rôle du calcium dans de nombreux processus physiologiques et pour manipuler les dynamiques calciques (oscillations, vagues, pics) dans différents types de cellules. Ainsi, cette technologie simple, facile à appliquer et disponible dans beaucoup de laboratoires serait envisageable pour la modulation et le contrôle de fonctions cellulaires basiques telles que la prolifération, la différenciation et l'apoptose.

Mots-clés: champ électrique pulsé microseconde, électroporation, électroperméabilisation, membrane plasmique, réticulum endoplasmique, pics calciques, cellules souches mésenchymateuses, oscillations calciques, différenciation osseuse.